**IN THE UNITED STATES DISTRICT COURT
FOR THE DISTRICT OF NEW JERSEY**

	)	
	)	
BRISTOL-MYERS SQUIBB COMPANY,	)	
	)	
Plaintiff,	)	
	)	Civil Action No. 3:10-cv-05810
v.	)	(MLC)(LHG)
	)	
APOTEX, INC., and	)	
APOTEX CORP.,	)	
	)	
Defendants.	)	
	)	

**DECLARATION OF JERRY ATWOOD
IN SUPPORT OF PLAINTIFF'S OPENING CLAIM CONSTRUCTION BRIEF**

I, Jerry L. Atwood, hereby declare the following:

I have been asked by Bristol Myers-Squibb's ("BMS") counsel to prepare an expert declaration addressing the meaning of ten (10) terms in the asserted claims of BMS's U.S. Patent No. 7,491,725 ("the '725 patent") (attached herein as Ex. A), which I understand are in dispute. In rendering my opinions, I have reviewed, *inter alia*, the '725 patent and its prosecution history, Apotex's proposed claim constructions, and the Summary of Proposed Testimony of Guatam Desiraju (Joint Claim Construction and Hearing Statement, Ex. F (Dkt. 51) (hereinafter "Desiraju Summary")).

I.   QUALIFICATIONS[1]

1.   Since 1994 to the present, I have been employed as Professor and Chairman of the Department of Chemistry at the University of Missouri-Columbia. From 1968 to 1994, I was employed by the University of Alabama, where I successively held the titles of Assistant

---

[1] Attached herein as Exhibit B is my curriculum vitae.

1

Professor, Associate Professor, and University Research Professor. I earned my Ph.D. degree in

Chemistry from the University of Illinois in 1968.

2.   From 1985 to 1998, I was Editor of the *Journal of Chemical Crystallography*. In

1999, I was named Consulting Editor for the *Journal of Chemical Crystallography*. From 1992

until 2000, I was Editor of *Supramolecular Chemistry*. From 1985 to 1993, I was Regional

Editor for the *Journal of Coordination Chemistry*. I have been a Co-Editor-in-Chief of the *New

Journal of Chemistry* since 2005. I am a Co-Editor of the *Inclusion Compounds* book series

(five volumes), *Comprehensive Supramolecular Chemistry* (ten volumes), and the *Encyclopedia

of Supramolecular Chemistry* (2 volumes). I currently serve on the editorial boards of *Crystal

Growth & Design, Chemical Communications,* the *Journal of Coordination Chemistry,* the *New

Journal of Chemistry,* and *Supramolecular Chemistry*.

3.   I currently run an active research laboratory of four postdoctoral fellows, eight

graduate students, and four undergraduate students. I have published more than 670 articles in

refereed journals, most of which focus on the fields of crystal growth, crystal engineering,

polymorphism, organic chemistry and polymer chemistry.

II.   BACKGROUND INFORMATION

4.   The following tutorial is provided as general scientific information to assist the

Court. There may be exceptions or caveats to the scientific statements made here, but I provide

the general concepts only to be concise.

a.   Polymorphs

5.   A compound is a substance made by joining together atoms of different chemical

elements (such as carbon, oxygen or hydrogen for example) in a specific ratio and connectivity,

resulting in a specific chemical structure. The different atoms are connected by chemical bonds.

A compound has properties that are different from those possessed by the elements that comprise it. The smallest fundamental unit of a compound that retains the compound's properties is a molecule.

6.   Some compounds can adopt crystalline forms. A crystal consists of repeating units made up of a regularly ordered arrangement of molecules or ions in three dimensional space. These units are referred to as unit cells. There are seven different unit cell shapes: triclinic, monoclinic, orthorhombic, tetragonal, hexagonal, trigonal and cubic.

7.   An example of a crystalline compound is table salt, NaCl. Table salt is a compound comprised of sodium (Na^+) ions and chloride (Cl^-) ions. A regularly ordered arrangement of these ions in three dimensional space results in a cubic lattice.
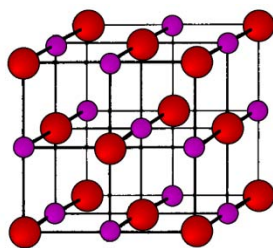

Sodium ions are shown as small spheres and chloride ions are shown as large spheres.

8.   It is possible for a compound to crystallize into more than one distinct crystalline form. These distinct crystalline forms are referred to as polymorphs. Polymorphs of a particular compound have identical chemical structures, but the arrangement of the molecules of the compound in three dimensional space, *i.e.*, the crystal structure, is different, resulting in different physical properties.

9.   Examples of polymorphs are graphite and diamond. Both are made up of carbon atoms, but the arrangement of the atoms in three dimensional space is different, resulting in very different properties. Graphite is opaque and has a dull metallic sheen, while diamonds are

transparent and brilliant. Another difference is that graphite is one of the softest natural substances whereas diamond is the hardest.
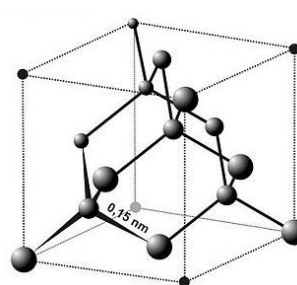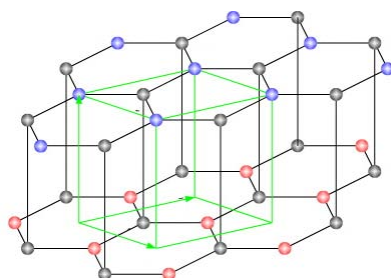
Graphite - a staggered arrangement of stacked hexagonal layers

Diamond - tetrahedrally bonded carbon atoms

10.   Some substances can trap solvent while undergoing crystallization in a definite ratio as an integral part of the crystal structure, resulting in a crystalline solvate. When the solvent is water, the polymorph is referred to as a hydrate. If a single water molecule is trapped for every single molecule of a substance, it is known as a monohydrate.

11.   Once obtained, polymorphs can be characterized by a variety of different techniques. As discussed in more detail below, one of these techniques is X-ray powder diffraction ("XRPD"), which provides information about the spacing between the planes of atoms in a crystal lattice. Another one of these techniques is differential scanning calorimetry ("DSC"), which provides information about the thermal behavior of a substance, such as loss of solvent, phase transitions, and/or the melting point of a crystal. Another technique is thermogravimetric analysis ("TGA"), which provides information about the amount of solvent or water a crystalline solvate or hydrate contains, respectively.

12.   Different polymorphs of a given molecule can display significantly different properties, such as different stabilities, different dissolution profiles, and different bioavailability. These different properties can be of great significance in the pharmaceutical industry. For

example, these differences can affect the manufacturability, performance, and quality of the drug product.

13.   An understanding of the different polymorphs of a particular pharmaceutical is important because information about how the polymorphs interconvert, and about their advantages over each other, may affect the properties of the final drug product. Thus, for a manufacturer to be able to control its drug manufacturing methods and have confidence in the end product of those methods, the manufacturer must have an understanding of whether polymorphs exist and the characteristics of the polymorphs if they do exist.

b.   X-ray Powder Diffraction

14.   A crystalline solid is one in which the molecules or atoms are uniformly arranged. This arrangement of molecules is called a "crystal lattice." This uniform arrangement gives rise to a unit cell, which is the simplest repeating three-dimensional portion of the crystal structure. The crystal lattice is therefore built up by stacking the unit cell in three dimensions. The size, shape, and contents of each unit cell within a crystal are identical. For example, diamond is a crystalline form of carbon and consists of an ordered arrangement of carbon atoms.

15.   X-ray powder diffraction data can be used to distinguish different polymorphs of a crystalline compound. X-ray powder diffraction is a method of characterizing solid substances in which a sample is bombarded with X-rays and the diffraction of the X-rays is recorded by a detector. A crystalline compound diffracts X-rays according to the arrangement of molecules in the crystal structure. Because crystalline solids are built in an ordered way, the same motifs repeat throughout the crystal in the three dimensions, which creates the lattice. These lattices exhibit "planes" in 3-D space. Different planes can occur in a particular crystal structure.

16. An X-ray powder diffraction pattern plots the intensity of an X-ray beam diffracted by the crystal lattice versus the angle of diffraction of the X-rays, usually represented with a measurement value of 2θ. Below is an example of an X-ray diffraction pattern where the X-axis plots the 2θ values and the Y-axis plots the intensity of the diffracted X-ray beam.
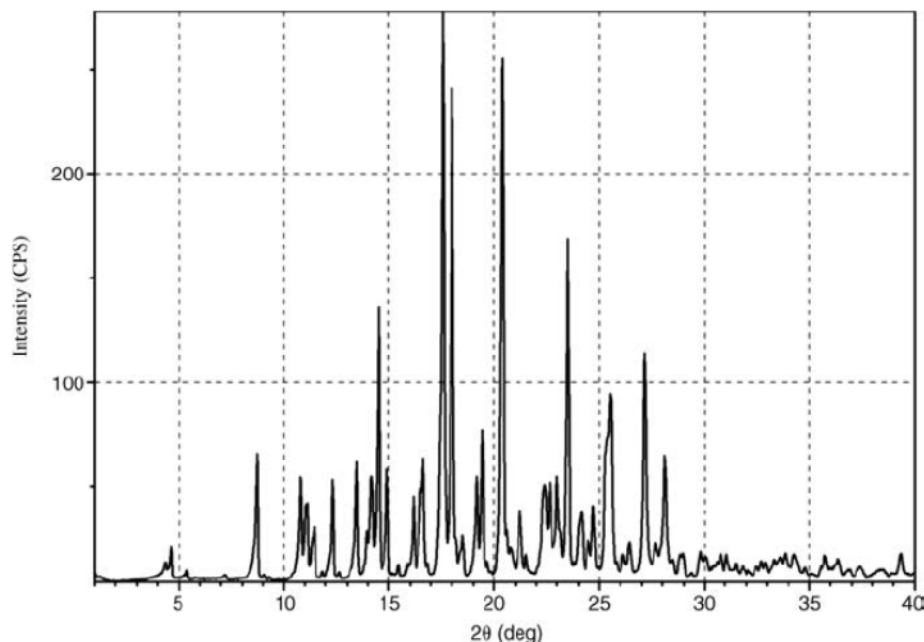
17. When preparing a sample for X-ray powder diffraction, the material of interest is generally ground into a fine crystalline powder. When X-rays of a particular wavelength are directed at the powder, an observable pattern is produced. This is because the X-rays are electromagnetic waves that interact with the planes of the lattice in a distinct manner. For purposes of illustration, the three-dimensional planes can be represented in two-dimensional space, wherein the lines represent planes. The wavelength of the X-rays that are used in such an experiment is of a length that is similar to the distance between the planes within the crystal, represented by the letter "d." The X-ray beam reflects off the crystallographic plane, and the angle of reflection is the same as the angle of incidence.

6
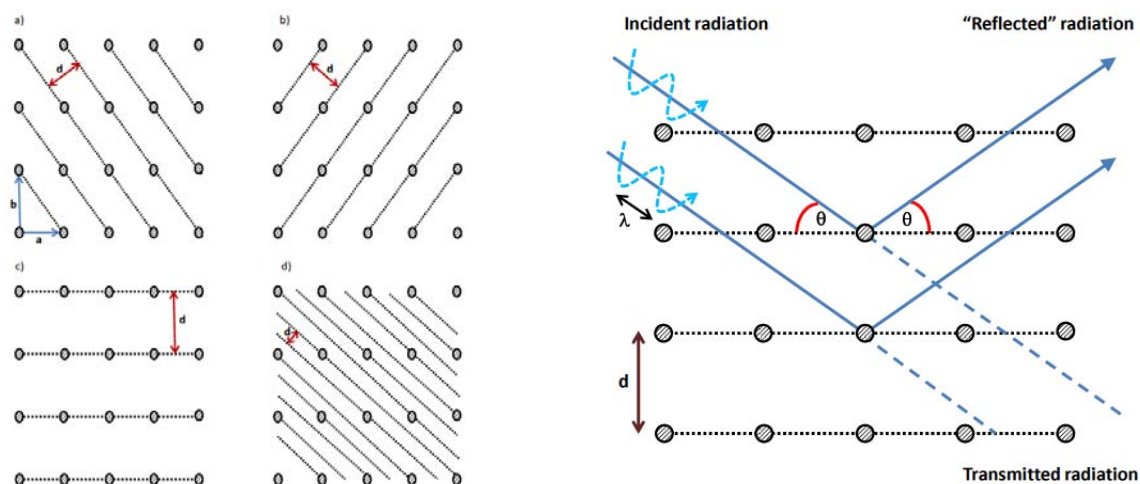
A lattice plane is a plane which intersects atoms of a unit cell across the whole three-dimensional lattice. The perpendicular separation between each plane is called the d-spacing.

18.   The result of an XRPD experiment is a pattern that can be used to identify a particular crystal structure or polymorph. This is possible because all possible lattice planes for the diffraction of X-rays are present in the powder sample of the crystalline powder sample. For every d-spacing between lattice planes, a device, called a diffractometer, plots the intensity of the diffracted X-rays versus the angle of incidence, usually represented as 2θ. The intensity of the diffracted X-rays relates to the arrangement of the molecules in the lattice, and is often provided as relative intensity, in which the various peaks are divided by the intensity of the maximum peak. Because different polymorphs have different lattice structures, and therefore different lattice "planes," different polymorphs have a different set of 2θ values compared to related polymorphs. This is what allows the X-ray diffraction pattern to act as an identifier for a given crystal form of a particular compound. It is possible for different crystals or polymorphs to have one or more peaks in common, because they might have different planes that have a similar d-spacing. However, it does not mean that the polymorphs share these particular planes. Therefore, the selection of multiple peaks from an XRPD pattern can be used to identify and

7

distinguish the crystalline form of a compound from other crystalline forms of the same compound (polymorphs).

19.   The method by which the XRPD analysis is performed can create some variations in the results. For example, the number of detected peaks and their intensities depend on the size of the sample, the scanning speed used in the diffractometer, the degree to which the sample was ground, and the crystallinity of the sample. Differences can also arise due to the type of equipment used to make the measurement, the care taken in making the measurement, and the number of samples measured. Because of these variations, substances are normally characterized by a number of the major or more intense peaks. However, the intensity of the peaks can vary among samples, so the intensities are not particularly informative in identifying a sample. (*See* I. Ivanisevic, R.B. McClurg, and P.J. Schields, *Uses of X-Ray Powder Diffraction In the Pharmaceutical Industry, in* Pharmaceutical Sciences Encyclopedia: Drug Discovery, Development, and Manufacturing 1, 6 (S.C. Gad ed., 2010) ("When comparing XRPD data of crystalline samples, one notes any differences in peak positions . . . which correspond to structural differences between the samples. Intensities are generally not relied upon for qualitative analysis due to previously mentioned instrument and sample artifacts. . . .") (attached herein as Ex. C); A.R. West, Basic Solid State Chemistry 142-43 (2nd ed. 1999) ("Intensities are more difficult to measure quantitatively and often vary from sample to sample especially if preferred orientation is present.") (attached herein as Ex. D).)

20.   In addition, the relative peak intensities can vary depending on the orientation of the sample. Severe preferential crystalline particle orientation can be induced by the particle size, leading to skewed X-ray powder diffraction data with regard to the intensities of the peaks. Preferred orientation is especially a problem with polymorphs that have needle-like or plate-like

crystals. (*See* Ex. D, West, at 139.) Even if the preferred orientation of the sample is accounted

for, the relative intensities can vary. For example, as described in The United States

Pharmacopoeia 1844 (23rd Rev. 1995) (attached herein as Ex. E), the "relative intensities

between sample and reference may vary up to 20 percent." Moreover, this potential variance is

on a peak-by-peak basis.

21.   Although XRPD can provide a lot of information about the structure of a

polymorph, another technique, single crystal X-ray diffraction, is the only technique that can

provide the space group or symmetry of the crystal, together with the position of all the atoms in

the unit cell. Single crystal X-ray diffraction is a technique where a beam of X-rays strikes a

single crystal as the crystal is gradually rotated, producing diffracted beams. The experimental

procedure and data collection are very similar to that of XRPD.

c.   Differential Scanning Calorimetry

22.   DSC is a method that uses heat to measure the physical properties of a crystal

polymorph. This can either be used to measure the melting point of a crystalline solid, to

measure phase changes, which occur at the temperature at which one polymorphic form converts

into another form, or to measure the desolvation or the removal of any solvent present in the

crystalline solid. In a DSC experiment, a test sample and a reference sample are placed on two

separate trays in a calorimeter, and heat flow to or from each of the samples is measured as the

temperature of the samples is increased. For example, the melting of a crystalline sample

requires an input of energy at the melting point. This is seen as an endothermic peak in the plot

of heat flow versus temperature.

23.   The melting point of a crystal requires the input of energy, but a phase change,

such as the conversion between two polymorphic structures, can either take up or give off

energy, or both. Dehydration of a crystalline hydrate requires the input of energy, giving rise to an endothermic peak

24.   Certain factors can affect DSC peaks. For example, impurities or excipients can affect DSC peaks. (*See, e.g.*, B.S. Furniss *et al*., Vogel's Textbook of Practical Organic Chemistry 236 (5th ed. 1989) ("The presence of small quantities of miscible, or partially miscible, impurities will usually produce a marked increase in the melting point range and cause the commencement of melting to occur at a temperature lower than the melting point of the pure substance. The melting point is therefore a valuable criterion of purity for an organic compound.") (attached herein as Ex. F); *see also* The United States Pharmacopeia, *Thermal Analysis*, 2394 (27th Rev. 2004) (attached herein as Ex. G).) Likewise, particle size may also affect DSC peaks. (*See, e.g.*, V. Ventkateswarlu & K. Manjunath, *Preparation, characterization and in vitro release kinetics of clozapine solid lipid nanoparticles*, 627 J. CONTROLLED RELEASE 634 (2004) (attached herein as Ex. H).)

d.   Thermogravimetric Analysis (TGA)

25.   TGA is a technique particularly suited for the measurement of the amount of solvent a solvate contains and/or the amount of water a hydrate contains. In the TGA experiment, the weight of a sample is monitored as the temperature of the sample is increased under a flow of nitrogen. The plot of weight of the sample versus temperature provides the percentage of water in a hydrate, and may provide an assessment of whether the water is surface-bound or more strongly held water of crystallization. *See* The United States Pharmacopeia, *Thermal Analysis*, 2394, 2395 (27th Rev. 2004) (attached herein as Ex. G).)

26.   Based on the weight loss obtained from the TGA and the corresponding transition temperature range of the DSC, the stoichiometry, *i.e.,* theoretical ratio, of bound water or solvent

to the "dry" form can be determined. Given the many experimental variables, the actual weight loss determined by TGA will rarely result in the exact stoichiometry.

III. CLAIM CONSTRUCTION ANALYSIS

27.   The '725 patent relates to crystalline forms of dasatinib. The art disclosed in this patent relates to solid-state chemistry and the design of a solid or crystalline form of an active pharmaceutical ingredient that is stable yet readily bioavailable. The person of ordinary skill in the art would be a medicinal or synthetic chemist with an advanced degree in solid-state chemistry with considerable study in pharmacology and crystal engineering. The person of ordinary skill would either work with a person with an advanced degree in molecular biology with education or experience in the field of cellular signal transduction or would have such training himself.
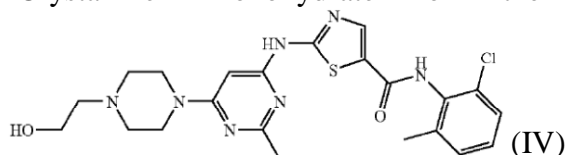
A.   "Crystalline monohydrate of the compound of formula (IV)

,"
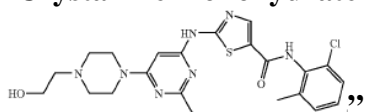
28.   This phrase appears in claims 1, 3 and 12 of the '725 patent.
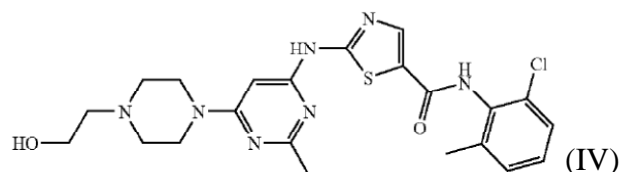
29.   Claim 1 of the '725 patent recites:

"Crystalline   monohydrate   of   the   compound   of   formula   (IV)

 (IV)

which is characterized by an x-ray powder diffraction pattern substantially in accordance with that shown in FIG. 1."

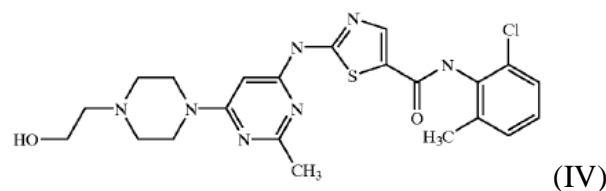30.   Claim 3 of the '725 patents recites:

"Crystalline monohydrate of the compound of formula (IV)

(IV)

which is characterized by an x-ray powder diffraction pattern (CuKα γ =1.5418 Å at a temperature of about 23° C.) comprising four or more 2θ values selected from the group consisting of: 18.0±0.2, 18.4±0.2, 19.2±0.2, 19.6±0.2, 21.2±0.2, 24.5±0.2, 25.9±0.2, and 28.0±0.2."

31.   Claim 12 of the '725 patent recites:

"Crystalline monohydrate of the compound of formula (IV)

(IV)

which is characterized by a differential scanning calorimetry having a broad peak between approximately 95° C and 130° C, which corresponds to the loss of one water of hydration on thermogravitmetric analysis."

32.   One of ordinary skill in the art would understand the term "[c]rystalline

monohydrate of the compound of formula (IV)

(IV)"
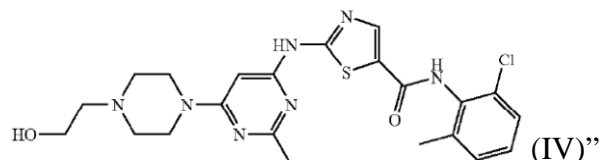
to have its ordinary meaning, i.e., the monohydrate of the compound of formula (IV) in a

crystalline form. (See The American Heritage Dictionary for the English Language 1137 (4th Ed.

2000) (defining "monohydrate" as "[a] compound, such as calcium chloride monohydrate,

$CaCl_2.H_2O$, that contains one molecule of water") (attached herein as Ex. I) (BMS01380886-

888).)

B.   **"which is characterized by an X-ray powder diffraction pattern substantially in accordance with that shown in FIG. 1"**

33.   This phrase appears in claim 1. (*See supra* ¶ 28)

34.   One of ordinary skill in the art would understand the term "which is characterized by an x-ray powder diffraction pattern substantially in accordance with that shown in FIG. 1" to mean that which is characterized by an x-ray powder diffraction ("XRPD") pattern that is substantially identical to that shown in FIG. 1 taking into account variations due to measurement errors dependent upon the measurement conditions employed, but not taking into account the exact order of intensity of the peaks. Further, the ability to ascertain substantial identities of X-ray diffraction patterns is within the purview of one of ordinary skill in the art.

35.   This construction is supported by, *inter alia*, the following statements in the '725 patent:

> One of ordinary skill in the art will appreciate that an X-ray diffraction pattern *may be obtained with a measurement error that is dependent upon the measurement conditions employed*. In particular, it is generally known that intensities in a X-ray diffraction pattern may fluctuate depending upon measurement conditions employed. *It should be further understood that relative intensities may also vary depending upon experimental conditions and, accordingly, the exact order of intensity should not be taken into account*. Additionally, a measurement error of diffraction angle for a conventional X-ray diffraction pattern is typically about 5% or less, and such degree of measurement error should be taken into account as pertaining to the aforementioned diffraction angles. Consequently, it is to be understood that the crystal forms of the instant invention are not limited to the crystal forms that provide X-ray diffraction patterns completely identical to the X-ray diffraction patterns depicted in the accompanying Figures disclosed herein. *Any crystal forms that provide X-ray diffraction patterns substantially identical to those disclosed in the accompanying Figures fall within the scope of the present invention*. *The ability to ascertain substantial identities of X-ray diffraction patterns is within the purview of one of ordinary skill in the art*. (Ex. A, '725 patent, col. 41, l. 58 - col. 42, l. 13.) (Emphasis added).

13

36.   Thus, the '725 patent specifically states that the exact order of intensity of the peaks should not be taken into account in determining whether an XRPD pattern is substantially in accordance with that shown in FIG. 1. (Ex. A, '725 patent, col. 41, l. 58 - col. 42, l. 13.) Further, a person of ordinary skill in the art knows that the peak intensities from an XRPD pattern are variable because they are dependent on the characteristics of a given sample and experimental conditions; thus no two XRPD patterns will have the same peak intensities. (*See supra*, ¶¶ 18, 19.)

C.   "which is characterized by differential scanning calorimetry thermogram and a thermogravimetric analysis substantially in accordance with that shown in FIG. 2"

37.   This phrase appears in claim 2 of the '725 patents which recites:

"The compound of claim 1, which is characterized by a differential scanning calorimetry thermogram and a thermogravimetric analysis substantially in accordance with that shown in FIG. 2."

38.   One of ordinary skill in the art would understand the term "which is characterized by a differential scanning calorimetry thermogram and a thermogravimetric analysis substantially in accordance with that shown in FIG. 2." to mean that which is characterized by differential scanning calorimetry thermogram and thermogravimetric analysis patterns that are substantially identical to those shown in FIG. 2, having one peak at approximately 287° C and one broad peak between approximately 95° C and approximately 130° C. Further, the ability to ascertain substantial identities of the patterns is within the purview of one of ordinary skill in the art.

39.   This construction is supported by the specification:

The monohydrate of the compound of formula (IV) is represented by the DSC as shown in FIG. 2. The DSC is characterized by a broad peak between approximately 95° C and 130° C. This peak is broad and variable and corresponds to the loss of one water of hydration as seen in the TGA graph.   The DSC also has a

14

characteristic peak at approximately 287° C. which corresponds to
the melt of the dehydrated form of the compound of formula IV.
(Ex. A, '725 patent, col. 45, ll. 15-22.)

40.   When peak values are measured, the apex of the peak is what is reported as the

peak value. The broad peak between approximately 95° C and approximately 130° C represents

the loss of one water of hydration. The peak at approximately 287° C is associated with the

melting point of the dehydrated (*i.e.*, loss of water) form of the compound of formula (IV). A

person of ordinary skill in the art would understand to take into account variations due to

measurement errors dependent upon the measurement conditions employed when reading the

DSC and TGA patterns.

41.   Apotex's expert, Dr. Desiraju[2] claims that the "differential scanning calorimetry

experiment is not described in sufficient detail because variations such as the instrument or

sample configuration (*e.g.*, open or closed pans) or how many times the sample has been tested

(*e.g.*, first or second run) can alter the nature of the transitions observed, the positions at which

transitions are observed, and the sharpness of said transitions, rendering the claim term

indefinite." (*See* Desiraju Summary, at ¶ 3"). I disagree. The '725 patent discloses in detail the

experimental conditions that were used to conduct the DSC analysis, *e.g.*, the experiment was

performed in an open aluminum DSC pan, rate of heating was 10°C per minute in the

temperature range between 25° and 350 C. (*See* Ex. A, '725 patent, col. 43, ll. 1-22.) Further,

DSC is typically treated as a destructive technique, so a second run is often not possible since the

sample is destroyed in the "first" run.

42.   Desiraju also claims that "'peak' is not a term of art appropriate for use in

reference to differential scanning calorimetry data given that the sample transitions observed by

---

[2] Since I have seen only a summary of the proposed testimony from Dr. Gautam Desiraju, I am addressing only
certain arguments raised therein to the extent they are understandable. I reserve the right to address all of the
arguments raised by Dr. Desiraju in any declaration he will submit to the Court.

this technique have events, which correlate with changes in the sample." (*See* Desiraju

Summary, at ¶ 4.) This is incorrect. The term "peaks" is used throughout the art to refer to the

enthalpic change resulting from a thermal event. (*See, e.g.,* H.G. Brittain, *Methods for the*

Characterization of Polymorphs and Solvates in Polymorphism in Pharmaceutical Solids, ed.

Harry G. Brittain, 227, 252-53 (1999) ("The area under a DSC peak. . . . ") (attached herein as

Ex. J); Y. Kim and R.W. Rousseau, *Characterization and Solid-State Transformations of the*

Pseudopolymorphic Forms of Sodium Naproxen, CRYSTAL GROWTH & DESIGN, 4, 1211, 1213-14

(2004) ("peaks," "DSC peak") (attached herein as Ex. K); Z. Dominguez *et al.*, *Molecular*

Compasses and Gyroscopes with Polar Rotors: Synthesis and Characterization of Crystalline

Forms, J. AM. CHEM. SOC., 125, 8827, 8835 (2003) ("the DSC thermograms . . . showed a broad

endothermic peak") (attached herein as Ex. L); The United States Pharmacopeia, *Thermal*

Analysis, 2394, 2395 (27th Rev. 2004) ("DSC Melting Peak Shape") (attached herein as Ex. G).)

> **D.** **"which is characterized by an x-ray powder diffraction pattern (CuKα γ =1.5418 Å at a temperature of about 23° C.) comprising four or more 2θ values selected from the group consisting of: 18.0±0.2, 18.4±0.2, 19.2±0.2, 19.6±0.2, 21.2±0.2, 24.5±0.2, 25.9±0.2, and 28.0±0.2."**

43.   This phrase appears in claim 3. (*See supra* ¶ 29)

44.   One of ordinary skill in the art would understand the claim term "which is

characterized by an x-ray powder diffraction pattern (CuKα γ =1.5418 Å at a temperature of

about 23° C.) comprising four or more 2θ values selected from the group consisting of: 18.0±0.2,

18.4±0.2, 19.2±0.2, 19.6±0.2, 21.2±0.2, 24.5±0.2, 25.9±0.2, and 28.0±0.2." to mean that which

is characterized by an x-ray powder diffraction pattern taken with CuKα λ =1.5418 Å at a

temperature of about 23° C, having at least four 2θ values, selected from the group consisting of:

18.0±0.2, 18.4±0.2, 19.2±0.2, 19.6±0.2, 21.2±0.2, 24.5±0.2, 25.9±0.2, and 28.0±0.2. One having

ordinary skill in the art would understand that "CuKα γ" is "CuKα λ." This is supported by the

specification. (*See, e.g.*, Ex. A, '725 patent, col. 25, ll. 14-21.) Further, a certificate correction

was filed on May 11, 2010 correcting the typographical error. (Attached herein as Ex. M)

(BMS01364004-05).

> **E.** **"characterized by unit cell parameters approximately equal to the following: Cell dimensions: a(Å)=13.8632(7); b(Å)=9.3307(3); c(Å)=38.390(2); Volume=4965.9(4) Å^3**
> **Space group Pbca**
> **Molecules/unit cell 8**
> **Density (calculated) (g/cm^3) 1.354"**

45.   This phrase appears in claim 5 of the '725 patent which recites:

> "The compound of claim 3, characterized by unit cell parameters approximately equal to the following:
>
> Cell dimensions:
> a(Å)=13.8632(7);
> b(Å)=9.3307(3);
> c(Å)=38.390(2);
> Volume=4965.9(4) Å^3
> Space group Pbca
> Molecules/unit cell 8
> Density (calculated) (g/cm^3) 1.354."

46.   The above phrase is well-understood by those of ordinary skill in the art. The

concept of characterizing compounds by unit cell parameters is well understood by one of

ordinary skill. (*See supra* ¶¶ 13, 20.)

> **F.** **"The compound of claim 1" or "The compound of claim 3" or "A process for preparing the compound of claim 3" or "The compound of claim 9" or "The compound of claim 12"**

47.   The phrase "[t]he compound of claim 1," "[t]he compound of claim 3," or "[a]

process for preparing the compound of claim 3," "[t]he compound of claim 9," or "[t]he

compound of claim 12" appears in claim 2, 4, 5, 6, 8, 9, 10, 11, 13, 14, 15 and 16 of the '725

patent. As detailed in paragraphs 47-50 below, one of ordinary skill in the art would understand

that the "compound" in these phrases refers to the crystalline monohydrate of the compound of

formula (IV).

48.   The specification makes clear that the compound being "characterized" in claims

2, 5, 9, 10, and 11 refers to the crystalline monohydrate of the compound of formula (IV). (*See,*

e.g., Ex. A, '725 patent, col. 4, ll. 62-67; col. 25, ll. 5-40; col. 44, ll. 53-60; col. 45, ll. 15-28.)

For example, the '725 patent states:

> "[T]he monohydrate form of the compound of Formula (IV) is
> characterized by an x-ray powder diffraction pattern substantially
> in accordance with that shown in Fig. 1." (Ex. A, '725 patent, col.
> 25, ll. 6-9.)

> "[T]he monohydrate form of the compound of Formula (IV) is
> characterized by differential calorimetry thermogram and a
> thermogravimetric analysis substantially in accordance with that
> shown in Fig. 2." (Ex. A, '725 patent, col. 25, ll. 10-13.)

> "[T]he monohydrate form of the compound of Formula (IV) is
> characterized by unit cell parameters approximately equal to the
> following:" (Ex. A, '725 patent, col. 25, ll. 28-31.)

> "The monohydrate of the compound of formula (IV) is represented
> by the DSC shown in Fig. 2." (Ex. A, '725 patent, col. 45, ll. 15-
> 16.)

> "The TGA for the monohydrate of the compound of Formula (IV)
> is shown in Fig. 2 along with the DSC." (Ex. A, '725 patent, col.
> 45, ll. 23-25.)

49.   The specification also states that the compound in the pharmaceutical composition

of claims 4 and 13-14 is a crystalline monohydrate of the compound of formula (IV). For

example, the specification states that "the present invention describes a pharmaceutical

composition comprising a therapeutically effective amount of at least one of the crystalline forms

of the compound of Formula (IV) . . . ." (Ex. A, '725 patent, col. 26, ll. 31-35.) The crystalline

monohydrate of the compound of formula (IV) is one of the crystalline forms of the invention. (Ex. A, '725 patent, col. 24, ll. 57-66.)

50.   The specification discloses that the compound being prepared in the process of claim 6 is the crystalline monohydrate of the compound of formula (IV). For example, the specification states "[a]n example of the crystallization procedure to obtain the crystalline monohydrate form is shown here." (Ex. A, '725 patent, col. 43, ll. 39-40.)

51.   Finally the specification makes clear that the substantially pure compound of claims 8, 15, and 16 refers to the crystalline monohydrate of the compound of formula (IV). For example the specification states:

> "[T]he monohydrate form is in substantially pure form." (Ex. A, '725 patent, col. 25, ll. 1-2.)

> "[T]he monohydrate form is in substantially pure form, wherein substantially pure is greater than 90 percent pure." (Ex. A, '725 patent, col. 25, ll. 3-5.)

G.   "being further characterized by a differential scanning calorimetry having a broad peak between approximately 95° C and 130° C"

52.   This phrase appears in claim 9 of the '725 patent which recites:

> "The compound of claim 3 being further characterized by a differential scanning calorimetry having a broad peak between approximately 95° C and 13° C, which corresponds to the loss of one water of hydration on thermogravitmetric analysis."

53.   One of ordinary skill in the art would understand the term "being further characterized by a differential scanning calorimetry having a broad peak between approximately 95° C and 13° C" as meaning being further characterized by a differential scanning calorimetry having a broad peak between about 95° C and about 130° C. (Ex. A, '725 patent, col. 45, ll. 16-19). A person of ordinary skill in the art would understand that "13° C" was a typographical error and should be "130° C." This is supported by the specification. (Ex. A, '725 patent, col.

45, ll. 16-19.) In addition, a Certificate of Correction was filed on May 11, 2010 correcting this error. (*See* Ex. M.) This peak can be variable but corresponds to the loss of one water of hydration on thermogravimetric analysis. Respecting the broad peak between approximately 95° C and 130° C, the specification states that "[t]his peak is broad and variable and corresponds to the loss of one water of hydration as seen in the TGA graph." (Ex. A, '725 patent, col. 45, ll. 16-19.)

54.   Desiraju states that the term "broad peak" is "indefinite as the breadth of a peak is not specified to an extent that it must clearly be interpreted as an instrumental response to a characteristic of the sample allegedly being claimed." (*See* Desiraju Summary, at ¶ 5.) I disagree. The specification states that the broad peak "corresponds to the loss of one water of hydration as seen in the TGA graph." (Ex. A, '725 patent, col. 45, ll. 18-19.) Thus, the breadth of the peak is defined. Further, within a given DSC thermogram of a specific material, "broad" is a comparative descriptor for a peak associated with the loss of a solvent or water, just as "sharp" is a comparative descriptor for the peak associated with the melting point. (*See, e.g.,* B.S. Furniss *et al*., Vogel's Textbook of Practical Organic Chemistry 236 (5th ed. 1989) ("A pure crystalline organic compound has, in general, a definite and sharp melting point."). "Broad peak" is commonly used in the art to describe the change in enthalpy associated with the loss of solvent or water. (*See, e.g.,* Ex. K, Kim *et al.*, at 1215 ("broader DSC and TGA traces"); Ex. L, Dominguez *et al.*, at 8835 ("broad endothermic peak").) Similarly, Desiraju's objection to the term "approximately" is unfounded. Interpretation of experimental data has to take into account variations due to measurement errors dependent upon the measurement conditions employed, and one of ordinary skill in the art would be able to do so. The use of "approximately" allows such variations.

H.   **"which corresponds to the loss of one water of hydration on thermogravitmetric analysis"**

55.   This phrase appears in claims 9 and 12 of the '725 patent. (*See supra* 30, 51)

56.   One of ordinary skill in the art would understand that the term "corresponds to the loss of one water of hydration on thermogravitmetric analysis" to mean that the broad peak between approximately 95° C and 130° C corresponds to the weight loss attributable to one water of hydration on thermogravimetric analysis. In the '725 patent, the sample undergoing analysis is a monohydrate and the broad peak is associated with the loss of one molecule of water. The literature has numerous examples of broad peaks corresponding to loss of water or other solvents. (*See, e.g.,* Ex. K, Kim *et al.*, at 1213 ("The dihydrate has one peak for melting and two peaks corresponding to removal of two different types of water from the unit cell. . . . The monohydrate of sodium naproxen exhibits two peaks, one for melting and the other associated with the endotherm for dehydration [loss of water]); Ex. L, Dominguez *et al.*, at 8835 ("the DSC thermograms . . . showed a broad endothermic peak between 60 and 140° C. That such a transition corresponds to the loss benzene [a solvent]. . . was confirmed by thermogravimetric analysis (TGA).")).

57.   Desiraju argues that the term "which corresponds to the loss of one water of hydration on thermogravimetric analysis" "does not make sense because a compound may not lose mass equivalent to one water and remain the same compound." (*See* Desiraju Summary, at ¶ 7.) This interpretation is flawed. As discussed above, the "compound of claim 3" recited in claim 9 refers to the crystalline monohydrate of the compound of formula (IV). Claim 9 and the specification state that this compound is "*characterized*" by a differential scanning calorimetry having a broad peak between approximately 95° C and 130° C which corresponds to the loss of one water of hydration on thermogravimetric analysis. (*See, e.g.*, Ex. A, '725 patent, col. 45, ll.

15-20, Fig. 2.) Thus, any one skilled in the art would understand the compound being

characterized is the monohydrate of the compound of formula (IV) and not the compound that

remains after the loss of one water of hydration. The literature has numerous examples of

characterizing solvated or hydrated compounds in such a manner. (*See, e.g.,* Ex. K, Kim *et al.*, at

1213; Ex. L, Dominguez *et al.*, at 8835.)

I.   **"which is further characterized by a weight loss of 3.48% by thermogravimetric analysis between 50° C and 175° C"**

58.   This phrase appears in claim 10 of the '725 patent which recites:

"The compound of claim 9, which is further characterized by a weight loss of 3.48% by thermogravimetric analysis between 50° C and 175° C."

59.   One of ordinary skill in the art would understand that the term "further

characterized by a weight loss of 3.48% by thermogravimetric analysis between 50° C and 175°

C" to mean being further characterized by a weight loss of 3.48% by thermogravimetric analysis

between 50° C and 175° C, taking into account variations due to measurement errors dependent

upon the measurement conditions employed.

J.   **"wherein the differential scanning calorimetry further has a peak at approximately 287° C"**

60.   This phrase appears in claim 11 of the '725 patent which recites:

"The compound of claim 9, wherein the differential scanning calorimetry further has a peak at approximately 287°C."

61.   One of ordinary skill in the art would understand that the term "wherein the

differential scanning calorimetry further has a peak at approximately 287°C" means being

characterized by differential scanning calorimetry with a peak located at about 287°C, which

corresponds to the melt of the dehydrated form of the compound of formula (IV). (Ex. A, '725

patent, col. 45, ll. 21-23.)

22

62.   Desiraju objects to claim 11, arguing that "the sample is no longer in the same form 'at approximately 287° C' as the form having a broad 'peak' at a temperature less than 180.50° C." (*See* Desiraju Summary, at ¶ 8.) This argument is a red herring. As with claim 9, claim 11 refers to characterizing the crystalline monohydrate of the compound of formula (IV) by differential scanning calorimetry, which shows a peak at approximately 287°C. As stated in the specification, this peak corresponds to the melt of the dehydrated form of the compound of formula (IV). (Ex. A, '725 patent, col. 45, ll. 21-23.) The literature has numerous examples of characterizing solvated or hydrated compounds by measuring the melting point of the desolvated or dehydrated form of the compounds. (*See, e.g.,* Ex. K, Kim *et al.,* at 1213 ("The dihydrate has one peak for melting and two peaks corresponding to removal of two different types of water from the unit cell."); Ex. L, Dominguez *et al.,* at 8835 ("Endothermic peaks corresponding to crystal melting were observed. . . .").

63.   I reserve the right to supplement my opinion as necessary to respond to the arguments raised by Apotex or its retained experts.

I declare under penalty of perjury that the foregoing is true and correct to the best of my knowledge and belief.

Date: May 3, 2012

Jerry L. Atwood

EXHIBIT A

US007491725B2

(12) **United States Patent**
Lajeunesse et al.

(10) **Patent No.:**   **US 7,491,725 B2**
(45) **Date of Patent:**   **Feb. 17, 2009**

(54) **PROCESS FOR PREPARING 2-AMINOTHIAZOLE-5-AROMATIC CARBOXAMIDES AS KINASE INHIBITORS**

(75) Inventors: **Jean Lajeunesse**, Candiac (CA); **John D. DiMarco**, East Brunswick, NJ (US); **Michael Galella**, Kendall Park, NJ (US); **Ramakrishnan Chidambaram**, Pennington, NJ (US)

(73) Assignee: **Bristol-Myers Squibb Company**, Princeton, NJ (US)

(*) Notice: Subject to any disclaimer, the term of this patent is extended or adjusted under 35 U.S.C. 154(b) by 251 days.

(21) Appl. No.: **11/192,867**

(22) Filed: **Jul. 29, 2005**

(65) **Prior Publication Data**

US 2006/0004067 A1   Jan. 5, 2006

Related U.S. Application Data

(63) Continuation-in-part of application No. 11/051,208, filed on Feb. 4, 2005, now abandoned.

(60) Provisional application No. 60/542,490, filed on Feb. 6, 2004, provisional application No. 60/624,937, filed on Nov. 4, 2004, provisional application No. 60/649, 722, filed on Feb. 3, 2005.

(51) **Int. Cl.**
A61K 31/506   (2006.01)
C07D 403/04   (2006.01)

(52) **U.S. Cl.** **514/252.19**; 544/295

(58) **Field of Classification Search** 544/295; 514/252.19
See application file for complete search history.

(56) **References Cited**

U.S. PATENT DOCUMENTS

3,547,917 A	12/1970	Kulka et al.	
5,114,940 A *	5/1992	Blade et al.	.... 514/248
6,596,746 B1	7/2003	Das et al.	
2004/0024208 A1	2/2004	Das et al.	
2004/0054186 A1	3/2004	Das et al.	
2004/0073026 A1	4/2004	Das et al.	
2004/0077875 A1	4/2004	Das et al.	
2004/0220233 A1	11/2004	Hynes et al.	
2005/0009891 A1	1/2005	Lee	
2005/0215795 A1	9/2005	Chen et al.	

FOREIGN PATENT DOCUMENTS

EP	639574	2/1995
WO	WO 0062778	10/2000
WO	WO 2004071440	8/2004
WO	WO 2004085388	10/2004
WO	WO 2005013983	2/2005

WO   WO2005/072826   8/2005

OTHER PUBLICATIONS

Byrn et al. (Sold-State Chemistry of Drugs, 2nd Edition, 1999, SSCI, Inc. Publishers).*

U.S. Appl. No. 11/049,815, filed Feb. 3, 2005, Chen et al.

Autenrieth, W., "Regarding our knowledge of the five isomeric acids $C_4H_6O_2$", Chem. Ber., vol. 38, pp. 2534-2551, *English Translation*.

Eremeev et al., "Absolute Configuration of Diastereomeric Derivatives of N-Substituted Aziridine-2-Carboxylic Acids", Chem. Heterocycl. Compd. Engl. Transl., vol. 20, pp. 1102-1107, 1984 (translated from Khimiya Geterotsiklicheskikh Soedinenii, No. 10, pp. 1342-1348, 1984).

Hartmann et al., "On the coupling of aryldiazonium salts with *N,N*-disubstituted 2-aminothiophenes and some of their carbocyclic and heterocyclic analogues", J. Chem. Soc.; Perkin Trans. vol. 1, pp 4316-4320, 2000.

Kantlehner et al., "Ein neues Herstellungsverfahren für 2,2,2-Trialkoxyacetonitrile und 2-Dialkylamino-2-alkoxycarbonsäurenitrile", Synthesis, pp. 358-360, 1984.

Kantlehner et al., "Orthoamides. IL Reaction of Orthoamide Derivatives with Sulfur and Selenium, Syntheses of 1,3-Thiazole- and 1,3-Selenazole Derivatives", J. prakt. Chem., vol. 338, pp. 403-413, 1996.

Knoll et al., "Formylation Products of Thioamides; VII[1] . Synthesis of New *N*-(3-AMinothioacryloyl)-formamidines and *N,N'*-Bis[aminomethylidene]thioureas by Bis-iminoformylation of Thioacetamides and Thiourea with Formamide Acetals", Synthesis Communications, pp. 51-53, 1984.

Landreau et al., "[4+2] Cycloaddition Reactions Between 2,4-Diamino-1-Thia-3-Azabutadienes and Ketene. Synthesis of New 1,3-Thiazin-6-ones, 1,3-Thiazine-6-Thiones and 2-Thioxopyrimidin-4-ones", Heterocycles, vol. 53, No. 12, pp. 2667-2677, 2000.
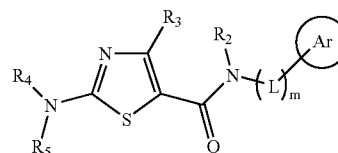
(Continued)

(57) **ABSTRACT**

The invention relates to processes for preparing compounds having the formula,

and crystalline forms thereof, wherein Ar is aryl or heteroaryl, L is an optional alkylene linker, and R_2, R_3, R_4, and R_5, are as defined in the specification herein, which compounds are useful as kinase inhibitors, in particular, inhibitors of protein tyrosine kinase and p38 kinase.

16 Claims, 7 Drawing Sheets

US 7,491,725 B2

Page 2

OTHER PUBLICATIONS

Landreau et al., "Cationic 1,3-Diazadienes in Annulation Reactions. Synthesis of Pyrimidine, Thiadiazinedioxide and Triazine Derivatives", J. Heterocyclic Chem., vol. 38, pp. 93-98, 2001.

Lin et al., "The Synthesis of Substituted 2-Aminothiazoles", J. Heterocyclic Chem., vol. 16, pp. 1377-1383, 1979.

Marsham et al., "Quinazoline Antifolate Thymidylate Synthase Inhibitors: Heterocyclic Benzoyl Ring Modifications", J. Med. Chem., vol. 34, pp. 1594-1605, 1991.

Noack et al., "Synthesis and characterization of N,N-disubstituted 2-amino-5-acylthiophenes and 2-amino-5-acylthiazoles", Tetrahedron, vol. 58, pp. 2137-2146, 2002.

Noack et al., "Synthesis and Spectral Characterisation of a New Class of Heterocyclic Analogues of Crystal Violet Dyes", Angew. Chem. Int. Ed., vol. 113, No. 16, pp. 3008-3011, 2001.

Roberts et al., "Folic Acid Analogs. Modifications in the Benzene-Ring Region. 2. Thiazole Analogs", J. Medicinal Chemistry, vol. 15, No. 12, pp. 1310-1312, 1972.

Zhao et al., "A new facile synthesis of 2-aminothiazole-5-carboxylates", Tetrahedron Letters, vol. 42, pp. 2101-2102, 2001.

Shah et al., "Overriding Imatinib Resistance with a Novel ABL Kinase Inhibitor", Science, vol. 35, pp. 339-401, 2004.

U.S. Appl. No. 11/271,626, Office Action Jan. 31, 2008.

* cited by examiner

Figure 1

Figure 2

U.S. Patent   Feb. 17, 2009   Sheet 3 of 7   US 7,491,725 B2

Figure 3

U.S. Patent   Feb. 17, 2009   Sheet 4 of 7   US 7,491,725 B2
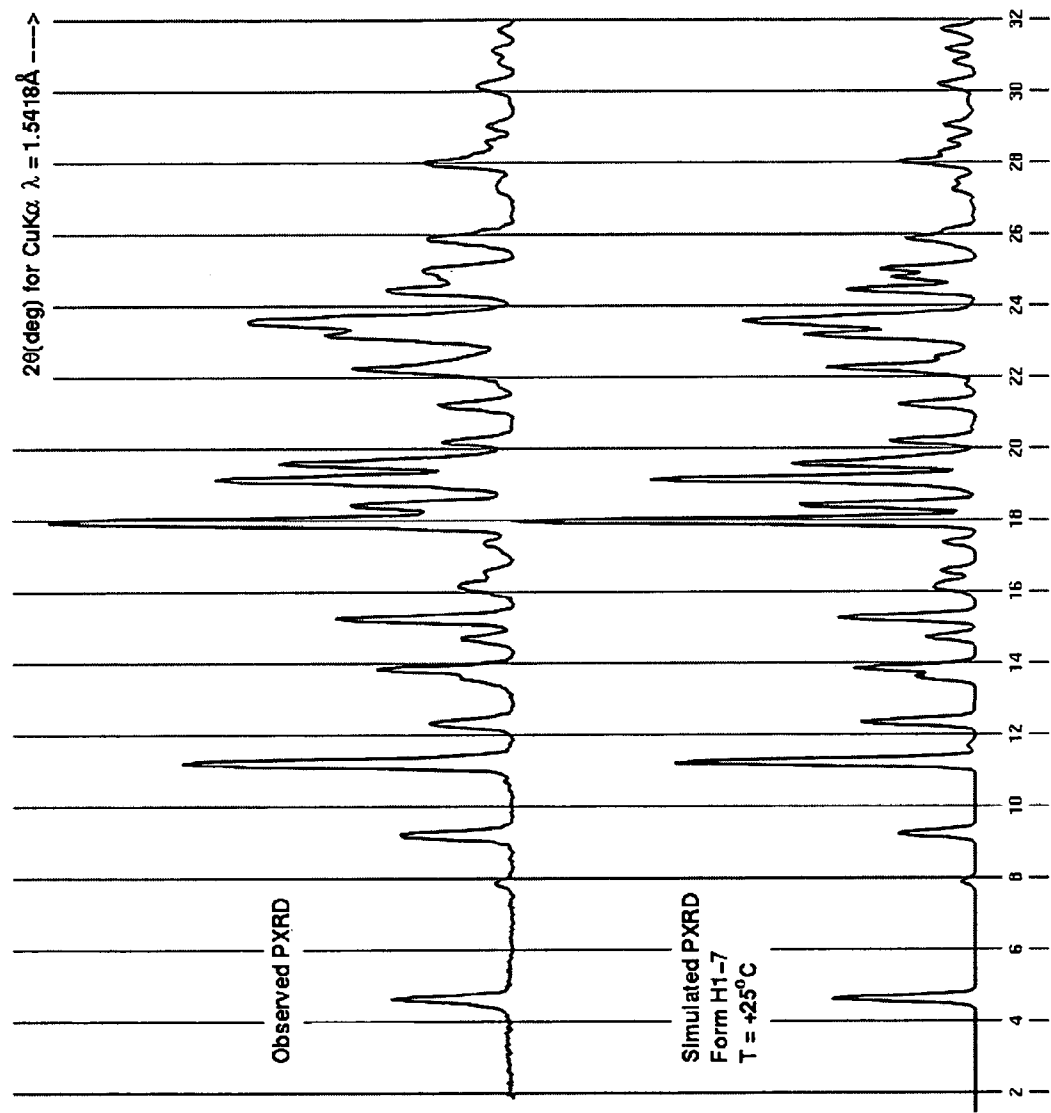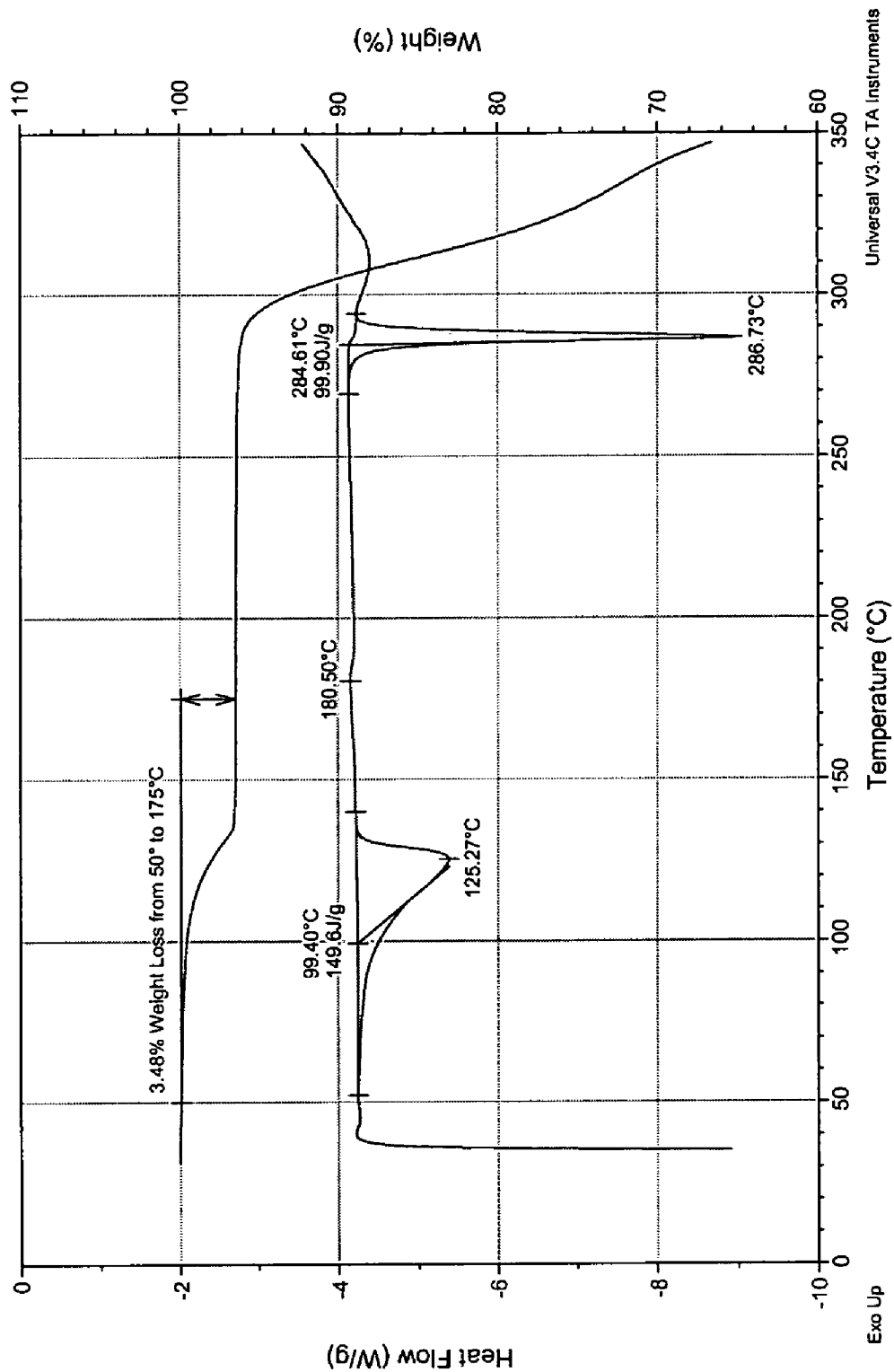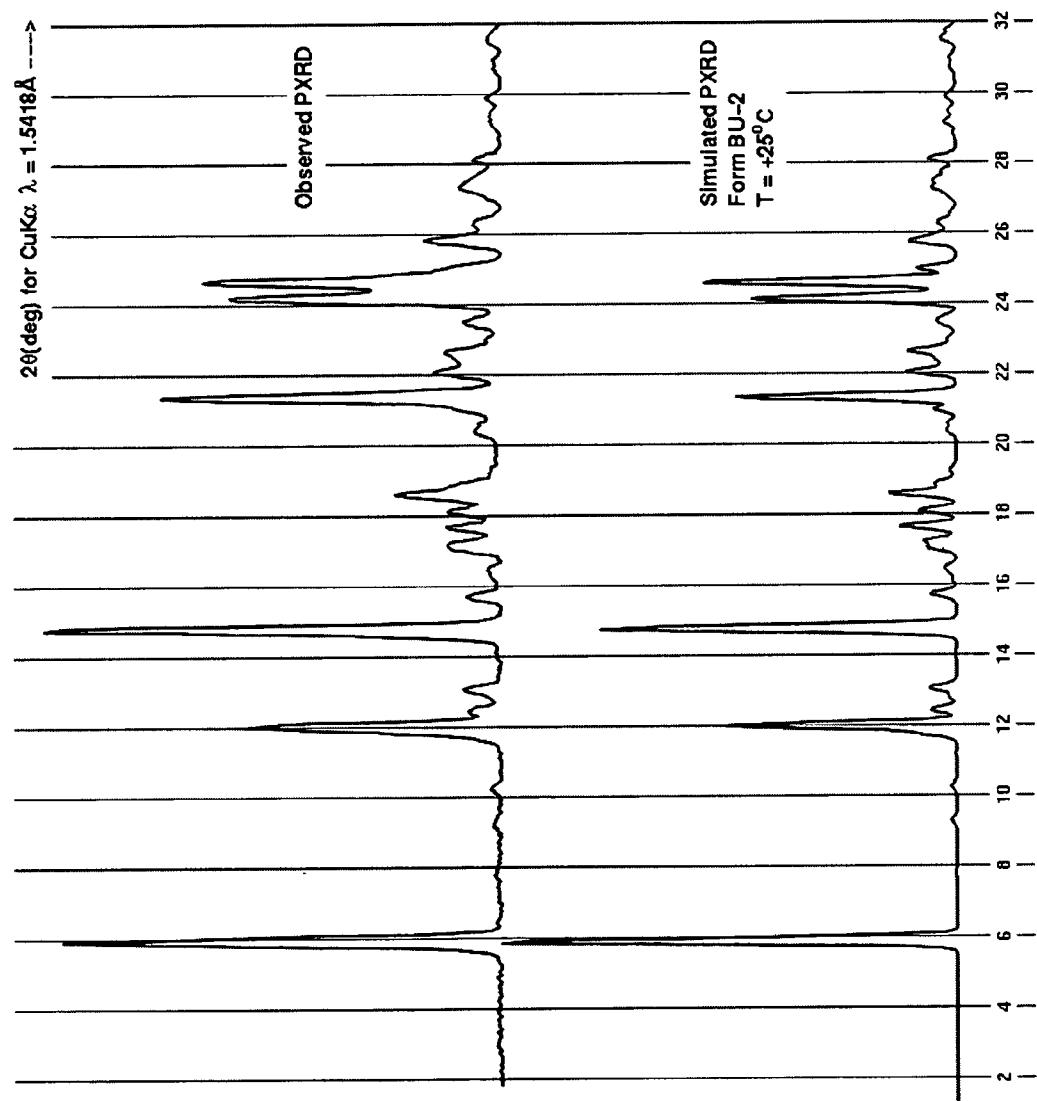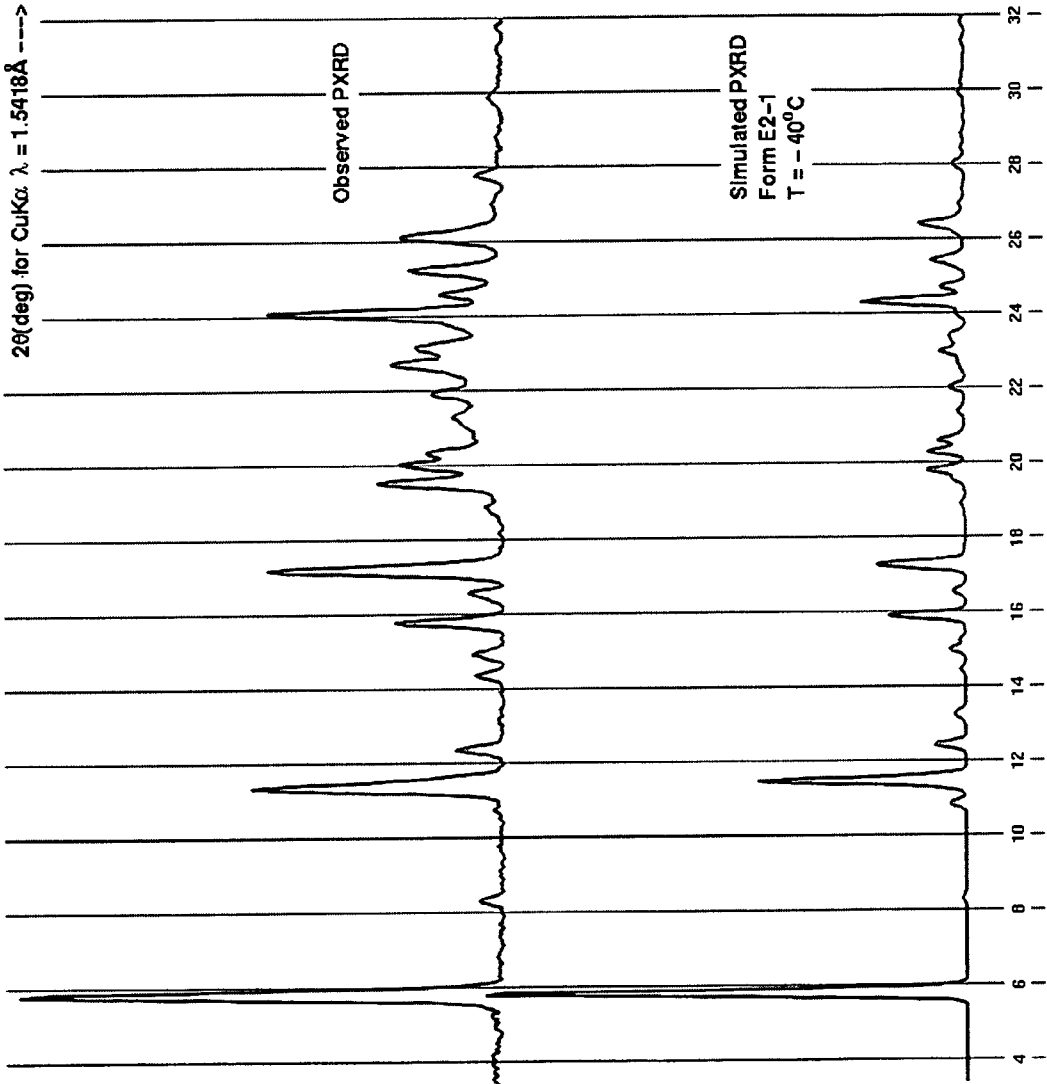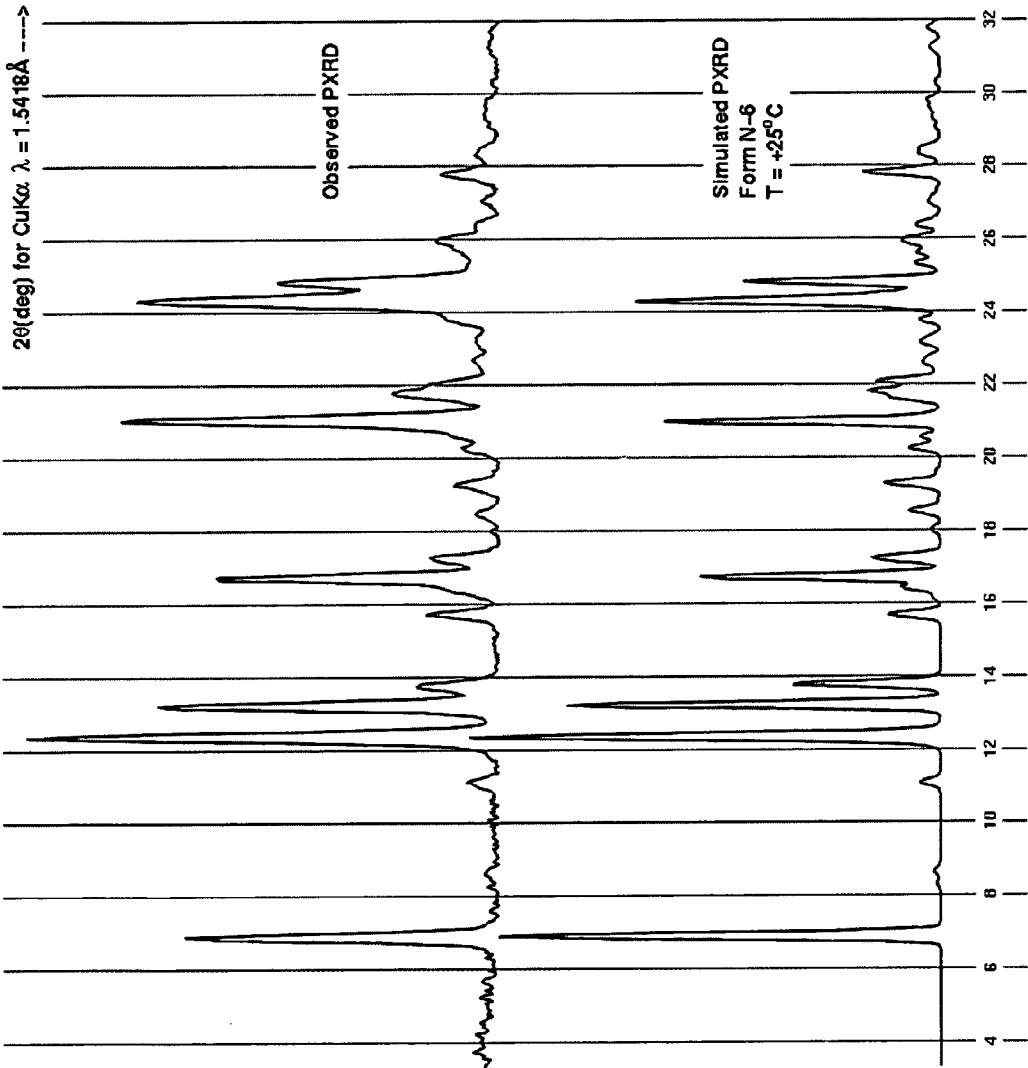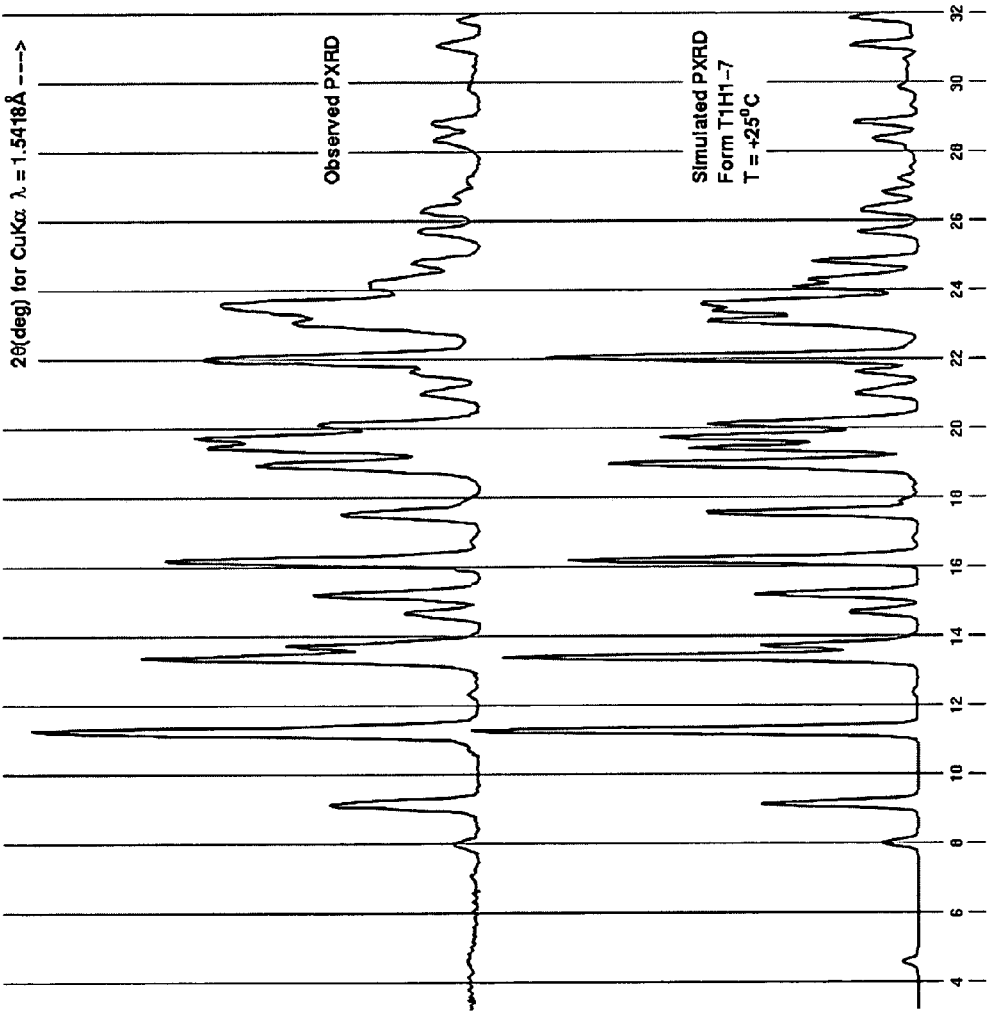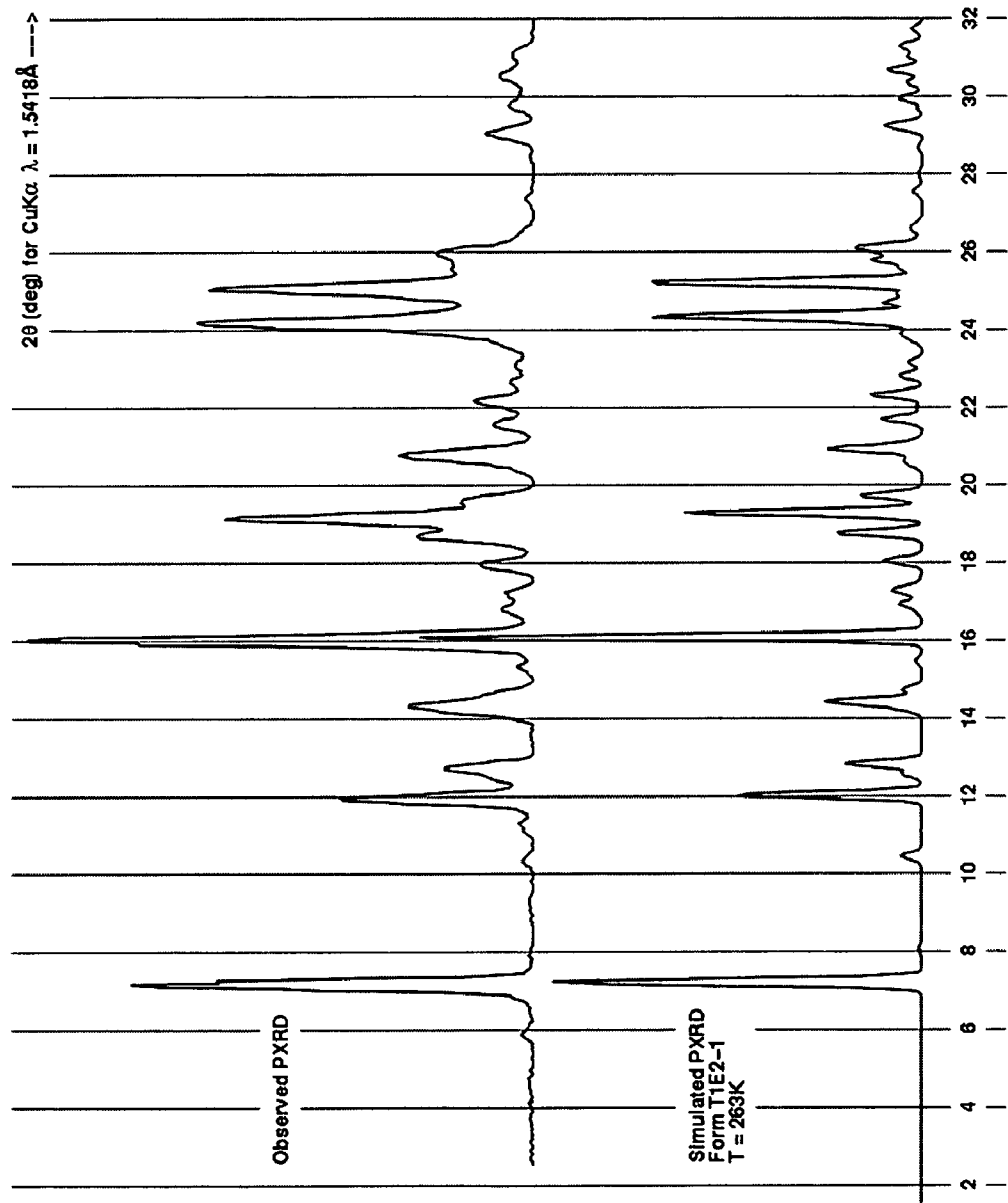

Figure 4

Figure 5

Figure 6

Figure 7

US 7,491,725 B2

1

PROCESS FOR PREPARING 2-AMINOTHIAZOLE-5-AROMATIC CARBOXAMIDES AS KINASE INHIBITORS

CROSS-REFERENCE TO RELATED APPLICATIONS

This application is a continuation-in-part of U.S. Non-Provisional Application Ser. No. 11/051,208, filed Feb. 4, 2005 now abandoned, which claims the benefit of U.S. Provisional Application No. 60/542,490, filed Feb. 6, 2004, U.S. Provisional Application No. 60/624,937, filed Nov. 4, 2004 and U.S. Provisional Application No. 60/649,722, filed Feb. 3, 2005, which are all hereby incorporated by reference in their entirety.

FIELD OF THE INVENTION

The present invention relates to processes for preparing 2-aminothiazole-5aromatic carboxamides which are useful as kinase inhibitors, such as inhibitors of protein tyrosine kinase and p38 kinase, intermediates and crystalline forms thereof.

BACKGROUND OF THE INVENTION

Aminothiazole-aromatic amides of formula I
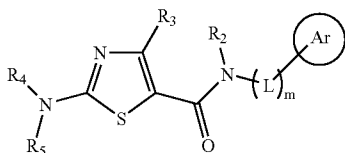
wherein Ar is aryl or heteroaryl, L is an optional alkylene linker, and R_2, R_3, R_4, and R_5, are as defined in the specification herein, are useful as kinase inhibitors, in particular, inhibitors of protein tyrosine kinase and p38 kinase. They are expected to be useful in the treatment of protein tyrosine kinase-associated disorders such as immunologic and oncological disorders [see, U.S. Pat. No. 6,596,746 (the '746 patent), assigned to the present assignee and incorporated herein by reference], and p38 kinase-associated conditions such as inflammatory and immune conditions, as described in U.S. patent application Ser. No. 10/773,790, filed Feb. 6, 2004, claiming priority to U.S. Provisional application Ser. No. 60/445,410, filed Feb. 6, 2003 (hereinafter the '410 application), both of which are also assigned to the present assignee and incorporated herein by reference.

The compound of formula (IV), 'N-(2-Chloro-6-methylphenyl)-2-[[6-[4-(2-hydroxyethyl)-1-piperazinyl]-2-methyl-4-pyrimidinyl]amino]-5-thiazolecarboxamide, is an inhibitor of SRC/ABL and is useful in the treatment of oncological diseases.

(IV)
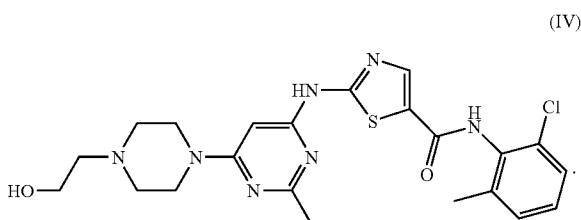
2

Other approaches to preparing 2-aminothiazole-5-carboxamides are described in the '746 patent and in the '410 application. The '746 patent describes a process involving treatment of chlorothiazole with n-BuLi followed by reaction with phenyl isocyanates to give chlorothiazole-benzamides, which are further elaborated to aminothiazole-benzamide final products after protection, chloro-to-amino substitution, and deprotection, e.g.,
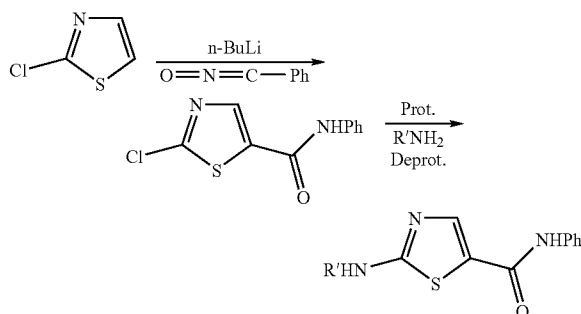

The '410 application describes a multi-step process involving first, converting N-unsubstituted aminothiazole carboxylic acid methyl or ethyl esters to bromothiazole carboxylic acid esters via diazotization with tert-butyl nitrite and subsequent $CuBr_2$ treatment, e.g.,
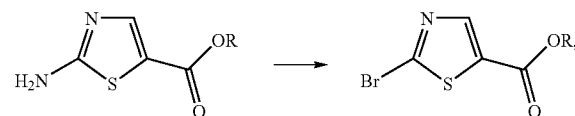
then, hydrolyzing the resulting bromothiazole esters to the corresponding carboxylic acids and converting the acids to the corresponding acyl chlorides, e.g.,
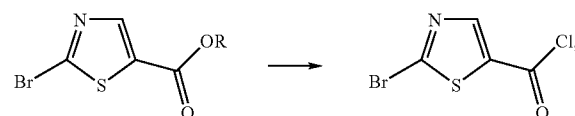
then finally, coupling the acyl chlorides with anilines to afford bromothiazole-benzamide intermediates which were further elaborated to aminothiazole-benzamide final products, e.g.,
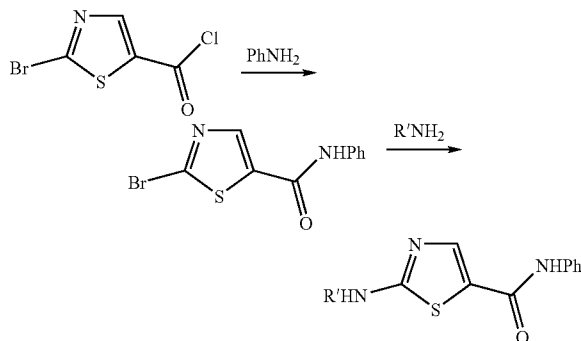
US 7,491,725 B2

3

Other approaches for making 2-aminothiazole-5-carboxamides include coupling of 2-aminothiazole-5-carboxylic acids with amines using various coupling conditions such as DCC [Roberts et al, *J. Med. Chem*. (1972), 15, at p. 1310], and DPPA [Marsham et al., *J. Med. Chem*. (1991), 34, at p. 1594)].

The above methods present drawbacks with respect to the production of side products, the use of expensive coupling reagents, less than desirable yields, and the need for multiple reaction steps to achieve the 2-aminothiazole-5-carboxamide compounds.

Reaction of N,N-dimethyl-N'-(aminothiocarbonyl)-formamidines with α-haloketones and esters to give 5-carbonyl-2-aminothiazoles has been reported. See Lin, Y. et al, *J. Heterocycl. Chem*. (1979), 16, at 1377; Hartmann, H. et al, *J. Chem. Soc. Perkin Trans*. (2000), 1, at 4316; Noack, A. et al; *Tetrahedron* (2002), 58, at 2137; Noack, A.; et al. *Angew. Chem*. (2001), 113, at 3097; and Kantlehner, W. et al., *J. Prakt. Chem./Chem.-Ztg*. (1996), 338, at 403. Reaction of β-ethoxy acrylates and thioureas to prepare 2-aminothiazole-5-carboxylates also has been reported. See Zhao, R., et al., *Tetrahedron Lett*. (2001), 42, at 2101. However, electrophilic bromination of acrylanilide and crotonanilide has been known to undergo both aromatic bromination and addition to the α,β-unsaturated carbon-carbon double bonds. See Autenrieth, *Chem. Ber*. (1905), 38, at 2550; Eremeev et al., *Chem. Heterocycl. Compd. Engl. Transl*. (1984), 20, at 1102.
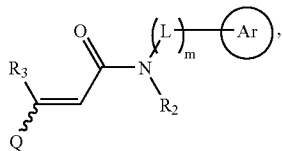
New and efficient processes for preparing 2-aminothiazole-5-carboxamides are desired.

SUMMARY OF THE INVENTION

This invention is related to processes for the preparation of 2-aminothiazole-5-aromatic amides having the formula (I)


(I)
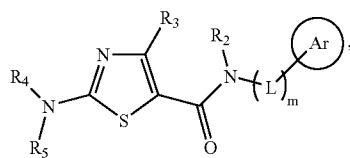
wherein L, Ar, R$_2$, R$_3$, R$_4$, R$_5$, and m are as defined below, comprising reacting a compound having the formula (II),

(II)

wherein Q is the group —O—P*, wherein P* is selected so that, when considered together with the oxygen atom to which P* is attached, Q is a leaving group, and Ar, L, R$_2$, R$_3$, and m are as defined below,
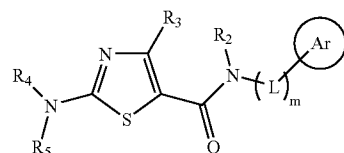
with a halogenating reagent in the presence of water followed by a thiourea compound having the formula (III),
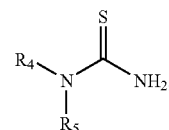
(III)

wherein, R$_4$ and R$_5$ are as defined below,
to provide the compound of formula (I),

(I)

wherein,
Ar is the same in formulae (I) and (II) and is aryl or heteroaryl;
L is the same in formulae (I) and (II) and is optionally-substituted alkylene;
R$_2$ is the same in formulae (I) and (II), and is selected from hydrogen, alkyl, substituted alkyl, alkenyl, substituted alkenyl, alkynyl, substituted alkynyl, aryl, heteroaryl, cycloalkyl, and heterocyclo;
R$_3$ is the same in formulae (I) and (II), and is selected from hydrogen, halogen, cyano, haloalkyl, alkyl, substituted alkyl, alkenyl, substituted alkenyl, aryl, heteroaryl, cycloalkyl, and heterocyclo;
R$_4$ is (i) the same in each of formulae (I) and (III), and (ii) is independently selected from hydrogen, alkyl, substituted alkyl, alkenyl, substituted alkenyl, alkynyl, substituted alkynyl, aryl, heteroaryl, cycloalkyl, and heterocyclo, or alternatively, R$_4$ is taken together with R$_5$, to form heteroaryl or heterocyclo;
R$_5$ is (i) the same in each of formulae (I) and (III), and (ii) is independently selected from hydrogen, alkyl, substituted alkyl, alkenyl, substituted alkenyl, alkynyl, substituted alkynyl, aryl, heteroaryl, cycloalkyl, and heterocyclo, or alternatively, R$_5$ is taken together with R$_4$, to form heteroaryl or heterocyclo; and
m is 0 or 1.

Applicants have surprisingly discovered said process for converting β-(P*)oxy acryl aromatic amides and thioureas to 2-aminothiazole derivatives, wherein the aromatic amides are not subject to further halogenation producing other side products. Aminothiazole-aromatic amides, particularly, 2-aminothiazole-5-benzamides, can thus be efficiently prepared with this process in high yield.

In another aspect, the present invention is directed to crystalline forms of the compound of formula (IV).

BRIEF DESCRIPTION OF THE DRAWINGS

The invention is illustrated by reference to the accompanying drawings described below.

FIG. **1** shows a simulated (bottom) (calculated from atomic coordinates generated at room temperature) and experimental (top) pXRD patterns for crystalline monohydrate of the compound of formula (IV).

FIG. **2** shows a DSC and TGA of the of the monohydrate crystalline form of the compound of Formula (IV).

US 7,491,725 B2

5

FIG. **3** shows a simulated (bottom) (from atomic parameters refined at room temperature) and experimental (top) pXRD patterns for crystalline butanol solvate of the compound of formula (IV).

FIG. **4** shows a simulated (bottom) (from atomic parameters refined at –40° C.) and experimental (top) pXRD patterns for crystalline ethanol solvate of the compound of formula (IV).

FIG. **5** shows a simulated (bottom) (from atomic parameters refined at room temperature) and experimental (top) pXRD patterns for crystalline neat form (N-6) of the compound of formula (IV).

FIG. **6** shows a simulated (bottom) (from atomic parameters refined at room temperature) and experimental (top) pXRD patterns for crystalline neat form (T1H1-7) of the compound of formula (IV).

FIG. **7** shows a simulated (bottom) (from atomic parameters refined at room temperature) and experimental (top) pXRD patterns for ethanolate form (T1E2-1) of the compound of formula (IV).

DETAILED DESCRIPTION OF THE INVENTION

Abbreviations

For ease of reference, the following abbreviations may be used herein:

Ph=phenyl
Bz=benzyl
t-Bu=tertiary butyl
Me=methyl
Et=ethyl
Pr=propyl
Iso-P=isopropyl
MeOH=methanol
EtOH=ethanol
EtOAc=ethyl acetate
Boc=tert-butyloxycarbonyl
CBZ=carbobenzyloxy or carbenzoxy or benzyloxycarbonyl
DMF=dimethyl formamide
DMF-DMA=N,N-dimethylformamide dimethyl acetal
DMSO=dimethyl sulfoxide
DPPA=diphenylphosphoryl azide
DPPF=1,1'-bis(diphenylphosphino)ferrocene
HATU=O-benzotriazol-1-yl0   N,N,N',N'-tetramethyluronium hexafluorphosphate
LDA=lithium di-isopropyl amide
TEA=triethylamine
TFA=trifluoroacetic acid
THF=tetrahydrofuran
KOH=potassium hydroxide
K_2CO_3=potassium carbonate
$POCl_3$=phosphorous oxychloride
EDC or EDCI=3-ethyl-3'-(dimethylamino)propyl-carbodiimide
DIPEA=diisopropylethylamine
HOBt=1-hydroxybenzotriazole hydrate
NBS=N-bromosuccinamide
NMP=N-methyl-2-pyrrolidinone
NaH=sodium hydride
NaOH=sodium hydroxide
$Na_2S_2O_3$=sodium thiosulfate
Pd=palladium
Pd—C or Pd/C=palladium on carbon
min=minute(s)
L=liter
mL=milliliter

6

μL=microliter
g=gram(s)
mg=milligram(s)
mol=moles
mmol=millimole(s)
meq=milliequivalent
RT or rt=room temperature
RBF=round bottom flask
ret. t.=HPLC retention time (minutes)
sat or sat'd=saturated
aq.=aqueous
TLC=thin layer chromatography
HPLC=high performance liquid chromatography
LC/MS=high performance liquid chromatography/mass spectrometry
MS=mass spectrometry
NMR=nuclear magnetic resonance
mp=melting point
DSC=differential scanning calorimetry
TGA=thermogravimetric analysis
XRPD=x-ray powder diffraction pattern
pXRD=x-ray powder diffraction pattern

Definitions

The following are definitions of terms used in this specification and appended claims. The initial definition provided for a group or term herein applies to that group or term throughout the specification and claims, individually or as part of another group, unless otherwise indicated.

The term "alkyl" as used herein by itself or as part of another group refers to straight and branched chain saturated hydrocarbons, containing 1 to 20 carbons, 1 to 10 carbons, or 1 to 8 carbons, such as methyl, ethyl, propyl, isopropyl, butyl, t-butyl, isobutyl, pentyl, hexyl, isohexyl, heptyl, 4,4-dimethylpentyl, octyl, 2,2,4-trimethyl-pentyl, nonyl, decyl, undecyl, dodecyl, the various branched chain isomers thereof, and the like. Lower alkyl groups, that is, alkyl groups of 1 to 4 carbon atoms.

The term "substituted alkyl" refers to an alkyl group substituted with one or more substituents (for example 1 to 4 substituents, or 1 to 2 substituents) at any available point of attachment. Exemplary substituents may be selected from one or more (or 1 to 3) of the following groups:

(i) halogen (e.g., a single halo substituent or multiple halo substitutents forming, in the latter case, groups such as a perfluoroalkyl group or an alkyl group bearing Cl_3 or CF_3), haloalkoxy, cyano, nitro, oxo (=O), —OR_a, —SR_a, —S(=O)R_e, —S(=O)$_2R_e$, —S(=O)$_3$H, —P(=O)$_2$—R_e, —S(=O)$_2OR_e$, —P(=O)$_2OR_e$, —U_1—NR_bR_c, —U_1—N(R_d)—U_2—NR_bR_c, —U_1—NR_d—U_2—R_b, —NR_bP(=O)$_2R_e$, —P(=O)$_2NR_bR_c$, —C(=O)OR_e, —C(=O)R_a, —OC(=O)R_a, —NR_dP(=O)$_2NR_bR_c$, —R_bP(=O)$_2R_e$, —U_1-aryl, —U_1-heteroaryl, —U_1-cycloalkyl, —U_1-heterocyclo, —U_1-arylene-R_e, —U_1-heteroarylene-R_e, —U_1-cycloalkylene-R_e, and/or —U_1-heterocyclene-R_e, wherein, in group (i),

(ii) —U_1— and —U_2— are each independently a single bond, —U_3—S(O)$_t$—U_4—, —U_3—C(O)—U_4—, —U_3—C(S)—U_4—, —U_3—O—U_4—, —U_3—S—U_4—, —U_3—O—C(O)—U_4—, —U_3—C(O)—O—U_4—, or —U_3—C(=NR_g)—U_4—;

US 7,491,725 B2

7

wherein,

(iii) U^3 and U^4 are each independently a single bond, alkylene, alkenylene, or alkynylene;

wherein, in group (i),

(iv) R_a, R_b, R_c, R_d, and R_e are each independently hydrogen, alkyl, alkenyl, alkynyl, cycloalkyl, aryl, heterocyclo, or heteroaryl, each of which is unsubstituted or substituted with one to four groups R_f, except R_e is not hydrogen; or R_b and R_c may be taken together to form a 3- to 8-membered saturated or unsaturated ring together with the atoms to which they are attached, which ring is unsubstituted or substituted with one to four groups listed below for R_f; or R_b and R_c together with the nitrogen atom to which they are attached may combine to form a group $—N=C\,R_gR_h$ where R_g and R_h are each independently hydrogen, alkyl, or alkyl substituted with a group R_f; and;

wherein,

(v) R_f is at each occurrence independently selected from alkyl, halogen, cyano, hydroxy, —O(alkyl), SH, —S(alkyl), amino, alkylamino, haloalkyl, haloalkoxy, or a lower alkyl substituted with one to two of halogen, cyano, hydroxy, —O(alkyl), SH, —S(alkyl), amino, alkylamino, haloalkyl, and/or haloalkoxy, and
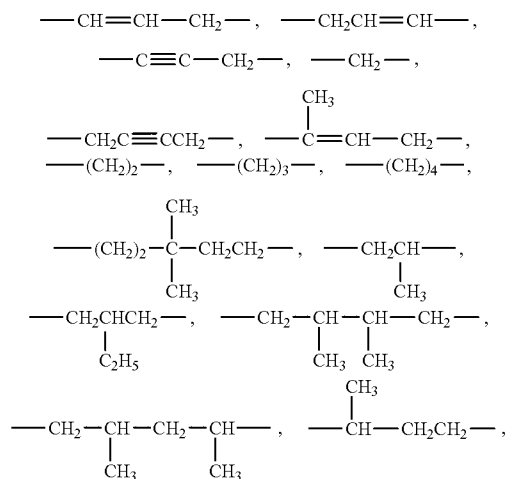
wherein,

(vi) t is 0, 1 or 2.

The term "alkenyl" as used herein by itself or as part of another group refers to straight or branched chain radicals of 2 to 20 carbons, alternatively 2 to 12 carbons, and/or 1 to 8 carbons in the normal chain, which include one to six double bonds in the normal chain, such as vinyl, 2-propenyl, 3-butenyl, 2-butenyl, 4-pentenyl, 3-pentenyl, 2-hexenyl, 3-hexenyl, 2-heptenyl, 3-heptenyl, 4-heptenyl, 3-octenyl, 3-nonenyl, 4-decenyl, 3-undecenyl, 4-dodecenyl, 4,8,12-tetradecatrienyl, and the like. A substituted alkenyl refers to an alkenyl having one or more substituents (for example 1 to 3 substituents, or 1 to 2 substituents), selected from those defined above for substituted alkyl.

The term "alkynyl" as used herein by itself or as part of another group refers to straight or branched chain hydrocarbon groups having 2 to 12 carbon atoms, alternatively 2 to 4 carbon atoms, and at least one triple carbon to carbon bond, such as ethynyl, 2-propynyl, 3-butynyl, 2-butynyl, 4-pentynyl, 3-pentynyl, 2-hexynyl, 3-hexynyl, 2-heptynyl, 3-heptynyl, 4-heptynyl, 3-octynyl, 3-nonynyl, 4-decynyl, 3-undecynyl, 4-dodecynyl and the like. A substituted alkynyl refers to an alkynyl having one or more substituents (for example 1 to 4 substituents, or 1 to 2 substituents), selected from those defined above for substituted alkyl.

When the term "alkyl" is used as a suffix with another group, such as in (aryl)alkyl or arylalkyl, this conjunction is meant to refer to a substituted alkyl group wherein at least one of the substituents is the specifically named group in the conjunction. For example, (aryl)alkyl refers to a substituted alkyl group as defined above wherein at least one of the alkyl substituents is an aryl, such as benzyl. However, in groups designated —O(alkyl) and —S(alkyl), it should be understood that the points of attachment in these instances are to the oxygen and sulfur atoms, respectively.

Where alkyl groups as defined are divalent, i.e., with two single bonds for attachment to two other groups, they are termed "alkylene" groups. Similarly, where alkenyl groups as defined above and alkynyl groups as defined above, respectively, are divalent radicals having single bonds for attachment to two other groups, they are termed "alkenylene groups" and "alkynylene groups" respectively. Examples of alkylene, alkenylene and alkynylene groups include:

8

$$—CH=CH—CH_2—, \quad —CH_2CH=CH—,$$

$$—C\equiv C—CH_2—, \quad —CH_2—,$$

$$—CH_2C\equiv CCH_2—, \quad —\overset{\displaystyle CH_3}{\underset{}{C}}=CH—CH_2—,$$

$$—(CH_2)_2—, \quad —(CH_2)_3—, \quad —(CH_2)_4—,$$

$$—(CH_2)_2—\overset{\displaystyle CH_3}{\underset{\displaystyle CH_3}{C}}—CH_2CH_2—, \quad —CH_2\overset{}{\underset{\displaystyle CH_3}{CH}}—,$$

$$—CH_2\overset{}{\underset{\displaystyle C_2H_5}{CHCH_2}}—, \quad —CH_2—\overset{}{\underset{\displaystyle CH_3}{CH}}—\overset{}{\underset{\displaystyle CH_3}{CH}}—CH_2—,$$

$$—CH_2—\overset{}{\underset{\displaystyle CH_3}{CH}}—CH_2—\overset{}{\underset{\displaystyle CH_3}{CH}}—, \quad —\overset{\displaystyle CH_3}{\underset{}{CH}}—CH_2CH_2—,$$

and the like. Alkylene groups may be optionally independently substituted as valence allows with one or more groups as defined for substituted alkyl groups. Thus, for example, a substituted alkylene group would include

$$—\overset{\displaystyle OCH_3}{\underset{}{CH}}—CH_2CH_2— \quad \text{and} \quad —(CH_2)_3—\overset{\displaystyle F}{\underset{\displaystyle F}{C}}—,$$
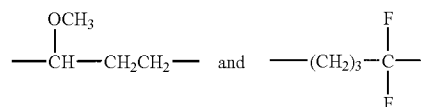
and so forth.

The term "cycloalkyl" as used herein by itself or as part of another group refers to optionally-substituted saturated and partially unsaturated (containing 1 or 2 double bonds) cyclic hydrocarbon groups containing 1 to 3 rings, including monocyclicalkyl, bicyclicalkyl and tricyclicalkyl, containing a total of 3 to 20 carbons forming the rings, or 3 to 7 carbons, forming the ring. The further rings of multi-ring cycloalkyls may be either fused, bridged and/or joined through one or more spiro unions. Exemplary cycloalkyl groups include cyclopropyl, cyclobutyl, cyclopentyl, cyclohexyl, cycloheptyl, cyclooctyl, cyclodecyl, cyclododecyl, cyclopentenyl, cycloheptenyl, cyclooctenyl, cyclohexadienyl, cycloheptadienyl,

US 7,491,725 B2

9

-continued
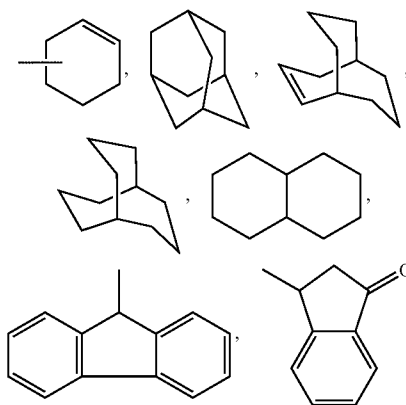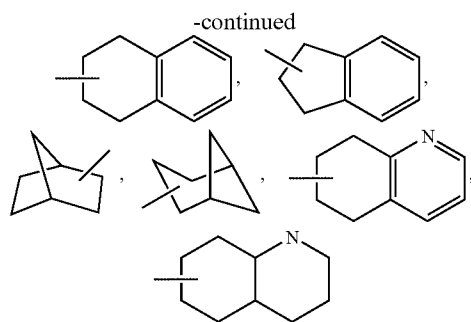
and the like.

Each reference to a cycloalkyl is intended to include both substituted and unsubstituted cycloalkyl groups as defined immediately below, unless reference is made to a particular selection of substituents to be made for the cycloalkyl (e.g., wherein cycloalkyl is substituted with one or more groups R_f) When no particular selection is recited, the optional substituents for the cycloalkyl groups may be selected from the following:

(i) halogen (e.g., a single halo substituent or multiple halo substitutents forming, in the latter case, groups such as a perfluoroalkyl group or an alkyl group bearing Cl_3 or CF_3), haloalkoxy, cyano, nitro, oxo (=O), —OR_a, —SR_a, —$S(=O)R_e$, —$S(=O)_2R_e$, —$S(=O)_3H$, —$P(=O)_2$—R_e, —$S(=O)_2OR_e$, —$P(=O)_2OR_e$, —U_1—NR_bR_c, —U_1—$N(R_d)$—U_2—NR_bR_c, —U_1—NR_d—U_2—R_b, —$NR_bP(=O)_2R_e$, —$P(=O)_2NR_bR_c$, —$C(=O)OR_e$, —$C(=O)R_a$, —$OC(=O)R_a$, —$NR_dP(=O)_2NR_bR_c$, —$R_bP(=O)_2R_e$, and/or —U_1—R_e, and/or

(ii) —U_1-alkyl, —U_1-alkenyl, or —U_1-alkynyl wherein the alkyl, alkenyl, and alkynyl are substituted with one or more (or 1 to 3) groups recited in (i),

wherein, in groups (i) and (ii),

(iii) —U_1— and —U_2— are each independently a single bond, —U_3—$S(O)_t$—U_4—, —U_3—$C(O)$—U_4—, —U_3—$C(S)$—U_4—, —U_3—O—U_4—, —U_3—S—U_4—, —U_3—O—$C(O)$—U_4—, —U_3—$C(O)$—O—U_4—, or —U_3—$C(=NR_g)$—U_4—;

wherein, in group (iii),

(iv) U_3 and U_4 are each independently a single bond, alkylene, alkenylene, or alkynylene;

wherein,

(v) R_a, R_b, R_c, R_d, and R_e are each independently hydrogen, alkyl, alkenyl, alkynyl, cycloalkyl, aryl, heterocyclo, or heteroaryl, each of which is unsubstituted or substituted with one or more groups R_f, except R_e is not hydrogen; or R_b and R_c may be taken together to form a 3- to 8-membered saturated or unsaturated ring together with the atoms to which they are attached, which ring is unsubstituted or substituted with one or more groups listed below for R_f or R_b and R_c together with the nitrogen atom to which they are attached may combine to form a group —N=$C R_gR_h$, where R_g and R_h are each independently hydrogen, alkyl, or alkyl substituted with a group R_f; and;

wherein,

(vi) R_f is at each occurrence independently selected from alkyl, halogen, cyano, hydroxy, —O(alkyl), SH, —S(alkyl), amino, alkylamino, haloalkyl, haloalkoxy, or a lower alkyl substituted with one to two of halogen,

10

cyano, hydroxy, —O(alkyl), SH, —S(alkyl), amino, alkylamino, haloalkyl, and/or haloalkoxy, and

wherein,

(vii) t is 0, 1 or 2.

When the suffix "ene" is used in conjunction with a cyclic group, this is intended to mean the cyclic group as defined herein having two single bonds as points of attachment to other groups. Thus, for example, the term "cycloalkylene" as employed herein refers to a "cycloalkyl" group as defined above which is a linking group such as
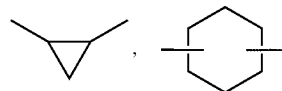

and the like.

The term "alkoxy" refers to an alkyl or substituted alkyl group as defined above bonded through an oxygen atom (—O—), i.e., the group —OR_i, wherein R_i is alkyl or substituted alkyl.
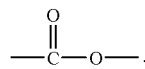
The term "alkylthio" refers to an alkyl or substituted alkyl group as defined above bonded through a sulfur atom (—S—), i.e., the group —SR_i, wherein R_i is alkyl or substituted alkyl.

The term "acyl" refers to a carbonyl group linked to a radical such as, but not limited to, alkyl, alkenyl, alkynyl, aryl, carbocyclyl, heterocyclyl, more particularly, the group $C(=O)R_j$, wherein R_j can be selected from alkyl, alkenyl, substituted alkyl, or substituted alkenyl, as defined herein.

The term "alkoxycarbonyl" refers to a carboxy group
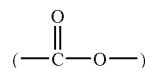
linked to an alkyl radical (i.e., to form CO_2R_j), wherein R_j is as defined above for acyl. When the designation "CO_2" is used herein, this is intended to refer to the group

The term "alkylamino" refers to amino groups wherein one or both of the hydrogen atoms is replaced with an alkyl group, i.e., NR_kR_l, wherein one of R_k and R_l is hydrogen and the other is alkyl, or both R_k and R_l are alkyl.

The term "halo" or "halogen" refers to chloro, bromo, fluoro and iodo.

The term "haloalkyl" means a substituted alkyl having one or more halo substituents. For example, "haloalkyl" includes mono, bi, and trifluoromethyl.

The term "haloalkoxy" means an alkoxy group having one or more halo substituents. For example, "haloalkoxy" includes OCF_3.

The terms "ar" or "aryl" as used herein by itself or as part of another group refer to optionally-substituted aromatic homocyclic (i.e., hydrocarbon) monocyclic, bicyclic or tricyclic aromatic groups containing 6 to 14 carbons in the ring portion [such as phenyl, biphenyl, naphthyl (including 1-naphthyl and 2-naphthyl) and antracenyl], and may optionally include one to three additional rings (either cycloalkyl, heterocyclo or heteroaryl) fused thereto. Examples include:

US 7,491,725 B2

11

12

pyrimidinyl, pyridazinyl, triazinyl, indolyl, benzothiazolyl, benzodioxolyl, benzoxazolyl, benzothienyl, quinolinyl, tetrahydroisoquinolinyl, isoquinolinyl, benzimidazolyl, benzopyranyl, indolizinyl, benzofuranyl, chromonyl, coumarinyl, benzopyranyl, cinnolinyl, quinoxalinyl, indazolyl, pyrrolopyridyl, furopyridyl, dihydroisoindolyl, tetrahydroquinolinyl, carbazolyl, benzidolyl, phenanthrollinyl, acridinyl, phenanthridinyl, xanthenyl

and the like.

Each reference to a heteroaryl is intended to include both substituted and unsubstituted heteroaryl groups as defined herein, unless reference is made to a particular selection of substituents to be made for the heteroaryl (e.g., as when heteroaryl is substituted with one or more groups R_f, above). When no particular selection is recited, the optional substituents for the heteroaryl groups may be selected from those recited above, as valence allows, for cycloalkyl groups.

The terms "heterocyclic" or "heterocyclo" as used herein by itself or as part of another group refer to non-aromatic, optionally substituted, fully saturated or partially unsaturated cyclic groups (for example, 3 to 13 member monocyclic, 7 to 17 member bicyclic, or 10 to 20 member tricyclic ring systems, or containing a total of 3 to 10 ring atoms) which have at least one heteroatom in at least one carbon atom-containing ring. Each ring of the heterocyclic group containing a heteroatom may have 1, 2, 3 or 4 heteroatoms selected from nitrogen atoms, oxygen atoms and/or sulfur atoms, where the nitrogen and sulfur heteroatoms may optionally be oxidized and the nitrogen heteroatoms may optionally be quaternized. The heterocyclic group may be attached at any heteroatom or carbon atom of the ring or ring system, where valence allows. The rings of multi-ring heterocycles may be fused, bridged and/or joined through one or more spiro unions.

Exemplary heterocyclic groups include oxetanyl, imidazolinyl, oxazolidinyl, isoxazolinyl, thiazolidinyl, isothiazolidinyl, piperidinyl, piperazinyl, 2-oxopiperazinyl, 2-oxopiperidinyl, 2-oxopyrrolodinyl, 2-oxoazepinyl, azepinyl,
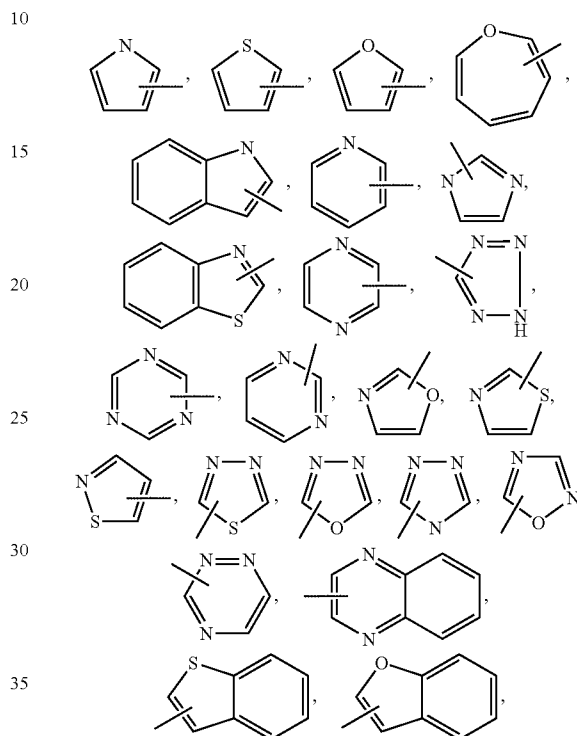
and the like.

Each reference to an aryl is intended to include both substituted and unsubstituted aryl groups as defined herein, unless reference is made to a particular selection of substituents to be made for the aryl (e.g., as when aryl is substituted with one or more groups R_f, above). When no particular selection is recited, the optional substituents for the aryl groups may be selected from those recited above, as valence allows, for cycloalkyl groups.

The term "heteroaryl" as used herein by itself or as part of another group refers to optionally-substituted monocyclic and bicyclic aromatic rings containing from 5 to 10 atoms, which includes 1 to 4 hetero atoms such as nitrogen, oxygen or sulfur, and such rings fused to an aryl, cycloalkyl, heteroaryl or heterocyclo ring, where the nitrogen and sulfur heteroatoms may optionally be oxidized and the nitrogen heteroatoms may optionally be quaternized. Examples of heteroaryl groups include pyrrolyl, pyrazolyl, pyrazolinyl, imidazolyl, oxazolyl, isoxazolyl, thiazolyl, thiadiazolyl, isothiazolyl, furanyl, thienyl, oxadiazolyl, pyridyl, pyrazinyl,

US 7,491,725 B2

13

4-piperidonyl, tetrahydropyranyl, morpholinyl, thiamorpholinyl, thiamorpholinyl sulfoxide, thiamorpholinyl sulfone, 1,3-dioxolane and tetrahydro-1,1-dioxothienyl,

and the like, which optionally may be substituted.

Each reference to a heterocyclo is intended to include both substituted and unsubstituted heterocyclo groups as defined herein, unless reference is made to a particular selection of substituents to be made for the heterocyclo (e.g., as when heterocyclo is substituted with one or more groups R_f, above). When no particular selection is recited, the optional substituents for the heterocyclo groups may be selected from those recited above, as valence allows, for cycloalkyl groups.
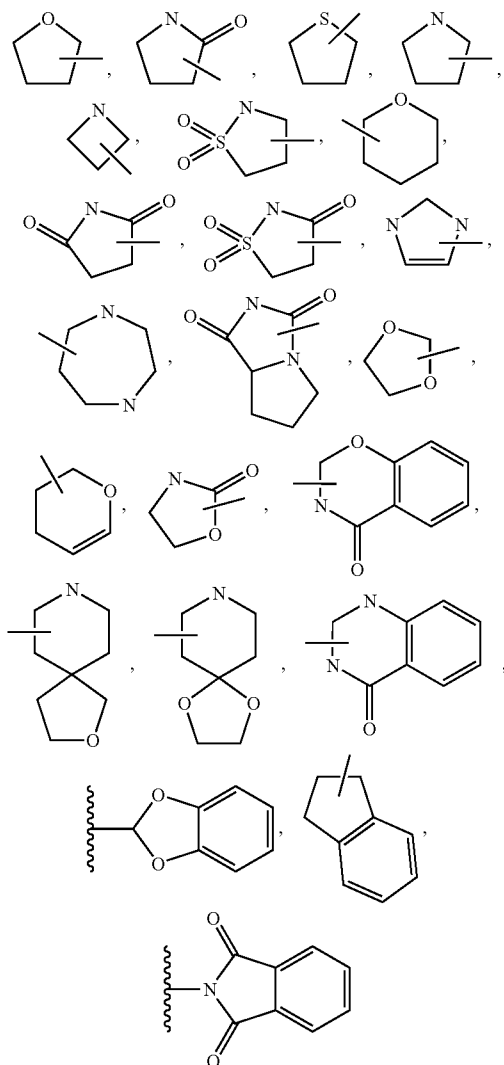
The term "ring" encompasses homocyclic (i.e., as used herein, all the ring atoms are carbon) or "heterocyclic" (i.e., as used herein, the ring atoms include carbon and one to four heteroatoms selected from N, O and/or S, also referred to as heterocyclo), where, as used herein, each of which (homocyclic or heterocyclic) may be saturated or partially or completely unsaturated.

Unless otherwise indicated, when reference is made to a specifically-named aryl (e.g., phenyl), cycloalkyl (e.g., cyclohexyl), heterocyclo (e.g., pyrrolidinyl) or heteroaryl (e.g., imidazolyl), unless otherwise specifically indicated, the reference is intended to include rings having 0 to 3, or 0 to 2,

14

substituents selected from those recited above for the aryl, cycloalkyl, heterocyclo and/or heteroaryl groups, as appropriate.

The term "heteroatoms" shall include oxygen, sulfur and nitrogen.

The term "carbocyclic" means a saturated or unsaturated monocyclic or bicyclic ring in which all atoms of all rings are carbon. Thus, the term includes cycloalkyl and aryl rings. The carbocyclic ring may be substituted in which case the substituents are selected from those recited above for cycloalkyl and aryl groups.

When the term "unsaturated" is used herein to refer to a ring or group, unless otherwise specified, the ring or group may be fully unsaturated or partially unsaturated.

"Base" when used herein includes metal oxides, hydroxides or alkoxides, hydrides, or compounds such as ammonia, that accept protons in water or solvent. Thus, exemplary bases include, but are not limited to, alkali metal hydroxides and alkoxides (i.e., MOR, wherein M is an alkali metal such as potassium, lithium, or sodium, and R is hydrogen or alkyl, as defined above, or where R is straight or branched chain C_{1-5} alkyl, thus including, without limitation, potassium hydroxide, potassium tert-butoxide, potassium tert-pentoxide, sodium hydroxide, sodium tert-butoxide, lithium hydroxide, etc.); other hydroxides such as magnesium hydroxide (Mg(OH)$_2$) or calcium hydroxide (Ca(OH)$_2$); alkali metal hydrides (i.e., MH, wherein M is as defined above, thus including, without limitation, sodium hydride and lithium hydride); alkylated disilazides, such as, for example, potassium hexamethyldisilazide and lithium hexamethyldisilazide; carbonates such as potassium carbonate (K_2CO_3), sodium carbonate (Na_2CO_3), potassium bicarbonate ($KHCO_3$), and sodium bicarbonate ($NaHCO_3$), alkyl ammonium hydroxides such as n-tetrabutyl ammonium hydroxide (TBAH); and so forth. The term "coupling reagent" as used herein refers to a reagent used to couple a carboxylic acid and an amine or an aniline to form an amide bond. It may include a coupling additive, such as CDI, HOBt, HOAt, HODhbt, HOSu, or NEPIS, used in combination with another coupling reagent to speed up coupling process and inhibit side reactions. Particular peptide-coupling reagents may include CDI, DCC, EDC, BBC, BDMP, BOMI, HATU, HAPyU, HBTU, TAPipU, AOP, BDP, BOP, PyAOP, PyBOP, TDBTU, TNTU, TPTU, TSTU, BEMT, BOP-Cl, BroP, BTFFH, CIP, EDPBT, Dpp-Cl, EEDQ, FDPP, HOTT-PF6, TOTT-BF4, PyBrop, PyClop, and TFFH. See "Peptide Coupling Reagents: Names, Acronyms and References," Albany Molecular Research, Inc., Technical Reports, Vol. 4, No. 1, incorporated herein by reference.

The terms "halogenating agent" or "halogenating reagent" mean an agent or agents capable of halogenating compounds of formula (II) herein. Halogenating reagents include inorganic and organic halogenating reagents. Examples of inorganic halogenating reagents include chlorine, bromine, iodine, fluorine, and sodium hypochlorite. Organic halogenting reagents include N-chlorosuccinimide (NCS), N-bromosuccinimide (NBS), N-iodosuccinimide (NIS), 1,3-dichloro-5,5-dimethylhydantoin, 1,3-dibromo-5,5-dimethylhydantoin, and 1,3-diiodo-5,5-dimethylhydantoin.

"High yield" as used herein means a yield of greater than 80%, greater than 85%, than 90%, or than 95%.

"Leaving group" means groups having the capability of being displaced upon reaction with a nucleophile including I, Br, Cl, $R_{10}SO_2O$— (wherein R_{10} is alkyl, substituted alkyl, aryl, or heteroaryl, as defined herein), and weak bases, such as, for example, HSO_4—. Examples of leaving groups include I, Br, Cl, and ions of methyl sulfate, mesylate (methane sulfonate), trifluromethanesulfonate, and tosylate (p-toluenesulfonate).

US 7,491,725 B2

15   16

In compounds of formula (II) herein, the group Q is —O—P*, wherein P* is selected so that, when considered together with the oxygen atom to which P* is attached, Q is a leaving group, i.e., Q has the capability of being displaced upon reaction with a nucleophile. Accordingly, the group P* may be selected from alkyl, —SO$_2$O R$_{10}$, —SO$_2$R$_{10}$, —C(═O)R$_{11}$ and —Si(R$_{12}$)$_3$, wherein R$_{10}$ is defined as above in the definition of "leaving group," R$_{11}$ is alkyl, aryl or heteroaryl, and R$_{12}$ is selected from alkyl and aryl.

"Suitable solvent" as used herein is intended to refer to a single solvent as well as mixtures of solvents. Solvents may be selected, as appropriate for a given reaction step, from, for example, aprotic polar solvents such as DMF, DMA, DMSO, dimethylpropyleneurea, N-methylpyrrolidone (NMP), and hexamethylphosphoric triamide; ether solvents such as diethyl ether, THF, 1,4-dioxane, methyl t-butyl ether, dimethoxymethane, and ethylene glycol dimethyl ether; alcohol solvents such as MeOH, EtOH, and isopropanol; and halogen-containing solvents such as methylene chloride, chloroform, carbon tetrachloride, and 1,2-dichloroethane. Mixtures of solvents may also include biphasic mixtures.

The term "slurry" as used herein is intended to mean a saturated solution of the compound of Formula (IV) and an additional amount of the compound of Formula (IV) to give a heterogeneous solution of the compound of Formula (IV) and a solvent.

The present invention describes crystalline forms of the compound of formula (IV) in substantially pure form. As used herein, "substantially pure" means a compound having a purity greater than 90 percent, including 90, 91, 92, 93, 94, 95, 96, 97, 98, 99, and 100 percent.

As one example, a crystalline form of the compound of the formula (IV) can be substantially pure in having a purity greater than 90 percent, where the remaining less than 10 percent of material comprises other form(s) of the compound of the formula (IV), and/or reaction and/or processing impurities arising from its preparation. A crystalline form of the compound of the formula (IV) in substantially pure form may therefore be employed in pharmaceutical compositions to which other desired components are added, for example, excipients, carriers, or active chemical entities of different molecular structure.

When dissolved, crystalline forms of the compound of formula (IV) loses its crystalline structure, and is therefore referred to as a solution of the compound of formula (IV). All forms of the present invention, however, may be used for the preparation of liquid formulations in which the drug is dissolved or suspended. In addition, the crystalline forms of the compound of formula (IV) may be incorporated into solid formulations.

A therapeutically effective amount of the crystalline forms of the compound of formula (IV) is combined with a pharmaceutically acceptable carrier to produce the pharmaceutical compositions of this invention. By "therapeutically effective amount" it is meant an amount that, when administered alone or an amount when administered with an additional therapeutic agent, is effective to prevent, suppress or ameliorate the disease or condition or the progression of the disease or condition.

General Methods

This invention is related to a process for the preparation of 2-aminothiazolyl-5-aromatic amides which are useful as inhibitors of kinases, particularly protein tyrosine kinase and p38 kinase. The process involves halogenation of β-(P*)oxy-α,β-unsaturated carboxyl aromatic amides (II) (wherein P* is as defined herein), such as β-(alkyl)oxy-α,β-unsaturated carboxylbenzamides, and reaction with thioureas (III) to give 2-aminothiazole-5-aromatic amides of formula (I). Desired

substituents on the 2-amino group and/or the 5-aromatic group can be attached either before or after the aminothiozole formation. For example, in one embodiment, the compound of formula (I) is prepared via reaction of a thiourea wherein R$_4$ is hydrogen, and the R$_4$ hydrogen atom is then elaborated to more functionalized groups such as, in one embodiment, substituted pyrimidines. In another embodiment, the compound of formula (I) is prepared via reaction of a thiourea wherein R$_4$ is a pyrimidinyl, and the pyrimidinyl optionally is further elaborated with additional substituents, as desired.

The process provides an efficient route for preparing 2-aminothiazolyl-5-aromatic amides, essentially in one step and in high yield, without use of expensive coupling reagents or catalysts. Surprisingly, with this process halogenation followed by reaction with thiourea to form the aminothizole is achieved without an undesired aromatic halogenation.

One embodiment of the invention is represented in Scheme 1.

Scheme 1
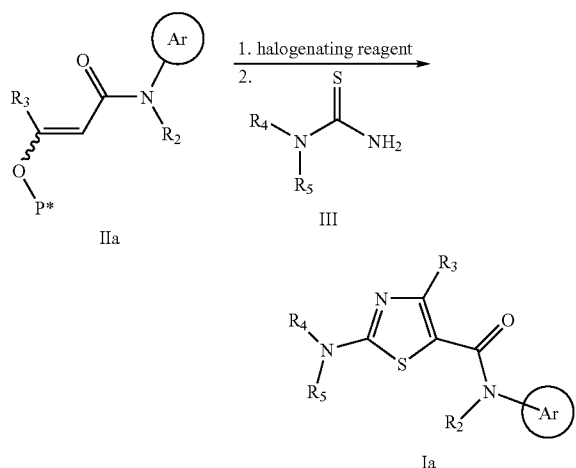
In Scheme 1, Ar is aryl or heteroaryl, more preferably aryl, even more preferably optionally-substituted phenyl. Most preferred is the process involving compounds wherein Ar is phenyl substituted with one to three of alkyl, halogen, —C(═O)NR$_8$, and/or NR$_8$C(═O), wherein R$_8$ is alkyl, cycloalkyl, or heteroaryl, more preferably wherein R$_8$ is cyclopropyl or methyl, and even more preferably wherein Ar is selected from 2-chloro-6-methylphenyl, N-cyclopropyl-1-methyl-benzamide, and N, 1-dimethyl-benzamide. The inventive process may be carried out where a linker group L is present, as in formula I, but advantageously the Ar group is directly attached to the carboxylamide nitrogen atom, as in formula (Ia).

As noted, the desired substituents may be attached to the group Ar either before or after the halogenation and cyclization process. Likewise, the thiourea compounds (III) may be prepared, prior to the cyclization, having desired groups R$_4$ and R$_5$, corresponding to the groups on the desired final product, or alternatively, the desired groups may be attached to the amino-thiazolyl after cyclization. For example, thiourea compounds (III) may be prepared and used in the reaction wherein R$_4$ and R$_5$ are both hydrogen, or R$_4$ and R$_5$ are other groups, different from those of the final desired product, and then, after formation of the aminothiazole (I) or (Ia), the

US 7,491,725 B2

17

groups R_4 and R_5 are elaborated to the substituents of the final desired product. All such alternative embodiments and variations thereof are contemplated as within the scope of the present invention.

In intermediates of formula (II) and (IIa), herein, preferably the group P* may be selected from alkyl, —SO_2OR_{10}, —SO_2R_{10}, —$C(\!=\!O)R_{11}$ and —$Si(R_{12})_3$, as defined above, but preferably P* is an alkyl, more preferably a lower alkyl, i.e., methyl, ethyl, n-propyl, isoP, or a straight or branched butyl. Preferably the group R_2 is hydrogen or lower alkyl, more preferably hydrogen, and R_3 is preferably hydrogen. For compounds (II), β-alkyloxy-α,β-unsaturated carboxyl-benzamides are thus preferred, including β-substituted and β-unsubstituted β-alkyloxy-α,β-unsaturated carboxyl benzamides, with the latter more preferred, wherein the phenyl group of the benzamide is optionally substituted as recited above for Ar in formula (Ia). Also preferred β-unsubstituted β-alkyloxy-α,β-unsaturated carboxylbenzamides are β-ethoxy acryl benzamides, again, wherein the phenyl group of the benzamide is optionally substituted as recited above for Ar. Intermediates (II) and (IIa) can be prepared upon reaction of the corresponding anilines, NHR_2—Ar, with alkoxyacryloyl compounds. Methods for making β-ethoxy acryl benzamides are also described, for example, in Ashwell, M. A. et al., *J. Bioorg. Med. Chem. Lett.* (2001), 24, at 3123; and Yoshizaki, S., et al. *Chem. Pharm. Bull.* (1980), 28, at 3441, incorporated herein by reference.

The halogenating agent(s) used in the process may be any agent or agents as defined herein capable of halogenating compounds (II), as previously defined herein. Preferred agents include NBS and the N-halohydantoins. Thiourea compounds (III) include unsubstituted thioureas, N-mono-substituted thioureas, and N,N-disubstituted thioureas. The steps of halogenation and cyclization are carried out in a suitable solvent which may include one or more solvents such as hydrocarbons, ethers, esters, amides and ketones with ethers, with dioxane preferred.

Another embodiment of the invention is illustrated in Scheme 2.

Scheme 2

18

-continued
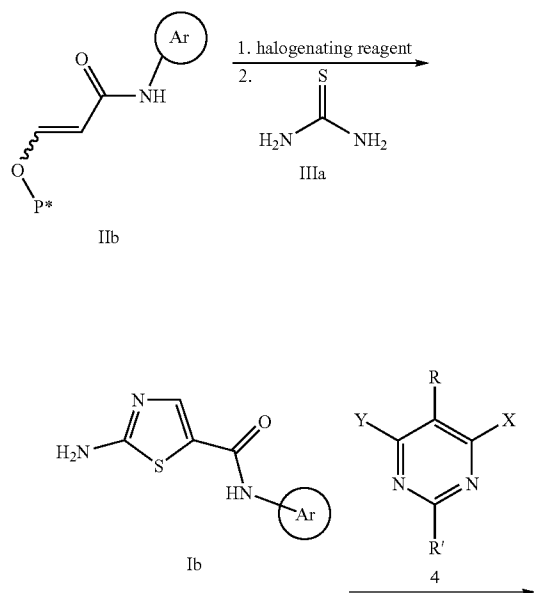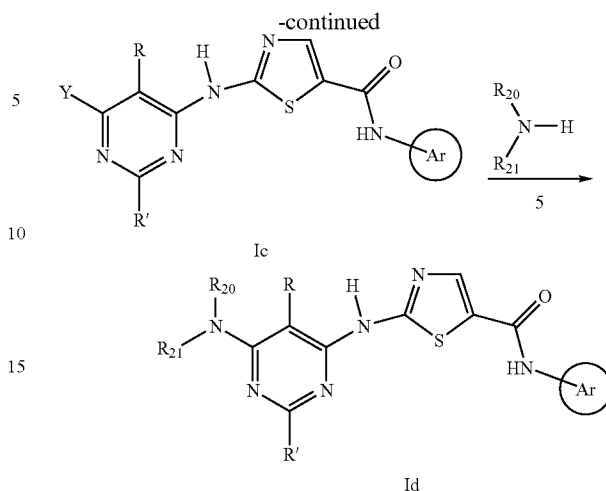
As can be seen, in Scheme 2, the β-(P*)oxy-acryl benzamides (IIb), wherein R_2 and R_3 are hydrogen, and P* is as previously defined herein, preferably a lower alkyl, are halogenated with a halogenating agent, such as NBS, in a suitable solvent, in the presence of water, then cyclized with unsubstituted thiourea (IIIa). The resulting 2-(unsubstituted) amino-thiazole-5-aromatic amide (Ib) is reacted with a pyrimidine compound 4, wherein R and R' are hydrogen or optional substituents, more preferably hydrogen or lower alkyl, and X and Y are both leaving groups, as defined herein, to produce compounds Ic. Leaving groups X and Y are preferably I, Br, Cl, or $R_{10}SO_2O$— (wherein R_{10} is alkyl, substituted alkyl, aryl, or heteroaryl, as defined herein), more preferably X and Y are selected from I, Br, Cl, methyl sulfate, mesylate, trifluoromethanesulfonate, and tosylate, even more preferably from Cl and Br. Thus, pyrimidines 4 include bis-halogen and sulfonyloxy substituted pyrimidines with the former such as bis-chloro substituted pyrimidines preferred. Advantageously, this step is carried out in the presence of a base, wherein the bases may include alkali hydride and alkoxides with the latter such as sodium t-butoxide preferred. Suitable solvent(s) include solvents such as hydrocarbons, ethers, esters, amides, ketones and alcohols, or mixtures of the above solvents, with ether such as THF preferred.

Compound (Ic) can then be reacted with amine $NHR_{20}R_{21}$ (5), to provide compounds of formula (Id). For example, R_{20} and R_{21} can both be hydrogen, or R_{20} and R_{21} can be independently selected from hydrogen, alkyl, substituted alkyl, cycloalkyl, heterocyclo, aryl, and heteroaryl, or R_{20} and R_{21} can be taken together to form a heterocyclo. Preferably, R_{20} and R_{21} are taken together so that $NHR_{20}R_{21}$ forms an optionally-substituted piperazine, more preferably a piperazine N'-substituted with substituted alkyl, more preferably hydroxyethyl. Advantageously, this step is carried out in the presence of a base, including inorganic and organic bases, with organic bases such as tertiary amines preferred. Suitable solvent(s) include solvents such as hydrocarbons, halogenated hydrocarbons, ethers, esters, amides, ketones, lactams and alcohols, and mixtures of the above solvents, with alcohols such as n-butanol as one nonlimiting example, and DMF (dimethylformamide), DMA (dimethylacetamide) and NMP (N-methylpyrrolidine) as other examples. The compounds of formula (Id) thus formed may optionally be further elaborated as desired and/or purified and crystallized.

An alternative approach is illustrated in Scheme 3, wherein a mono-substituted thiourea compound (IIIb) is used.

US 7,491,725 B2

19

Scheme 3

IIb

IIIb

Ic

Id
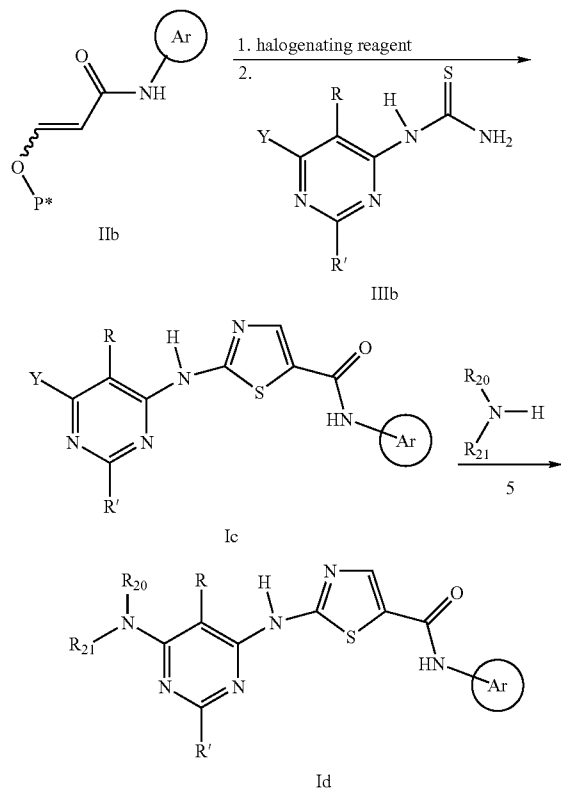
As can be seen, in Scheme 3, the β-(P*)oxy-acryl benzamides (IIb), as in Scheme 2, are halogenated with a halogenating agent, then further reacted with a monosubstituted thiourea (IIIb) having attached thereto a functional pyrimidine group, wherein R, R' and Y are as in Scheme 2, to provide intermediate 2-substituted-aminothiazole-aromatic amides of formula (Ic). The compounds of formula (Ic) may optionally then be reacted with amines $NHR_{20}R_{21}$ (5), to provide compounds of formula (Id), and/or optionally further elaborated as desired, and/or purified and crystallized.

FURTHER EMBODIMENTS

In one embodiment, the process comprises preparing a compound of the formula (Ie),

(Ie)
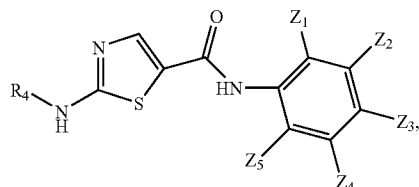
wherein Z_1 and Z_5 are selected from hydrogen, alkyl, halogen, hydroxy, and alkoxy;

20

Z_2, Z_3 and Z_4 are selected from hydrogen, alkyl, halogen, hydroxy, alkoxy, $C(=O)NR_8$, and/or $NR_8C(=O)$, wherein R_8 is alkyl, cycloalkyl, or heteroaryl; comprising reacting a compound having the formula,
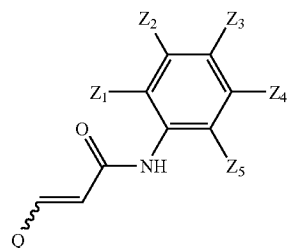
IIc

wherein Q is the group —O—P*, wherein P* is selected so that, when considered together with the oxygen atom to which P* is attached, Q is a leaving group, and Z_1, Z_2, Z_3, Z_4, and Z_5 are as defined above, with a halogenating reagent followed in the presence of water by a thiourea compound having the formula,

IIIc
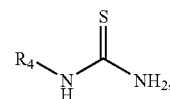
to provide the compound having the formula (Ie),

(Ie)
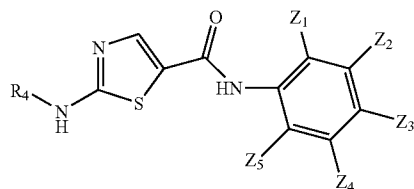
In the above process, in one embodiment, R_4 is hydrogen, whereby the process provides a compound having the formula (If),

(If)
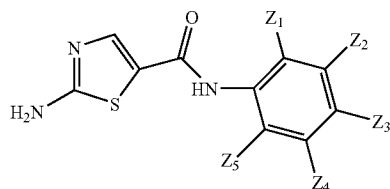
In another embodiment, R_4 may be a group having the formula,
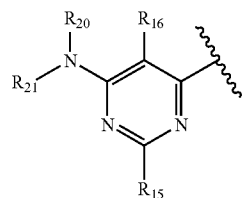
US 7,491,725 B2

21

wherein R_{15} and R_{16} are as defined herein, whereby said process provides a compound having the formula (Ih),

(Ih)
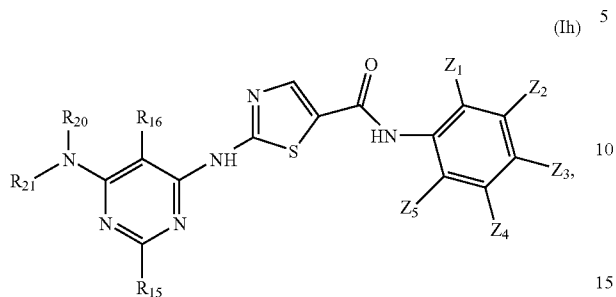
wherein R_{15}, R_{16}, Z_1, Z_2, Z_3, Z_4, Z_5, R_{20} and R_{21} are as defined herein.

In yet another embodiment, R_4 is a group having the formula,
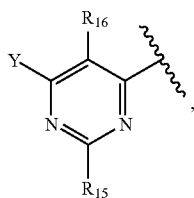
wherein Y, R_{15} and R_{16} are as defined herein, wherein said process provides a compound having the formula (Ii),

(Ii)
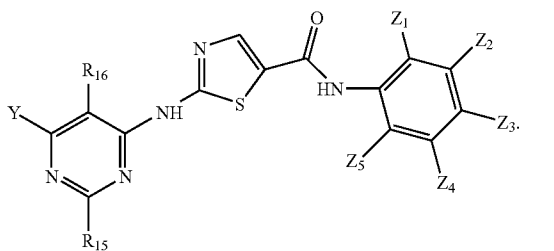
In yet another embodiment, R_4 is a group having the formula,
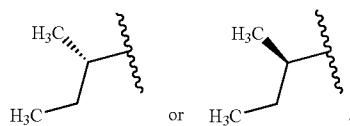
22

In another embodiment of the above process, e.g., when R_4 is hydrogen to provide compounds (If), the process may further comprise reacting the compound of the formula

(If)

with a pyrimidine compound having the formula,

4a

wherein X and Y are leaving groups, and R_{15} and R_{16} are independently selected from hydrogen, alkyl and substituted alkyl, to provide a compound having the formula,

(Ig)
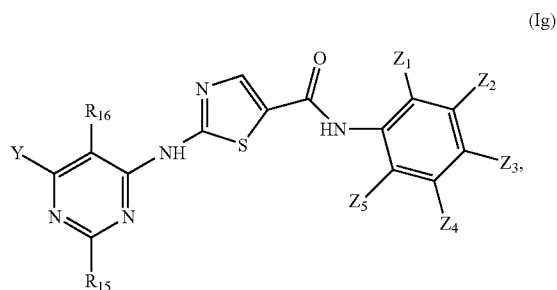
wherein Y, R_{15}, R_{16}, Z_1, Z_2, Z_3, Z_4, and Z_5 are as defined above.

In another embodiment of the above process, e.g., when R_4 is hydrogen to provide compounds (If), the process may further comprise reacting the compound of the formula

(If)
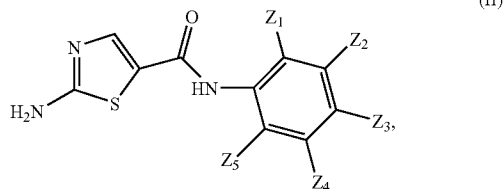
with a pyrimidine compound having the formula,

US 7,491,725 B2

<div style="display:flex">
<div>

23

(4a)
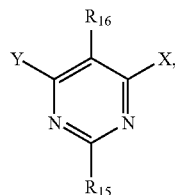
(for example reacting with a base or by metal catalysis)

wherein X and Y are leaving groups, and R_{15} and R_{16} are independently selected from hydrogen, alkyl and substituted alkyl,

to provide a compound having the formula,

(Ig)
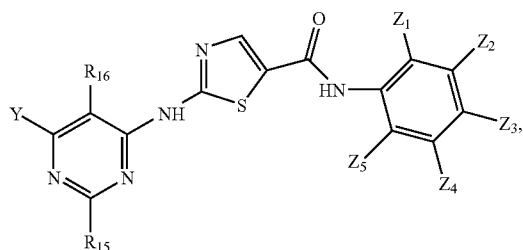
wherein Y, R_{15}, R_{16}, Z_1, Z_2, Z_3, Z_4, and Z_5 are as defined above.

Compounds (Ig) may optionally further be reacted with an amine having the formula $NHR_{20}R_{21}$, wherein R_{20} and R_{21} are independently selected from hydrogen, alkyl, substituted alkyl, cycloalkyl, heterocyclo, aryl, and heteroaryl, or R_{20} and R_{21} can be taken together to form a heterocyclo, to provide a compound having the formula (Ih),

(Ih)
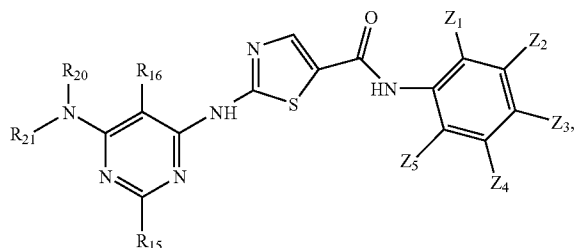
wherein R_{15}, R_{16}, Z_1, Z_2, Z_3, Z_4, Z_5, R_{20} and R_{21} are as defined above.

In one embodiment, the amine $NHR_{20}R_{21}$ is piperazine in turn optionally substituted with hydroxy(alkyl), more preferably hydroxyethyl.

</div>
<div>

24

In one embodiment, the amine $NHR_{20}R_{21}$ is
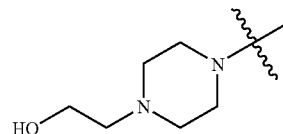
In another embodiment, when R_4 is hydrogen to provide compounds (If), the process may further comprise reacting the compound of the formula

(If)
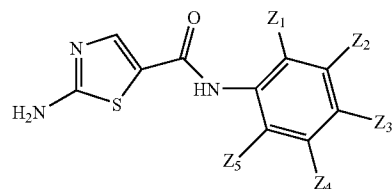
with a pyrimidine compound having the formula,

(4b)
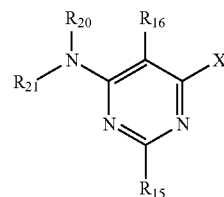
wherein R_{15}, R_{16}, R_{20} and R_{21} are defined as above, to provide a compound having the formula (Ih),

(Ih)
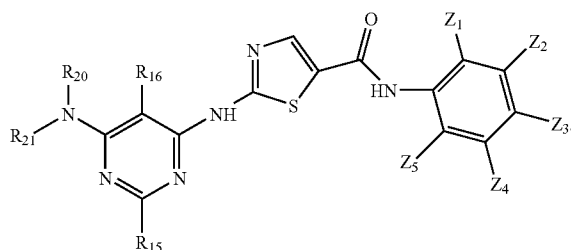
Other variations of the above processes are also contemplated as within the scope of the invention, including processes involving further elaboration of the 2-amino-thiazole-5-aromatic amides.

In one embodiment, the present invention provides a crystalline monohydrate of the compound of formula (IV)

(IV)

</div>
</div>
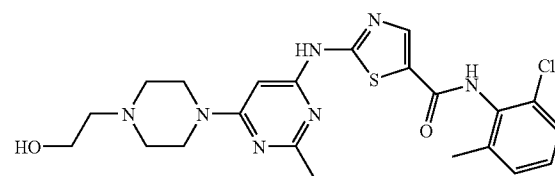
US 7,491,725 B2

25

In another embodiment, the monohydrate form is in substantially pure form.

In another embodiment, the monohydrate form is in substantially pure form, wherein substantially pure is greater than 90 percent pure.

In another embodiment, the monohydrate form of the compound of Formula (IV) is characterized by an x-ray powder diffraction pattern substantially in accordance with that shown in FIG. **1**.

In another embodiment, the monohydrate form of the compound of Formula (IV) is characterized by differential scanning calorimetry thermogram and a thermogravimetric anaylsis substantially in accordance with that shown in FIG. **2**.

In another embodiment, the monohydrate form of the compound of Formula (IV) is characterized by an x-ray powder diffraction pattern (CuKα λ=1.5418 Å at a temperature of about 23° C.) comprising four or more 2θ values (alternatively, comprising five or more, six or more, or comprising 2θ values) selected from the group consisting of: 18.0±0.2, 18.4±0.2, 19.2±0.2, 19.6±0.2, 21.2±0.2, 24.5±0.2, 25.9±0.2, and 28.0±0.2.

In another embodiment, the monohydrate form of the compound of Formula (IV) is characterized by an x-ray powder diffraction pattern (CuKα λ=1.5418 Å at a temperature of about 23° C.) comprising four or more 2θ values (alternatively, comprising five or more, six or more, or comprising 2θ values) selected from the group consisting of: 4.6±0.2, 11.2±0.2, 13.8±0.2, 15.2±0.2, 17.9±0.2, 19.1±0.2, 19.6±0.2, 23.2±0.2, 23.6±0.2.

In another embodiment, the monohydrate form of the compound of Formula (IV) is characterized by unit cell parameters approximately equal to the following:

Cell dimensions:
a(Å)=13.862(1);
b(Å)=9.286(1);
c(Å)=38.143(2);
Volume=4910(1) Å^3
Space group Pbca
Molecules/unit cell 8
Density (calculated) (g/cm^3) 1.369

wherein the compound is at a temperature of about −50° C.

In another embodiment, the monohydrate form of the compound of Formula (IV) there is one water molecule per molecule of formula (IV).

In another embodiment, the present invention provides a crystalline butanol solvate of the compound of formula (IV)

(IV)
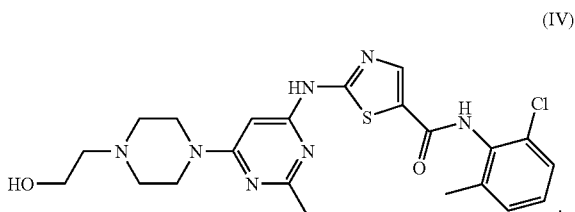
In another embodiment, the butanol solvate form of the compound of Formula (IV) is characterized by unit cell parameters approximately equal to the following:

Cell dimensions:
a(Å)=22.8102(6);
b(Å)=8.4691(3);
c(Å)=15.1436(5);
β=95.794(2);
Volume=2910.5(2) Å^3
Space group P2$_1$/a

26

Molecules/unit cell 4
Density (calculated) (g/cm^3) 1.283.

In another embodiment, the crystalline butanol solvate of the compound of Formula (IV) is characterized by an x-ray powder diffraction pattern (CuKα λ=1.5418 Å at a temperature of about 23° C.) comprising four or more 2θ values (alternatively, comprising five or more, six or more, or comprising 2θ values) selected from the group consisting of: 5.9±0.2, 12.0±0.2, 13.0±0.2, 17.7±0.2, 24.1±0.2, and 24.6±0.2.

In another embodiment, the present invention is directed to the crystalline ethanol solvate of the compound of formula (IV).

In another embodiment, the crystalline ethanol solvate of the compound of Formula (IV) is characterized by an x-ray powder diffraction pattern (CuKα λ=1.5418 Å at a temperature of about 23° C.) comprising four or more 2θ values (alternatively, comprising five or more, six or more, or comprising 2θ values) selected from the group consisting of: 5.8±0.2, 11.3±0.2, 15.8±0.2, 17.2±0.2, 19.5±0.2, 24.1±0.2, 25.3±0.2, and 26.2±0.2.

In another embodiment, the present invention is directed to the crystalline neat form of the compound of formula (IV).

In another embodiment, the crystalline neat form of the compound of Formula (IV) is characterized by an x-ray powder diffraction pattern (CuKα λ=1.5418 Å at a temperature of about 23° C.) comprising four or more 2θ values (alternatively, comprising five or more, six or more, or comprising 2θ values) selected from the group consisting of: 6.8±0.2, 11.1±0.2, 12.3±0.2, 13.2±0.2, 13.7±0.2, 16.7±0.2, 21.0±0.2, 24.3±0.2, and 24.8±0.2.

In another embodiment, the present invention describes a pharmaceutical composition comprising a therapeutically effective amount of at least one of the crystalline forms of the compound of Formula (IV) and a pharmaceutically acceptable carrier.

In another embodiment, the present invention describes a method for the treatment of cancer which comprises administering to a host in need of such treatment a therapeutically effective amount of at least one of the crystalline forms of the compound of Formula (IV).

In another embodiment, the present invention describes a method of treating oncological disorders which comprises administering to a host in need of such treatment a therapeutically effective amount of at least one of the crystalline forms of the compound of Formula (IV), wherein the disorders are selected from chronic myelogenous leukemia (CML), gastrointestinal stromal tumor (GIST), small cell lung cancer (SCLC), non-small cell lung cancer (NSCLC), ovarian cancer, melanoma, mastocytosis, germ cell tumors, acute myelogenous leukemia (AML), pediatric sarcomas, breast cancer, colorectal cancer, pancreatic cancer, and prostate cancer.

In another embodiment, the present invention is directed to a use of at least one of the crystalline forms of the compound of Formula (IV), in the preparation of a medicament for the treatment of oncological disorders, such as those described herein.

In another embodiment, the present invention is directed to a method of treating of oncological disorders, as described herein, which are resistant or intolerant to Gleevec® (STI-571), comprising administering to a host in need of such treatment a therapeutically effective amount of the compound of Formula (IV) or at least one of the crystalline forms of the compound of Formula (IV).

This invention also encompasses all combinations of alternative aspects of the invention noted herein. It is understood that any and all embodiments of the present invention may be taken in conjunction with any other embodiment to describe additional embodiments of the present invention. Furthermore, any elements of an embodiment are meant to be com-

US 7,491,725 B2

27

28

bined with any and all other elements from any of the embodiments to describe additional embodiments.

Utility

The compounds of formula (I) prepared according to the inventive process herein inhibit protein tyrosine kinases, especially Src-family kinases such as Lck, Fyn, Lyn, Src, Yes, Hck, Fgr and Blk, and are thus useful in the treatment, including prevention and therapy, of protein tyrosine kinase-associated disorders such as immunologic and oncologic disorders. The compounds of formula (I) also may inhibit receptor tyrosine kinases including HER1 and HER2 and therefore be useful in the treatment of proliferative disorders such as psoriasis and cancer. The ability of these compounds to inhibit HER1 and other receptor kinases will permit their use as anti-angiogenic agents to treat disorders such as cancer and diabetic retinopathy. "Protein tyrosine kinase-associated disorders" are those disorders which result from aberrant tyrosine kinase activity, and/or which are alleviated by the inhibition of one or more of these enzymes. For example, Lck inhibitors are of value in the treatment of a number of such disorders (for example, the treatment of autoimmune diseases), as Lck inhibition blocks T cell activation. The treatment of T cell mediated diseases, including inhibition of T cell activation and proliferation, is a particularly preferred use for compounds of formula (I) prepared according to the process herein.

Use of the compounds of formula (I) in treating protein tyrosine kinase-associated disorders is exemplified by, but is not limited to, treating a range of disorders such as: transplant (such as organ transplant, acute transplant or heterograft or homograft (such as is employed in burn treatment)) rejection; protection from ischemic or reperfusion injury such as ischemic or reperfusion injury incurred during organ transplantation, myocardial infarction, stroke or other causes; transplantation tolerance induction; arthritis (such as rheumatoid arthritis, psoriatic arthritis or osteoarthritis); multiple sclerosis; chronic obstructive pulmonary disease (COPD), such as emphysema; inflammatory bowel disease, including ulcerative colitis and Crohn's disease; lupus (systemic lupus erythematosis); graft vs. host disease; T-cell mediated hypersensitivity diseases, including contact hypersensitivity, delayed-type hypersensitivity, and gluten-sensitive enteropathy (Celiac disease); psoriasis; contact dermatitis (including that due to poison ivy); Hashimoto's thyroiditis; Sjogren's syndrome; Autoimmune Hyperthyroidism, such as Graves' Disease; Addison's disease (autoimmune disease of the adrenal glands); Autoimmune polyglandular disease (also known as autoimmune polyglandular syndrome); autoimmune alopecia; pernicious anemia; vitiligo; autoimmune hypopituatarism; Guillain-Barre syndrome; other autoimmune diseases; cancers, including cancers where Lck or other Src-family kinases such as Src are activated or overexpressed, such as colon carcinoma and thymoma, and cancers where Src-family kinase activity facilitates tumor growth or survival; glomerulonephritis; serum sickness; uticaria; allergic diseases such as respiratory allergies (asthma, hayfever, allergic rhinitis) or skin allergies; scleracierma; mycosis fungoides; acute inflammatory responses (such as acute respiratory distress syndrome and ishchemia/reperfusion injury); dermatomyositis; alopecia greata; chronic actinic dermatitis; eczema; Behcet's disease; Pustulosis palmoplanteris; Pyoderma gangrenum; Sezary's syndrome; atopic dermatitis; systemic schlerosis; and morphea.

The compounds of the present invention are useful for the treatment of cancers such as chronic myelogenous leukemia (CML), gastrointestinal stromal tumor (GIST), small cell lung cancer (SCLC), non-small cell lung cancer (NSCLC), ovarian cancer, melanoma, mastocytosis, germ cell tumors,

acute myelogenous leukemia (AML), pediatric sarcomas, breast cancer, colorectal cancer, pancreatic cancer, prostate cancer and others known to be associated with protein tyrosine kinases such as, for example, SRC, BCR-ABL and c-KIT. The compounds of the present invention are also useful in the treatment of cancers that are sensitive to and resistant to chemotherapeutic agents that target BCR-ABL and c-KIT, such as, for example, Gleevec® (STI-571). In one embodiment of the invention, for example, the compound of the formula (IV) (including, but not limited to the crystalline forms of that compound described herein, such as the crystalline monohydrate) is useful in the treatment of patients resistant or intolerant to Gleevec® (STI-571) of AMN-107 for diseases such as chronic myelogenous leukemias (CML), or other cancers (including other leukemias) as described herein.

In another embodiment of the invention a compound of Formulas I is administered in conjunction with at least one anti-neoplastic agent.

As used herein, the phrase "anti-neoplastic agent" or "anti-cancer agent" is synonymous with "chemotherapeutic agent" and/or "anti-proliferative agent" and refers to compounds that prevent cancer, or hyperproliferative cells from multiplying. Anti-proliferative agents prevent cancer cells from multiplying by: (1) interfering with the cell's ability to replicate DNA and (2) inducing cell death and/or apoptosis in the cancer cells.

Classes of compounds that may be used as anti-proliferative cytotoxic agents and/or anti-proliferative agents include the following:

Alkylating agents (including, without limitation, nitrogen mustards, ethylenimine derivatives, alkyl sulfonates, nitrosoureas and triazenes): Uracil mustard, Chlormethine, Cyclophosphamide (Cytoxan@), Ifosfamide, Melphalan, Chlorambucil, Pipobroman, Triethylene-melamine, Triethylenethiophosphoramine, Busulfan, Carmustine, Lomustine, Streptozocin, Dacarbazine, and Temozolomide.

Antimetabolites (including, without limitation, folic acid antagonists, pyrimidine analogs, purine analogs and adenosine deaminase inhibitors): Methotrexate, 5-Fluorouracil, Floxuridine, Cytarabine, 6-Mercaptopurine, 6-Thioguanine, Fludarabine phosphate, Pentostatine, and Gemcitabine.

Natural products and their derivatives (for example, vinca alkaloids, antitumor antibiotics, enzymes, lymphokines and epipodophyllotoxins): Vinblastine, Vincristine, Vindesine, Bleomycin, Dactinomycin, Daunorubicin, Doxorubicin, Epirubicin, Idarubicin, Ara-C, paclitaxel (paclitaxel is commercially available as Taxol®), Mithramycin, Deoxyco-formycin, Mitomycin-C, L-Asparaginase, Interferons (especially IFN-a), Etoposide, and Teniposide.

Other anti-proliferative cytotoxic agents and/or anti-proliferative agents are navelbene, CPT-11, anastrazole, letrazole, capecitabine, reloxafine, cyclophosphamide, ifosamide, and droloxafine.

The phrase "radiation therapy" includes, but is not limited to, x-rays or gamma rays which are delivered from either an externally applied source such as a beam or by implantation of small radioactive sources. Radiation therapy may be useful in combination with compounds of the present invention.

The following may also be useful when administered in combination with compounds of the present invention.

Microtubule affecting agents interfere with cellular mitosis and are well known in the art for their anti-proliferative cytotoxic activity. Microtubule affecting agents useful in the invention include, but are not limited to, allocolchicine (NSC 406042), Halichondrin B (NSC 609395), colchicine (NSC 757), colchicine derivatives (e.g., NSC 33410), dolastatin 10 (NSC 376128), maytansine (NSC 153858), rhizoxin (NSC 332598), paclitaxel (Taxol®, NSC 125973), Taxol® derivatives (e.g., derivatives (e.g., NSC 608832), thiocolchicine

US 7,491,725 B2

29

NSC 361792), trityl cysteine (NSC 83265), vinblastine sulfate (NSC 49842), vincristine sulfate (NSC 67574), natural and synthetic epothilones including but not limited to epothilone A, epothilone B, epothilone C, epothilone D, desoxyepothilone A, desoxyepothilone B, [1S-[1R*,3R*(E), 7R*,10S*,11R*,12R*,16S*]]-7-11-dihydroxy-8,8,10,12, 16-pentamethyl-3-[1-methyl-2-(2-methyl-4-thiazolyl) ethenyl]-4-aza-17 oxabicyclo [14.1.0]heptadecane-5,9-dione (disclosed in U.S. Pat. No. 6,262,094, issued Jul. 17, 2001), [1S-[1R*,3R*(E),7R*,10S*,11R*,12R*,16S*]]-3-[2-[2-(aminomethyl)-4-thiazolyl]-1-methylethenyl]-7,11-dihydroxy-8,8,10,12,16-pentamethyl-4-17-dioxabicyclo [14.1.0]-heptadecane-5,9-dione (disclosed in U.S. Ser. No. 09/506,481 filed on Feb. 17, 2000, and examples 7 and 8 herein), [1S1R*,3R*(E),7R*,10S*,11R*,12R*,16S*]]-7,11-dihydroxy-8,8,10,12,16-pentamethyl-3-[1-methyl-2-(2-methyl-4-thiazolyl)ethenyl]-4-aza-17oxabicyclo[14.1.0]-heptadecane-5,9-dione, [1S-[1R*,3R*(E),7R*,10S*,11R*, 12R*,16S*]]-3-[2-[2-(Aminomethyl)-4-thiazolyl]-1-methylethenyl]-7,11-dihydroxy-8,8,10,12,16-pentamethyl-4,17-dioxabicyclo[14.1.0]heptadecane-5,9-dione, and derivatives thereof; and other microtubule-disruptor agents. Additional antineoplastic agents include, discodermolide (see Service, (1996) Science, 274:2009) estramustine, nocodazole, MAP4, and the like. Examples of such agents are also described in the scientific and patent literature, see, e.g., Bulinski (1997) *J. Cell Sci.* 110:3055 3064; Panda (1997) Proc. Natl. Acad. Sci. USA 94:10560-10564; Muhlradt (1997) Cancer Res. 57:3344-3346; Nicolaou (1997) *Nature* 387:268-272; Vasquez (1997) *Mol. Biol. Cell.* 8:973-985; Panda (1996) *J. Biol. Chem* 271:29807-29812.

In cases where it is desirable to render aberrantly proliferative cells quiescent in conjunction with or prior to treatment with the chemotherapeutic methods of the invention, hormones and steroids (including synthetic analogs): 17a-Ethinylestradiol, Diethylstilbestrol, Testosterone, Prednisone, Fluoxymesterone, Dromostanolone propionate, Testolactone, Megestrolacetate, Methylprednisolone, Methyltestosterone, Prednisolone, Triamcinolone, hlorotrianisene, Hydroxyprogesterone, Aminoglutethimide, Estramustine, Medroxyprogesteroneacetate, Leuprolide, Flutamide, Toremifene, Zoladex can also be administered to the patient.

Also suitable for use in the combination chemotherapeutic methods of the invention are antiangiogenics such as matrix metalloproteinase inhibitors, and other VEGF inhibitors, such as anti-VEGF antibodies and small molecules such as ZD6474 and SU6668 are also included. Anti- Her2 antibodies from Genetech may also be utilized. A suitable EGFR inhibitor is EKB-569 (an irreversible inhibitor). Also included are Imclone antibody C225 immunospecific for the EGFR, and src inhibitors.

Also suitable for use as an antiproliferative cytostatic agent is Casodex™ which renders androgen-dependent carcinomas non-proliferative. Yet another example of a cytostatic agent is the antiestrogen Tamoxifen which inhibits the proliferation or growth of estrogen dependent breast cancer. Inhibitors of the transduction of cellular proliferative signals are cytostatic agents. Examples are epidermal growth factor inhibitors, Her-2 inhibitors, MEK-1 kinase inhibitors, MAPK kinase inhibitors, PI3 inhibitors, Src kinase inhibitors, and PDGF inhibitors.

As mentioned, certain anti-proliferative agents are antiangiogenic and antivascular agents and, by interrupting blood flow to solid tumors, render cancer cells quiescent by depriving them of nutrition. Castration, which also renders androgen dependent carcinomas non-proliferative, may also be utilized. Starvation by means other than surgical disruption of blood flow is another example of a cytostatic agent. A particular class of antivascular cytostatic agents is the combretastatins. Other exemplary cytostatic agents include MET

30

kinase inhibitors, MAP kinase inhibitors, inhibitors of non-receptor and receptor tyrosine kinases, inhibitors of integrin signaling, and inhibitors of insulin-like growth factor receptors.

Also suitable are anthracyclines (e.g., daunorubicin, doxorubicin), cytarabine (ara-C; Cytosar-U®); 6-thioguanine (Tabloid®), mitoxantrone (Novantrone®) and etoposide (Ve-Pesid®), amsacrine (AMSA), and all-trans retinoic acid (ATRA).

The compounds of the present invention may be useful in combination with BCR-ABL inhibitors such as, but not limited to, Gleevec® (imatinib, STI-571) or AMN-107, the compound shown below
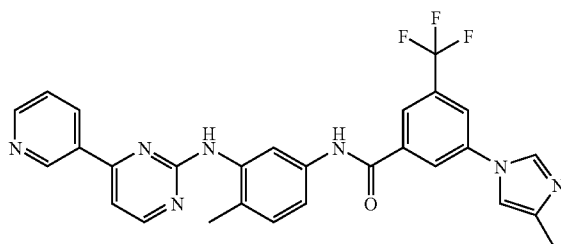
The compounds of the present invention may be useful in combination with anti-cancer compounds such as fentanyl, doxorubicin, interferon alfa-n3, palonosetron dolasetron anastrozole, exemestane, bevacizumab, bicalutamide, cisplatin, dacarbazine, cytarabine, clonidine, epirubicin, levamisole, toremifene, fulvestrant, letrozole, tamsulosin, gallium nitrate, trastuzumab, altretamine, hydroxycarbamide, ifosfamide, interferon alfacon-1, gefitinib, granisetron, leuprorelin, dronabinol, megestrol, pethidine, promethazine, morphine, vinorelbine, pegfilgrastim, filgrastim, nilutamide, thiethylperazine, leuprorelin, pegaspargase, muromonab-CD3, porfimer sodium, cisplatin, abarelix, capromab, samarium SM153 lexidronam, paclitaxel, docetaxel, etoposide, triptorelin, valrubicin, nofetumomab merpentan technetium 99m Tc, vincristine, capecitabine, strptozocin, and ondansetron.

Thus, the present invention provides methods for the treatment of a variety of cancers, including, but not limited to, the following:

carcinoma including that of the bladder (including accelerated and metastatic bladder cancer), breast, colon (including colorectal cancer), kidney, liver, lung (including small and non-small cell lung cancer and lung adenocarcinoma), ovary, prostate, testes, genitourinary tract, lymphatic system, rectum, larynx, pancreas (including exocrine pancreatic carcinoma), esophagus, stomach, gall bladder, cervix, thyroid, and skin (including squamous cell carcinoma);

hematopoietic tumors of lymphoid lineage including leukemia, acute lymphocytic leukemia, acute lymphoblastic leukemia, B-cell lymphoma, T-cell lymphoma, Hodgkin's lymphoma, non-Hodgkin's lymphoma, hairy cell lymphoma, histiocytic lymphoma, and Burketts lymphoma;

hematopoietic tumors of myeloid lineage including acute and chronic myelogenous leukemias, myelodysplastic syndrome, myeloid leukemia, and promyelocytic leukemia;

tumors of the central and peripheral nervous system including astrocytoma, neuroblastoma, glioma, and schwannomas;

tumors of mesenchymal origin including fibrosarcoma, rhabdomyoscarcoma, and osteosarcoma; and

US 7,491,725 B2

31

other tumors including melanoma, xenoderma pigmentosum, keratoactanthoma, seminoma, thyroid follicular cancer, and teratocarcinoma.

The present invention provides methods for the treatment of a variety of non-cancerous proliferative diseases.

The invention is useful to treat GIST, breast cancer, pancreatic cancer, colon cancer, NSCLC, CML, and ALL, sarcoma, and various pediatric cancers.

The compounds of the present invention are protein tyrosine kinase inhibitors and as such are useful in the treatment of immunological disorders in addition to oncological disorders. U.S. Pat. No. 6,596,746 describes the utility of the compound in immunological disorders and is hereby incorporated by reference for the description of the compound in such immunological disorders.

The present invention also encompasses a pharmaceutical composition useful in the treatment of cancer, comprising the administration of a therapeutically effective amount of the combinations of this invention, with or without pharmaceutically acceptable carriers or diluents. The pharmaceutical compositions of this invention comprise an anti-proliferative agent or agents, a formula I compound, and a pharmaceutically acceptable carrier. The methods entail the use of a neoplastic agent in combination with a Formula I compound. The compositions of the present invention may further comprise one or more pharmaceutically acceptable additional ingredient(s) such as alum, stabilizers, antimicrobial agents, buffers, coloring agents, flavoring agents, adjuvants, and the like. The antineoplastic agents, Formula I, compounds and compositions of the present invention may be administered orally or parenterally including the intravenous, intramuscular, intraperitoneal, subcutaneous, rectal and topical routes of administration.

The present invention also provides using the compounds obtained with the inventive process to further prepare pharmaceutical compositions capable of treating Src-kinase associated conditions, including the conditions described above. The said compositions may contain other therapeutic agents. Pharmaceutical compositions may be formulated by employing conventional solid or liquid vehicles or diluents, as well as pharmaceutical additives of a type appropriate to the mode of desired administration (e.g., excipients, binders, preservatives, stabilizers, flavors, etc.) according to techniques such as those well known in the art of pharmaceutical formulations.

The said pharmaceutical compositions may be administered by any means suitable for the condition to be treated, which may depend on the need for site-specific treatment or quantity of drug to be delivered. Topical administration is generally preferred for skin-related diseases, and systematic treatment preferred for cancerous or pre-cancerous conditions, although other modes of delivery are contemplated. For example, the compounds of formula (I) may be delivered orally, such as in the form of tablets, capsules, granules, powders, or liquid formulations including syrups; topically, such as in the form of solutions, suspensions, gels or ointments; sublingually; bucally; parenterally, such as by subcutaneous, intravenous, intramuscular or intrasternal injection or infusion techniques (e.g., as sterile injectable aq. or non-aq. solutions or suspensions); nasally such as by inhalation spray; topically, such as in the form of a cream or ointment; rectally such as in the form of suppositories; or liposomally. Dosage unit formulations containing non-toxic, pharmaceutically acceptable vehicles or diluents may be administered. The compounds of formula (I), prepared according to the inventive process, may be administered in a form suitable for immediate release or extended release. Immediate release or extended release may be achieved with suitable pharmaceutical compositions or, particularly in the case of extended release, with devices such as subcutaneous implants or osmotic pumps.

32

Exemplary compositions for topical administration include a topical carrier such as PLASTIBASE® (mineral oil gelled with polyethylene).

Exemplary compositions for oral administration include suspensions which may contain, for example, microcrystalline cellulose for imparting bulk, alginic acid or sodium alginate as a suspending agent, methylcellulose as a viscosity enhancer, and sweeteners or flavoring agents such as those known in the art; and immediate release tablets which may contain, for example, microcrystalline cellulose, dicalcium phosphate, starch, magnesium stearate and/or lactose and/or other excipients, binders, extenders, disintegrants, diluents and lubricants such as those known in the art. The compounds of formula (I) may also be orally delivered by sublingual and/or buccal administration, e.g., with molded, compressed, or freeze-dried tablets. Exemplary compositions may include fast-dissolving diluents such as mannitol, lactose, sucrose, and/or cyclodextrins. Also included in such formulations may be high molecular weight excipients such as celluloses (AVICEL®) or polyethylene glycols (PEG); an excipient to aid mucosal adhesion such as hydroxypropyl cellulose (HPC), hydroxypropyl methyl cellulose (HPMC), sodium carboxymethyl cellulose (SCMC), and/or maleic anhydride copolymer (e.g., GANTREZ®); and agents to control release such as polyacrylic copolymer (e.g., CARBOPOL 934®). Lubricants, glidants, flavors, coloring agents and stabilizers may also be added for ease of fabrication and use.

An example of a composition for oral administration is the compound of formula (IV), lactose monohydrate(intragranular phase), microcrystalline cellulose(intra-granular phase), croscarmellose sodium(intra-granular phase), hydroxypropyl cellulose(intra-granular phase), microcrystalline cellulose(extra-granular phase), croscarmellose sodium (extra-granular phase), and magnesium stearate(extragranular phase).

Exemplary compositions for nasal aerosol or inhalation administration include solutions which may contain, for example, benzyl alcohol or other suitable preservatives, absorption promoters to enhance absorption and/or bioavailability, and/or other solubilizing or dispersing agents such as those known in the art.

Exemplary compositions for parenteral administration include injectable solutions or suspensions which may contain, for example, suitable non-toxic, parenterally acceptable diluents or solvents, such as mannitol, 1,3-butanediol, water, Ringer's solution, an isotonic sodium chloride solution, or other suitable dispersing or wetting and suspending agents, including synthetic mono- or diglycerides, and fatty acids, including oleic acid.

Exemplary compositions for rectal administration include suppositories which may contain, for example, suitable nonirritating excipients, such as cocoa butter, synthetic glyceride esters or polyethylene glycols, which are solid at ordinary temperatures but liquefy and/or dissolve in the rectal cavity to release the drug.

The effective amount of a compound of formula (I) may be determined by one of ordinary skill in the art, and includes exemplary dosage amounts for a mammal of from about 0.05 to 100 mg/kg of body weight of active compound per day, which may be administered in a single dose or in the form of individual divided doses, such as from 1 to 4 times per day. It will be understood that the specific dose level and frequency of dosage for any particular subject may be varied and will depend upon a variety of factors, including the activity of the specific compound employed, the metabolic stability and length of action of that compound, the species, age, body weight, general health, sex and diet of the subject, the mode and time of administration, rate of excretion, drug combination, and severity of the particular condition. Preferred subjects for treatment include animals, most preferably mamma-

US 7,491,725 B2

33

lian species such as humans, and domestic animals such as dogs, cats, horses, and the like. Thus, when the term "patient" is used herein, this term is intended to include all subjects, most preferably mammalian species, that are affected by mediation of Src kinase levels.

When administered intravenously, the compounds of the present invention, including the crystalline forms of the compounds of formula IV, are administered using the formulations of the invention. In one embodiment, the compounds of the present invention, are administered by IV infusion over a period of from about 10 minutes to about 3 hours, preferably about 30 minutes to about 2 hours, more preferably about 45 minutes to 90 minutes, and most preferably about 1 hour. Typically, the compounds are administered intravenously in a dose of from about 0.5 mg/m^2 to 65 mg/m^2, preferably about 1 mg/m^2 to 50 mg/m^2, more preferably about 2.5 mg/m^2 to 30 mg/m^2, and most preferably about 25 mg/m^2.

One of ordinary skill in the art would readily know how to convert doses from mg/kg to mg/m^2 given either or both the height and or weight of the patient (See, e.g., http://www.fda.gov/cder/cancer/animalframe.htm).

As discussed above, compounds of the present invention, including the crystalline forms of the compounds of formula IV can be administered orally, intravenously, or both. In particular, the methods of the invention encompass dosing protocols such as once a day for 2 to 10 days, preferably every 3 to 9 days, more preferably every 4 to 8 days and most preferably every 5 days. In one embodiment there is a period of 3 days to 5 weeks, alternatively 4 days to 4 weeks, or 5 days to 3 weeks, or 1 week to 2 weeks, in between cycles where there is no treatment. In another embodiment the compounds of the present invention, including the crystalline forms of the compounds of formula IV can be administered orally, intravenously, or both, once a day for 3 days, with a period of 1 week to 3 weeks in between cycles where there is no treatment. In yet another embodiment the compounds of the present invention, the crystalline forms of the compounds of formula IV, can be administered orally, intravenously, or both, once a day for 5 days, with a period of 1 week to 3 weeks in between cycles where there is no treatment.

In another embodiment the treatment cycle for administration of the compounds of the present invention, the crystalline forms of the compounds of formula IV, is once daily for 5 consecutive days and the period between treatment cycles is from 2 to 10 days, or alternatively one week. In one embodiment, a compound of the present invention, for example, a compound of formula IV, is administered once daily for 5 consecutive days, followed by 2 days when there is no treatment.

The compounds of the present invention, the crystalline forms of the compounds of formula IV, can also be administered orally, intravenously, or both once every 1 to 10 weeks, every 2 to 8 weeks, every 3 to 6 weeks, alternatively every 3 weeks.

In another method of the invention, the compounds of the present invention, the crystalline forms of the compounds of formula IV, are administered in a 28 day cycle wherein the compounds are intravenously administered on days 1, 7, and 14 and orally administered on day 21. Alternatively, the compounds of the present invention, the crystalline forms of the compounds of formula IV, are administered in a 28 day cycle wherein the compound of formulae IV are orally administered on day 1 and intravenously administered on days 7, 14, and 28.

In another embodiment of the invention, the compound of formula IV may be administered in a dose of 15-200 mg twice a day, or 30-100 mg twice a day. In one embodiment, the compound of formula IV may be administered at 70 mg twice a day. In another embodiment, the compound of formula IV may be administered in a dose of 50-300 mg once a day, or

34

100-200 mg once a day. Alternatively, the compound of formula IV may be administered in a dose of 75-150 mg twice a day or 140-250 mg once a day. Alternatively, the compound of formula IV may be administered at 50, 60, 70, 80, 90, 100, 110, 120, 130 or 140 mg twice a day, or doses in between. Alternatively, the compound of formula IV may be administered at 100, 120, 140, 160, 180, 200, 220 or 240 mg once a day, or doses in between. The compound of formula IV may be administered either continuously or on an alternating schedule, such as 5 days on, 2 days off, or some other schedule as described above.

According to the methods of the invention, the compounds of the present invention, including compounds of formulae IV, are administered until the patient shows a response, for example, a reduction in tumor size, or until dose limiting toxicity is reached.

Compounds within the scope of formula (I) may be tested for activity as inhibitors of protein kinases using the assays described below, or variations thereof that are within the level ordinary skill in the art.

Cell Assays

(1) Cellular Tyrosine Phosphorylation

Jurkat T cells are incubated with the test compound and then stimulated by the addition of antibody to CD3 (monoclonal antibody G19-4). Cells are lysed after 4 minutes or at another desired time by the addition of a lysis buffer containing NP-40 detergent. Phosphorylation of proteins is detected by anti-phosphotyrosine immunoblotting. Detection of phosphorylation of specific proteins of interest such as ZAP-70 is detected by immunoprecipitation with anti-ZAP-70 antibody followed by anti-phosphotyrosine immunoblotting. Such procedures are described in Schieven, G. L., Mittler, R. S., Nadler, S. G., Kirihara, J. M., Bolen, J. B., Kanner, S. B., and Ledbetter, J. A., "ZAP-70 tyrosine kinase, CD45 and T cell receptor involvement in UV and H$_2$O$_2$ induced T cell signal transduction", *J. Biol. Chem., 269, 20718-20726 (1994), and the references incorporated therein. The Lck inhibitors inhibit the tyrosine phosphorylation of cellular proteins induced by anti-CD3 antibodies.

For the preparation of G19-4, see Hansen, J. A., Martin, P. J., Beatty, P. G., Clark, E. A., and Ledbetter, J. A., "Human T lymphocyte cell surface molecules defined by the workshop monoclonal antibodies," in *Leukocyte Typing I*, A. Bernard, J. Boumsell, J. Dausett, C. Milstein, and S. Schlossman, eds. (New York: Springer Verlag), p. 195-212 (1984); and Ledbetter, J. A., June, C. H., Rabinovitch, P. S., Grossman, A., Tsu, T. T., and Imboden, J. B., "Signal transduction through CD4 receptors: stimulatory vs. inhibitory activity is regulated by CD4 proximity to the CD3/T cell receptor", *Eur. J. Immunol., 18, 525 (1988).

(2) Calcium Assay

Lck inhibitors block calcium mobilization in T cells stimulated with anti-CD3 antibodies. Cells are loaded with the calcium indicator dye indo-1, treated with anti-CD3 antibody such as the monoclonal antibody G19-4, and calcium mobilization is measured using flow cytometry by recording changes in the blue/violet indo-1 ratio as described in Schieven, G. L., Mittler, R. S., Nadler, S. G., Kirihara, J. M., Bolen, J. B., Kanner, S. B., and Ledbetter, J. A., "ZAP-70 tyrosine kinase, CD45 and T cell receptor involvement in UV and H$_2$O$_2$ induced T cell signal transduction", *J. Biol. Chem., 269, 20718-20726 (1994), and the references incorporated therein.

(3) Proliferation Assays

Lck inhibitors inhibit the proliferation of normal human peripheral blood T cells stimulated to grow with anti-CD3 plus anti-CD28 antibodies. A 96 well plate is coated with a monoclonal antibody to CD3 (such as G19-4), the antibody is

US 7,491,725 B2

35   **36**

allowed to bind, and then the plate is washed. The antibody bound to the plate serves to stimulate the cells. Normal human peripheral blood T cells are added to the wells along with test compound plus anti-CD28 antibody to provide co-stimulation. After a desired period of time (e.g., 3 days), the [3H]-thymidine is added to the cells, and after further incubation to allow incorporation of the label into newly synthesized DNA, the cells are harvested and counted in a scintillation counter to measure cell proliferation.
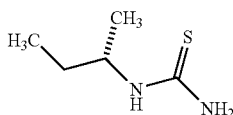
The following examples illustrate the invention but should not be interpreted as a limitation thereon.

EXAMPLES

Example 1

Preparation of Intermediate:

(S)-1-sec-Butylthiourea

To a solution of S— sec-butyl-amine (7.31 g, 0.1 mol) in chloroform (80 mL) at 0° C. was slowly added benzoyl isothiocyanate (13.44 mL, 0.1 mol). The mixture was allowed to warm to 10° C. and stirred for 10 min. The solvent was then removed under reduced pressure, and the residue was dissolved in MeOH (80 mL). An aqueous solution (10 mL) of NaOH (4 g, 0.1 mol) was added to this solution, and the mixture was stirred at 60° C. for another 2 h. The MeOH was then removed under reduced pressure, and the residue was stirred in water (50 mL). The precipitate was collected by vacuum filtration and dried to provide S-1-sec-butyl-thiourea (12.2 g, 92% yield). mp 133-134° C.; ^{1}H NMR (500 MHz, DMSO-D$_6$) δ 7.40 (s, 1H), 7.20 (br s, 1H), 6.76 (s, 1H), 4.04 (s, 1H), 1.41 (m, 2H), 1.03 (d, J=6.1 Hz, 3H), 0.81 (d, J=7.7 Hz, 3H); ^{13}C NMR (125 MHz, DMSO-D$_6$) δ 182.5, 50.8, 28.8, 19.9, 10.3; LRMS m/z 133.2 (M+H); Anal. Calcd for C$_5$H$_{12}$N$_2$S: C, 45.41; H, 9.14; N, 21.18; S, 24.25. Found: C, 45.49; H, 8.88; N, 21.32; S, 24.27.

Example 2

Preparation of Intermediate:

(R)-1-sec-Butylthiourea
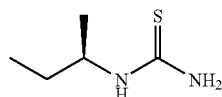
(R)-1-sec-Butylthiourea was prepared in 92% yield according to the general method outlined for Example 1. mp 133-134° C.; ^{1}H NMR(500 MHz, DMSO) δ 0.80(m, 3H, J=7.7), 1.02(d, 3H, J=6.1), 1.41(m, 2H), (3.40, 4.04)(s, 1H), 6.76(s, 1H), 7.20(s, br, 1H), 7.39(d, 1H, J=7.2); ^{13}C NMR (500 MHz, DMSO) δ: 10.00, 19.56, 28.50, 50.20, 182.00; m/z 133.23 (M+H); Anal. Calcd for C$_5$H$_{12}$N$_2$S: C, 45.41; H, 9.14; N, 21.18; S, 24.25. Found: C, 45.32; H, 9.15; N, 21.14; S, 24.38.

Example 3

Preparation of:

3A.

(3A)
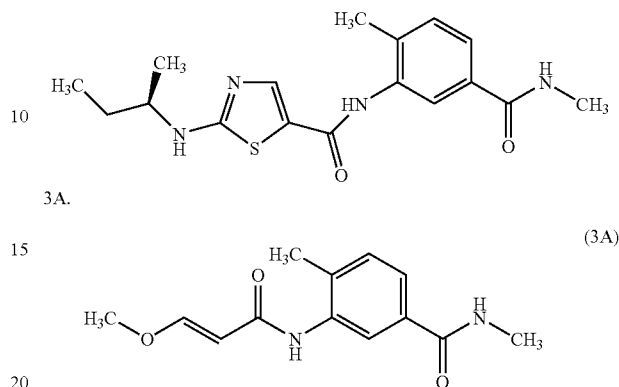
To a solution of 3-amino-N-methyl-4-methylbenzamide hydrochloride (1.0 g, 5 mmol) in acetone (10 mL) at 0° C. was added pyridine (1.2 mL, 15 mmol) dropwise via syringe. 3-Methoxyacryloyl chloride (0.72 mL. 6.5 mmol) was added and the reaction stirred at room temperature for 1 h. The solution was cooled again to 0° C. and 1N HCl (1.5 mL) was added dropwise via pipet. The reaction mixture was stirred for 5 min, then water (8.5 mL) was added via an addition funnel. The acetone was removed in vacuo and the resulting solution stirred for 4h. Crystallization began within 15 min. After stirring for 4 h, the vessel was cooled in an ice bath for 30 min, filtered, and rinsed with ice cold water (2×3 mL) to give compound 3A (0.99 g, 78% yield) as a white solid. ^{1}H NMR (400 MHz, CDCl$_3$) δ 8.95 (s, 1H), 8.12 (br s, 1H), 7.76 (s, 1H), 7.29 (m, 2H), 7.05 (d, J=7.9 Hz, 1H), 5.47 (d, J=12.3 Hz, 1H), 3.48 (s, 3H), 2.54 (d, J=4.7 Hz, 3H), 2.03 (s, 3H); HPLC rt 2.28 min (Condition A).

3B. Example 3

To a 50 mL RBF containing the above compound 3A (0.5 g, 2.0 mmol) was added THF (2.5 mL) and water (2 mL), followed by NBS (0.40 g, 2.22 mmol), and the solution was stirred for 90 min. R-sec-butylthiourea (Ex. 2) (267 mg), was added, and the solution was heated to 75° C. for 8 h. Conc. NH$_4$OH was added to adjust the pH to 10 followed by the addition of EtOH (15 mL). Water (15 mL) was added and the slurry stirred for 16 h, filtered, and washed with water to give Example 3 as a light brown solid (0.48 g, 69% yield, 98% purity). MS 347.1; HPLC 2.59.

Example 4

Preparation of:
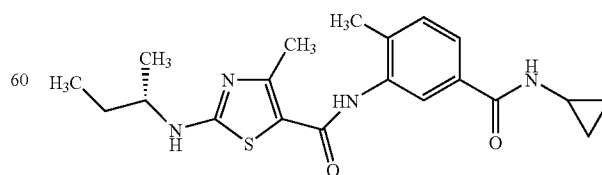
Example 4 is prepared following the methods of Example 3 but using the appropriate acryl benzamide and Example 1.

US 7,491,725 B2

37

Example 5

Preparation of:

N-(2-chloro-6-methylphenyl)-2-(6-(4-(3-hydroxy-
ethyl)piperazin-1-yl)-2-methylpyrimidin-4-ylamino)
thiazole-5-carboxamide (The Compound of Formula
(IV))

(IV)
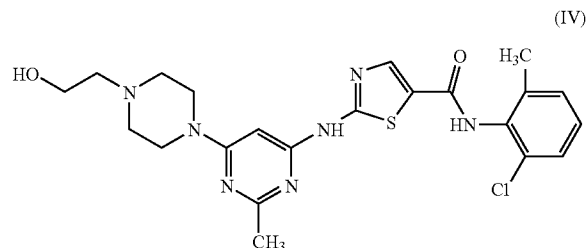
5A. 1-(6-Chloro-2-methylpyrimidin-4-yl)thiourea

(5A)
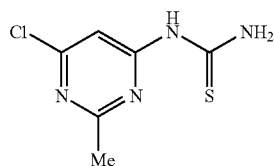
To a stirring slurry of 4-amino-5-chloro-2-methylpyrimi-
dine (6.13 g, 42.7 mmol) in THF (24 mL) was added ethyl
isothiocyanatoformate (7.5 mL, 63.6 mmol), and the mixture
heated to reflux. After 5h, another portion of ethyl isothiocy-
anato formate (1.0 mL, 8.5 mmol) was added and after 10h, a
final portion (1.5 mL, 12.7 mmol) was added and the mixture
stirred 6h more. The slurry was evaporated under vacuum to
remove most of the solvent and heptane (6 mL) added to the
residue. The solid was collected by vacuum filtration and
washed with heptane (2×5 mL) giving 8.01 g (68% yield) of
the intermediate ethyl 6-chloro-2-methylpyrimidin-4-ylcar-
bamothioylcarbamate.

A solution of ethyl 6-chloro-2-methylpyrimidin-4-ylcar-
bamothioylcarbamate (275 mg, 1.0 mmol) and 1N sodium
hydroxide (3.5 eq) was heated and stirred at 50° C. for 2h. The
resulting slurry was cooled to 20-22° C. The solid was col-
lected by vacuum filtration, washed with water, and dried to
give 185 mg of 1-(6-chloro-2-methylpyrimidin-4-yl)thiourea
(91% yield). ^{1}H NMR (400 MHz, DMSO-d6): δ2.51 (S, 3H),
7.05 (s, 1H), 9.35 (s,1H), 10.07 (s, 1H), 10.91 (s, 1H); [13]C
NMR (125 MHz, DMSO-d6) δ: 25.25, 104.56, 159.19,
159.33, 167.36, 180.91.

38

5B. (E)-N-(2-Chloro-6-methylphenyl)-3-ethoxyacry-
lamide

(5B)
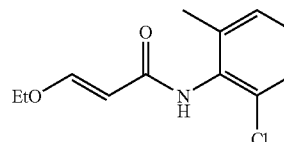
To a cold stirring solution of 2-chloro-6-methylaniline
(59.5 g 0.42 mol) and pyridine (68 ml, 0.63 mol) in THF (600
mL) was added 3-ethoxyacryloyl chloride (84.7 g, 0.63 mol)
slowly keeping the temp at 0-5° C. The mixture was then
warmed and stirred for 2 h. at 20° C. Hydrochloric acid (1N,
115 mL) was added at 0-10° C. The mixture was diluted with
water (310 mL) and the resulting solution was concentrated
under vacuum to a thick slurry. The slurry was diluted with
toluene (275 mL) and stirred for 15 min. at 20-22° C. then 1
h. at 0° C. The solid was collected by vacuum filtration,
washed with water (2×75 mL) and dried to give 74.1 g (73.6%
yield) of (E)-N-(2-chloro-6-methylphenyl)-3-ethoxyacryla-
mide). ^{1}H NMR (400 Hz, DMSO-d6) δ 1.26 (t, 3H, J=7 Hz),
2.15 (s, 3H), 3.94 (q, 2H, J=7 Hz), 5.58 (d, 1H, J=12.4 Hz),
7.10-7.27 (m, 2H, J=7.5 Hz), 7.27-7.37 (d, 1H, J=7.5 Hz),
7.45(d, 1H, J=12.4 Hz), 9.28 (s, 1H); ^{13}C NMR (100 MHz,
CDCl3) δ: 14.57, 18.96, 67.17, 97.99, 126.80, 127.44,
129.07, 131.32, 132.89, 138.25, 161.09, 165.36.

5C. 2-Amino-N-(2-chloro-6-methylphenyl)thiazole-
5-carboxamide

(5C)
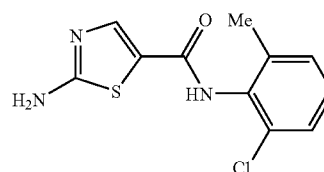
To a mixture of compound 5B (5.00 g, 20.86 mmol) in
1,4-dioxane (27 mL) and water (27 mL) was added NBS (4.08
g, 22.9 mmol) at −10 to 0° C. The slurry was warmed and
stirred at 20-22° C. for 3h. Thiourea (1.60 g, 21 mmol) was
added and the mixture heated to 80° C. After 2h, the resulting
solution was cooled to 20-22° and conc. ammonium hydrox-
ide (4.2 mL) was added dropwise. The resulting slurry was
concentrated under vacuum to about half volume and cooled
to 0-5° C. The solid was collected by vacuum filtration,
washed with cold water (10 mL), and dried to give 5.3 g
(94.9% yield) of 2-amino-N-(2-chloro-6-methylphenyl)thia-
zole-5-carboxamide. ^{1}H NMR (400 MHz, DMSO-d6) δ δ
2.19 (s, 3H), 7.09-7.29 (m, 2H, J=7.5), 7.29-7.43 (d, 1H,
J=7.5), 7.61 (s, 2H), 7.85 (s, 1H), 9.63 (s, 1H); ^{13}C NMR (125
MHz, DMSO-d6) δ: 18.18, 120.63, 126.84, 127.90, 128.86,
132.41, 133.63, 138.76, 142.88, 159.45, 172.02.

US 7,491,725 B2

<table>
<tr><td>39</td><td>40</td></tr>
</table>

5D. 2-(6-Chloro-2-methylpyrimidin-4-ylamino)-N-(2-chloro-6-methylphenyl)thiazole-5-carboxamide

(5D)
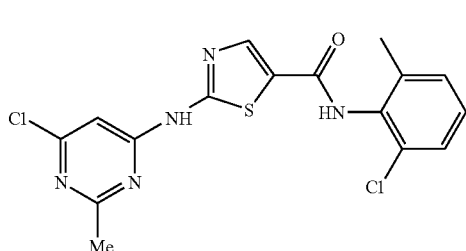
To a stirring solution of compound 5C (5.00 g, 18.67 mmol) and 4,6-dichloro-2-methylpyrimidine (3.65 g 22.4/ mmol) in THF (65 mL) was added a 30% wt. solution of sodium t-butoxide in THF (21.1 g, 65.36 mmol) slowly with cooling to keep the temperature at 10-20° C. The mixture was stirred at room temperature for 1.5 h and cooled to 0-5° C. Hydrochloric acid, 2N (21.5 mL) was added slowly and the mixture stirred 1.75 h at 0-5° C. The solid was collected by vacuum filtration, washed with water (15 mL) and dried to give 6.63 g (86.4% yield) of compound 5D. ^{1}H NMR (400 MHz, DMSO-d$_6$) δ 2.23 (s, 3H), 2.58 (s, 3H), 6.94 (s, 1H), 7.18-7.34, (m, 2H, J=7.5), 7.34-7.46 (d, 1H, J=7.5), 8.31 (s, 1H), 10.02 (s, 1H), 12.25 (s, 1H).

5E. Example 5

To a mixture of compound 5D (4.00 g, 10.14 mmol) and hydroxyethylpiperazine (6.60 g, 50.69 mmol) in n-butanol (40 mL) was added DIPEA (3.53 mL, 20.26 mmol). The slurry was heated at 118° C. for 4.5 h, then cooled slowly to room temperature. The solid was collected by vacuum filtration, washed with n-butanol (5 mL), and dried. The product (5.11 g) was dissolved in hot 80% EtOH—H$_2$O (80 mL), and the solution was clarified by filtration. The hot solution was slowly diluted with water (15 mL) and cooled slowly to room temperature. The solid was collected by vacuum filtration, washed with 50% ethanol-water (5 mL) and dried affording 4.27 g (83.2% yield) of N-(2-chloro-6-methylphenyl)-2-(6-(4-(3-hydroxyethyl)piperazin-1-yl)-2-methylpyrimidin-4-ylamino)thiazole-5-carboxamide as monohydrate. ^{1}H NMR (400 MHz, DMSO-d$_6$) δ 2.23 (s, 3H), 2.40 (s, 3H), 2.42 (t, 2H, J=6), 2.48 (t, 4H, J=6.3), 3.50 (m, 4H), 3.53 (q, 2H, J=6), 4.45 (t, 1H, J=5.3), 6.04 (s, 1H), 7.25 (t, 1H, J=7.6), 7.27 (dd, 1H, J=7.6, 1.7), 7.40 (dd, 1H, J=7.6, 1.7), 8.21 (s, 1H), 9.87 (s, 1H), 11.47.

Example 6

Preparation of:

N-(2-chloro-6-methylphenyl)-2-(6-(4-(3-hydroxy-ethyl)piperazin-1-yl)-2-methylpyrimidin-4-ylamino)thiazole-5-carboxamide

(IV)
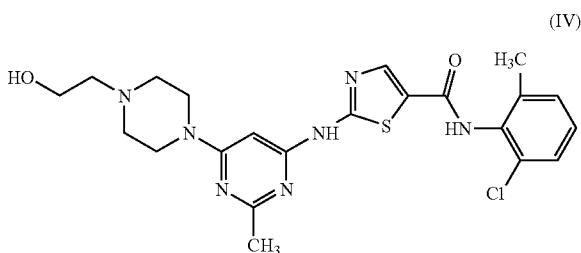
To a slurry of (E)-N-(2-chloro-6-methylphenyl)-3-ethoxy-acrylamide 5B (120 mg, 0.50 mmol) in THF (0.75 ml) and water (0.5 mL) was added NBS (98 mg, 0.55 mmol) at 0° C. The mixture was warmed and stirred at 20-22° C. for 3h. To this was added 1-(6-chloro-2-methylpyrimidin-4-yl)thiourea 5A (100 mg, 0.49 mmol), and the slurry heated and stirred at reflux for 2h. The slurry was cooled to 20-22° C. and the solid collected by vacuum filtration giving 140 mg (71% yield) of 2-(6-chloro-2-methylpyrimidin-4-ylamino)-N-(2-chloro-6-methylphenyl)thiazole-5-carboxamide 5D. ^{1}H NMR (400 MHz, DMSO-d$_6$) δ 2.23 (s, 3H), 2.58 (s, 3H), 6.94 (s, 1H), 7.18-7.34, (m, 2H, J=7.5), 7.34-7.46 (d, 1H, J=7.5), 8.31 (s, 1H), 10.02 (s, 1H), 12.25 (s, 1H).

Compound 5D was elaborated to N-(2-chloro-6-meth-ylphenyl)-2-(6-(4-(3-hydroxyethyl)piperazin-1-yl)-2-meth-ylpyrimidin-4-ylamino)thiazole-5-carboxamide, following Step 5E.

Example 7

Preparation of:

N-(2-chloro-6-methylphenyl)-2-(6-(4-(3-hydroxy-ethyl)piperazin-1-yl)-2-methylpyrimidin-4-ylamino)thiazole-5-carboxamide

7A. 2-[4-(6-Chloro-2-methyl-pyrimidin-4-yl)-piper-azin-1-yl]-ethanol
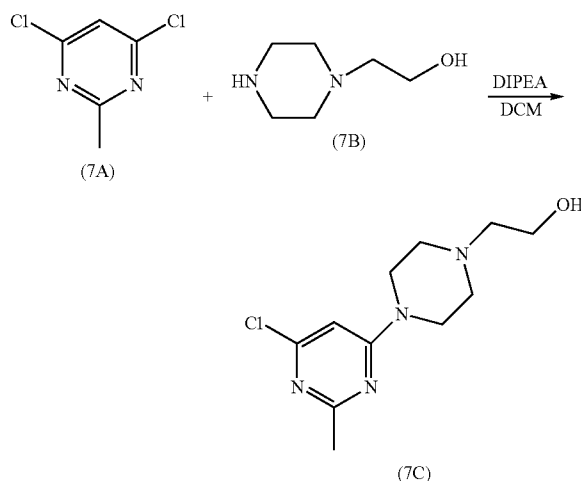
2-piperazin-1-yl-ethanol (8.2 g, 63.1 mmol) was added to a solution of 4,6-dichloro-2-methylpyrimidine (5.2 g, 31.9 mmol) in dichloromethane (80 ml) at rt. The mixture was stirred for two hours and triethylamine (0.9 ml) was added. The mixture was stirred at rt for 20h. The resultant solid was filtered. The cake was washed with dichloromethane (20 ml). The filtrate was concentrated to give an oil. This oil was dried under high vacuum for 20h to give a solid. This solid was stirred with heptane (50 ml) at rt for 5h. Filtration gave 7C (8.13 g) as a white solid

US 7,491,725 B2

41

7B. Example 7

(5C)

(7C)

Pd(OAc)2/BINAP/Toluene

(IV)
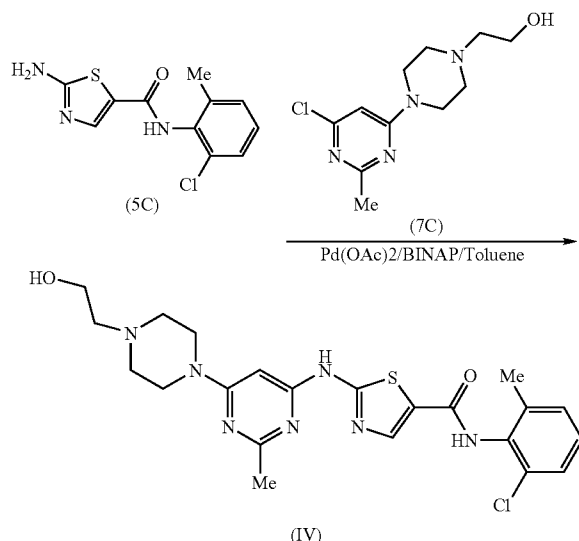
To a 250 ml of round bottom flask were charged compound 5C (1.9 g, 7.1 mmol), compound 7C (1.5 g, 5.9 mmol), K_2CO_3 (16 g, 115.7 mmol), Pd $(OAc)_2$ (52 mg, 0.23 mmol) and BINAP (291 mg, 0.46 mmol). The flask was placed under vacuum and flushed with nitrogen. Toluene was added (60 ml). The suspension was heated to 100-110° C. and stirred at this temperature for 20h. After cooling to room temperature, the mixture was applied to a silica gel column. The column was first eluted with EtOAC, and then with 10% of MeOH in EtOAC. Finally, the column was washed with 10% 2M ammonia solution in MeOH/90% EtOAC. The fractions which contained the desired product were collected and concentrated to give compound IV as a yellow solid (2.3 g).

Analytical Methods

Solid State Nuclear Magnetic Resonance (SSNMR)

All solid-state C-13 NMR measurements were made with a Bruker DSX-400, 400 MHz NMR spectrometer. High resolution spectra were obtained using high-power proton decoupling and the TPPM pulse sequence and ramp amplitude cross-polarization (RAMP-CP) with magic-angle spinning (MAS) at approximately 12 kHz (A. E. Bennett et al, *J. Chem. Phys.*, 1995, 103, 6951), (G. Metz, X. Wu and S. O. Smith, *J. Magn. Reson. A.,* 1994, 110, 219-227). Approximately 70 mg of sample, packed into a canister-design zirconia rotor was used for each experiment. Chemical shifts (δ) were referenced to external adamantane with the high frequency resonance being set to 38.56 ppm (W. L. Earl and D. L. Vander-Hart, *J. Magn. Reson.,* 1982, 48, 35-54).

X-Ray Powder Diffraction

One of ordinary skill in the art will appreciate that an X-ray diffraction pattern may be obtained with a measurement error that is dependent upon the measurement conditions employed. In particular, it is generally known that intensities in a X-ray diffraction pattern may fluctuate depending upon measurement conditions employed. It should be further understood that relative intensities may also vary depending upon experimental conditions and, accordingly, the exact order of intensity should not be taken into account. Additionally, a measurement error of diffraction angle for a conven-

42

tional X-ray diffraction pattern is typically about 5% or less, and such degree of measurement error should be taken into account as pertaining to the aforementioned diffraction angles. Consequently, it is to be understood that the crystal forms of the instant invention are not limited to the crystal forms that provide X-ray diffraction patterns completely identical to the X-ray diffraction patterns depicted in the accompanying Figures disclosed herein. Any crystal forms that provide X-ray diffraction patterns substantially identical to those disclosed in the accompanying Figures fall within the scope of the present invention. The ability to ascertain substantial identities of X-ray diffraction patterns is within the purview of one of ordinary skill in the art.

X-Ray powder diffraction data for the crystalline forms of Compound (IV) were obtained using a Bruker GADDS (BRUKER AXS, Inc., 5465 East Cheryl Parkway Madison, Wis. 53711 USA) (General Area Detector Diffraction System) manual chi platform goniometer. Powder samples were placed in thin walled glass capillaries of 1 mm or less in diameter; the capillary was rotated during data collection. The sample-detector distance was 17 cm. The radiation was Cu Kα (45 kV 111 mA, λ=1.5418 Å). Data were collected for 3<2θ<35° with a sample exposure time of at least 300 seconds.

Single Crystal X-Ray

All single crystal data were collected on a Bruker-Nonius (BRUKER AXS, Inc., 5465 East Cheryl Parkway Madison, Wis. 53711 USA) Kappa CCD 2000 system using Cu Kα radiation (λ=1.5418 Å) and were corrected only for the Lorentz-polarization factors. Indexing and processing of the measured intensity data were carried out with the HKL2000 software package (Otwinowski, Z. & Minor, W. (1997) in *Macromolecular Crystallography*, eds. Carter, W. C. Jr & Sweet, R. M. (Academic, NY), Vol. 276, pp. 307-326) in the Collect program suite (Data collection and processing user interface: Collect: Data collection software, R. Hooft, Nonius B. V., 1998).

The structures were solved by direct methods and refined on the basis of observed reflections using either the SDP (SDP, Structure Determination Package, Enraf-Nonius, Bohemia NY 11716 Scattering factors, including f' and f", in the SDP software were taken from the "International Tables for Crystallography", Kynoch Press, Birmingham, England, 1974; Vol IV, Tables 2.2A and 2.3.1) software package with minor local modifications or the crystallographic package, MAXUS (maXus solution and refinement software suite: S. Mackay, C. J. Gilmore, C. Edwards, M. Tremayne, N. Stewart, K. Shankland. maXus: a computer program for the solution and refinement of crystal structures from diffraction data).

The derived atomic parameters (coordinates and temperature factors) were refined through full matrix least-squares. The function minimized in the refinements was $\Sigma_w(|F_o|-|F_c|)^2$. R is defined as $\Sigma||F_o|-|F_c||/\Sigma|F_o|$ while $R_w=[\Sigma_w(|F_o|-|F_c|)_2/\Sigma_w|F_o|^2]^{1/2}$ where w is an appropriate weighting function based on errors in the observed intensities. Difference maps were examined at all stages of refinement. Hydrogens were introduced in idealized positions with isotropic temperature factors, but no hydrogen parameters were varied.

The derived atomic parameters (coordinates and temperature factors) were refined through full matrix least-squares. The function minimized in the refinements was $\Sigma_w(|F_o|-|F_c|)^2$. R is defined as $\Sigma||F_o|-|F_c||/\Sigma|F_o|$ while $R_w=[\Sigma_w(|F_o|-|F_c|)_2/\Sigma_w|F_o|^2]^{1/2}$ where w is an appropriate weighting function based on errors in the observed intensities. Difference maps were examined at all stages of refinement. Hydrogens were introduced in idealized positions with isotropic temperature factors, but no hydrogen parameters were varied

US 7,491,725 B2

<div style="text-align:center">43</div>

Differential Scanning Calorimetry

The DSC instrument used to test the crystalline forms was a TA Instruments® model Q1000. The DSC cell/sample chamber was purged with 100 ml/min of ultra-high purity nitrogen gas. The instrument was calibrated with high purity indium. The accuracy of the measured sample temperature with this method is within about +/−1° C., and the heat of fusion can be measured within a relative error of about +/−5%. The sample was placed into an open aluminum DSC pan and measured against an empty reference pan. At least 2 mg of sample powder was placed into the bottom of the pan and lightly tapped down to ensure good contact with the pan. The weight of the sample was measured accurately and recorded to a hundredth of a milligram. The instrument was programmed to heat at 10° C. per minute in the temperature range between 25 and 350° C.

The heat flow, which was normalized by a sample weight, was plotted versus the measured sample temperature. The data were reported in units of watts/gram ("W/g"). The plot was made with the endothermic peaks pointing down. The endothermic melt peak was evaluated for extrapolated onset temperature, peak temperature, and heat of fusion in this analysis.

Thermogravimetric Analysis (TGA)

The TGA instrument used to test the crystalline forms was a TA Instruments® model Q500. Samples of at least 10 milligrams were analyzed at a heating rate of 10° C. per minute in the temperature range between 25° C. and about 350° C.

<div style="text-align:center">Example 8</div>

Preparation of:

<div style="text-align:center">crystalline monohydrate of N-(2-chloro-6-meth-
ylphenyl)-2-(6-(4-(3-hydroxyethyl)piperazin-1-yl)-2-
methylpyrimidin-4-ylamino)thiazole-5-carboxamide
(IV)</div>

An example of the crystallization procedure to obtain the crystalline monohydrate form is shown here:

Charge 48 g of the compound of formula (IV).

Charge approximately 1056 mL (22 mL/g) of ethyl alcohol, or other suitable alcohol.

Charge approximately 144 mL of water.

Dissolve the suspension by heating to approximately 75° C.

Optional: Polish filter by transfer the compound of formula (IV) solution at 75° C. through the preheated filter and into the receiver.

Rinse the dissolution reactor and transfer lines with a mixture of 43 mL of ethanol and 5 mL of water.

Heat the contents in the receiver to 75-80° C. and maintain 75-80° C. to achieve complete dissolution.

Charge approximately 384 mL of water at a rate such that the batch temperature is maintained between 75-80° C.

Cool to 75° C., and, optionally, charge monohydrate seed crystals. Seed crystals are not essential to obtaining monohydrate, but provide better control of the crystallization.

Cool to 70° C. and maintain 70° C. for ca. 1 h.

Cool from 70 to 5 C over 2 h, and maintain the temperature between 0 at 5° C. for at least 2 h.

Filter the crystal slurry.

Wash the filter cake with a mixture of 96 mL of ethanol and 96 mL of water.

Dry the material at ≦50° C. under reduced pressure until the water content is 3.4 to 4.1% by KF to afford 41 g (85 M %).

<div style="text-align:center">44</div>

Alternately, the monohydrate can be obtained by:

1) An aqueous solution of the acetate salt of compound IV was seeded with monohydrate and heated at 80° C. to give bulk monohydrate.

2) An aqueous solution of the acetate salt of compound IV was seeded with monohydrate. On standing several days at room temperature, bulk monohydrate had formed.

3) An aqueous suspension of compound IV was seeded with monohydrate and heated at 70° C. for 4 hours to give bulk monohydrate. In the absence of seeding, an aqueous slurry of compound IV was unchanged after 82 days at room temperature.

4) A solution of compound IV in a solvent such as NMP or DMA was treated with water until the solution became cloudy and was held at 75-85° C. for several hours. Monohydrate was isolated after cooling and filtering.

5) A solution of compound IV in ethanol, butanol, and water was heated. Seeds of monohydrate were added to the hot solution and then cooled. Monohydrate was isolated upon cooling and filtration.

One of ordinary skill in the art will appreciate that the monohydrate of the compound of formula (IV) may be represented by the XRPD as shown in FIG. 1 or by a representative sampling of peaks as shown in Table 1.

Representative peaks taken from the XRPD of the monohydrate of the compound of formula (IV) are shown in Table 1.

<div style="text-align:center">TABLE 1</div>

2-Theta	d(Å)	Height
17.994	4.9257	915
18.440	4.8075	338
19.153	4.6301	644
19.599	4.5258	361
21.252	4.1774	148
24.462	3.6359	250
25.901	3.4371	133
28.052	3.1782	153

The XRPD is also characterized by the following list comprising 2θ values selected from the group consisting of: 4.6 ± 0.2, 11.2 ± 0.2, 13.8 ± 0.2, 15.2 ± 0.2, 17.9 ± 0.2, 19.1 ± 0.2, 19.6 ± 0.2, 23.2 ± 0.2, 23.6 ± 0.2. The XRPD is also characterized by the list of 2θ values selected from the group consisting of: 18.0 ± 0.2, 18.4 ± 0.2, 19.2 ± 0.2, 19.6 ± 0.2, 21.2 ± 0.2, 24.5 ± 0.2, 25.9 ± 0.2, and 28.0 ± 0.2.

Single crystal x-ray data was obtained at room temperature ($+25°$ C.). The molecular structure was confirmed as a monohydrate form of the compound of Formula (IV).

The following unit cell parameters were obtained for the monohydrate of the compound of formula (IV) from the x-ray analysis at 25° C.:

a(Å)=13.8632(7); b(Å)=9.3307(3); c(Å)=38.390(2);

V(Å^3) 4965.9(4); Z'=1; Vm=621

Space group Pbca

Molecules/unit cell 8

Density (calculated) (g/cm^3) 1.354

Wherein Z'=number of drug molecules per asymmetric unit. Vm=V(unit cell)/(Z drug molecules per cell).

Single crystal x-ray data was also obtained at −50° C. The monohydrate form of the compound of Formula (IV) is characterized by unit cell parameters approximately equal to the following:

US 7,491,725 B2

<table>
<tr><td>45</td><td>46</td></tr>
</table>

Cell dimensions:

a(Å)=13.862(1);

b(Å)=9.286(1);

c(Å)=38.143(2);

Volume=4910(1) Å^3

Space group Pbca

Molecules/unit cell 8

Density (calculated) (g/cm^3) 1.369

wherein the compound is at a temperature of about −50° C.

The simulated XRPD was calculated from the refined atomic parameters at room temperature.

The monohydrate of the compound of formula (IV) is represented by the DSC as shown in FIG. **2**. The DSC is characterized by a broad peak between approximately 95° C. and 130° C. This peak is broad and variable and corresponds to the loss of one water of hydration as seen in the TGA graph. The DSC also has a characteristic peak at approximately 287° C. which corresponds to the melt of the dehydrated form of the compound of formula (IV).

The TGA for the monohydrate of the compound of Formula (IV) is shown in FIG. **2** along with the DSC. The TGA shows a 3.48% weight loss from 50° C. to 175° C. The weight loss corresponds to a loss of one water of hydration from the compound of Formula (IV).

The monohydrate may also be prepared by crystallizing from alcoholic solvents, such as methanol, ethanol, propanol, i-propanol, butanol, pentanol, and water.

Example 9

Preparation of:

crystalline n-butanol solvate of N-(2-chloro-6-methylphenyl)-2-(6-(4-(3-hydroxyethyl)piperazin-1-yl)-2-methylpyrimidin-4-ylamino)thiazole-5-carboxamide (IV)

The crystalline butanol solvate of the compound of formula (IV) is prepared by dissolving compound (IV) in 1-butanol at reflux (116-118° C.) at a concentration of approximately 1 g/25 mL of solvent. Upon cooling, the butanol solvate crystallizes out of solution. Filter, wash with butanol, and dry.

The following unit cell parameters were obtained from the x-ray analysis for the crystalline butanol solvate, obtained at room temperature:

a(Å)=22.8102(6);   b(Å)=8.4691(3);   c(Å)=15.1436(5); β=95.794(2);

V(Å^3) 2910.5(2); Z'=1; Vm=728

Space group P2$_1$/a

Molecules/unit cell 4

Density (calculated) (g/cm^3) 1.283

Wherein Z'=number of drug molecules per asymmetric unit. Vm=V(unit cell)/(Z drug molecules per cell).

One of ordinary skill in the art will appreciate that the butanol solvate of the compound of formula (IV) may be represented by the XRPD as shown in FIG. **3** or by a representative sampling of peaks. Representative peaks for the crystalline butanol solvate are 2θ values of: 5.9±0.2, 12.0±0.2, 13.0±0.2, 17.7±0.2, 24.1±0.2, and 24.6±0.2.

Example 10

Preparation of:

crystalline ethanol solvate of N-(2-chloro-6-methylphenyl)-2-(6-(4-(3-hydroxyethyl)piperazin-1-yl)-2-methylpyrimidin-4-ylamino)thiazole-5-carboxamide (IV)
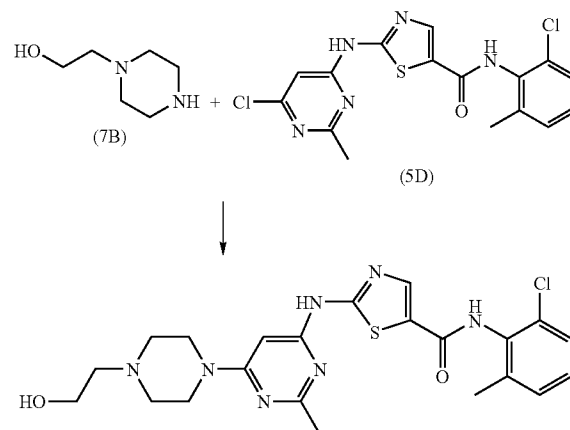
To a 100-mL round bottom flask was charged 4.00 g (10.1 mmol) of 5D (contained 2.3 Area % 5C) 6.60 g (50.7 mmol) of 7B, 80 mL of n-butanol and 2.61 g (20.2 mmol) of DIPEA. The resulting slurry was heated to 120° C. and maintained at 120° C. for 4.5 h whereby HPLC analysis showed 0.19 relative Area % of residual 5D to compound IV. The homogeneous mixture was cooled to 20° C. and left stirring overnight. The resulting crystals were filtered. The wet cake was washed twice with 10-mL portions of n-butanol to afford a white crystalline product. HPLC analysis showed this material to contain 99.7 Area % compound IV and 0.3 Area % 5C.

The resulting wet cake was returned to the 100-mL reactor, and charged with 56 mL (12 mL/g) of 200 proof ethanol. At 80° C. an additional 25 mL of ethanol was added. To this mixture was added 10 mL of water resulting in rapid dissolution. Heat was removed and crystallization was observed at 75-77° C. The crystal slurry was further cooled to 20° C. and filtered. The wet cake was washed once with 10 mL of 1:1 ethanol: water and once with 10 mL of n-heptane. The wet cake contained 1.0% water by KF and 8.10% volatiles by LOD. The material was dried at 60° C./30 in Hg for 17 h to afford 3.55 g (70 M %) of material containing only 0.19% water by KF, 99.87 Area % by HPLC. The ^{1}H NMR spectrum, however revealed that the ethanol solvate had been formed.

The following unit cell parameters were obtained from the x-ray analysis for the crystalline ethanol solvate (di-ethanolate, E2-1), obtained at −40° C.:

a(Å)=22.076(1);   b(Å)=8.9612(2);   c(Å)=16.8764(3); β=114.783(1);

V(Å^3) 3031.1(1); Z'=1; Vm=758

Space group P2$_1$/a

Molecules/unit cell 4

Density (calculated) (g/cm^3) 1.271

Wherein Z'=number of drug molecules per asymmetric unit. Vm=V(unit cell)/(Z drug molecules per cell).

One of ordinary skill in the art will appreciate that the ethanol solvate (E2-1) of the compound of formula (IV) may be represented by the XRPD as shown in FIG. **4** or by a representative sampling of peaks. Representative peaks for

US 7,491,725 B2

47

the crystalline ethanol solvate are 2θ values of: 5.8±0.2, 11.3±0.2, 15.8±0.2, 17.2±0.2, 19.5±0.2, 24.1±0.2, 25.3±0.2, and 26.2±0.2.

In addition, during the process to form the ethanolate (diethanolate) the formation of another ethanol solvate (½ ethanolate, T1E2-1) has been observed. To date this additional ethaonol solvate is known strictly as a partial desolvation product of the original diethanolate form E2-1, and has only been observed on occasion during crystallization of E2-1

The following unit cell parameters were obtained from the x-ray analysis for the crystalline ½ ethanol solvate T1E2-1, obtained at −10° C.:

a(Å)=22.03(2); b(Å)=9.20(1); c(Å)=12.31(1);
β=93.49(6)
V(Å^3) 2491(4)); Z'=1; Vm=623;
Space group P2$_1$/a
Molecules/unit cell 4
Density (calculated) (g/cm^3) 1.363

Wherein Z'=number of drug molecules per asymmetric unit. Vm=V(unit cell)/(Z drug molecules per cell).

One of ordinary skill in the art will appreciate that the ethanol solvate (T1E2-1) of the compound of formula (IV) may be represented by the XRPD as shown in FIG. 7 or by a representative sampling of peaks. Representative peaks for the crystalline ethanol solvate are 2θ values of: 7.20±0.2, 12.01±0.2, 12.81±0.2, 18.06±0.2, 19.30±0.2, and 25.24±0.2.

Example 11

Preparation of:

crystalline N-(2-chloro-6-methylphenyl)-2-(6-(4-(3-hydroxyethyl)piperazin-1-yl)-2-methylpyrimidin-4-ylamino)thiazole-5-carboxamide (IV) (Neat form N-6)

To a mixture of compound 5D (175.45 g, 0.445 mol) and hydroxyethylpiperazine (289.67 g, 2.225 mol) in NMP (1168 mL) was added DIPEA (155 mL, 0.89 mol). The suspension was heated at 110° C. (solution obtained) for 25 min., then cooled to about 90° C. The resulting hot solution was added dropwise into hot (80° C.) water (8010) mL, keeping the temperature at about 80° C. The resulting suspension was stirred 15 min at 80° C. then cooled slowly to room temperature. The solid was collected by vacuum filtration, washed with water (2×1600 mL) and dried in vacuo at 55-60° C. affording 192.45 g (88.7% yield) of N-(2-chloro-6-methylphenyl)-2-(6-(4-(3-hydroxyethyl)piperazin-1-yl)-2-methylpyrimidin-4-ylamino)thiazole-5-carboxamide. ^{1}H NMR (400 MHz, DMSO-d$_6$): δ 2.24 (s, 3H), 2.41 (s, 3H), 2.43 (t, 2H, J=6), 2.49 (t, 4H, J=6.3), 3.51 (m, 4H), 3.54 (q, 2H, J=6), 4.46 (t, 1H, J=5.3), 6.05 (s, 1H), 7.26 (t, 1H, J=7.6), 7.28 (dd, 1H, J=7.6, 1.7), 7.41 (dd, 1H, J=7.6, 1.7), 8.23 (s, 1H), 9.89 (s, 1H), 11.48. KF0.84; DSC: 285.25° C. (onset), 286.28° C. (max).

The following unit cell parameters were obtained from the x-ray analysis for the neat crystalline compound IV, obtained at 23° C.:

a(Å)=22.957(1);   b(Å)=8.5830(5);   c(Å)=13.803(3);
β=112.039(6);
V(Å^3)=2521.0(5); Z'=1; Vm=630
Space group P2$_1$/a
Molecules/unit cell 4
Density (calculated) (g/cm^3) 1.286

Wherein Z'=number of drug molecules per asymmetric unit. Vm=V(unit cell)/(Z drug molecules per cell).

One of ordinary skill in the art will appreciate that the crystalline form of the compound of formula (IV) may be

48

represented by the XRPD as shown in FIG. 5 or by a representative sampling of peaks. Representative peaks for the crystalline neat form (N-6) are 2θ values of: 6.8±0.2, 11.1±0.2, 12.3±0.2, 13.2±0.2, 13.7±0.2, 16.7±0.2, 21.0±0.2, 24.3±0.2, and 24.8±0.2.

Example 12

Preparation of:

crystalline N-(2-chloro-6-methylphenyl)-2-(6-(4-(3-hydroxyethyl)piperazin-1-yl)-2-methylpyrimidin-4-ylamino)thiazole-5-carboxamide (IV) (neatform T1H1-7)

The title neat form may be prepared by heating the monohydrate form of the compound of formula (IV) above the dehydration temperature.

The following unit cell parameters were obtained from the x-ray analysis for the neat crystalline (T1H1-7) compound IV, obtained at 25° C.:

a(Å)=13.4916; b(Å)=9.3992(2); c(Å)=38.817(1);
V(Å^3)=4922.4(3); Z'=1; Vm=615
Space group Pbca
Density (calculated) (g/cm^3) 1.317

Wherein Z'=number of drug molecules per asymmetric unit. Vm=V(unit cell)/(Z drug molecules per cell).

One of ordinary skill in the art will appreciate that the neat crystalline form (T1H1-7) of the compound of formula (IV) may be represented by the XRPD as shown in FIG. 6 or by a representative sampling of peaks. Representative peaks for the crystalline neat form (T1H1-7)) are 2θ values of: 8.0±0.2, 9.7±0.2, 11.2±0.2, 13.3±0.2, 17.5±0.2, 18.9±0.2, 21.0±0.2, 22.0±0.2.

Obviously, numerous modifications and variations of the present invention are possible in light of the above teachings. It is therefore to be understood that within the scope of the appended claims, the invention may be practiced otherwise than as specifically described herein.

What we claim is:

1. Crystalline monohydrate of the compound of formula (IV)
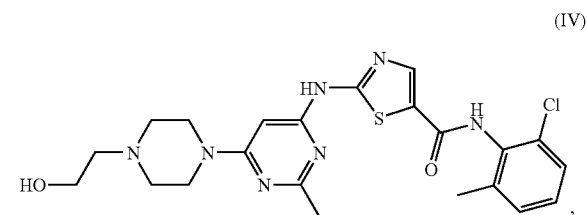
(IV)

which is characterized by an x-ray powder diffraction pattern substantially in accordance with that shown in FIG. 1.

2. The compound of claim 1, which is characterized by differential scanning calorimetry thermogram and a thermogravimetric anaylsis substantially in accordance with that shown in FIG. 2.

US 7,491,725 B2

49 50

3. Crystalline monohydrate of the compound of formula (IV)
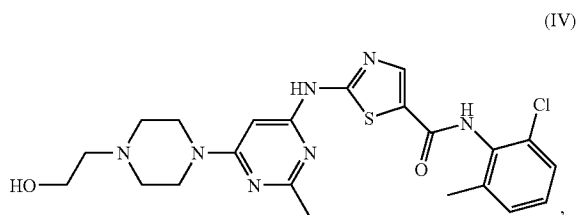
(IV)

,

which is characterized by an x-ray powder diffraction pattern (CuKα γ=1.5418 Å at a temperature of about 23° C.) comprising four or more 2θ values selected from the group consisting of: 18.0±0.2, 18.4±0.2, 19.2±0.2, 19.6±0.2, 21.2±0.2, 24.5±0.2, 25.9±0.2, and 28.0±0.2.

4. A solid pharmaceutical composition comprising a therapeutically effective amount of the compound of claim **3** and a pharmaceutically acceptable carrier.

5. The compound of claim **3**, characterized by unit cell parameters approximately equal to the following:

Cell dimensions:
a(Å)=13.8632(7);
b(Å)=9.3307(3);
c(Å)=38.390(2);
Volume=4965.9(4) Å^3
Space group Pbca
Molecules/unit cell 8
Density (calculated) (g/cm^3) 1.354.

6. A process for preparing the compound of claim **3** comprising heating and dissolving the compound of formula (IV) in an ethanol/water mixture and crystallizing the monohydrate from the ethanol/water mixture as it cools.

7. The process of claim **6**, wherein a butanol solvate of the compound of formula (IV) is dissolved in the ethanol/water mixture.

8. The compound of claim **3**, wherein the compound is substantially pure.

9. The compound of claim **3**, the compound being further characterized by a differential scanning calorimetry having a broad peak between approximately 95° C. and 13° C. which corresponds to the loss of one water of hydration on thermogravitmetric analysis.

10. The compound of claim **9**, which is further characterized by a weight loss of 3.48% by thermogravimetric analysis between 50° C. and 175° C.

11. The compound of claim **9**, wherein the differential scanning calorimetry further has a peak at approximately 287° C.

12. Crystalline monohydrate of the compound of formula (IV)

(IV)

which is characterized by a differential scanning calorimetry having a broad peak between approximately 95° C. and 130° C. which corresponds to the loss of one water of hydration on thermogravitmetric analysis.
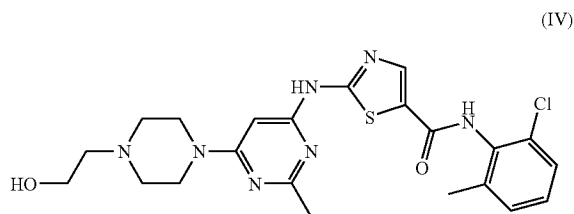
13. A solid pharmaceutical composition comprising a therapeutically effective amount of the compound of claim **12** and a pharmaceutically acceptable carrier.

14. A solid pharmaceutical composition comprising a therapeutically effective amount of the compound of claim **9** and a pharmaceutically acceptable carrier.

15. The compound of claim **12**, wherein the compound is substantially pure.

16. The compound of claim **9**, wherein the compound is substantially pure.

* * * * *

UNITED STATES PATENT AND TRADEMARK OFFICE
CERTIFICATE OF CORRECTION

PATENT NO.   : 7,491,725 B2   Page 1 of 1
APPLICATION NO. : 11/192867
DATED   : February 17, 2009
INVENTOR(S)   : Lajeunesse et al.

It is certified that error appears in the above-identified patent and that said Letters Patent is
hereby corrected as shown below:
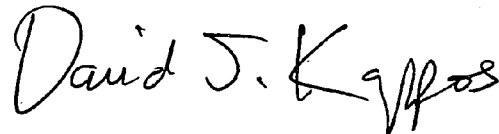
On the Title page,

[*] Notice: Subject to any disclaimer, the term of this patent is extended or adjusted
under 35 USC 154(b) by 251 days.

Delete the phrase "by 251 days" and insert -- by 214 days --

Signed and Sealed this

Third Day of November, 2009

David J. Kappos
Director of the United States Patent and Trademark Office

UNITED STATES PATENT AND TRADEMARK OFFICE
CERTIFICATE OF CORRECTION

PATENT NO.   : 7,491,725 B2   Page 1 of 1
APPLICATION NO. : 11/192867
DATED   : February 17, 2009
INVENTOR(S)   : LaJeunesse et al.

It is certified that error appears in the above-identified patent and that said Letters Patent is hereby corrected as shown below:
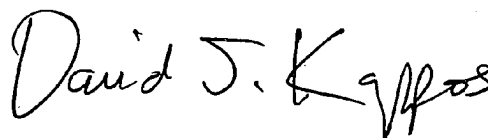
On the Title Page:

The first or sole Notice should read --

Subject to any disclaimer, the term of this patent is extended or adjusted under 35 U.S.C. 154(b)
by 417 days.

Signed and Sealed this

Fifth Day of October, 2010

David J. Kappos
Director of the United States Patent and Trademark Office

EXHIBIT B

CURRICULUM VITAE

Jerry L. Atwood

Personal

Date of Birth: July 27, 1942
Place of Birth: Springfield, Missouri

Education

B.S., Southwest Missouri State, Chemistry and Mathematics, 1964
Ph.D., University of Illinois, 1968

Professional Experience

Assistant Professor, University of Alabama, 1968-1972
Associate Professor, University of Alabama, 1972-1978
Professor, University of Alabama, 1978-1987
Visiting Professor, Imperial College, 1977
Visiting Professor, University of Sussex, 1985
University Research Professor, University of Alabama, 1987 - 1994
Professor and Chairman, University of Missouri-Columbia, 1994-
Curators' Professor, University of Missouri-Columbia, 1999-

Professional Activities

Co-Editor-in-Chief, *New Journal of Chemistry* (2005-)
Editor, *Journal of Supramolecular Chemistry* (2000-2004)
Editor, *Supramolecular Chemistry* (1992-2000)
Associate Editor, *Chemical Communications* (1996-2006)
Consulting Editor, *Journal of Chemical Crystallography* (1999-)
Editor, *Journal of Chemical Crystallography* (1985-1998)
Regional Editor, *Journal of Coordination Chemistry*, A & B (1985-1993)
Editor, *Journal of Inclusion Phenomena* (1983-1991)
Editorial Advisory Board, *Crystal Growth & Design* (2000-)
International Advisory Editorial Board, *New Journal of Chemistry* (2003-)
Editorial Board, *Supramolecular Chemistry* (2000-)
Editorial Board, *Journal of Coordination Chemistry* (1993-)
Editorial Board, *Journal of Organometallic Chemistry* (1986-2000)
Editorial Board, *Crystal Engineering* (1998-)
Co-Editor, *Inclusion Compounds* (five volumes)
Co-Editor, *Comprehensive Supramolecular Chemistry* (ten volumes)
Co-Editor, *Encyclopedia of Supramolecular Chemistry* (two volumes)
Member, American Chemical Society
Member, American Institute of Chemical Engineers
Member, Royal Society of Chemistry
Member, American Crystallographic Association
Institute of Scientific Information, Highly Cited Researchers, isihighlycited.com

Publications Summary

Publications in Refereed Journals	668
Patents	13

Honors and Awards:

1986	Burnum Award for Teaching and Research, U of Alabama
1987	University Research Professor, U of Alabama
1989	von Humboldt Senior Scientist Award, Germany
1992	Japanese Society for the Promotion of Science Award
1996	Outstanding Alumni Award, SMSU
1999	Curators' Professor, University of Missouri (MU)
2000	President's Award for Research and Creative Activity, MU
2000	Izatt-Christensen International Macrocyclic Chemistry Award
2000	Polish Academy of Science, Elected Foreign Member
2002	Alumni-Faculty Award, MU
2005	Royal Society of Chemistry, Elected Fellow
2005	Honorary Medal of the Institute of Physical Chemistry, Polish Academy of Sciences
2005	Midwest Chemist Award, American Chemical Society
2010	Distinguished Faculty Alumni Award, MU

PUBLICATIONS

Jerry L. Atwood

1. J. L. Atwood and G. D. Stucky, "The Crystal and Molecular Stucture of [Al(CH$_3$)$_3$]$_2$·C$_4$H$_8$O$_2$," *J. Amer. Chem. Soc.*, **89**, 5362 (1967).

2. J. L. Atwood and G. D. Stucky, "Dative Nitrogen-to-Metal π-bonding in Bis(dimethylamino)beryllium," *Chem. Comm.*, 1169 (1967).

3. J. L. Atwood and G. D. Stucky, "Mg[Al(OCH$_3$)$_2$(CH$_3$)$_2$]$_2$·C$_4$H$_8$O$_2$ A Novel Coordination Compound of a Metal Alkoxide and a Donor Molecule," *J. Organometal. Chem.*, **13**, 53 (1968).

4. J. L. Atwood and G. D. Stucky, "The Stereochemistry of Polynuclear Compounds of the Main Group Elements. VII. The Structure of Octamethyldialuminummonomagnesium," *J. Amer. Chem. Soc.*, **91**, 2538 (1969).

5. J. L. Atwood and G. D. Stucky, "The Stereochemistry of Polynuclear Compounds of the Main Group Elements. XI. The Structure of Bis(dimethylamino)beryllium and Its Reaction with Trimethylaluminum," *J. Amer. Chem. Soc.*, **91**, 4426 (1969).

6. J. L. Atwood and G. D. Stucky, "The Stereochemistry of Polynuclear Compounds of the Main Group Elements. XII. The Synthesis and Structure of the Ethyleniminodimethylaluminum Trimer," *J. Amer. Chem. Soc.*, **92**, 285 (1970).

7. J. L. Atwood, P. A. Milton, and S. K. Seale, "Thermal Decomposition of Anionic Organoaluminum Thiocyanates," *J. Organometal. Chem.*, **28**, C29 (1971).

8. C. D. Whitt and J. L. Atwood, "The Structure of Dimethylbis(quinuclidine)-beryllium," *J. Organometal. Chem.*, **32**, 17 (1971).

9. C. D. Whitt, L. M. Parker, and J. L. Atwood, "The Crystal Structure of Trimethyl(quinuclidine)aluminum," *J. Organometal. Chem.*, **32**, 291 (1971).

10. P. G. Laubereau, L. Ganguly, J. H. Burns, B. M. Benjamin, J. Selbin, and J. L. Atwood, "Triindenylthoriumchloride and Triindenyluraniumchloride," *Inorg. Chem.*, **10**, 2274 (1971).

11. J. L. Atwood and P. A. Milton, "Thermolysis of Tetramethylammonium Iodotrimethylaluminate," *J. Organometal. Chem.*, **36**, C1 (1972).

12. K. D. Smith and J. L. Atwood, "The Nature of the Scandium-Carbon Bond. The Crystal and Molecular Structure of [$(C_5H_5)_2ScCl]_2$," *J. C. S. Chem. Comm.*, 593 (1972).

13. J. L. Atwood and W. R. Newberry, III, "Solid State Structure and Solution Behavior of Compounds of the Type $M[Al_2(CH_3)_6X]$," *J. Organometal. Chem.*, **42**, C77 (1972).

14. R. A. Abramovitch, G. Grins, R. B. Rogers, J. L. Atwood, M. D. Williams, and S. Crider, "A Novel β-Alkylation of Pyridine and Quinoline 1-Oxides," *J. Org. Chem.*, **37**, 3383 (1972).

15. M. L. Simms, J. L. Atwood, and D. A. Zatko, "The Crystal Structure of Ethylenebis(biguanide)silver(III) Perchlorate," *J. C. S. Chem. Comm.*, 46 (1973).

16. J. L. Atwood and R. E. Cannon, "The Synthesis and Structure of Potassium Cyanotrimethylaluminate," *J. Organometal. Chem.*, **47**, 321 (1973).

17. J. L. Atwood and K. D. Smith, "The Nature of the Scandium-Carbon Bond. II. The Crystal and Molecular Structure of Tricyclopentadienylscandium," *J. Amer. Chem. Soc.*, **95**, 1488 (1973).

18. J. L. Atwood, J. H. Burns, and P. G. Laubereau, "The Crystal Structure of Triindenylsamarium," *J. Amer. Chem. Soc.*, **95**, 1830 (1973).

19. J. L. Atwood, S. K. Seale, and D. H. Roberts, "Thermal Decomposition of Anionic Organoaluminum Compounds. III. The Preparation and Structure of the Neutral Addition Complex of Acetonitrile and Trimethylaluminum," *J. Organometal. Chem.*, **51**, 105 (1973).

20. J. L. Atwood, M. L. Simms, and D. A. Zatko, "Bis(2,2'-bipyridine)silver(II) Nitrate Monohydrate, $Ag(N_2C_{10}H_8)_2 \cdot (NO_3)_2 \cdot H_2O$," *Cryst. Struct. Comm.*, **2**, 279 (1973).

21. J. L. Atwood and P. A. Milton, "The Crystal Structure of Iododimethyl-(trimethylamine)aluminum," *J. Organometal. Chem.*, **52**, 275 (1973).

22. J. L. Atwood and D. C. Hrncir, "Thermal Decomposition of Anionic Organoaluminum Compounds. IV. The Formation of Alkali Metal Tetramethylaluminates and the Crystal Structure of $Rb[Al(CH_3)_4]$," *J. Organometal. Chem.*, **61**, 43 (1973).

23. J. L. Atwood, B. L. Bailey, B. L. Kindberg, and W. J. Cook, "Ferrocenylalanes. The Preparation and Properties of $(C_5H_5)Fe[\pi-C_5H_4Al_2(CH_3)_4Cl]$," *Aust. J. Chem.*, **26**, 2297 (1973).

24. J. L. Atwood, C. F. Hains, M. Tsutsui, and A. E. Gebala, "X-ray Crystallographic Characterization of the Uranium-Carbon Sigma bond in Tricyclopentadienyl-phenylethynyluranium (IV)," *J. C. S. Chem. Comm.*, 452 (1973).

25. J. L. Atwood and K. D. Smith, "Crystal Structure of Di-μ-chloro-bis[di-η-cyclo-pentadienylscandium(III)] Dimer," *J. C. S. Dalton Trans.*, 2487 (1973).

26. M. Tsutsui, N. Ely, A. E. Gebala, and J. L. Atwood, "Sigma-Bonded Organometallic Derivatives of the Lanthanides and Actinides," *Ann. N. Y. Acad. Sci.*, **239**, 160 (1973).

27. S. K. Seale and J. L. Atwood, "Cationic Influence in Anionic Organoaluminum Chemistry Synthesis and Structure of Dimethylthallium Isothiocyana-totrimethylaluminate," *J. Organometal. Chem.*, **64**, 57 (1974).

28. J. L. Atwood and W. R. Newberry, III, "The Interaction of Aromatic Hydrocarbons with Organometallic Compounds of the Main Group Elements III. The Crystal Structure of $K[Al_2(CH_3)_6F]\cdot C_6H_6$," *J. Organometal. Chem.*, **66**, 15 (1974).

29. J. L. Atwood and W. R. Newberry, III, "The Interaction of Aromatic Hydrocarbons with Organometallic Compounds of the Main Group Elements. II. Solution Behavior and Crystal Structure of $K[Al_2(CH_3)_6N_3]$," *J. Organometal. Chem.*, **65,** 145 (1974).

30. J. L. Atwood and K. D. Smith, "Synthesis and Structure of Bis(indenyl)magnesium," *J. Amer. Chem. Soc.*, **96**, 994 (1974).

31. J. L. Atwood and K. D. Smith, "Crystal and Molecular Structure of Trichlorotris-(tetrahydrofuran)scandium(III)," *J. C. S. Dalton Trans.*, 921 (1974).

32. S. K. Seale and J. L. Atwood, "Thermal Decomposition of Anionic Organoaluminum Compounds. V. The Preparation and Crystal Structure of the (Isopropylidenamino)dimethylaluminum Dimer," *J. Organometal. Chem.*, **73**, 27 (1974).

33. J. L. Atwood, M. D. Williams, R. H. Garner, and E. J. Cone, "The Crystal and Molecular Structure of 4-Bromo-2,3-carbomethoxyl-2-cyclohepten-1-one," *Acta Cryst.*, B**30**, 2066 (1974).

34. J. L. Atwood, D. C. Hrncir, C. Wong, and W. W. Paudler, "The Structure of a Hydrazino-Bridged[12]Annulene. A 12 π-monocyclic Antiaromatic Compound," *J. Amer. Chem. Soc.*, **96**, 6132 (1974).

35. J. L. Atwood, D. K. Krass, and W. W. Paudler, "1,2,4-Triazines XIII: The Bond Lengths and Bond Angles of a 1,2,4-Triazine," *J. Heterocyclic Chem.*, **11**, 743 (1974).

36. J. L. Atwood, D. C. Hrncir, and W. R. Newberry, III, "Potassium Methyltri-chloroaluminate, K[CH$_3$AlCl$_3$]," *Cryst. Struct. Comm.*, **3**, 615 (1974).

37. J. L. Atwood and W. A. Sheppard, "The Crystal and Molecular Structure of 4,5-Dicyano-1-imidazolyl(phenyl)bromonium Ylide, C$_{11}$H$_5$N$_4$Br," *Acta Cryst.*, B**31**, 2638 (1975).

38. J. L. Atwood, W. E. Hunter, D. C. Hrncir, E. Samuel, H. Alt, and M. D. Rausch, "Molecular Structures of the Bis(η^5-indenyl)dimethyl-Derivatives of Titanium, Zirconium, and Hafnium," *Inorg. Chem.*, **14**, 1757 (1975).

39. J. L. Atwood and W. R. Newberry, III, "The Crystal Structure of Cesium Azidotrimethylaluminate," *J. Organometal. Chem.*, **87**, 1 (1975).

40. J. L. Atwood, W. E. Hunter, C. Wong, and W. W. Paudler, "The X-ray Crystallographically Determined Confirmation of [2.2](2,5)Furano(2,5)-pyridinophane," *J. Heterocyclic Chem.*, **12**, 433 (1975).

41. J. L. Atwood, K. E. Stone, H. G. Alt, D. C. Hrncir, and M. D. Rausch, "Crystal and Molecular Structure of Titanocene Dicarbonyl, (η^5-C$_5$H$_5$)$_2$Ti(CO)$_2$," *J. Organometal. Chem.*, **95**, C4 (1975).

42. J. R. Chang, G. L. McPherson, and J. L. Atwood, "The Electron Paramagnetic Resonance Spectra of V(II) and Ni(II) Doped into Crystals of CsCdCl$_3$," *Inorg. Chem.*, **14**, 3079 (1975).

43. R. A. Abramovitch, J. L. Atwood, M. L. Good, and B. A. Lampert, "Crystal Structure and Mössbauer Spectrum of [2]-Ferrocenophanethiazine 1,1-Dioxide," *Inorg. Chem.*, **14**, 3085 (1975).

44. D. H. Miles, U. Kokpol, J. L. Atwood, K. E. Stone, T. A. Bryson, and C. Wilson, "Structure of Sarracenin. An Unusual Diacteal Monoterpene from the Insectivorous Plant *Sarrcenia Flava*," *J. Amer. Chem. Soc.*, **98** 1569 (1976).

45. J. L. Atwood, W. E. Hunter, H. Alt, and M. D. Rausch, "The Molecular Structure of

1,1-Bis(η^5-cyclopentadienyl)2,3,4,5-tetraphenyltitanole and its Hafnium Analogue," *J. Amer. Chem. Soc.*, **98**, 2454 (1976).

46. J. L. Atwood, M. Tsutsui, N. Ely, and A. E. Gebala, "The Crystal and Molecular Structure of Tricyclopentadienylethynyluranium(IV)," *J. Coord. Chem.*, **5**, 209 (1976).

47. I. Bernal, J. L. Atwood, F. Calderazzo, and D. Vitali, "Structural Studies on Organodisulfides as Ligands. I. The Crystal and Molecular Structure of $[Re_2Br_2(CO)_6S_2(C_6H_5)_2]$, a Compound Containing Both Disulfide and Bromide Bridges and Capable of Reversible Coordination of an Intact Disulfide Ligand," *Gazz. Chim. Italiana*, **106**, 971 (1976).

48. J. L. Atwood and S. K. Seale, "The Interaction of Aromatic Hydrocarbons with Organometallic Compounds of the Main Group Elements IV. The Preparation and Structure of the Novel Selenide $K[CH_3Se\{Al(CH_3)_3\}_3] \cdot 2C_6H_6$," *J. Organometal. Chem.*, **114**, 107 (1976).

49. J. Holton, M. F. Lappert, D. G. H. Ballard, R. Pearce, J. L. Atwood, and W. E. Hunter, "Dimeric-Dimethyl Lanthanide Complexes, a New Class of Electron-Deficient Compounds, and the Crystal and Molecular Structure of $[(\eta^5\text{-}C_5H_5)_2YbCH_3]_2$," *J. C. S. Chem. Comm.*, 480 (1976).

50. J. Holton, M. F. Lappert, G. R. Schollary, D. G. H. Ballard, R. Pearce, J. L. Atwood, and W. E. Hunter, "μ-Dialkyl Inner Transition Metal (III) Tetra-alkyl-aluminates. The Crystal and Molecular Structure of $[(\eta^5\text{-}C_5H_5)_2M(CH_3)_2Al(CH_3)_2]$ (M = Y or Yb)," *J. C. S. Chem. Comm.*, 425 (1976).

51. K. D. Smith and J. L. Atwood, "Diindenylmagnesium," *Inorg. Syn.*, **16,** 137 (1976).

52. J. L. Atwood and J. D. Atwood, "Liquid Clathrates," *Advan. Chem. Ser.*, **150**, 112 (1976).

53. R. A. Abramovitch, I. Shinkai, B. W. Cue, F. A. Ragan, and J. L. Atwood, "A New Ring Transformation of 3-Halo-2-azido-pyridine 1-Oxides. A Novel Synthesis of 1,2-Oxazin-6-ones," *J. Heterocycl. Chem.*, **13**, 415 (1976).

54. M. M. Goodman, J. L. Atwood, R. T. Carlin, W. E. Hunter, and W. W. Paudler, "Tetrazolo[1.5-b]-1,2,4-Triazines: Syntheses and Structure Determination," *J. Org. Chem.*, **41**, 2860 (1976).

55. J. L. Atwood, J. K. Newell, W. E. Hunter, I. Bernal, F. Calderazzo, I. P. Mavani, and

D. Vitali, "Synthesis, Crystal and Molecular Structure of μ-Dibromo-μ-tetraphenyldiphosphinebis(tricarbonylrhenium(I)), a Molecule Containing a New Type of Tetraphenyldiphosphane Bridge," *J. C. S. Chem. Comm.,* 441 (1976).

56. R. L. Mahaffey, J. L. Atwood, M. B. Humphrey, and W. W. Paudler, "N-(p-Bromphenyl)[2.2](2,5)pyrrolophane: Synthesis and Self-Condensation," *J. Org. Chem.,* **41**, 2963 (1976).

57. J. L. Atwood and A. L. Shoemaker, "Synthesis and Crystal Structure of the Novel Ferrocenylalane [(η^5-C$_5$H$_5$)Fe(η^5-C$_5$H$_3$)Al$_2$Me$_3$Cl]$_2$," *J. C. S. Chem. Comm.,* 536 (1976).

58. J. L. Atwood, W. E. Hunter, B. A. Lampert, and R. H. Garner, "The Crystal and Molecular Structure of 1-Hydroxy-2,3-dicarbomethoxy-1,3-cycloheptadiene," *J. Cryst. Mol. Struct.,* **6**, 291 (1976).

59. B. Kalyanaraman, J. L. Atwood, and L. D. Kispert, "The Crystal Structure of α-Chloroacetic Acid," *J. C. S. Chem. Comm.,* 715 (1976).

60. B. Kalyanaraman, J. L. Atwood, and L. D. Kispert, "The Crystal Structure of Chlorodifluroacetamide," *J. Cryst. Mol. Struct.,* **6**, 311 (1976).

61. I. Bernal, J. L. Atwood, F. Calderazzo, and D. Vitali, "Structural Studies on Organodisulfides as Metal Ligands. II. The Crystal and Molecular Structure of [Re$_2$Br$_2$(CO)$_6$]S$_2$(CH$_3$)$_2$, a Compound Containing an Intact Dimethyldisulfide Bridge Across the Two Metals," *Israel J. Chem.,* **15**, 153 (1976/77).

62. J. L. Atwood, "Liquid Clathrates," *Rec. Adv. Separation Sci.,* **3**, 195 (1977).

63. J. L. Atwood, W. E. Hunter, and K. D. Crissinger, "The Synthesis and Crystal Structure of Tetramethylammonium Acetatotrimethylaluminate," *J. Organometal. Chem.,* **127**, 403 (1977).

64. D. H. Miles, J. Bhattacharyya, N. Mody, J. L. Atwood, S. Black, and P. A. Hedin, "The Structure of Juncusol. Novel Cytotoxic Dihydrophenanthrene from the Estuarine Marsh Plant *Juncus Roemerianus*," *J. Amer. Chem. Soc.,* **99**, 200 (1977).

65. J. L. Atwood, K. E. Stone, H. G. Alt, D. C. Hrncir, and M. D. Rausch, The Crystal Structure of Dicarbonyldicyclopentadienyltitanium(II), (η^5-C$_5$H$_5$)$_2$Ti(CO)$_2$," *J. Organometal. Chem.,* **132**, 367 (1977).

66. J. L. Atwood, G. K. Barker, J. Holton, W. E. Hunter, and M. F. Lappert, "Silylmethyl

and Related Complexes. V. Metallocene Bis(trimethylsilyl)- methyls and Benzhydryls of Early Transition Metals [M(η^5-C$_5$H$_5$)$_2$R] (M = Ti or V) and [M(η^5-C$_5$H$_5$)$_2$X(R)] (M = Zr or Hf) and the Crystal and Molecular Structures of [M(η^5-C$_5$H$_5$)$_2$(CHPh$_2$)$_2$] (M = Zr or Hf)," *J. Amer. Chem. Soc.*, **99**, 6645 (1977).

67. J. L. Atwood and D. J. Darensbourg, "Intramolecular Hydrogen Bonding Implications of the Lability of the Molybdenum-Piperidine Bond. The Molecular Structure of *cis*-Mo(CO)$_4$[P(OCH$_3$)$_3$]NHC$_5$H$_{10}$," *Inorg. Chem.*, **16**, 2314 (1977).

68. R. Gruning and J. L. Atwood, "The Crystal Structure of N-sodiohexamethyldi-silazane, Na[N{Si(CH$_3$)$_3$}$_2$]," *J. Organometal. Chem.*, **137**, 101 (1977).

69. J. L. Atwood, R. D. Rogers, C. Kutal, and P. Grutsch, "X-ray Crystallographic Characterization of the Single Hydrogen Bridge Attachment of the Tetrahydroborate Group in [(MePh$_2$P)$_3$CuBH$_4$]," *J. C. S. Chem. Comm.*, 593 (1977).

70. J. L. Atwood and J. M. Cummings, "The Crystal Structure of Rubidium Azidotrimethylaluminate," *J. Cryst. Mol. Struct.*, **7**, 257 (1977).

71. B. Kalyanaraman, L. D. Kispert, and J. L. Atwood, "The Disordered Crystal Structure of Bromodifluoroacetamide and Trifluoroacetamide," *Acta Crystallogr.*, B**34**, 1131 (1978).

72. J. L. Atwood, J. K. Newell, W. E. Hunter, I. Bernal, F. Calderazzo, I. P. Mavani, and D. Vitali, "The Crystal and Molecular Structure of μ-Dibromo-μ-tetraphen-yldiphosaphanebis[tricarbonylrhenium(I)]," *J. C. S. Dalton Trans.*, 1189 (1978).

73. J. L. Atwood, R. D. Rogers, W. E. Hunter, J. Holton, R. Pearce, and M. F. Lappert, "Neutral and Anionic Silylmethyl Complexes of the Group 3a and Lanthanoid Metals; the Crystal and Molecular Structure of [Li(thf)][Yb{CH(SiMe$_3$)$_2$}$_3$Cl] (thf = Tetrahydrofuran)," *J. C. S. Chem. Comm.*, 140 (1978).

74. E. Carmona-Guzman, G. Wilkinson, J. L. Atwood, W. E. Hunter, and R. D. Rogers, "Interaction for Bis(trimethylsilylmethyl)magnesium and Molybden-umtetrachloridebis(tetrahydrofuran). The Crystal Structure of Chlorotris(tri-methylsilylmethyl)(trimethylphosphine)molybdenum(IV)," *J. C. S. Chem. Comm.*, 465 (1978).

75. R. D. Rogers, J. L. Atwood, and R. Gruning, "The Crystal Structure of N-Lithiohexamethyldisilazane," *J. Organometal. Chem.*, **157**, 229 (1978).

76. J. L. Atwood, R. D. Rogers, W. E. Hunter, I. Bernal, R. Lukas, and H. Brunner, "X-ray Structure of $(C_{15}H_{15})W(CO)_2$: A Compound Containing Three Unusually Bonded Five-Membered Rings," *J. C. S. Chem. Comm.*, 451 (1978).

77. R. D. Rogers, R. V. Bynum, and J. L. Atwood, "The Crystal and Molecular Structures of Tetra(cyclopentadienyl)zirconium," *J. Amer. Chem. Soc.*, **100**, 5238 (1978).

78. R. J. Radel, J. L. Atwood, and W. W. Paudler, "Brominations of some 1,2,4-Triazine 2-Oxides," *J. Org. Chem.*, **43**, 2514 (1978).

79. K. D. Crissinger, R. D. Rogers, and J. L. Atwood, "The Synthesis of $M[Al_2(CH_3)_6NO_3]$ (M = K^+, Rb^+, Cs^+, NR_4^+) and the Crystal Structures of $K[Al_2(CH_3)_6NO_3]$ and $K[Al(CH_3)_3NO_3]\cdot C_6H_6$," *J. Organometal. Chem.*, **155**, 1 (1978).

80. J. L. Atwood, L. G. Canada, A. N. K. Lau, A. G. Ludwick, and L. M. Ludwick, "Crystal Structure of exo-6-Chloromercury-7-dihydro-exo-7-methoxyaldrin (1,2,3,4,10,10-Hexachloro-exo-6-chloromercurio-1,4,4a,5,6,7,8,8a-octahydro-endo, exo-1, 4:5, 8-dimethano-exo-7-ethoxynaphthalenel)," *J. C. S. Dalton Trans.*, 1573 (1978).

81. J. Mattia, M. B. Humphrey, J. L. Atwood, and M. D. Rausch, "The Syntheses and Molecular Structures of Two Metalloindene Complexes: 1,1-Bis(η^5-cyclopentadienyl)-2,3,-bis-(pentafluorophenyl)benzotitanole and 1,1-Bis(η^5-cyclopentadienyl)-2-trimethylsilyl-3-phenylbenzotitanole," *Inorg. Chem.*, **17**, 3257 (1978).

82. C. Kutal, P. Grutsch, J. L. Atwood, and R. D. Rogers, "Structural Characterization of the Single Hydrogen Bridge Attachment of the Tetrahydroborate Group in Tris-(methyldiphenylphosphine)tetrahydroborate-copper," *Inorg. Chem.*, **17**, 3558 (1978).

83. F. Calderazzo, I. P. Mavani, D. Vitali, I. Bernal, J. K. Korp, and J. L. Atwood, "Studies on Organometallic Compounds with Hetero Multiple Bridges. V. Crystal and Molecular Structure of the Parent Rhenium Complex $Re_2Br_2(CO)_6(thf)_2$ and Products of the Tricarbonylrhenium(I) Derived from It," *J. Organometal. Chem.*, **160**, 207 (1978).

84. J. L. Atwood, H. T. Mayfield, and W. A. Sheppard, "4,5-Dicayno-2-imidazolyl(diethyl)sulfonium Ylide, $(CN)_2C_3N_2S(C_2H_5)_2$," *Cryst. Struct. Comm.*, **7**, 739 (1978).

85. J. Jeffery, M. F. Lappert, N. T. Luong-Thi, J. L. Atwood, and W. E. Hunter, "Bulky Alkyls and Hydridoalkyls of Zirconium(IV): Influence of Steric Constraints Upon

(i) Conformation and the Zr-C Rotational Barrier, and (ii) the Zr-C Bond Length. X-ray Crystal and Molecular Structure of [Zr(η-C$_5$H$_5$)$_2${CH(SiMe$_3$)$_2$}Ph]," *J. C. S. Chem. Comm.*, 1081 (1978).

86. B. Kalyanaraman, L. D. Kispert, and J. L. Atwood, "Crystal Structure of 2-Chloroacetamide (α Form): A Reinvestigation," *J. Cryst. Mol. Struct.*, **8**, 175 (1978).

87. G. R. Newkome, V. Majestic, F. Fronczek, and J. L. Atwood, "Synthesis and X-ray Structure of N[(CH$_2$)$_2$O(2,6-C$_6$H$_3$N)O$_2$-(CH$_2$)$_2$]$_3$N: A D$_3$ Macrobicyclic Ligand Capped by Two sp Nitrogen Atoms," *J. Amer. Chem. Soc.*, **101**, 1047 (1979).

88. J. Holton, M. F. Lappert, D. G. H. Ballard, R. Pearce, J. L. Atwood, and W. E. Hunter, "Alkyl-bridged Complexes of the d- and f-block Elements. Part 1. Di-μ-cyclopentadienylmetal (III) Tetra-alkylaluminates [M(η-C$_5$H$_5$)$_2$R$_2$AlR$_2$] (M = Sc, Y, or Ho, with R = Et), and the Crystal and Molecular Structure of [Yb(η-C$_5$H$_5$)$_2$Me$_2$AlMe$_2$]," *J. C. S. Dalton Trans.*, 45, (1979).

89. J. Holton, M. F. Lappert, D. G. H. Ballard, R. Pearce, J. L. Atwood, and W. E. Hunter, "Alkyl-bridged Complexes of the d- and f-block elements. Part 2. Di-μ-cyclopentadienylmetal (III) Methyls [{M(ηC$_5$H$_5$)$_2$Me}$_2$] (M = Y, Dy, Ho, Er, Tm, or Yb) and the Crystal and Molecular Structures of [{M(η-C$_5$H$_5$)$_2$Me}$_2$] (M = Yb)," *J. C. S. Dalton Trans.*, 54. (1979).

90. J. Korp, I. Bernal, J. L. Atwood, F. Calderazzo, and D. Vitali, "Synthesis, Properties, and Crystal and Molecular Structure of [Re$_2$Br$_2$(CO)$_6$(Se$_2$Ph$_2$)], a Binuclear Rhenium(I) Complex Containing a Diphenyl Diselenide Bridge," *J. C. S. Dalton Trans.*, 1492 (1979).

91. J. D. Korp, I. Bernal, J. L. Atwood, W. E. Hunter, F. Calderazzo, and D. Vitali, "Studies on Organometallic Compounds with Hetero Multiple Bridges. X-ray Crystal and Molecular Structure of Mn$_2$Br$_2$(CO)$_6$P$_2$Ph$_4$, the Product Resulting from Co-ordinative Addition of P$_2$Ph$_4$ to Manganese (I)," *J. C. S. Chem. Comm.*, 576 (1979).

92. J. Holton, M. F. Lappert, D. G. H. Ballard, R. Pearce, J. L. Atwood, and W. E. Hunter, "Kinetically-Stable Lanthanide Metal Alkyls and Bridging Methyls," in "Organometallics of the f-Elements," edited by T. J. Marks and R. D. Fischer, D. Reidel, Boston, 1979, pp. 179-220.

93. J. L. Atwood, R. Shakir, J. T. Malito, M. Herberhold, W. Kremnitz, W. P. E. Bernhagen, and H. G. Alt, "The Preparation and Crystal Structures of Dicarbonylcyclopentadienylnitrosylchromium and Dicarbonylfluoroenyl-

11

nitrosylchromium," *J. Organometal. Chem.*, **165**, 65 (1979).

94. R. Shakir, M. J. Zaworotko, and J. L. Atwood, "The Crystal and Molecular Structure of $K[Al_2(CH_3)_6SCN]$, a Compound which Contains an S,N-Bridging Thiocyanate Ligand," *J. Organometal. Chem.*, **171**, 9 (1979).

95. M. Y. Darensbourg, J. L. Atwood, R. R. Burch, W. E. Hunter, and N. Walker, "Structural and Chemical Characterization of a Phosphine Bound M-H-M Bridged Carbonylate: $[NEt_4][(\mu\text{-}H)Mo_2(Co)_9PPh_3]$," *J. Amer. Chem. Soc.*, **101**, 2631 (1979).

96. R. D. Rogers, W. J. Cook, and J. L. Atwood, "Ferrocenylalanes 3. The Synthesis and Crystal Structure of $(\eta^5\text{-}C_5H_5)Fe[\eta^5\text{-}C_5H_4Al_2(CH_3)_4Cl]$," *Inorg. Chem.*, **18**, 279 (1979).

97. W. W. Paudler, R. L. Mahaffey, and J. L. Atwood, "Novel Rearrangement of a [2.2](2,5)Pyrrolophane," *J. Org. Chem.*, **44**, 2498 (1979).

98. D. J. Sikora, M. D. Rausch, R. D. Rogers, and J. L. Atwood, "The Structure and Reactivity of the First Hafnium Carbonyl, $(\eta^5\text{-}C_5H_5)_2Hf(CO)_2$," *J. Amer. Chem. Soc.*, **101**, 5079 (1979).

99. J. L. Atwood, W. E. Hunter, R. D. Rogers, E. Carmona-Guzman, and G. Wilkinson, "The Crystal Structures of $(\eta\text{-}C_6H_6)MoMe_2(PPhMe_2)_2$ and $(\eta\text{-}C_6H_5Me)MoMe_2(PPhMe_2)_2$," *J. C. S. Dalton Trans.*, 1519 (1979).

100. M. B. Honan, J. L. Atwood, I. Bernal, and W. Herrmann, "The Crystal and Molecular Structure of 1-Bromobenzocymantrene, $(\eta^5\text{-}C_9H_6Br)Mn(CO)_3$. *J. Organometal. Chem.*, **179**, 403 (1979).

101. R. D. Rogers and J. L. Atwood, "The Interaction of Aromatic Hydrocarbons with Organometallic Compounds of the Main Group Elements. VI. The Synthesis and Crystal Structure of Cesium Diiododimethylaluminate p-Xylene Solvate," *J. Cryst. Mol. Struct.*, **9**, 45 (1979).

102. R. Shakir, M. J. Zaworotko, and J. L. Atwood, "The Crystal and Molecular Structure of Cesium Isothiocyanotrimethylaluminate, $Cs[Al(CH_3)_3NCS]$," *J. Cryst. Mol. Struct.*, **9**, 135 (1979).

103. M. J. Zaworotko, J. L. Atwood, and L. Floch, "The Crystal and Molecular Structure of 5-Amino-1,2,3,4-thiatriazole," *J. Cryst. Mol. Struct.*, **9**, 173 (1979).

104. M. J. Zaworotko and J. L. Atwood, "Crystal and Molecular Structure of $Cl_2AlN(C_2H_2)C_2H_4N(CH_3)_2$, a Neutral, Chelated Four-Coordinate Aluminum Compound, which Contains Two Types of Al-N Bond," *Inorg. Chem.*, **19**, 268 (1980).

105. P. H. Daniels, J. L. Wong, J. L. Atwood, L. G. Canada, and R. D. Rogers, "Unreactive 1-Azadiene and Reactive 2-Azadiene in Diels-Alder Reaction of Pentachloroazacyclopentadienes," *J. Org. Chem.*, **45**, 435 (1980).

106. E. Carmona-Guzman, G. Wilkinson, R. D. Rogers, W. E. Hunter, M. J. Zaworotko, and J. L. Atwood, "Synthesis and Crystal Structures of Chloro(trimethylphosphine)tris(trimethylsilylmethyl)molybdenum(IV) and Di-μ-chloro-bis[bis(carbonyl)trimethylphosphine (1-2-η-trimethylsilylmethyl-carbonyl)molybdenum(II)]," *J. C. S. Dalton Trans.*, 229 (1980).

107. J. L. Atwood, W. E. Hunter, E. Carmona-Guzman, and G. Wilkinson, "The Synthesis and Crystal Structure of Hydrido(tetrahydroborato)tetrakis(trimethyl-phosphine)molybdenum(II)," *J. C. S. Dalton Trans.*, 467 (1980).

108. B. Cetinkaya, I. Gumrukcu, M. F. Lappert, J. L. Atwood, and R. Shakir, "Lithium and Sodium 2,6-Di-t-butylphenoxides and the Crystal and Molecular Structure of $[Li(OC_6H_2CH_3)\text{-}4\text{-}Bu^t\text{-}2,6(OEt_2)]_2$," *J. Amer. Chem. Soc.*, **102**, 2086 (1980).

109. B. Cetinkaya, I. Gumrukcu, M. F. Lappert, J. L. Atwood, R. D. Rogers, and M. J. Zaworotko, "Bivalent Germanium, Tin, and Lead 2,6-Di-t-butylphenoxides and the Crystal and Molecular Structures of $M(OC_6H_2Me\text{-}4\text{-}Bu^t\text{-}2,6)_2$ (M = Ge or Sn)," *J. Amer. Chem. Soc.*, **102**, 2088 (1980).

110. B. Cetinkaya, P. B. Hitchcock, M. F. Lappert, C. Torroni, J. L. Atwood, W. E. Hunter, and M. J. Zaworotko, "Transition-metal Complexes of Two Tautomers of a Bulky Phenoxide, $2,6\text{-}Bu^t_2\text{-}4\text{-}MeC_6H_2O(ArO)$; Preparation and the Crystal and Molecular Structure of a Phenoxytitanium(III) and a Cyclohexadienoneyl-rhodium(I) Complex, $[Ti(C_5H_5\text{-}\eta)_2OAr]$ and $[Rh(ArO\text{-}\eta)_2OAr]$ and $[Rh(ArO\text{-}\eta^5)(PPh_3)_2]$," *J. Organometal. Chem.*, **188**, C31 (1980).

111. R. Shakir, J. L. Atwood, T. S. Janik, and J. D. Atwood, "Synthesis and Crystal Structure of the Novel Hexanuclear Manganese Complex $[Mn_6(CO)_9\{OP(OEt)_2\}_9]$," *J. Organometal. Chem.*, **190**, C14 (1980).

112. J. T. Malito, R. Shakir, and J. L. Atwood, "Synthesis and Structural Studies of

13

Chromium, Molybdenum and Tungsten Compounds containing Cyclopentadienyl-like Ligands. 3. Dicarbonylnitrosyl(η^5-pentamethylcyclopentadienyl) Complexes," *J. C. S. Dalton Trans.*, 1253 (1980).

113. R. D. Rogers, R. V. Bynum, and J. L. Atwood, "Synthesis and Structure of (η^5-C_5H_5)$_3$Gd·OC_4H_8," *J. Organometal. Chem.*, **192**, 65 (1980).

114. D. F. Foust, M. D. Rausch, W. E. Hunter, J. L. Atwood, and E. Samuel, "The Formation and Molecular Structure of Bis (η^5-cyclopentadienyl)bis(pentafluorophenyl)vinylene-vanadium: An Acetylene derivative of Vanadocene," *J. Organometal. Chem.*, **197**, 217 (1980).

115. M. D. Rausch, W. P. Hart, J. L. Atwood, and M. J. Zaworotko, "The Formation and Molecular Structure of (η^5-Nitrocyclopentadienyl)dicarbonylrhodium," *J. Organometal. Chem.*, **197**, 225 (1980).

116. M. Y. Darensbourg, R. R. Burch, J. L. Atwood, and W. E. Hunter, "The μ-H[Mo(CO)$_4$(PMePh$_2$)]$_2$ Anion: An Example of Phosphine Enhancement of Metal-Metal Interaction," *J. Amer. Chem. Soc.*, **102**, 3290 (1980).

117. R. V. Bynum, W. E. Hunter, R. D. Rogers, and J. L. Atwood, "Pyrrolyl Complexes of the Early Transition Metals. 1. Synthesis and Crystal Structure of (η^5-C_5H_5)$_2$Zr(η^1-NC_4H_4)$_2$, (η^5-C_5H_5)$_2$Zr(η^1-NC_4H_4)$_2$, and [Na(THF)$_6$]$_2$[Zr-(η^1-NC_4H_4)$_6$]," *Inorg. Chem.*, **19**, 2368 (1980).

118. R. D. Rogers, W. E. Hunter, and J. L. Atwood, "The Nature of the Novel ($C_{15}H_{15}$) Ligand in [W(CO)$_2$(η^5-C_5H_5)(η^3-$C_{15}H_{15}$)]," *J. C. S. Dalton Trans.*, 1032 (1980).

119. G. L. McPherson, A. M. McPherson, and J. L. Atwood, "Structures of CsMgBr$_3$, CsCdBr$_3$, CsCdBr$_3$, and CsMgI$_3$-Diamagnetic Linear Chain Lattices, *J. Phys. Chem. Solids*, **41**, 495 (1980).

120. J. A. Paulson, D. A. Krost, G. L. McPherson, R. D. Rogers, and J. L. Atwood, "Structural, Spectroscopic and Theoretical Studies of an Exchange Coupled Manganese(II)-Copper(II) Dimer," *Inorg. Chem.*, **19**, 2519 (1980).

121. R. D. Rogers, L. B. Stone, and J. L. Atwood, "Tetramethylammonium Iodotri-methylaluminate," *Cryst. Struct. Comm.*, **9**, 143 (1980).

122. J. D. Atwood, T. S. Janik, J. L. Atwood, and R. D. Rogers, "Synthesis of

Bis(benzene)tetracarbonyldivanadium, $(C_6H_6)_2V_2(CO)_4$," *Syn. Reac. Inorg. Met. Org. Chem.*, **10**, 397 (1980).

123. M. F. Lappert, T. R. Martin, J. L. Atwood, and W. E. Hunter, "Metal Complexes Derived from the o-Xylidene Ligand, o-$C_6H_4(CH_2\}_2$, and the Crystal and Molecular Structure of the Metallocycle [Zr(η-$C_5H_5)_2\{(CH_2)_2C_6H_4$-o}]," *J. C. S. Chem. Comm.*, 476 (1980).

124. M. F. Lappert, T. R. Martin, C. R. C. Milne, J. L. Atwood, W. E. Hunter, and R. E. Penttila, "Synthesis and Structure of the Nb[IV] Metallocycle [M- (η-$C_5H_4SiMe_3)_2\{CH_2C_6H_4CH_2$-o}] (M = Nb, R = Me_3Si) and Reductive Cleavage of d Analogues (M = Ti, Zr, or Hf; R = H or Me_3Si) by Na[$C_{10}H_8$]," *J. Organometal. Chem.*, **192**, C35 (1980).

125. S. R. Stobart, K. R. Dixon, D. T. Eadie, J. L. Atwood, and M. J. Zaworotko, "Transition-Metal Complexes with Pyrazolyl Bridging Ligands Between Very Different Metal Centers," *Angew. Chem. Int. Ed. Engl.*, **19**, 931 (1980).

126. M. F. Lappert, M. J. Slade, J. L. Atwood, and M. J. Zaworotko, "Monomeric, Coloured Germanium(II) and Tin(II) Di-t-Butylamides, and the Crystal and Molecular Structure of Ge[$NCMe_2(CH_2)_3CMe_2]_2$," *J. C. S. Chem. Comm.*, 621 (1980).

127. M. D. Rausch, D. J. Sikora, D. C. Hrncir, W. E. Hunter, and J. L. Atwood, "Formation and Molecular Structure of a Novel Organometallic Titanoxane Derived from the Reaction of Dicarbonyltitanocene and Hexafluorobut-2-yne," *Inorg. Chem.*, **19**, 3817 (1980).

128. J. L. Atwood, R. D. Rogers, W. E. Hunter, C. Floriani, G. Fachinetti, and A. Chiesi-Villa, "The Crystal and Molecular Structure of Two Early Transition Metal Dicarbonyldicyclopentadienyl Complexes: (η^5-$C_5H_5)_2Zr(CO)_2$ and [(η^5-$C_5H_5)_2V(CO)_2][B(C_6H_5)_4$]," *Inorg. Chem.*, **19**, 3812 (1980).

129. M. F. Lappert, P. I. W. Yarrow, J. L. Atwood, R. Shakir, and J. Holton, "Preparation and Properties of Some Bis(cyclopentadienyl)ytterbium(II) Complexes and the X-ray Crystal and Molecular Structure of [Yb- (η-$C_5H_4SiMe_3)_2(thf)_2$]," *J. C. S. Chem. Comm.*, 987 (1980).

130. D. Pace, W. E. Hunter, R. Shakir, L. D. Kispert, and J. L. Atwood, "Crystal and Molecular Structure of Dichlorofluoroacetamide," *J. Cryst. Mol. Struct.*, **10**, 115 (1980).

131. E. Carmona, F. Gonzalez, M. L. Poveda, J. L. Atwood, and R. D. Rogers, "Alkyl and Acyl Derivatives of Nickel(II) Containing Tertiary Phosphine Ligands," *J. C. S. Dalton Trans.*, 2108 (1980).

132. D. J. Sikora, M. D. Rausch, R. D. Rogers, and J. L. Atwood, "New Syntheses and Molecular Structures of the Decamethylmetallocene Dicarbonyls, (η^5-C$_5$H$_5$)$_2$M(CO)$_2$ (M = Ti, Zr, Hf)," *J. Amer. Chem. Soc.*, **103**, 1265 (1981).

133. K. O. Devaney, M. R. Freedman, G. L. McPherson, and J. L. Atwood, "Electron Paramagnetic Resonance Studies of Manganese (II) and Nickel (II) in Three Structural Phases of Rubidium Magnesium Chloride and the Crystal Structure of α-Rubidium Magnesium Chloride," *Inorg. Chem.*, **20**, 140 (1981).

134. M. F. Lappert, P. I. Riley, P. I. W. Yarrow, J. L. Atwood, W. E. Hunter, and M. J. Zaworotko, "Metallocene Derivatives of Early Transition Elements. Part 3. Synthesis, Characterization, Conformation, and Rotational Barriers, Zr-C$_{sp}$3 of the Zirconium (IV) Chlorides [Zr (η-C$_5$H$_4$R)$_2${CH(SiMe$_3$)$_2$}Cl] and the Crystal and Molecular Structures of the t-Butyl and Trimethylsilyl Complexes (R = Me$_3$C of Me$_3$Si)," *J. C. S. Dalton Trans.*, 814 (1981).

135. S. Randle, D. H. Miles, R. Shakir, and J. L. Atwood, "The Structure of Juncunone: A Biogenetically Intriguing Molecule from the Marsh Plant *Juncus roemerianus*," *J. Org. Chem.*, **46**, 2813 (1981).

136. D. J. Sikora, M. D. Rausch, R. D. Rogers, and J. L. Atwood, "The Formation and Molecular Structure of Bis(η^5-cyclopentadienyl)bis(trifluorophosphine)- titanium," *J. Amer. Chem. Soc.*, **103**, 982 (1981).

137. W. E. Hunter, J. L. Atwood, G. Fachinetti, and C. Floriani, "The Crystal Structure of 1,1-Bis(η^5-cyclopentadienyl)2,3,4,5-tetraphenylzirconole," *J. Organometal. Chem.*, **204**, 67 (1981).

138. R. Shakir and J. L. Atwood, "The Crystal and Molecular Structure of Dicarbonylindenylnitrosylchromium, (η^5-C$_9$H$_7$)Cr(CO)$_2$(NO)," *Acta Crystallogr.*, B**37**, 1656 (1981).

139. J. L. Atwood, R. D. Rogers, J. M. Cummings, I. Bernal, F. Calderazzo, and D. Vitali, "Studies on Organometallic Compounds with Hetero Multiple Bridges. VI. Synthesis and Crystal and Molecular Structure of a Diphenylditelluride-Bridged

Complex, a Member of a Family of Rhenium(I) Compounds Containing Chalcogens as Donor Atoms," *J. C. S. Dalton Trans.*, 1004 (1981).

140. R. D. Rogers, B. Kalyanaraman, M. S. Dalton, W. Smith, L. D. Kispert, and J. L. Atwood, "Crystal Structure of Bromofluoroacetic Acid: A Chiral Molecule," *J. Cryst. Mol. Struct.*, **11**, 105 (1981).

141. F. R. Fronczek, V. K. Majestic, G. R. Newkome, W. E. Hunter, and J. L. Atwood, "The Crystal Structures of a Macrocycle Containing 2,6-Pyridino and Piperazino Subunits, and of the Tetrachlorocobalt(III)ate Salt of its Diprotoned Cation," *J. C. S. Perkin II*, 331 (1981).

142. R. D. Rogers, J. L. Atwood, D. Foust, and M. D. Rausch, "The Crystal Structure of Vanadocene, $(\eta^5\text{-}C_5H_5)_2V$," *J. Cryst. Mol. Struct.*, **11**, 183 (1981).

143. R. D. Rogers, R. V. Bynum, and J. L. Atwood, "The First Authentic Example of a Difference in the Structural Organometallic Chemistry of Zirconium and Hafnium: The Crystal and Molecular Structure of $(\eta^5\text{-}C_5H_5)_2Hf$ $(\eta^1\text{-}C_5H_5)_2$," *J. Amer. Chem. Soc.*, **103**, 692 (1981).

144. R. D. Rogers, J. L. Atwood, A. Emad, D. J. Sikora, and M. D. Rausch, "The Formation and Molecular Structures of $(\eta^5\text{-}C_5H_5)_3Y\cdot OC_4H_8$ and $(\eta^5\text{-}C_5H_5)_3La\cdot OC_4H_8$," *J. Organometal. Chem.*, **216**, 383 (1981).

145. E. Carmona, F. Gonzales, M. L. Poveda, J. L. Atwood, and R. D. Rogers, "Synthesis and Properties of Dialkyl Complexes of Nickel(II). The Crystal Structure of Bis(trimethylsilylmethyl)bis(pyridine)nickel(II)," *J. C. S. Dalton Trans.*, 777 (1981).

146. D. C. Hrncir, R. D. Rogers, and J. L. Atwood, "New Bonding Mode for a Bridging Dioxygen Ligand: The Crystal and Molecular Structure of [K·dibenzo-18-crown-6][$Al_2Me_6O_2$]·$2C_6H_6$," *J. Amer. Chem. Soc.*, **103**, 4277 (1981).

147. J. L. Atwood, W. E. Hunter, A. H. Cowley, R. A. Jones, and C. A. Stewart, "The Solid State Structures of Bis(cyclopentadienyl)tin, Bis(cyclopentadienyl)lead, and Bis(pentamethylcyclopentadienyl)lead," *J. C. S. Chem. Comm.*, 925 (1981).

148. W. J. Evans, A. L. Wayda, W. E. Hunter, and J. L. Atwood, "Heteroleptic tert-Butyl Lanthanide Complexes: Synthesis and Structure of Monomeric Bis(cyclopentadienyl)(tert-butyl)lutetium Tetrahydrofuranate," *J. C. S. Chem. Comm.*, 292 (1981).

17

149. F. Calderazzo, D. Vitali, I. P. Mavani, F. Marchetti, I. Bernal, J. D. Korp, J. L. Atwood, R. D. Rogers, and M. S. Dalton, "Preparation and Properties and Crystal and Molecular Structure of Bis(Sec-Amine) Complexes of Rhenium(I)," *J. C. S. Dalton Trans.*, 2523 (1981).

150. M. F. Lappert, S. J. Miles, J. L. Atwood, M. J. Zaworotko, and A. J. Carty, "Oxidative Addition of an Alcohol to the Ge(II) Alkyl Ge[CH(SiMe$_3$)$_2$]$_2$; Molecular Structure of Ge[CH(SiMe$_3$)$_2$]$_2$(H)OEt," *J. Organometal. Chem.*, **212**, C4 (1981).

151. J. L. Atwood, D. C. Hrncir, R. D. Rogers, and J. A. K. Howard, "Novel Linear Al-H-Al Electron-Deficient Bond in Na[(CH$_3$)$_3$Al-H-Al(CH$_3$)$_3$]," *J. Amer. Chem. Soc.*, **103**, 6787 (1981).

152. W. J. Evans, A. L. Wayda, W. E. Hunter, and J. L. Atwood, "Organolanthanoid Activation of Carbon Monoxide: Single and Multiple Insertion of CO into t-Butyl Lanthanoid Bonds; X-ray Crystallographic Identification of a New Bonding Mode for a Bridging Enedione Diolate Ligand Formed By Formal Coupling of Four CO Molecules," *J. C. S. Chem. Comm.*, 706 (1981).

153. W. J. Evans, I. Bloom, W. E. Hunter, and J. L. Atwood, "Synthesis and X-ray Crystal Structure of a Soluble Divalent Organosamarium Complex," *J. Amer. Chem. Soc.*, **103**, 6507 (1981).

154. J. Jeffrey, M. F. Lappert, N. T. Luong-Thi, M. Webb, J. L. Atwood, and W. E. Hunter, "Metallocene Derivatives of Early Transition Metals. Part 4. Chemistry of the Complexes [M(η-C$_5$H$_5$)$_2$RR'][M = Ti, Zr, or Hf; R = CH$_3$M'Me$_3$ (M' = C, Si, Ge or Sn) or CH(SiMe$_3$)$_2$; R' = Cl or alkyl] and the X-ray Structures of [Zr(η-C$_5$H$_5$)$_2$(CH$_2$M'Me$_3$)$_2$] (M' = C or Si)," *J. C. S. Dalton Trans.*, 1593 (1981).

155. J. L. Atwood, W. E. Hunter, A. L. Wayda, and W. J. Evans, "Synthesis and Crystallographic Characterization of a Dimeric Alkynide Bridged Organolanthanide: [(C$_5$H$_5$)$_2$ErC+CC(CH$_3$)$_3$]$_2$," *Inorg. Chem.*, **20**, 4115 (1981).

156. M. F. Lappert, A. Singh, J. L. Atwood, and W. E. Hunter, "Organometallic Complexes of the Group 3A and Lanthanoid Metals Containing MCl$_2$Li Bridging Units; the X-ray Structure of [Nd(η-Cp")$_2$(μ-Cl)$_2$Li(thf)$_2$][Cp" = C$_5$H$_3$(SiMe$_3$)$_2$; thf = tetrahydrofuran]," *J. C. S. Chem. Comm.*, 1191 (1981).

157. M. F. Lappert, A. Singh, J. L. Atwood, and W. E. Hunter, "The Use of the Bis(trimethylsilyl)cyclopentadienyl Ligand for Stabilizing Early (f^0-f^3) Lanthanocene Chlorides; X-ray Structure of [(Pr(η-Cp")$_2$Cl)$_2$] [Cp" =

$C_5H_3(SiMe_3)_2$] and of Isoleptic Scandium and Ytterbium Complexes," *J. C. S. Chem. Comm.*, 1190 (1981).

158. W. Liese, K. Dehnicke, R. D. Rogers, R. Shakir, and J. L. Atwood, "A Spectroscopic and Crystallographic Study of the [ReNCl$_4$]$^-$ Ion," *J. C. S. Dalton Trans.*, 1061 (1981).

159. J. L. Atwood, D. C. Hrncir, R. Shakir, M. S. Dalton, R. D. Priester, and R. D. Rogers, "Reaction of Trimethylaluminum with Crown Ethers. The Synthesis and Structure of (Dibenzo-18-crown-6)bis(trimethylaluminum) and of (15-crown-5)tetrakis(trimethylaluminum)," *Organometallics*, **1**, 1021 (1982).

160. M. D. Rausch, D. W. Macomber, W. P. Hart, J. L. Atwood, and R. D. Rogers, "The Formation and Molecular Structure of Acetylcyclopentadienyl-sodium·tetrahydrofuranate," *J. Organometal. Chem.*, **238**, 79 (1982).

161. J. L. Atwood, M. B. Honan, and R. D. Rogers, "Crystal and Molecular Structure of (η^5-C_5H_5)Ta (η^5-C_2H_4)Cl$_2$(PMe$_2$Ph)$_2$, a Crowded Molecule which Exhibits a Distorted η^5-Coordination Mode of the Cyclopentadienyl Ligand," *J. Cryst. Spec. Res*, **12**, 205 (1982).

162. M. J. Zaworotko, R. D. Rogers, and J. L. Atwood, "Interaction of Trimethylaluminum and Trimethylgallium with the Acetate Ion. Synthesis and Crystal Structures of [N(CH_3)$_4$][Al$_2$(CH_3)$_6$$CH_3$COO] and Rb[Ga$_2$($CH_3$)$_6$$CH_3$COO]," *Organometallics*, **1**, 1179 (1982).

163. M. J. Zaworotko, R. Shakir, J. L. Atwood, V. Sriyunyongwat, S. D. Reynolds, and T. A. Albright, "Synthesis and Structure of Dicarbonyl(η^5-methylcyclo-pentadienyl)triphenylphosphinemanganese(I)," *Acta Crystallogr.*, B**38**, 1572 (1982).

164. J. L. Atwood, A. H. Cowley, W. E. Hunter, and S. K. Mehrotra, "The Crystal and Molecular Structure of Sulfamide (t-BuNH)$_2$SO$_2$," *Inorg. Chem.*, **21**, 435 (1982).

165. K. A. Beveridge, G. W. Bushnell, K. R. Dixon, D. T. Eadie, S. R. Stobart, M. J. Zaworotko, and J. L. Atwood, "Pyrazolyl-bridged Iridium Dimers. 1. Accommodation of Both Weak and Strong Metal-Metal Interactions by a Bridging Pyrazolyl Framework in Dissymetric Dimeric Structures," *J. Amer. Chem. Soc.*, **104**, 920 (1982).

166. A. W. Coleman, D. T. Eadie, S. R. Stobart, M. J. Zaworotko, and J. L. Atwood, "Pyrazolyl-bridged Iridium Dimers. 2. Contrasting Modes of Two-Center Oxidative Addition to a Bimetallic System and Reductive Access to the Starting

19

Complex: Three Key Di-iridium Structures Representing Short Non-bonding and Long and Short Bonding Metal-Metal Interactions," *J. Amer. Chem. Soc.*, **104**, 922 (1982).

167.   W. J. Evans, J. H. Meadows, A. L. Wayda, W. E. Hunter, and J. L. Atwood, "Organolanthanide Hydride Chemistry. 1. Synthesis and X-ray Crystallographic Characterization of Dimeric Organolanthanide and Organoyttrium Hydride Complexes," *J. Amer. Chem. Soc.*, **104**, 2008 (1982).

168.   W. J. Evans, J. H. Meadows, A. L. Wayda, W. E. Hunter, and J. L. Atwood, "Organolanthanide Hydride Chemistry. 2. Synthesis and X-ray Crystallographic Characterization of Trimetallic Organolanthanide Polyhydride Complex," *J. Amer. Chem. Soc.*, **104**, 2015 (1982).

169.   D. F. Foust, R. D. Rogers, M. D. Rausch, and J. L. Atwood, "Photo-induced Reactions of (η^5-C$_5$H$_5$)$_2$MH$_3$, (η^5-C$_5$H$_5$)$_2$M(CO)H (M = Nb, Ta), and the Molecular Structure of (η^5-C$_5$H$_5$)$_2$Ta(CO)H," *J. Amer. Chem. Soc.*, **104**, 5646 (1982).

170.   R. D. Rogers, R. V. Bynum, and J. L. Atwood, "Synthesis and Crystal Structure of [(η^5-C$_5$H$_5$)$_2$HfO]$_3$·C$_6$H$_5$Me," *J. Cryst. Spec. Res.*, **12**, 239 (1982).

171.   E. Carmona, J. M. Marin, M. L. Poveda, J. L. Atwood, R. D. Rogers, and G. Wilkinson, "Bis-dinitrogen and Diethylene Complexes of Molybdenum(0)," *Angew. Chem.*, **21**, 441 (1982).

172.   J. L. Atwood, A. H. Cowley, W. E. Hunter, and S. K. Mehrotra, "Pyrrolyl Compounds of Main-Group Elements. 1. Synthesis of (η^1-C$_4$H$_4$N)$_3$As and Crystal and Molecular Structures of (η^1-C$_4$H$_4$N)$_3$As," *Inorg. Chem.*, **21**, 1354 (1982).

173.   M. D. Rausch, B. H. Edwards, J. L. Atwood, and R. D. Rogers, "Formation and Molecular Structure of (η^4-Tetraphenylcyclobutadiene)dicarbonylnitrosyl-manganese)," *Organometallics*, **1**, 1567 (1982).

174.   R. A. Jones, A. L. Stuart, J. L. Atwood, W. E. Hunter, and R. D. Rogers, "Steric Effects of Phosphido Ligands. Synthesis and Crystal Structure of Di-tert-butylphosphido-Bridged Dinuclear Metal-Metal Bonded Complexes of Fe(II), Co(I,II), and Ni(I)," *Organometallics,* **1**, 1721 (1982).

175.   R. D. Holmes-Smith, S. R. Stobart, J. L. Atwood, and W. E. Hunter, "Transition-metal Silacyclohexyl Derivatives. Crystal and Molecular Structure of Carbonyl(η-

cyclopentadienyl)(1-phenyl-1-silacyclohex-1-yl)(triphenylphosphine)iron(II)," *J. C. S. Dalton Trans.*, 2461 (1982).

176. G. Erker, K. Engel, U. Dorf, J. L. Atwood, and W. E. Hunter, "The Reaction of (Butadiene)zirconocene and -hafnocene with Ethylene," *Agnew. Chem. Int. Ed. Engl.*, **21**, 914 (1982).

177. E. Carmona, J. M. Marin, M. L. Poveda, R. D. Rogers, and J. L. Atwood, "Preparation and Properties of Dinitrogen Complexes of Molybdenum and Tungsten with Trimethylphosphine as Coligand. III. Synthesis and Properties of cis-$[W(N_2)_2(PMe_3)_4]$, trans-$[W(C_2H_4)_2(PMe_3)_4]$ and $[M(N_2)(PMe_3)_5](M = Mo, W)$. The Crystal and Molecular Structure of $[Mo(N_2)(PMe_3)_5]$," *J. Organometal. Chem.*, **238**, C63 (1982).

178. W. E. Hunter, D. C. Hrncir, R. V. Bynum, R. A. Penttila, and J. L. Atwood, "The Search for Dimethylzirconocene: Crystal Structures of Dimethylzirconocene, Dimethylhafnocene, Chloromethylzirconocene, and μ-Oxobis(methylzircono-cene)," *Organometallics,* **2**, 750 (1983).

179. J. L. Atwood, D. C. Hrncir, R. D. Priester, and R. D. Rogers, "Decomposition of High-Oxygen Content Organoaluminum Compounds. The Formation and Structure of the $[Al_7O_6Me_{16}]^-$ Anion," *Organometallics*, **2**, 985 (1983).

180. G. Erker, K. Kropp, J. L. Atwood, and W. E. Hunter, "Reactions of Vinylzirconocene Complexes with a Zirconiumhydride-the Unexpected Formation of μ-(β-η^1:α-β-η^2-Styryl)-μ-chlorobisbis-Zirconocene Complex," *Organometallics*, **2**, 1555 (1983).

181. J. L. Atwood, W. E. Hunter, R. A. Jones, and T. C. Wright, "Reversible Metal-metal Bond Cleavage Accompanied by a Geometrical Isomerism. Synthesis and Crystal Structures of Isomers of $[Rh(μ-^tBu_2P)(CO)_2]_2$. Catalysis of Alkene Hydroformylation," *Organometallics*, **2**, 470 (1983).

182. R. A. Jones, A. L. Stuart, J. L. Atwood, and W. E. Hunter, "Structure of Chlorotristrimethylphosphinecobalt(I), $C_9H_{27}ClCoP_3$," *J. Cryst. Spec. Res.*, **13**, 273 (1983).

183. J. L. Atwood, W. E. Hunter, H.-M. Zhang, M. F. Lappert, and A. Singh, "Synthesis and Characterization of Stable Anionic Structure of $[AsPh_4][Nd\{\eta-C_5H_3(SiMe_3)_2\}_2Cl_2]$." *J. C. S. Chem. Comm.*, 69 (1983).

184. W. J. Evans, I. Bloom, W. E. Hunter, and J. L. Atwood, "Organolanthanide Hydride Chemistry.   3. Reactivity of Low Valent Samarium with Unsaturated Hydrocarbons Leading to a Structurally Characterized Samarium Hydride Complex," *J. Amer. Chem. Soc.*, **105**, 1401 (1983).

185. W. J. Evans, I. Bloom, W. E. Hunter, and J. L. Atwood "Synthesis of Organosamarium Complexes Containing Sm-C and Sm-P Bonds. Crystallographic Characterization of [(CH$_3$C$_5$H$_4$)$_2$SmC+CC(CH$_3$)$_3$]$_2$," *Organometallics*, **2**, 709 (1983).

186. J. L. Atwood, K. R. Dixon, D. T. Eadie, S. R. Stobart, and M. J. Zaworotko, "Crystal and Molecular Structures of Tetrafluoroborate Salts of the *cis*-Chlorobis(triethylphosphine)(3-trifluoromethyl,5-methylpyrazole)platinum (II) and *cis*-Chlorobis(triethylphosphine)(indazole)platinum(II) Cations," *Inorg. Chem.*, **22**, 774 (1983).

187. M. D. Rausch, B. H. Edwards, R. D. Rogers, and J. L. Atwood, "The Formation of Diphenylphosphinocyclopentadienylthallium, and Its Utility in the Synthesis of Heterobimetallic Ti-Mn Complexes: The Molecular Structure of (η^5-cyclopentdienyl)(η^5-cyclopentadienyl)(η^5-diphenylphosphincyclopentadienyl) dichlorotitanium-[P]manganese," *J. Amer. Chem. Soc.*, **105**, 3882 (1983).

188. J. L. Atwood, R. D. Priester, R. D. Rogers, and L. G. Canada, "Reaction of Trimethylaluminum with Crown Ethers. II. The Synthesis and Structure of (Dibenzo-18-crown-6)tris(trimethylaluminum) and of (18-crown-6)tetrakis-(trimethylaluminum)," *J. Incl. Phenomena*, **1**, 61 (1983).

189. E. Carmona, J. M. Marin, M. L. Poveda, J. L. Atwood, and R. D. Rogers, "Preparation and Properties of Dinitrogen Trimethylphosphine Complexes of Molybdenum and Tungsten. 4. Synthesis, Chemical Properties and X-ray Structure of cis-[Mo(N$_2$)$_2$(PMe$_3$)$_4$]. The Crystal and Molecular Structures of trans-[Mo(C$_2$H$_4$)$_2$(PMe$_3$)$_4$] and trans, mer-[Mo(C$_2$H$_4$)$_2$(CO)(PMe$_3$)$_3$]," *J. Amer. Chem. Soc.*, **105**, 3014 (1983).

190. E. Carmona, L. Sanchez, M. L. Poveda, J. M. Marin, J. L. Atwood, and R. D. Rogers, "β-C-H Interaction versus Dihaptoacyl Coordination in a Molybdenum Acetyl Complex. X-ray Crystal Structure of [Mo(COCH$_3$)(S$_2$CNMe$_2$)- (CO)(PMe$_3$)$_2$]," *J. C. S. Chem. Comm.*, 161 (1983).

191. R. B. Hallock, O. T Beachley, Jr., W. E. Hunter, and J L. Atwood, "A Re-examination of the Product from the Ga(CH$_2$SiMe$_3$)$_3$ - KH Reaction: KGa(CH$_2$SiMe$_3$)$_3$H," *Inorg. Chem.*, **22**, 3683 (1983).

192. B. H. Edwards, R. D. Rogers, D. J. Sikora, J. L. Atwood, and M. D. Rausch, "Formation, Reactivities, and Molecular Structure of Phosphine Derivatives of Titanocene. Isolation and Characterization of a Titanium Monoolefin π Complex," *J. Amer. Chem. Soc.*, **105**, 416 (1983).

193. M. F. Lappert, M. J. Slade, A. Singh, J. L. Atwood, R. D. Rogers, and R. Shakir, "Structure and Reactivity of Sterically Hindered Lithium Amides and Their Diethyl Etherates; Crystal and Molecular Structures of $[LiN(SiMe_3)_2(OEt_2)]_2$ and $[Li(NCMe_2CH_2CH_2CH_2CMe_2)]_4$," *J. Amer. Chem. Soc.*, **105**, 302 (1983).

194. W. J. Evans, J. H. Meadows, W. E. Hunter, and J. L. Atwood, "Organolanthanide and Organoyttrium Hydride Chemistry. 4. Reaction of Isocyanides with $[(C_5H_4R)_2Yb(THF)]_2$ to Form a Structurally Characterized N-Alkyl Forminidoyl Complex," *Organometallics*, **2**, 1252 (1983).

195. J. L. Atwood and M. J. Zaworotko, "The Formation and Structure of the Novel Aluminoxane Anion $[Me_2AlO \cdot AlMe_3]_2$," *J. C. S. Chem. Comm.*, 302 (1983).

196. M. F. Lappert, A. Singh, J. L. Atwood, and W. E. Hunter, "Metallocene(III) Tetrahydroborates of the Group 3a Elements and the X-ray Structure of $[Sc(C_5H_3(SiMe_3)_2)_2(H_2)BH_2]$," *J. C. S. Chem. Comm.*, 206 (1983).

197. R. A. Jones, A. L. Stuart, J. L. Atwood, and W. E. Hunter, "Substitution Reactions of Bis-tertbutylphosphido Complexes of Nickel(I). Crystal Structures of $Ni_2(^tBu_2P)_2(CO)_2(PMe_3)$, (Ni-Ni) and $Ni_2(^tBu_2P)_2(CO)_3$, (Ni-Ni)," *Organometallics*, **2**, 874 (1983).

198. J. L. Atwood, I. Bernal, F. Calderazzo, L. G. Canada, R. Poli, R. D. Rogers, C. A. Veracini, and D. Vitali, "Studies on Organometallic Hetero-Multiple-Bridged Molecules. 8. Preparation and Crystal and Molecular Structures of Diphenyl Dichalcogenide Complexes of Manganese (I). Kinetic, Spectroscopic and Equilibrium Data: A Quantitative Assessment of the Solid-State and Solution Properties Within Members of Homogeneous Families of Chalcogenide Low-Valent Metal Complexes," *Inorg. Chem.*, **22**, 1797 (1983).

199. E. Carmona, J. M. Marin, M. L. Poveda, J. L. Atwood, and R. D. Rogers, "Preparation and Properties of Dinitrogentrimethylphosphine Complexes of Molybdenum and Tungsten. II. Synthesis and Crystal Structures of $[MCl(N_2)(PMe_3)_4]$ (M = Mo, W) and trans-$[MoCl_2(PMe_3)_4]$, *Polyhedron*, **2**, 185 (1983).

23

200. A. H. Cowley, J. E. Kilduff, N. C. Norman, M. Pakulski, J. L. Atwood, and W. E. Hunter, "Electrophilic Additions to Diphosphenes (RP=PR)," *J. Amer. Chem. Soc.*, **105**, 4845 (1983).

201. D. L. Reger, K. A. Belmore, J. L. Atwood, and W. E. Hunter, "Cis Addition of Hydride to η^5-Ring. Crystal and Molecular Structure of $(\eta^5\text{-}C_5H_5)FeCO(PPh_3)(E\text{-}C(CO_2Et)=C(H)Me)$." *J. Amer. Chem. Soc.*, **105,** 5743 (1983).

202. A. H. Cowley, R. A. Jones, C. A. Stewart, A. L. Stuart, J. L. Atwood, W. E. Hunter, and H.-M. Zhang, "Synthesis and Structure of an η^5-Phosphaalkene Nickel Complex," *J. Amer. Chem. Soc.*, **105**, 3737 (1983).

203. E. Carmona, F. Gonzalez, M. L. Poveda, J. M. Marin, J. L. Atwood, and R. D. Rogers, "Reaction of cis-$[Mo(N_2)_2(PMe_3)_4]$ with CO_2. Synthesis and Characterization of Products of Disproportionation and the X-ray Structure of a Tetrametallic Mixed-Valence $Mo^{II}\text{-}Mo^V$ Carbonate with a Novel Mode of Carbonate Binding," *J. Amer. Chem. Soc.*, **105**, 3365 (1983).

204. R. A. Jones, M. H. Seeberger, J. L. Atwood, and W. E. Hunter, "Diazasilametallacycles: Crystal and Molecular Structure of $Ti(NBuSiMe_2NBu)Cl_2$," *J. Organometal. Chem.*, **247**, 1 (1983).

205. E. Carmona, J. M. Marin, M. L. Poveda, L. Sanchez, R. D. Rogers, and J. L. Atwood, "Synthesis of Chloro(trimethylphosphine)tris(trimethylsilylmethyl)- tungsten(IV); Synthesis and Molecular Structure of Di-μ-chloro-bis[dicarbonyl-(trimethylphosphine)(1-2-η-trimethylsilylmethyl-carbonyl)tungsten(II)]," *J. Chem. Soc. Dalton Trans.*, 1003 (1983).

206. R. D. Rogers and J. L. Atwood, "The Crystal and Molecular Structure of $SnBr[N(SiMe_3)_2]_3$," *J. Cryst. Spec. Res.*, **13**, 1 (1983).

207. R. A. Jones, N. C. Norman, M. H. Seeberger, J. L. Atwood, and W. E. Hunter, "Synthesis and X-ray Crystal Structures of $[M(\mu\text{-}(^tBu)(H)P)(PMe_3)_2]_2$, M = Rh, Ni, Containing Rh=Rh Double and Ni-Ni Single Bonds, *Organometallics*, **2**, 1629 (1983).

208. W. A. Herrmann, J. Plank, J. L. Hubbard, G. W. Kriechbaum, W. Kalcher, B. Koumbouris, G. Ihl, A. Schafer, M. L. Ziegler, H. Pfisterer, C. Pahl, J. L. Atwood, and R. D. Rogers, "Transition Metal Methylene Complexes. LI. Carbocyclic Carbenes, Carbene Bridges, Small Hydrocarbon Ligands, and Metallacycles: Examples of a General Synthetic Concept," *Z. Naturforsch.*, **38**b, 1392 (1983).

209. J. L. Atwood, D. C. Hrncir, and R. D. Rogers, "The Use of Crown Ethers to Access New M[Al$_2$R$_6$X] Species. Synthesis and Crystal Structure of [K·dibenzo-18-crown-6][Al$_2$Me$_6$Cl]·2C$_6$H$_6$," *J. Incl. Phenom.*, **1**, 199 (1983).

210. R. A. Jones, A. L. Stuart, J. L. Atwood, and W. E. Hunter, "Synthesis of Di-tert-butylphosphido-Bridged Dimers of Cobalt (I) Containing Cobalt-Cobalt Double Bonds. Crystal Structures of [Co(μ-t-Bu$_2$P)(CO)$_2$]$_2$ and [Co(μ-t-Bu$_2$P)(PMe$_3$)L]$_2$ (L = CO or N$_2$)," *Organometallics*, **2**, 1437 (1983).

211. K. A. Beveridge, G. W. Bushnell, S. R. Stobart, J. L. Atwood, and W. E. Hunter, "Pyrazolyl-Bridged Iridium Dimers. 4. Crystal and Molecular Structures of Bis(cycloocta-1,5-diene)bis(μ-pyrazolyl)diiridium(I), Its Dirhodium(I) Isomorph, and Two Bis(cycloocta-1,5-diene)diiridium(I) Analogues Incorporating 3.5-Disubstituted μ-Pyrazolyl Ligands," *Organometallics*, **2**, 1447 (1983).

212. J. L. Atwood, D. E. Berry, S. R. Stobart, and M. J. Zaworotko, "Aspects of Organocadmium Chemistry. Part 3. Cyclometallated Alkyls and Aryls of Zn, Cd, and Hg and the Crystal and Molecular Structure of Bis[(o-N,N-dimethylaminomethyl)phenyl]mercury(II)," *Inorg. Chem.*, **22,** 3480 (1983**).**

213. J. L. Atwood, W. E. Hunter, R. A. Jones, and T. C. Wright, "Synthesis and X-ray Crystal Structure of Tris(bis-tertbutylphosphido)tricarbonyltrirhodium(I)," *Inorg. Chem.*, **22**, 993 (1983).

214. F. Calderazzo, R. Poli, D. Vitali, J. D. Korp, I. Bernal, G. Pelizzi, J. L. Atwood, and W. E. Hunter, "Studies on Organometallic Hetero-Multiple-Bridged (HMB) Molecules. IX. Synthesis and Crystal and Molecular Structure of Mn$_2$X$_2$(CO)$_6$P$_2$Ph$_4$ (X = Br, I) and Mn$_2$Br$_2$(CO)$_6$As$_2$Ph$_4$, the Products Arising from Co-ordinative Addition of P$_2$Ph$_4$ and As$_2$Ph$_4$ to Manganese(I)." *Gazz. Chim. Ital.*, **113**, 761 (1983).

215. G. Erker, K. Engel, J. L. Atwood, and W. E. Hunter, "The Zirconocene-Induced Coupling of Butadiene with Carbonyl Compounds," *Angew. Chem. Int. Ed. Engl.*, **22**, 494 (1983).

216. R. D. Rogers, R. V. Bynum, and J. L. Atwood, "The Crystal Structure of LiBr·(CH$_3$OCH$_2$CH$_2$OCH$_3$)$_2$," *J. Cryst. Spec. Res.*, **14**, 29 (1984).

217. R. D. Rogers and J. L. Atwood, "Reaction of K$_2$SO$_4$ with AlMe$_3$ and the Crystal

Structures of $K_2[Al_4Me_{12}SO_4]$ with $K_2[Al_4Me_{12}SO_4]\cdot0.5p$-Xylene," *Organometallics,* **3**, 271 (1984).

218. G. S. Bristow, M. F. Lappert, T. R. Martin, J. L. Atwood, and W. E. Hunter, "Metallocyclopentenes. Part 2. The Preparation of o-Xylidene Derivatives of Ti, Zr, Hf, or Nb; the Crystal and Molecular Structures of $[M(\eta$-$C_5H_4R)_2(p$-$(CH_2)_2C_6H_4)]$ (R = H, M = Ti, Zr or Hf; R = SiMe$_3$, M = Nb)," *J. C. S. Dalton Trams.*, 399 (1984).

219. R. D. Rogers, R. V. Bynum, and J. L. Atwood, "Synthesis and Crystal Structure of $(\eta^5$-$C_5H_5)_2Hf(\eta^1$-$NC_4H_4)_2$," *J. Cryst. Spec. Res.*, **14**, 21 (1984).

220. R. D. Rogers and J. L. Atwood, "The Crystal and Molecular Structure of [K·DB-18-C-6][AlMe$_3$NO$_3$]·3C$_6$H$_6$," *J. Cryst. Spec. Res.*, **14**, 1 (1984).

221. R. A. Jones, B. R. Whittlesey, J. L. Atwood, and W. E. Hunter, "Synthesis and X-ray Crystal Structure of $OsBr_2(CN^tBu)_4\cdot2CH_2Cl_2$," *Polyhedron*, **3**, 385 (1984).

222. R. D. Rogers, J. L. Atwood, T. A. Albright, W. A. Lee, and M. D. Rausch, "The Structure of Biphenylene- and Triphenylene-Cr(CO)$_3$. An Analysis of the Bonding of Cr(CO)$_3$ to Bicyclic Polyenes," *Organometallics*, **3**, 263 (1984).

223. R. D. Rogers, J. C. Baker, and J. L. Atwood, "The Crystal Structure of [NBu$_4$][AlI$_4$]," *J. Cryst. Spec. Res.*, **14**, 334 (1984).

224. J. L. Atwood, A. D. McMaster, R. D. Rogers, and S. R. Stobart, "Stereochemically Non-rigid Silanes, Germanes, and Stannanes. 12. Crystal and Molecular Structures Tetra(η^1-indenyl) Derivatives of Germanium and Tin: *meso* Diastereoisomers with S$_4$ Symmetry," *Organometallics,* **3**, 1500 (1984).

225. G. Erker, W. Fromberg, J. L. Atwood, and W. E. Hunter, "Hydrozirconation of Nitriles: Proof of a Linear Heteroallene Structure in (Benzylideneamido)-zirconocene Chloride," *Angew. Chem. Int. Ed. Engl.*, **23**, 68 (1984).

226. J. L. Atwood, T. Fjeldberg, M. F. Lappert, N. T. Luong-Thi, R. Shakir, and A. J. Thorne, "Molecular Structures of Bis(trimethylsilylmethyl)lithium (LiR)$_n$, R = [CH(SiMe$_3$)$_2$] in the Vapour (Gas-phase Electron Diffraction: a Monomer, n = 1) and the Crystal (X-ray: a Polymer, n = $\square$)," *J. Chem. Soc. Chem. Commun.,* 1163 (1984).

227. A. H. Cowley, R. A. Jones, J. G. Lasch, N. C. Norman, C. A. Stuart, J. L. Atwood, W. E. Hunter, and H.-M. Zhang, "Synthesis and Structures of Free and Coordinated Phosphaalkenes," *J. Amer. Chem. Soc.*, **106**, 7015 (1984).

228. A. L. Wayda, J. L. Atwood, and W. E. Hunter, "Homoleptic Organolathanoid Hydrocarbyls. The Synthesis and X-ray Crystal Structure of Tris(ortho-N,N-dimethylaminomethylphenyl)lutetium," *Organometallics*, **3**, 939 (1984).

229. E. Carmona, M. Paneque, M. L. Poveda, R. D. Rogers, and J. L. Atwood, "Further Studies on Organonickel Compounds: the Synthesis of some New Alkyl-, Acyl- and Cyclopentadienyl-Derivatives and the Crystal Structure of trans-[Ni(CH$_2$SiMe$_3$)$_2$(PMe$_3$)$_2$]," *Polyhedron*, **3**, 317 (1984).

230. C. M. Means, N. C. Means, S. G. Bott, and J. L. Atwood, "How Short is a Bond of Order Zero? A Close Cs...Cs Contact in the [Cs$_2$(18-crown-6)]$^{2+}$ Cation," *J. Am. Chem. Soc.*, **106**, 7627 (1984).

231. J. L. Atwood, R. D. Rogers, and R. V. Bynum, "Tris(1,2-dimethoxyethane)lithium μ-Chloro-μ-oxo-bis[chloro(pentamethylcyclopentadienyl)(1-pyrrolyl)zirco-nate(IV)] Dimethoxyethane solvate, [Li(C$_4$H$_{10}$O$_2$)$_3$][Zr$_2$Cl$_3$O(C$_4$H$_4$N)$_2$-(C$_{10}$H$_{15}$)$_2$]·C$_4$H$_{10}$O$_2$," *Acta Crystallogr.* **C40**, 1812 (1984).

232. J. L. Atwood, K. A. Beveridge, G. W. Bushnell, K. R. Dixon, D. T. Eadie, S. R. Stobart, and M. J. Zaworotko, "Pyrazolyl-Bridged Iridium Dimers. 4. Two Fragment, Two Center Oxidative Addition of Halogens and Methyl Halides to *trans*-Bis(triphenylphosphine)dicarbonyldi(μ-pyrazolato)diiridium(I)." *Inorg. Chem.*, **23**, 4050 (1984).

233. E. Samuel, R. D. Rogers, and J. L. Atwood, "Synthesis and Crystal Structure of [(η^5-C$_9$H$_{11}$)TiCl(μ-O)]$_4$," *J. Cryst. Spec. Res.*, **14**, 573, (1984).

234. W. J. Evans, J. H. Meadows, W. E. Hunter, and J. L. Atwood, "Organolanthanide and Organoyttrium Hydride Chemistry. 5. Improved Synthesis of [C$_5$H$_4$R)$_2$YH(THF)]$_2$ Complexes and Their Reactivity With Alkenes, Alkynes, 1,2-Propadiene, Nitriles, and Pyridine, Including Structural Characterization of an Alkylideneamido Product," *J. Amer. Chem. Soc.*, **106**, 1291 (1984).

235. A. H. Cowley, J. E. Kilduff, J. G. Lasch, S. K. Mehrotra, N. C. Norman, M. Pakulski, B. R. Whittlesey, J. L. Atwood, and W. E. Hunter, "Synthesis and Structures of Compounds Containing Double Bonds Between the Heavier Group VA Elements:

Diphosphenes, Diarsenes, Phosphaarsenes, and Phosphastibenes," *Inorg. Chem.*, **23**, 2582 (1984).

236. W. A. Herrmann, J. Plank, G. W. Kriechbaum, M. L. Ziegler, H. Pfisterer, J. L. Atwood, and R. D. Rogers, "Komplexchemie reaktiver organischer Verbindungen. XLVII. Synthese, Strukturchemie und Druckcarbonylierung von Metallcarben-Komplexen," *J. Organometal. Chem.*, **264**, 327 (1984).

237. M. D. Rausch, D. F. Foust, R. D. Rogers, and J. L. Atwood, "The Formation and Molecular Structure of Bis(η^5-cyclopentadienyl)(2-[(dimethylamino)methyl]-phenyl-C,N)yttrium." *J. Organometal. Chem.*, **265**, 241 (1984).

238. R. D. Rogers, E. Carmona, A. Galindo, J. L. Atwood, and L. G. Canada, "Trimethylphosphine Complexes of Molybdenum and Tungsten. The Synthesis and Chemical Properties of $MoCl_4(PMe_3)_3$ and $MoO(acac)_2PMe_3$." *J. Organometal. Chem.*, **277**, 403 (1984).

239. E. Carmona, L. Sanchez, J. M. Marin, M. L. Poveda, J. L. Atwood, R. D. Priester, and R. D. Rogers, "η^2-Acyl Coordination and β-C-H Interaction in Acyl Complexes of Molybdenum. Crystal and Molecular Structures of $Mo(\eta^2$-$COCH_2SiMe_3)Cl(CO)(PMe_3)_3$ and $Mo(COCH_3)(S_2CNMe_2)(CO)(PMe_3)_2$," *J. Amer. Chem. Soc.*, **106**, 3214 (1984).

240. J. L. Atwood, "Liquid Clathrates," in "Inclusion Compounds," Vol. 1, Eds., J. L. Atwood, J. E. D. Davies, and D. D. MacNicol, Academic Press, London, 1984, pp. 375-405.

241. J. L. Atwood, "New Inclusion Methods for Separations Problems," *Sep. Sci. Tech.*, **19**, 751 (1984).

242. J. L. Atwood, H. Elgamal, G. H. Robinson, S. G. Bott, J. A. Weeks, and W. E. Hunter, "From Crown Ethers to Zeolites: Reaction of $EtAlCl_2$ with Crown Ethers," *J. Incl. Phenom.*, **2**, 367 (1984).

243. J. L. Atwood, "The Interaction of Alkali Metal Cations with Aromatic Molecules in Complexes of the Type $M[AlMe_3X]\cdot$aromatic, $M[Al_2Me_6X]\cdot$aromatic, and Related," *J. Incl. Phenom.*, **3**, 13 (1985).

244. W. J. Evans, I. Bloom, W. E. Hunter, and J. L. Atwood, "Metal Vapor Synthesis of $(C_5Me_5)_2Sm(THF)_2$ and $(C_5Me_4Et)_2Sm(THF)_2$ and Their Reactivity with Organomercurial Reagents. Synthesis and X-ray Structural Analysis of

28

(C_5Me_5)$_2$Sm(C_6H_5)(THF)," *Organometallics*, **4**, 112 (1985).

245. H. Zhang, C. M. Means, N. C. Means, and J. L. Atwood, "Reaction of Trimethylaluminum with Crown Ethers. IV. Crystal Structure of (18-Crown-6)Tetrakis(trimethylaluminum)·p-xylene Solvate," *J. Cryst. Spec. Res.*, **15**, 445 (1985).

246. W. J. Evans, J. W. Grate, I. Bloom, W. E. Hunter, and J. L. Atwood, "Reactivity of (C_5Me_5)$_2$Sm(THF)$_2$ with Oxygen Containing Substrates: Synthesis and X-ray Crystallographic Characterization of an Oxo-bridged Bimetallic Organosamarium Complex, [(C_5Me_5)$_2$Sm]$_2$(μ-O)," *J. Am. Chem. Soc.*, **107**, 405 (1985).

247. H. D. H. Showalter, E. M. Berman, J. L. Johnson, J. L. Atwood and W. E. Hunter, "A Facile Synthesis of Functionalized 9,10-Anthracenediones via Tosylate and Triflate Phenolic Activation," *Tetrahedron Letters*, **26**, 157 (1985).

248. G. H. Robinson, S. G. Bott, H. Elgamal, W. E. Hunter, and J. L. Atwood, "Reaction of Trimethylaluminum with Crown Ethers. III. The Synthesis and Crystal Structure of (12-crown-4)-bis(trimethylaluminum)," *J. Incl. Phenom.*, **3**, 65 (1985).

249. W. J. Evans, T. T. Peterson, M. D. Rausch, W. E. Hunter, and J. L. Atwood, "Synthesis and X-ray Crystallographic Characterization of an Asymmetric Organoyttrium Hallide Dimer: (C_5Me_5)$_2$Y[(μ-Cl)YCl(C_5Me_5)$_2$]," *Organometallics*, **4**, 554 (1985).

250. R. B. Hallock, W. E. Hunter, J. L. Atwood, and O. T. Beachley, "Synthesis and Structural Study of Ga(CH_2SiMe_3)$_3$. $Me_2NC_2H_4NMe_2$.Ga(CH_2SiMe_3)$_3$," *Organometallics*, **4**, 547 (1985).

251. M. J. Zaworotko, C. R. Kerr, and J. L. Atwood, "Reaction of the Phenoxide Ion with Trimethylaluminum. Isolation and Crystal Structure of [K.dibenzo-18-crown-6][Al_2Me_6OPh] and K[$AlMe_3$(OPh)$_2$]," *Organometallics*, **4**, 238 (1985).

252. W. J. Evans, J. W. Grate, H. W. Choi, I. Bloom, W. E. Hunter, and J. L. Atwood, "Solution Synthesis and Crystallographic Characterization of the Divalent Organosamarium Complexes [(C_5Me_5)SmI(THF)$_2$]$_2$," *J. Amer. Chem. Soc.*, **107**, 941 (1985).

253. J. H. Medley, F. R. Fronczek, N. Ahmad, M. C. Day, R. D. Rogers, C. R. Kerr, and J. L. Atwood, "The Crystal Structures of NaAlR$_4$, R = Methyl, Ethyl, and n-Propyl," *J. Cryst. Spec. Res.*, **15**, 99 (1985).

29

254 O. T. Beachley, T. D. Getman, R. U. Kirss, R. B. Hallock, W. E. Hunter, and J. L. Atwood, "Preparation and Properties of Cyclopentadienylgallium(III) Compounds," *Organometallics*, **4**, 751 (1985).

255. A. H. Cowley, S. K. Mehrotra, W. E. Hunter, and J. L. Atwood, "Synthesis and Crystal Structure of the Bis(cyclopentadienyl)gallium Ethoxide Dimer," *Organometallics*, **4**, 1115 (1985).

256. J. L. Atwood, W. E. Hunter, R. D. Rogers, and J. A. Weeks, "Behavior of $M[Al_2Me_6N_3](M = K, Rb, Cs)$ with Aromatic Solvents and the Crystal Structures Two Related Complexes," *J. Incl. Phenom.*, **3**, 113 (1985).

257. W. J. Evans, J. W. Grate, L. A. Hughes, H. Zhang, and J. L. Atwood, "Reductive Homologation of CO to a Ketenecarboxylate by a Low Valent Organolanthanide Complex: Synthesis and X-ray Crystal Structure of $[(C_5Me_5)_4Sm_2(OCCCO_2)(THF)]_2$," *J. Amer. Chem. Soc.*, **107**, 3728 (1985).

258. M. J. Zaworotko, R. J. Stamps, M. T. Ledet, H. Zhang, and J. L. Atwood, "Heterocyclophane Complexes of Transition Metals. 1. Synthesis and Crystal Structure of Both the η^5- and the η^6-[2.2](2,5)Pyrroloparacyclophanetri-carbonylchromium," *Organometallics*, **4**, 1697 (1985).

259. S. G. Bott, H. Elgamal, and J. L. Atwood, "Seven-Coordinate Aluminum in $[AlCl_2.benzo-15-crown-5][AlCl_3Et]$," *J. Amer. Chem. Soc.*, **107**, 1796 (1985).

260. J. L. Atwood, S. G. Bott, C. Eaborn, M. N. El-Kheli, and J. D. Smith, "The Crystal and Molecular Structure of Fluoro(hydroxy){tris(dimethylphenylsilyl)-methyl}borane," *J. Organometal. Chem.*, **294**, 23 (1985).

261. O. T. Beachley, Jr., R. B. Hallock, H. Zhang, and J. L. Atwood, "Synthesis, Characterizations and Crystal and Molecular Structures of Pentamethylcyclopentadienyl Gallium Chloride Compounds, $Ga(C_5Me_5)_2Cl$ and $Ga(C_5Me_5)Cl_2$," *Organometallics*, **4**, 1675 (1985).

262. S. P. McManus, J. A. Knight, E. J. Meehan, R. A. Abramovitch, M. N. Offor, J. L. Atwood, and W. E. Hunter, "Ferrocenesulfonyl Azide: Structure and Kinetics of Solution Thermolysis," *J. Org. Chem.*, **50**, 2742 (1985).

263. M. J. Wovkulich, J. L. Atwood, L. Canada, and J. D. Atwood, "A Crystallographic Determination of the Influence of the Trans Ligand on the Bonding of Triphenylphosphine. Crystal and Molecular Structures of $Cr(CO)_4(PPh_3)L$ (L =

PBu$_3$, P(OMe)$_3$, and P(OPh)$_3$)," *Organometallics*, **4**, 867 (1985).

264. W. J. Evans, I. Bloom, J. W. Grate, L. A. Hughes, W. E. Hunter, and J. L. Atwood, "Synthesis and Characterization of the Samarium-Cobalt Complexes (C$_5$Me$_5$)$_2$(THF)SmCo(CO)$_4$ and [SmI$_2$(THF)$_5$][Co(CO)$_4$]: X-ray Crystal Structure of a Seven-Coordinate Samarium(III) Cation Complex," *Inorg. Chem.*, **24**, 4620 (1985).

265. D. R. Corbin, J. L. Atwood, and G. D. Stucky, "Hydrogenation of Unsaturated Dicarboxylic Acids by Dicarbonylbis(η^5-cyclopentadienyl)titanium(II) and the Molecular Structure of μ-Acetylenedicarboxylatobis[bis(η^5-methylcyclopenta-dienyl)titanium(III)]," *Inorg. Chem.*, **25**, 98 (1986).

266. R. V. Bynum, H.-M. Zhang, W. E. Hunter, and J. L. Atwood, "Pyrrolyl Complexes of the Early Transition Metals. 3. Preparation and Crystal Structure of (η^5-C$_5$H$_5$)$_2$Zr-(η^1-NC$_4$H$_2$Me$_2$)$_2$ and Zr(η^1-NC$_4$H$_2$Me$_2$)$_4$," *Can. J. Chem.*, **64**, 1304 (1986).

267. G. Erker, U. Dorf, J. L. Atwood, and W. E. Hunter, "The Metallaoxirane Type Structure of Cp$_2$ZrCl(CPh$_2$OCH$_3$) and the Question of Modeling the Chemistry of Alkylidene Units on a Metal Oxide Surface," *J. Amer. Chem. Soc.*, **108**, 2251 (1986).

268. S. G. Bott, A. W. Coleman, and J. L. Atwood, "Preparation and Structure of the First Complex of an Early Transition Metal and a Calixarene, Calix[6]arene[TiCl$_2$(μ-O)TiCl$_3$]$_2$," *J. Chem. Soc., Chem. Commun.*, 610 (1986).

269. S. G. Bott, A. W. Coleman, and J. L. Atwood, "Inclusion of both Cation and Neutral Molecule by a Calixarene. Structure of the [p-tert-Butylmethoxycalix[4]arene·Na·toluene]$^+$ Cation," *J. Amer. Chem. Soc.*, **108**, 1709 (1986).

270. W. J. Evans, L. A. Hughes, D. K. Drummond, H. Zhang, and J. L. Atwood, "Facile Stereospecific Synthesis of a Dihydroxyindenoindene Unit from an Alkyne and CO Via Samarium-mediated CO and CH Activation," *J. Amer. Chem. Soc.*, **108**, 1722 (1986).

271. M. D. Rausch, K. J. Moriarty, J. L. Atwood, J. A. Weeks, W. E. Hunter, and H. G. Brittian, "Synthetic, X-ray Structural and Luminescence Studies on Pentamethylcyclopentadienyl Derivatives of Lanthanum, Cerium and Praseodymium," *Organometallics*, **5**, 1281 (1986).

272. R. A. Jones, T. C. Wright, J. L. Atwood, and W. E. Hunter, "Structure of Bis(m-di-tert-butylphosphido)-bis(dicarbonylrhodium)(Rh-Rh) in P1," *Acta Crystallogr.*, **C42**, 294 (1986).

273. H. Prinz, S. G. Bott, and J. L. Atwood, "Decyclization of Crown Ethers. Ring-opening Reaction of 18-Crown-6 with $ZrCl_4$," *J. Am. Chem. Soc.*, **108**, 2113 (1986).

274. W. J. Evans, J. W. Grate, K. R. Levan, I. Bloom, T. T. Peterson, R. J. Doedens, H. Zhang, and J. L. Atwood, "Synthesis and X-ray Crystal Structure of Bis(pentamethylcyclopentadienyl) Lanthanide and Yttrium Halide Complexes," *Inorg. Chem.*, **25**, 3614 (1986).

275. E. Samuel, J. L. Atwood, and W. E. Hunter, "Cyclization of Phenylpropiolic Acid on Titanocene. Synthesis and Molecular Structure of Bis(η^5-cyclopenta-dienyl)(cynamylato-C^3,0)-titanium Phenylpropiolic Acid (1/1), a Novel Titanacycle. Synthesis of Bis(cyclopentadienyl)bis(phenylpropiolato)- titanium," *J. Organometal. Chem.*, **311**, 325 (1986).

276. J. L. Atwood, "Applications of Inclusion in Separation Science," in "Chemical Separations," Ed. J. Navratil and C. J. King, Litarvan, Golden, CO, 1986.

277. S. G. Bott, U. Kynast, and J. L. Atwood, "Reaction of Early Transition Metal Complexes with Macrocycles. II. Synthesis and Structure of $TiCl_3(H_2O)\cdot$18-crown-6, a Compound with a Unique Bidentate Bonding Mode for the 18-crown-6 Molecule," *J. Incl. Phenom.*, **4**, 241 (1986).

278. J. Z. Cayias, E. A. Babaian, D. C. Hrncir, S. G. Bott, and J. L. Atwood, "Crystal Structure of $[Zr(dmpe)(CH_2SiMe_3)_4]$ (dmpe = $PMe_2CH_2CH_2PMe_2$). Evidence in Support of the Postulation for the Presence of an Agostic Hydrogen," *J. Chem. Soc., Dalton Trans.*, 2743 (1986).

279. Y. P. Singh, P. Rupani, A. Singh, A. K. Rai, R. C. Mehrotra, R. D. Rogers, and J. L. Atwood, "Synthesis and IR, UV, NMR (^{1}H and ^{11}B) and Mass Spectral Studies of Some New β-ketonamine Complexes of Boron: Crystal and Molecular Structure of $OC_6H_4OBOC(R)CHC(R')NR''$ (R = p-ClC_6H_4, R' = C_6H_5, R'' = CH_3)," *Inorg. Chem.*, **25**, 3076 (1986).

280. P. C. Blake, M. F. Lappert, R. G. Taylor, J. L. Atwood, W. E. Hunter, and H. Zhang, "A Complete Series of U(III) Halides, $[(UCp''_2X)_n]$ (X = F, Cl, Br or I; Cp'' = η-$C_5H_3(SiMe_3)_2$); Single-crystal X-ray Structure Determinations of the Chloride and

32

Bromide (n = 2 for X = μ-Cl⁻ or μ-Br⁻)," *J. Chem. Soc., Chem. Commun.*, 1394 (1986).

281. A. W. Coleman, S. G. Bott, and J. L. Atwood, "Preparation and Structure of (Calix[8]arene Methyl Ether)·2 $CDCl_3$," *J. Incl. Phenom.*, **4**, 247 (1986).

282. P. C. Blake, M. F. Lappert, J. L. Atwood, and H. Zhang, "The Synthesis and Characterisation, Including X-ray Diffraction Study, of [Th{η-C_5H_3(SiMe$_3$)$_2$}$_3$]; the First Thorium(III) Crystal Structure," *J. Chem. Soc., Chem. Commun.*, 1148 (1986).

283. W. J. Evans, D. K. Drummond, S. G. Bott, and J. L. Atwood, "Reductive Distortion of Azobenzene by an Organosamarium(II) Reagent to Form [(C_5Me_5)$_2$Sm]$_2$(C_6H_5)$_2$N$_2$: An X-ray Crystallographic Snapshot of an Agostic Hydrogen Complex on an Ortho Metalation Reaction Coordinate," *Organometallics*, **5**, 2389 (1986).

284. J. W. Chambers, A. J. Baskar, S. G. Bott, J. L. Atwood, and M. D. Rausch, "Formation and Molecular Structures of ($η^5$-Pentabenzylcyclopentadienyl)- and ($η^5$-Pentaphenylcyclopentadienyl)dicarbonyl Derivatives of Cobalt and Rhodium," *Organometallics*, **5**, 1635 (1986).

285. E. A. Babaian, D. C. Hrncir, S. G. Bott, and J. L. Atwood, "Siloxy-Zirconium Chemistry. I. Reaction of Zr-C σ-Bonds with R_3SiOH and the Crystal Structure of (1,2-dimethoxyethane)-bis(triphenylsiloxy)dichlorozirconium(IV), (DME) ZrCl$_2$(OSiPh$_3$)$_2$," *Inorg. Chem.*, **25**, 4818 (1986).

286. D. A. Atwood, S. G. Bott, and J. L. Atwood, "Preparation and Structure of the [YbCl$_2$·15-crown-5]$^+$ Cation, a New Synthetic Intermediate for Organolanthanide Chemistry," *J. Coord. Chem.*, **16**, 93 (1987).

287. W. J. Evans, T. P. Hanusa, J. H. Meadows, W. E. Hunter, and J. L. Atwood, "Synthesis and X-ray Crystal Structure of μ, v^2-N-Alkylformimidoyl Complexes of Erbium and Yttrium: A Structural Comparison," *Organometallics*, **6**, 295 (1987).

288. D. H. Miles, A. A. de la Cruz, A. M. Ly, D. -S. Lho, E. Gomez, J. A. Weeks, and J. L. Atwood, "Toxicants from Mangrove Plants IV: Ichthyotoxins from the Philippine Plant *Heritiera Littoralis*," *ACS Symposium Series*, **330**, 491 (1987).

289. A. W. Coleman, H. Zhang, S. G. Bott, J. L. Atwood, and P. H. Dixneuf, "Reactivity of the Diphosphine Ph$_2$PCH$_2$PPh$_2$ with [($η^6$-p-CH$_3$C$_6$H$_4$Pr^i)RuCl$_2$]$_2$. Crystal

33

Structures of Ruthenium Complexes Containing Monodentate and Singly-Bridging Diphosphine Ligands," *J. Coord. Chem.,* **16**, 9 (1987).

290. O. T. Beachley, Jr., J. P. Kopasz, H. Zhang, W. E. Hunter, and J. L. Atwood, "Synthesis and Characterization of Amphoteric Ligands Including the Crystal and Molecular Structure of [(Me$_3$SiCH$_2$)$_2$InPPh$_2$]$_2$," *J. Organometal. Chem.,* **325**, 69 (1987).

291. A. W. Coleman, S. G. Bott, and J. L. Atwood, "Reaction of Trimethylaluminum with Calixarenes. I. Synthesis and Structure of [Calix[8]arene Methyl Ether][AlMe$_3$]$_6$·2 Toluene and of [p-tert-Butylcalix[8]arene Methyl Ether][AlMe$_3$]$_6$·4 Benzene," *J. Incl. Phenom.,* **5**, 581 (1987).

292. S. G. Bott, M. Clark, J. S. Thrasher, and J. L. Atwood, "Crystal and Molecular Structure of S-Methyl(pentafluorosulfanyl)thiocarbamate," *J. Cryst. Spec. Res.,* **17**, 187 (1987).

293. G. H. Robinson, W. E. Hunter, S. G. Bott, and J. L. Atwood, "The Interation of Group III Metal Alkyls with Crown Ethers. The Synthesis and Structure of [Ga(CH$_3$)$_3$]$_2$[Dibenzo-18-crown-6] and [Al(CH$_3$)$_3$]$_2$[Dicyclohexano-18-crown-6]," *J. Organomet. Chem.,* **326**, 9 (1987).

294. E. A. Babaian, L. M. Barden, D. C. Hrncir, W. E. Hunter, and J. L. Atwood, "Indium-Based Liquid Clathrates. I. The Preparation of the First Indium Liquid Inclusion Compound and Crystal Structure of its Parent Complex, [K·18-Crown-6]$_2$-[In$_2$I$_3$Cl$_2$(CH$_3$)$_3$]," *J. Incl. Phenom.,* **5**, 605 (1987).

295. M. D. Rausch, K. J. Moriarty, J. L. Atwood, W. E. Hunter, and E. Samuel, "The Formation, Crystal and Molecular Structures of Bis(η^5-indenyl)di-carbonylzirconium," *J. Organomet. Chem.,* **327**, 39 (1987).

296. N. C. Means, C. M. Means, S. G. Bott, and J. L. Atwood, "Interaction of AlCl$_3$ with Tetrahydrofuran. Formation and Crystal Structure of [AlCl$_2$(THF)$_4$][AlCl$_4$]," *Inorg. Chem.,* **26**, 1466 (1987).

297. E. Hey, M. F. Lappert, J. L. Atwood, and S. G. Bott, "Bis(trimethylsilyl)phosphinodithioformates, the P-Analogues of Dithiocarbamates; X-ray Structures of [ZrCp$_2$(Cl)(η^2-S$_2$CPR$_2$)](1a) and [(ZrCp$_2$(μ-S))$_2$], a Thermolysis Product of (1a) (Cp = η-C$_5$H$_5$, R = SiMe$_3$)," *J. Chem. Soc.,*

Chem. Commun., 421 (1987).

298. E. Hey, M. F. Lappert, J. L. Atwood, and S. G. Bott, "A Hexaphosphorus Chain as Part of a Dimeric P,P'-containing Ligand; 1,3-Phosphozirconation of White Phosphorus; X-ray Structure of [Zr(η-C_5H_5)$_2$(O(PR$_2$)PP(PR$_2$)P)] (R = SiMe$_3$)," *J. Chem. Soc., Chem. Commun.*, 597 (1987).

299. W. J. Evans, D. K. Drummond, J. W. Grate, H. Zhang, and J. L. Atwood, "Structural Diversity in Bis(pentamethylcyclopentadienyl) Lanthanide Halide Complexes: X-ray Crystal Structures of [(C_5Me_5)$_2$SmCl]$_3$ and (C_5Me_5)$_{10}$Sm$_5$Cl$_5$[Me(OCH$_2$CH$_2$)$_4$OMe]," *J. Amer. Chem. Soc.*, **109**, 3928 (1987).

300. G. H. Robinson, H. Zhang, and J. L. Atwood, "Reaction of Trimethylaluminum with a Macrocyclic Tetradentate Tertiary Amine. Synthesis and Molecular Structure of [Al(CH$_3$)$_3$]$_4$[N-tetramethylcyclam]," *J. Organometal. Chem.*, **331**, 153 (1987).

301. J. L. Atwood, "Inclusion (Clathrate) Compounds," Encyclopedia of Physical Science and Technology, Vol. 6, 583-594 (1987).

302. A. W. Coleman, A. J. Baskar, S. G. Bott, and J. L. Atwood, "Synthesis and Crystal Structure of a Novel Mixed Valence Iron Compound, [(η^5-cyclopentadienyl)(η^6-tetralin)Fe(II)]$_3$[Fe(III)(NCS)$_6$]," *J. Coord. Chem.*, **17**, 339 (1988).

303. S. G. Bott, A. Alvanipour, S. D. Morley, D. A. Atwood, C. M. Means, A. W. Coleman, and J. L. Atwood, "Stabilization of the AlMe$_2^+$ Cation by Crown Ethers," *Angew. Chem. Int. Engl. Ed.*, **26**, 485 (1987).

304. W. J. Evans, R. A. Keyer, H. Zhang, and J. L. Atwood, "Synthesis and X-ray Crystal Structure of [(C_5Me_5)$_2$Sm]$_2$C$_4$(C$_6$H$_5$)$_2$, a Complex Containing η^2-Alkyne Coordination to Samarium," *J. Chem. Soc., Chem. Commun.*, 837 (1987).

305. D. Caine, C. J. McCloskey, J. L. Atwood, S. G. Bott, H. Zhang, and D. VanDerveer, "The Synthesis and Base-Induced Methylation Reactions of Cis-7a-Hydroxy-3a-phenylsulfenyl-3z,4,5,6,7,7a-hexahydro-4-indano ne," *J. Org. Chem.*, **52**, 1280 (1987).

306. J. L. Atwood, S. G. Bott, P. B. Hitchcock, C. Eaborn, R. S. Shariffudin, J. D. Smith, and A. C. Sullivan, "The Chemistry of Trichloro(tris(trimethylsilyl)methyl) and Trichloro(tris(dimethylphenyl)silyl) methyl gallates, -indates and -thallates. Crystal and Molecular Structures of [Li(thf)$_2$(μ-Cl)$_2$Ga(Cl)C(SiMe$_2$Ph)$_3$]thf, [Li(thf)$_3$-(μ-Cl)InCl$_2$C(SiMe$_3$)$_3$] and [(SiMe$_3$)$_3$CIn(μ-Cl)(μ-Fe(CO)$_4$InC(SiMe$_3$)$_3$]

(thf = tetrahydrofuran)," *J. Chem. Soc., Dalton Trans.*, 747 (1987).

307. G. H. Robinson, H. Zhang, and J. L. Atwood, "Reaction of Trimethylaluminum with Thiacrown Ethers. Crystal and Molecular Structure of [AlMe$_3$]$_4$[14]anesS$_4$," *Organometallics*, **6**, 887 (1987).

308. M. V. Lakshmikantham, M. S. Raasch, M. P. Cava, S. G. Bott, and J. L. Atwood, "Thioquinones. A Reinvestigation of Perkin and Green's Diaminodithio- quinone," *J. Org. Chem.*, **52,** 1875 (1987).

309. J. A. Ewen, L. Haspeslagh, J. L. Atwood, and H. Zhang, "Synthesis, Crystal Structure, and Isospecific Propylene Polymerizations with Ethylenebis(4,5,6,7-tetrahydro-1-indenyl)hafnium(IV) Dichloride," *J. Amer. Chem. Soc.*, **109**, 6544 (1987).

310. G. H. Robinson, S. G. Bott, and J. L. Atwood, "Triethylaluminum-based Ferrocenylalanes. Synthesis and Crystal Structure of [(η-C$_5$H$_5$)Fe (η-C$_5$H$_4$)Al(C$_2$H$_5$)$_4$Cl]," *J. Coord. Chem.,* **16**, 219 (1987).

311. S. G. Bott, A. W. Coleman, and J. L. Atwood, "The Synthesis and Molecular Structure of t-Butylcalix[4]arene Methyl Ether complexed with Aluminum Alkyl Species," *J. Incl. Phenom.,* **6**, 747 (1987).

312. S. G. Bott, H. Prinz, A. Alvanipour, and J. L. Atwood, "Reaction of Early Transition Metals with Macrocycles.   III. Synthesis and Structure of 18-Crown-6·MCl$_4$ (M=Ti, Sn)," *J. Coord. Chem.,* **16**, 303 (1987).

313. M. A. Edelman, M. F. Lappert, J. L. Atwood, and H. Zhang, "The Synthesis and X-ray Structure of a Novel Monocyclopentadienyluranium(IV) Chloride [UCp'''Cl$_2$(THF)(μ-Cl)$_2$Li(THF)$_2$][Cp'''=η-C$_5$H$_2$(SiMe$_3$)$_3$-1,2,4]," *Inorg. Chim. Acta*, **139**, 185 (1987).

314. P. C. Blake, M. F. Lappert, R. G. Taylor, J. L. Atwood, and H. Zhang, "Some Aspects of the Coordination and Organometallic Chemistry of Thorium and Uranium (M^{III}, M^{IV}, U^{V}) in +3 and +4 Oxidation States," *Inorg. Chim. Acta.,* **139**, 13 (1987).

315. P. C. Stark, M. Huff, E. A. Babaian, L. M. Barden, D. C. Hrncir, S. G. Bott, and J. L. Atwood, "Indium-based Liquid Clathrates. II. Inclusion Compounds Derived from Salts of the Tetrachloroindate Anion, InCl$_4$$^-$ and the Crystal Structure of [Li-15-Crown-5][In(CH$_3$)$_3$Cl]," *J. Incl. Phenom.,* **6**, 683 (1987).

316. J. L. Atwood, S. G. Bott, A. W. Coleman, K. D. Robinson, S. B. Whetstone, and C. M. Means, "The H_3O^+ Cation in Aromatic Solvents. Synthesis, Structure and Behavior of [H_3O·18-Crown-6][Cl-H-Cl]," *J. Am. Chem. Soc.*, **109**, 8100 (1987).

317. A. M. Arif, D. E. Heaton, R. A. Jones, K. B. Kidd, T. C. Wright, B. R. Whittlesey, J. L. Atwood, W. E. Hunter, and H. Zhang, "Synthesis and Structures of Di- and Tri-nuclear Di-tert-butylphosphido and Di-tert-butylarsenido Complexes of Iridium. X-ray Crystal Structures of [$Ir(\mu$-t-$Bu_2E)(CO)_2]_2$ (E=P, As), [$Ir(tOBu_2PH)(CO)]_2(\mu$-H)$(\mu$-t-Bu_2P), [$Ir(t$-$Bu_2PH)(CO)(\mu$-H)]$_2$(H)$(\mu$-t-Bu_2P) and $Ir_3(\mu$-t-$Bu_2P)_3(CO)_5$," *Inorg. Chem.*, **26**, 4065 (1987).

318. U. Kynast, S. G. Bott, and J. L. Atwood, "Reaction of Early Transition Metal Complexes with Macrocycles. IV. Synthesis and Structure of [$PPh_4]_2$[18-Crown-6·($VCl_4)_2$] and 18-Crown-6·$VCl_3.H_2O$," *J. Coord. Chem.*, **17**, 53 (1988).

319. A. W. Coleman, S. G. Bott, S. D. Morley, C. M. Means, K. D. Robinson, H. Zhang, and J. L. Atwood, "Novel Layer Structure of Sodium Calix[4]arene Sulphonate Complexes - a Class of Organic Clays?" *Angew. Chem. Int. Ed. Engl.*, **27**, 1361 (1988).

320. W. J. Evans, J. M. Olofson, H. Zhang, and J. L. Atwood, "Synthesis and X-ray Crystal Structure of an Unusual Oligomeric Bis(pentamethylcyclopentadienyl) Halide Complex of Cerium: [$(C_5Me_5)_2CeCl_2K(THF)]_n$," *Organometallics*, **7**, 629 (1988).

321. W. J. Evans, M. A. Hozbar, S. G. Bott, G. H. Robinson, and J. L. Atwood, "Utility of Cyclodichlorophosphazane as a NaC_5H_5 Scavenging Reagent: Synthesis of an Organoyttrium Hydroxide Complex and the X-ray Crystal Structure of the Layered Compound [$(C_5H_5)_2Y(\mu$-OH)$_2]C_6H_5C$ C_6H_5," *Inorg. Chem.*, **27**, 1990 (1988).

322. S. G. Bott, A. W. Coleman, and J. L. Atwood, "Intercalation of Cationic, Anionic and Molecular Species by Organic Hosts. Preparation and Crystal Structure of [$NH_4]_6$[calix[4]arenesulphonate][$MeOSO_3]$·($H_2O)_2$," *J. Amer. Chem. Soc.*, **110**, 610 (1988).

323. W. J. Evans, D. K. Drummond, H. Zhang, and J. L. Atwood, "Synthesis and X-ray Crystal Structure of the Divalent [Bis-(trimethylsilyl)amido]samarium Complexes [$(Me_3Si)_2N]_2Sm(THF)_2$ and ([$(Me_3Si)_2N]Sm(\mu$-I)(DME)(THF))$_2$," *Inorg. Chem.*, **27**, 575 (1988).

324. E. Hey, S. G. Bott, and J. L. Atwood, "Synthesis of Bis(η-cyclopentadienyl)- (1,2,3-triphosphanto-P,P)zirconium(IV) and hafnium(IV), [(η-C$_5$H$_5$)M- (PPh-PPh-PPh)] (M=Zr, Hf) and Structure of the Hafnocene Derivative," *Chem. Ber.*, **121**, 561 (1988).

325. J. S. Thrasher, J. B. Nielsen, S. G. Bott, D. J. McClure, S. A. Morris, and J. L. Atwood,"Bis[pentafluorosulfanyl(trifluoromethyl)amino]mercury, Hg[N(CF$_3$)-SF$_5$]$_2$, and Bis[pentafluorotellurium(trifluoromethyl)amino]mercury, Hg[N(CF$_3$)TeF$_5$]$_2$," *Inorg. Chem.*, **27**, 570 (1988).

326. P. J. Cragg, S. G. Bott, and J. L. Atwood, "Lanthanide and Actinide Complexes of Monoaza-15-Crown-5. Syntheses and Crystal Structure of [La(monoaza-15-Crown-5)(NO$_3$)$_3$] and [UO$_2$(NO$_3$)$_2$]$_2$(μ-H$_2$O)(monoaza-15-crown-5)," *J. Lanth. Act. Res.* **2,** 265 (1988).

327. G. H. Robinson, E. S. Appel, S. A. Sangokoyo, H. Zhang, and J. L. Atwood, "Synthesis and Molecular Structure of [Al(CH$_3$)]$_2$[15] and N$_4$[Al(CH$_3$)$_3$]$_2$: An Aluminum-Nitrogen Macrocyclic Cage," *J. Coord. Chem.*, **17**, 373 (1988).

328. W. J. Evans, D. K. Drummond, L. R. Chamberlain, R. J. Doedens, S. G. Bott, H. Zhang, and J. L. Atwood, "Synthetic, Structural and Reactivity Studies of the Reduction and CO Derivatization of Azobenzene Mediated by Divalent Lanthanide Complexes," *J. Amer. Chem. Soc.*, **110,** 4983 (1988).

329. W. J. Evans, D. K. Drummond, L. A. Hughes, R. J. Doedens, H. Zhang, and J. L. Atwood, "Variable Coordination Numbers in Crystalline Bis(pentamethylcyclopentadienyl) Samarium Oxide, Iodide, and Alkoxide Complexes," *Polyhedron*, **7**, 1693 (1988).

330. R. Shakir, R. D. Rogers, J. L. Atwood, D. W. Macomber, Y.-P. Wang, and M. D. Rausch, "The Formation and Molecular Structures of Formyl-, Cyano-, and Aminocyclopentadienyldicarbonylnitrosylchromium," *J. Cryst. Spec. Res.*, **18**, 767 (1988).

331. A. Alvanipour, H. Zhang, and J. L. Atwood, "Synthesis, Structure, and Solution Behavior of [Na·15-Crown-5][Mn(CO)$_5$]," *J. Organomet. Chem.*, **358**, 295 (1988).

332. P. C. Blake, E. Hey, M. F. Lappert, J. L. Atwood, and H. Zhang, "Bis(trimethylsilyl)phosphido complexes. II. Bis(trimethylsilyl)phosphidobis-(tetrahydrofuran)lithium as a reducing agent; X-ray structure of [UCp"$_2$(μ-Cl)$_2$Li(THF)$_2$][Cp"=η-C$_5$H$_3$(SiMe$_3$)$_2$-1,3; THF=OC$_4$H$_8$]," *J. Organomet. Chem.*, **353**,

307 (1988).

333. J. L. Atwood, M. F. Lappert, R. G. Smith, and H. Zhang, "Four-co-ordinate Lanthanide Metal(III) Chloro(alkyls)s: Synthesis and X-ray Structure of [LaR$_3$(μ-Cl)Li(pmdeta)] [R=CH(SiMe$_3$)$_2$, pmdeta = N,N,N',N",N"-pentamethyl-diethylenetriamine]," *J. Chem. Soc., Chem. Commun.*, 1308 (1988).

334. E. Hey, M. F. Lappert, J. L. Atwood, and S. G. Bott,   "Insertion of Diphenyl-diazomethane into [ZrCp$_2$(Cl)PR$_2$] (Cp = η-C$_5$H$_5$, R = SiMe$_3$), X-Ray Structures of [ZrCp$_2$(PR$_2$)X] (X = Cl or Me) and [ZrCp$_2$(Cl){N(CPh$_2$)NPR$_2$}]," *Polyhedron*, **7**, 2083 (1988).

335. J. L. Atwood, "Inclusion Compounds in Separation Science: An Overview," in Separation Technology, Eds., N. N. Li and H. Strathmann, Engineering Foundation, New York, 1988, pp. 46-56.

336. J. A. Ewen, L. Haspeslagh, M. J. Elder, J. L. Atwood, H. Zhang, and H. N. Cheng, "Catalysts for Propylene Polymerization," *Transition Metals and Organometallics as Catalysts for Olefin Polymerization*, W. Kaminsky and H. Sinn, Eds., Springer-Verlag, Berlin, 1988, p. 281.

337. P. C. Blake, M. F. Lappert, J. L. Atwood, and H. Zhang, "A Series of Bis(η-cyclopentadienyl)uranium(III) Dichloro-bridged-alkali-metal and Dihalogenobis(η-cyclopentadienyl)uranate(III) Complexes," *J. C. S. Chem. Comm.*, 1436 (1988).

338. A. Antinolo, G. S. Bristow, G. K. Campbell, A. W. Duff, P. B. Hitchcock, R. A. Kamarudin, M. F. Lappert, R. J. Norton, N. Sarjudeen, D. J. W. Winterborn, J. L. Atwood, W. E. Hunter, and H. Zhang, "Synthetic and Structural Studies on Some Organic Compounds of Zirconium," *Polyhedron*, **8**, 1601 (1989).

339. J. L. Atwood, A. W. Coleman, H. Zhang, and S. G. Bott, "Organic Clays. Synthesis and Structure of Na$_5$[calix[4]arene sulfonate] ·12 H$_2$O, K$_5$[calix[4]arene sulfonate] ·8 H$_2$O, Rb$_5$[calix[4]arene sulfonate] ·5 H$_2$O, and Cs$_5$[calix[4]arene sulfonate] ·4 H$_2$O," *J. Incl. Phenom.*, **7,** 203 (1989).

340. H. Yoo, H. Zhang, J. L. Atwood, and G. W. Gokel, "A Lariat Ether that Forms a Pseudo-sandwich Complex," *Tetrahderon Lett.*, **30**, 2489 (1989).

341. M. D. Rausch, W. C. Spink, J. L. Atwood, A. J. Baskar, and S. G. Bott "Dimethyl- and Diphenylphosphino-cyclopentadienyl Derivatives of Cobalt, Rhodium and

Iridium: The Crystal and Molecular Structure of Dicarbonyl-{π-[η^5-Cyclo-pentadienyl)dimethylphosphine-P]}Dirhodium," *Organometallics*, **8**, 2627 (1989).

342. E. Hey, S. B. Wild, S. G. Bott, and J. L. Atwood, "The Synthesis and Crystal Structure of (R*,R*)-(±)-[(η^5-C$_5$H$_5$){1,2-C$_6$H$_4$(PMePh)$_2$}Fe(PCl$_3$)Cl.2 MeCN," *Z. Naturforsch.*, **44b**, 615 (1989).

343. A. Nakano, Y. Li, P. Geoffroy, M. Kim, J. L. Atwood, S. G. Bott, L. Echegoyen, and G. W. Gokel, "Cistulynes: Proton NMR and Single Crystal X-ray Evidence for Structure and Cation Encapsulation in a Rigid Molecular Channel Model System," *Tetrahedron Lett.*, 5099 (1989).

344. J. L. Atwood, "Inclusion Compounds," in Ullman's Encyclopedia of Industrial Chemistry, Vol. A14, 119 (1989).

345. J. L. Atwood, S. G. Bott, C. M. Means, A. W. Coleman, H. Zhang, and M. T. May, "Synthesis of Salts of the Hydrogen Dichloride Anion in Aromatic Solvents. II. The Synthesis and Crystal Structure of [K·18-crown-6]- [Cl-H-Cl], [Mg·18-crown-6][Cl-H-Cl]$_2$, [H$_3$O$^+$·18-crown-6][Cl-H-Cl], and the Related [H$_3$O$^+$·18-crown-6][Br-H-Br]," *Inorg. Chem.*, **29**, 467 (1990).

346. F. Hamada, S. G. Bott, G. W. Orr, A. W. Coleman, H. Zhang, and J. L. Atwood, "Thiocalix[4]arenes, I. Synthesis and Structure of Ethylthiocalix[4]arene Methyl Ether and the Related Structure of Bromocalix[4]arene Methyl Ether," *J. Incl. Phenom.*, **9,** 195 (1990).

347. G. M. Gray, N. Takada, M. Jan, H. Zhang, and J. L. Atwood, "Synthesis and Characterization of a Series of trans-[(CO)$_5$MPh$_2$PX(CH$_2$)$_3$M=CHC$_6$H$_4$-o-O]$_2$M' (M = Mo; X = NH or M = Cr, W; X = CH$_2$; M' = Ni, Cu, Zn) Complexes and the X-ray Crystal Structure of trans-[(CH)$_5$MoP(OCH$_2$CMe$_2$CH$_2$O)NH(CH$_2$)$_2$N= CHC$_6$H$_4$-o-O)]$_2$Cu," *J. Organometal. Chem.*, **381**, 53 (1990).

348. H. Zhang and J. L. Atwood, "Crystal and Molecular Structure of Cyclotriveratrylene," *J. Cryst. Spec. Res.*, **20**, 465 (1990).

349. M. B. Power, A. R. Barron, J. L. Atwood, and S. G. Bott, "π-Face Selectivity of Coordinated Ketones to Nucleophilic Additions: The Importance of Aluminum-Oxygen π-Bonding," *J. Am. Chem. Soc.*, **112**, 3446 (1990).

350. T. Lu, H. K. Yoo, H. Zhang, S. G. Bott, J. L. Atwood, L. Echegoyen, and G. W. Gokel, "Podand-Catalyzed Nucleophilic Aromatic   Substitutions of Anthra-

quinones: A Novel Synthetic Approach and a Mechanistic Suggestion from Solid State Data," *J. Org. Chem.*, **55**, 2269 (1990).

351. M. B. Power, A. W. Applett, S. G. Bott, J. L. Atwood, and A. R. Barron, "Aldol Condensation of Ketones Promoted by Sterically Crowded Aryloxide Compounds of Aluminum," *Organometallics*, **9**, 2529 (1990).

352. J. L. Atwood, S. G. Bott, R. A. Jones, and S. U. Koschmieder, "Synthesis and Structure of Cp*BePBu$^t_2$: The First Diorganophosphide Derivative of Beryllium," *J. Chem. Soc., Chem. Commun.*, 692 (1990).

353. R. D. Rogers, J. L. Atwood, M. D. Rausch, and D. W. Macomber, "Crystal Stuctures of (η^5-C$_5$H$_4$COMe)M(CO)$_3$Me (M = Mo, W)," *J. Cryst. Mol. Struct.*, **20**, 555 (1990).

354. M. J. Zaworotko, J. L. Atwood, and R. D. Priester, "Structure, Conformation and Reactivity of Organotransition Metal π-Complexes. Part 2. X-Ray Crystallographic Characterization of Two Neutral Half-Sandwich Cr(CO)$_3$ Complexes," *J. Coord. Chem.*, **22**, 209 (1990).

355. A. W. Coleman, C. M. Means, S. G. Bott, and J. L. Atwood,   "Air-Stable Liquid Clathrates, I. Crystal Structure of [NBu$_4$][Br$_3$] and Reactivity of the [NBu$_4$][Br$_3$]·7 C$_6$H$_6$ Liquid Clathrate," *J. Cryst. Spec. Res.*, **20,** 199, (1990).

356. D. A. Atwood, R. A. Jones, A. H. Cowley, J. L. Atwood, and S. G. Bott, "X-ray Crystal Structure of the Dimethylgallium Azide Polymer and Its Use as a Gallium Nitride Precursor," *J. Organomet. Chem.*, **394**, C6 (1990).

357. J. L. Atwood, "Cation Complexation by Calixarenes," in *Cation Binding by Macrocycles*, Eds., G. W. Gokel and Y. Inoue, Dekker, New York, 1990, pp. 581-597.

358. S. G. Bott, A. Alvanipour, and J. L. Atwood, "Stabilization of H$_2$O.BF$_3$ by Hydrogen-Bonding to 18-Crown-6," *J. Incl. Phenom.* **10**, 153 (1990).

359. M. D. Rausch, W. C. Spink, B. G. Conway, R. D. Rogers, J. L. Atwood, and L. G. Canada, "Synthetic and Structural Studies on (η^5: η^5-Fulvalene)bimetallic Compounds Derived from (η^5: η^5-Fulvalene)dithallium" *J. Organomet. Chem.*, **383**, 227 (1990).

360. J. L. Atwood and S. G. Bott "Water Soluble Calixarene Salts. A Class of Compounds with Solid-State Structures Resembling those of Clays", in *Calixarenes*, Eds., J. Vicens and V. Böhmer, Kluwer, 1990, pp. 209-221.

41

361. C. M. Means, S. G. Bott, and J. L. Atwood, "Reduction of Sugars with Aluminum Alkyls. Preparation and Structure of $[AlCl_2(NC_5H_5)(OEt_2)]_2(\mu$-O)- $(\mu$-AlCl.2NC_5H_5$)," *Polyhedron*, **9**, 309, (1990).

362. M. B. Power, S. G. Bott, D. L. Clark, J. L. Atwood, and A. R. Barron, "The Interaction of Organic Carbonyls with Sterically Crowded Aryloxide Compounds of Aluminum," *Organometallics,* **9**, 3086 (1990).

363. A. H. Cowley, R. A. Jones, M. A. Mardones, J. Ruiz, J. L. Atwood, and S. G. Bott, "Synthesis and Structure of a Diphosphagalletane: A Novel Base-Stabilized Ga_2P_2 Ring System," *Angew. Chem. Int. Ed. Engl.,* **29**, 1150 (1990).

364. A. H. Cowley, R. A. Jones, M. A. Mardones, J. Ruiz, J. L. Atwood, and S. G. Bott, "Cleavage of a Phosphorus-Carbon Double Bond and Formation of a Linear Terminal Phosphinidene Complex," *J. Amer. Chem. Soc.,* **112**, 6734 (1990).

365. J. L. Atwood, S. G. Bott, and R. L. Vincent, "Crystal Structure of Dinitrato - tris(pyridine)nickel (II), $Ni(NC_5H_5)_3(NO_3)_2$," *J. Cryst. Spec. Res.,* **20**, 631 (1990).

366. D. H. Miles, J. M. R. del Medeiros, V. Chittawond, C. Swithenbank, Z. Lidert, J. A. Weeks, J. L. Atwood, and P. A. Hedin, "3'-Formyl-2',4',6'-Trihydroxy-5'-methyldihydrochalcone, A Prospective New Agrochemical from Psidium acutangulum," *J. Nat. Products*, **53**, 1548 (1990).

367. A. H. Cowley, R. A. Jones, M. Mardones, S. G. Bott and J. L. Atwood, "An Aluminum - Phosphorus Cubane, a New Aluminum Phosphide Precursor," *Angew. Chem. Int. Ed. Engl.,* **29**, 1409 (1990).

368. F. Hamada, T. Fukugaki, K. Murai, G. W. Orr, and J. L. Atwood, "Liquid-Liquid Extraction of Transition and Alkali Metal Cations by a New Calixarene: Diphenyl Phosphino Calix[4]arene Methyl Ether," *J. Incl. Phenom.*, **10**, 57 (1991).

369. J. L. Atwood, S. G. Bott, K. D. Robinson, E. J. Bishop, and M. T. May, "Preparation and X-ray Structure of $[H_3O^+\cdot 18$-Crown-6][$H_5O_2^+$](Cl^-)$_2$, a Compound Containing both H_3O^+ and $H_5O_2^+$ Crystallized from Aromatic Solution," *J. Cryst. Spec. Res.,* **21**, 458 (1991).

370. E. Hey-Hawkins, M. F. Lappert, J. L. Atwood, and S. G. Bott, "Bis(trimethylsilyl)phosphido Complexes. Part 3. Synthesis Structures and Reactions of [Bis(trimethylsilyl)phosphido]zirconocene(IV) and the X-ray Structure

of {AlMe$_2$μ-P(SiMe$_3$)$_2$}$_2$." *J. Chem. Soc., Dalton Trans.*, 939 (1991).

371. M. B. Power, S. G. Bott, E. J. Bishop, K. D. Tierce, J. L. Atwood, and A. R. Barron, "Acylation and Esterification of the Aryloxide Ligand in AlMe(BHT)$_2$" *J. Chem. Soc., Dalton Trans.,* 241 (1991).

372. C. J. Harlan, T. C. Wright, J. L. Atwood, and S. G. Bott, "Hydrazinophosphine Complexes of Iron: Metallocycle Formation via Attack on Coordinated Carbon Monoxide," *Inorg. Chem.,* **30**, 1955 (1991).

373. J. C. Medina, T. T. Goodnow, S. Bott, J. L. Atwood, A. E. Kaifer, and G. W. Gokel, Ferrocenyldimethyl-[2.2]-Cryptand: Solid State Structure of the External Hydrate and Alkali and Alkaline-earth-dependent Electrochemical Behaviour," *J. Chem. Soc., Chem. Commun.,* 290 (1991).

374. R. Alvarez, J. L. Atwood, E. Carmona, P. J. Perez, M. L. Poveda, and R. D. Rogers, "Formation of Carbonyl-Carbonate Complexes of Molybdenum by Reductive Disproportionation of Carbon Dioxide. X-Ray Structure of Mo$_4$(μ$_4$-CO$_3$)(CO)$_2$(O)$_2$(μ$_2$-OH)$_4$ (PMe$_3$)$_6$," *Inorg. Chem.,* **30**, 1493 (1991).

375. J. C. Medina, C. Li, S. G. Bott, J. L. Atwood, and G. W. Gokel, "A Molecular Receptor Based on the Ferrocene System: Selective Complexation Using Atomic Ball-bearings," *J. Am. Chem. Soc.,* **113**, 366 (1991).

376. J. L. Atwood, G. W. Orr, F. Hamada, R. L. Vincent, S. G. Bott, and K. D. Robinson,"Second Sphere Coordination of a Transition Metal Complex by a Calix[4]arene," *J. Am. Chem. Soc.*, **113**, 2760 (1991).

377. J. L. Atwood, F. Hamada, K. D. Robinson, G. W. Orr, and R. L. Vincent, "X-Ray diffraction evidence for aromatic π hydrogen bonding to H$_2$O," *Nature*, **349**, 683 (1991).

378. D. H. Miles, V. Chittawong, D.-S. Lho, A. M. Payne, A. A. de la Cruz, E. D. Gomez, J. A. Weeks, and J. L. Atwood, "Toxicants from Mangrove Plants, VII. Vallapin and Vallapianin, Novel Sesquiterpene Lactones from the Mangrove Plant Heritiera littoralis," *J. Natural Prod.*, **54**, 286 (1991).

379. N. S. Kishore, T. Lu, L. J. Knoll, A. Katoh, D. A. Rudnick, P. P. Mehta, B. Devadas, M. Huhn, J. L. Atwood, S. P. Adams, G. W. Gokel, and J. I. Gordon, "The Substrate Specificity of Saccharomyces cerevisiae Myristoyl-CoA:Protein N-Myristoyltransferase," *J. Biol. Chem.*, **266**, 8835 (1991).

380. J. L. Atwood, S. G. Bott, F. M. Elms, C. Jones, and C. L. Raston, "Tertiary Amine Adducts of Gallane," *Inorg. Chem.*, **30**, 3792 (1991).

381. J. A. Ewen, M. J. Elder, R. L. Jones, L. Haspeslagh, J. L. Atwood, S. G. Bott, and K. Robinson, "Metallocene/Polypropylene Structural Relationships: Implications on Polymerization and Stereochemical Control Mechanisms" *Makromol. Chem., Macromol Symp.*, **48/49**, 253 (1991).

382. E. Carmona, L. Contreras, M. L. Poveda, L. J. Sanchez, J. L. Atwood, and R. D. Rogers," η^2-Acyl and Methyl complexes of Tungsten. Crystal and Molecular Structures of $W(\eta^2\text{-COCH}_2\text{SiMe}_3)\text{Cl(CO)(PMe}_3)_3$ and $W(\text{CH}_3)(S_2\text{CNMe}_2)$-$(\text{CO})_2(\text{PMe}_3)_2$," *Organometallics*, **10**, 61 (1991).

383. L. M. Clarkson, W. Clegg, D. C. R. Hockless, N. C. Norman, L. J. Farrugia, S. G. Bott, and J. L. Atwood, "Synthetic and Structural Studies on Group 13 Complexes Containing the $M(\text{CO})_3(\eta\text{-C}_5\text{H}_5)$ Fragment (M = Cr, Mo); Part 2," *J. Chem. Soc., Dalton Trans.*, 2241 (1991).

384. J. C. W. Chien, G. H. Llinas, M. D. Rausch, J. L. Atwood, and S. G. Bott, Two-State Propagation Mechanism for Propylene Polymerization Catalyzed by "rac[anti-Ethylidene(1-η^5-tetramethylcyclopentadienyl)(1-η^2-indenyl)dimethyl- titanium]," *J. Am. Chem. Soc.*, **113**, 8569 (1991).

385. J. L. Atwood, S. G. Bott, C. Jones, and C. L. Raston, "Oligomeric Gallium Amide/Hydride Complexes, $[\text{Ga}_2\text{H}_2((\text{NPr}^i\text{CH}_2)_2)_2]$ and $[\text{Ga}_3\text{H}_5((\text{NMeCH}_2)_2)_2]$, via Hydromethallation and Metalation," *Inorg. Chem.*, **30**, 4868 (1991).

386. O. F. Schall, K. Robinson, J. L. Atwood, and G. W. Gokel, "Self-Assembling, Alkali-Metal-Complexing Nickel Salicylaldimine Complexes," *J. Am. Chem. Soc.*, **113**, 7434 (1991).

387. J. L. Atwood, F. R. Bennett, F. M. Elms, C. Jones, C. L. Raston, and K. D. Robinson "Tertiary Amine Stabilized Dialane," *J. Amer. Chem. Soc.*, **113**, 8183 (1991).

388. J. L. Atwood, K. D. Robinson, C. Jones, and C. L. Raston "Cationic Aluminum Hydrides: $[\text{H}_2\text{AlL}]^+[\text{AlH}_4]^-$, L = N,N,N,',N",N"-Penta- methyldiethylene- triamine and N,N',N",N'"-Tetramethylcyclam," *J. Chem. Soc., Chem. Commun.*, 1697 (1991).

389. D. A. Atwood, R. A. Jones, A. H. Cowley, S. G. Bott, and J. L. Atwood, "Primary Amido and Amine Adduct Complexes of Gallium: Synthesis and Structures of [t-$\text{Bu}_2\text{Ga}(\mu\text{-NHPh})]_2$ and t-$\text{Bu}_3\text{Ga}\cdot\text{NH}_2\text{Ph}$," *Polyhedron,* **10**, 1897 (1991).

390.   A. H. Cowley, R. A. Jones, M. A. Mardones, J. L. Atwood, and S. G. Bott, "A Novel Gallium-Phosphorus Cage Compound," *Angew. Chem. Int. Ed. Engl.*, **30**, 1141 (1991).

391.   A. H. Cowley, R. A. Jones, M. A. Mardones, J. L. Atwood, and S. G. Bott, "Reaction of (t-BuGaCl$_2$)$_2$ with Ar'PHLi (Ar' = 2,4,6-t-Bu$_3$C$_6$H$_2$): Preparation of the Chloride-Bridged Dimer (t-BuGa(Cl)P(H)Ar')$_2$," *Heteroatom. Chem.*, **2**, 11(1991).

392.   S. G. Bott, A. Alvanipour, and J. L. Atwood, "Stabilization of Boron Trifluoride Monohydrate by Hydrogen Bonding to 18-Crown-6," *J. Incl. Phenom.*, **10**, 153 (1991).

393.   J. L. Atwood, S. G. Bott, and M. T. May, "Synthesis and Crystal Structure of [(ClAl(μ-OH)$_2$AlCl]$\cdot$18-crown-6][AlCl$_4$]$_2\cdot$8/3 C$_6$H$_5$NO$_2$, a Complex Featuring a Binuclear Aluminum-Containing Cation Threaded through 18-Crown-6," *J. Coord. Chem.*, **23**, 313 (1991).

394.   J. A. Ewen, M. J. Elder, C. J. Harlan, R. L. Jones, J. L. Atwood, S. G. Bott, and K. Robinson, "π-Face Selectivity in Syndiospecific Propylene Polymerizations with Zirconium (IV) Monoalkyl Cations," *Polym. Prepr.* (Am. Chem. Soc., Div. Polym. Chem.), **32**, 469 (1991).

395.   M. Tsesarskaja, T. P. Cleary, S. R. Miller, J. E. Trafton, S. Bott, J. L. Atwood, and G. W. Gokel, "Tribracchial Lariat Ethers: Syntheses, Binding, and Formation of an Intramolecular Macroring-sidearm Complex in the Absence of Any Cation," *J. Incl. Phenom.*, **12**, 187 (1992).

396.   R. K. Juneja, K. D. Robinson, G. W. Orr, R. H. Dubois, K. A. Belmore, and J. L. Atwood, "Inclusion of Multi-ring Compounds by p-tert-Butylcalix[5]arene," *J. Incl. Phenom.*, **13**, 93 (1992).

397.   J. L. Atwood, F. R. Bennett, C. Jones, G. A. Koutsantonis, C. L. Raston, and K. D. Robinson, "Polydentate Tertiary Amine Alane Adducts: Monomeric versus Polymeric Species," *J. Chem. Soc., Chem. Commun.*, 541 (1992).

398.   J. L. Atwood, D. L. Clark, R. K. Juneja, G. W. Orr, K. D. Robinson, and R. L. Vincent, "Double Partial Cone Conformation for Na$_8$[calix[6]arene sulfonate]$\cdot$20.5 H$_2$O and Its Parent Acid," *J. Am. Chem. Soc.*, **114**, 7558 (1992).

399.   C. J. Harlan, T. C. Wright, S. G. Bott, and J. L. Atwood, "Synthesis and Structure of

45

[CpFe(CO){(Ph$_2$P)$_2$NNMe$_2$}][I]·CH$_2$Cl$_2$," *J. Cryst. Spec. Res.*, **22**, 91 (1992).

400. C. J. Harlan, T. C. Wright, S. G. Bott, and J. L. Atwood, "Synthesis and X-ray Crystal Structure of a Five Coordinate d^8 Complex: [Pt((Me$_2$NN)(PMe$_2$)-(PPh$_2$))$_2$Cl][Cl]," *J. Cryst. Spec. Res.*, **22**, 71 (1992).

401. J. L. Atwood, G. W. Orr, N. C. Means, F. Hamada, H. Zhang, S. G. Bott, and K. D. Robinson, "Metal Ion Complexes of Water Soluble Calix[4]arenes," *Inorg. Chem.*, **31**, 603 (1992).

402. J. L. Atwood, G. W. Orr, F. Hamada, S. G. Bott, and K. D. Robinson, "Supramolecular Assemblies of Calix[4]arenes Organized by Weak Forces," *Supramol. Chem.*, **1**, 15 (1992).

403. R. O. C. Hart, S. G. Bott, J. L. Atwood, and S. R. Cooper, "Higher Valent Manganese Chemistry. [Mn(biguanide)$_3$]$^+$, a Structurally Characterized Mn^{IV} Complex with All-Nitrogen Coordination," *J. Chem. Soc., Chem. Commun.*, 894 (1992).

404. D. A. Atwood, R. A. Jones, A. H. Cowley, S. G. Bott, and J. L. Atwood, "Primary Amide and Amine Complexes of Gallium and Indium: X-ray Crystal Structures of [Me$_2$Ga(μ-NH(Bu))]$_2$, Me$_3$Ga·NH$_2$(Bu) and Me$_3$In·NH$_2$(Bu)," *J. Organomet. Chem.*, **434**, 143 (1992).

405. J. L. Atwood, A. Alvanipour, and H. Zhang, "Synthesis and Structure of ((H$_2$O)·HBF$_4$)$_2$(18-crown-6)," *J. Cryst. Spec. Res.*, **22**, 349 (1992).

406. J. L. Atwood, F. R. Bennett, K. D. Robinson, F. M. Elms, G. A. Koutsantonis, C. L. Raston, and D. J. Young "Gallane/Phosphine Adducts: Air Stable [H$_3$Ga{P(C$_6$H$_{11}$)$_3$}] and Gallane Rich [(H$_3$Ga)$_2${(PMe$_2$CH$_2$)$_2$}]," *Inorg. Chem.*, **31**, 2673 (1992).

407. M. Clark, C. J. Kellen, K. D. Robinson, H. Zhang, Z.-Y. Yang, K. V. Madappat, J. W. Fuller, J. L. Atwood, and J. S. Thrasher "Naked SF$_5^-$ Anion: The Crystal and Molecular Structure of [Cs$^+$·(18-Crown-6)$_2$][SF$_5^-$]," *Eur. J. Solid State Inorg. Chem.*, **29**, 809 (1992).

408. R. H. Wallace, Y. S. Lu, J. C. Liu, and J. L. Atwood, "Synthesis of alpha-Pinene Derived C-2 Symmetrical, Optically-Active 1,2-Diols," *Synlett*, 992 (1992).

409. H. Kim, O. F. Schall, J. Fang, J. E. Trafton, T. Lu, J. L. Atwood, and G. W. Gokel, "Direct Nucleophilic Aromatic Substitution Reactions in the Syntheses of Anthraquinone Derivatives: Chemistry and Binding of Podands, Crown Ethers, and a Cryptand," *J. Phys. Org. Chem.*, **5**, 482 (1992).

410. J. L. Atwood, S. G. Bott, C. Jones, and C. L. Raston, "Aluminum Fused Bis-p-tert-Butylcalix[4]arene: A Double Cone with Two π-Arene...H-Interactions for Included Methylene Chloride," *J. Chem. Soc., Chem. Commun.*, 1349 (1992).

411. R. Chukwu, A. D. Hunter, B. D. Santarsiero, S. G. Bott, J. L. Atwood, and J. Chassalgnac, "Electrochemical, Spectroscopic, and Structural Studies of Mono- and Bimetallic Complexes of Iron," *Organometallics*, **11**, 589 (1992).

412. D. A. Atwood, A. H. Cowley, R. A. Jones, M. A. Mardones, J. L. Atwood, and S. G. Bott, "Synthesis and Structures of Two Bulky Gallium Chlorides," *J. Coord. Chem.*, **25**, 233 (1992).

413. D. A. Atwood, R. A. Jones, A. H. Cowley, S. G. Bott, and J. L. Atwood, "Structural Characterization of a Dialkylgallium Cation: X-ray Crystal Structure of [Me$_2$Ga(BuNH$_2$)$_2$]Br," *J. Organomet. Chem.*, **425**, C1 (1992).

414. R. A. Jones, S. U. Koschmieder, J. L. Atwood, and S. G. Bott, "Insertion of LiPEt$_2$ into Poly(dimethylsiloxane) to Give [LiOSiMe$_2$PEt$_2$]$_6$," *J. Chem. Soc., Chem. Commun.,* 726 (1992).

415. J. L. Atwood, S. D. Christie, M. D. Clerk, D. A. Osmond, K. C. Sturge, and M. J. Zaworotko, "Interaction of Alkylaluminum Reagents with Organotransition Metal Arene Complexes: Net Addition of Alkide, Haloalkide and Dichloromethide to [(arene)$_2$Fe]$^{2+}$ Cations," *Organometallics*, **11**, 337 (1992).

416. J. L. Atwood, G. W. Orr, F. Hamada, R. L. Vincent, S. G. Bott, and K. D. Robinson, "Calixarenes as Second-Sphere Ligands for Transition Metal Ions," *J. Incl. Phenom.*, **14**, 37 (1992).

417. D. A. Atwood, A. H. Cowley, R. A. Jones, M. A. Mardones, J. L. Atwood, and S. G. Bott, "Synthesis and Structures of [NMe$_2$(μ-NMe$_2$)GaCl]$_2$ and [TMP(μ-OEt)GaCl]$_2$ (TMP = 2,6-tetramethylpipyridine)," *J. Coord. Chem.*, **26**, 285 (1992).

418. C. Balagopalakrishna, M. V. Rajasekharan, S. Bott, J. L. Atwood, and B. L. Ramakrishna, "Synthesis, Crystal Structure, Magnetic Susceptibility, and Single Crystal EPR Studies of Bis(diazafluorenone)dichlorocopper(II): A Novel

Cu(NN)$_2$X$_2$ System with an Unusual Distortion," *Inorg. Chem.*, **31**, 2843 (1992).

419. D. A. Atwood, A. H. Cowley, R. A. Jones, J. L. Atwood, and S. G. Bott, "Synthesis and X-ray Structure of Me$_2$InI(NH$_2$(t-Bu)): The First Structurally Characterized Amine Adduct of a Dialkyl Indium Iodide," *J. Coord. Chem.*, **26**, 293 (1992).

420. D. A. Atwood, V. O. Atwood, A. H. Cowley, J. L. Atwood, and E. Roman, "Macrocyclic (C$_{22}$H$_{22}$ N$_4$) Complexes of Ge(II), Sn(II), Ga(III), and In(III). Main Group Functionalities in an Unusual Environment," *Inorg. Chem.*, **31**, 3871 (1992).

421. J. Fang, R. Lu, H. Kim, I. Delgado, P. Geoffroy, J. L. Atwood, and G. W. Gokel, "Alkynes and Polyethylene Glycol Derivatives as Nucleophiles and Catalysts in Substitution Reactions of 1-Chloroanthraquinones," *J. Org. Chem.*, **56**, 7059 (1992).

422. J. C. W. Chien, G. H. Llinas, M. D. Rausch, Y.-G. Lin, H. H. Winter, J. L. Atwood, and S. G. Bott, "Metallocene Catalysts for Olefin Polymerizations. XXIV. Stereoblock Propylene Polymerization Catalyzed by rac-[anti-Ethylidene(1-η^5-Tetramethylcyclopentadienyl)(1-η^5-Indenyl)dimethyltitanium]: A Two-State Propagation," *J. Poly. Sci. A. Poly. Chem.*, **30**, 2601 (1992).

423. J. C. Medina, T. T. Goodnow, M. T. Rojas, J. L. Atwood, B. C. Lynn, A. E. Kaifer, and G. W. Gokel, "Ferrocenyl Iron as a Donor Group for Complexed Silver in Ferrocenyldimethyl[2.2]cryptand: A Redox-Switched Receptor Effective in Water," *J. Am. Chem. Soc.*, **114**, 10583 (1992).

424. J. Li, A. D. Hunter, R. McDonald, B. D. Santarsiero, S. G. Bott, and J. L. Atwood, "π-Donor Interactions and the Origin of Arene Nonplanarity in Heterobimetallic (η^6-arene)Cr(CO)$_3$ Complexes Having σ-Bonded Organometallic Substituents," *Organometallics*, **11**, 3050 (1992).

425. J. L. Atwood, "Inclusion (Clathrate) Compounds," in Encyclopedia of Physical Science and Technology, Vol. 8, 25-36 (1992).

426. F. Hamada, K. D. Robinson, G. W. Orr, and J. L. Atwood, "Alkali Metal Salts of Oxyanions of p-*tert*-Butylcalix[4]arene," *Supramol. Chem.*, **2**, 19 (1993).

427. G. Facey, R. H. Dubois, M. Zakrzewski, C. I. Ratcliffe, J. L. Atwood, and J. A. Ripmeester, "Phase Transition and Dynamic Structure of the Toluene Complex of t-Butylcalix[4]arene," *Supramol. Chem.*, **1**, 199 (1993).

428. D. A. Atwood, A. H. Cowley, P. R. Harris, R. A. Jones, J. L. Atwood, and S. G. Bott,

"Cyclic Trimeric Hydroxy, Amido, Phosphido and Arsenido Derivatives of Al and Ga. X-ray Structures of [t-Bu$_2$Ga(μ-OH)]$_3$ and [t-Bu$_2$Ga(μ-NH$_2$)]$_3$," *Organometallics*, **12**, 24 (1993).

429. J. L. Atwood and G. W. Gokel, "Molecular Recognition," in McGraw-Hill Dictionary of Science, 244-247 (1993).

430. R. M. Metzger, J. L. Atwood, W.-J. Lee, S. M. Rao, R. B. Lal, and B. H. Loo, "Structure of MAP:MNA, a New Nonlinear Optical Crystal," *Acta Crystallogr.*, **C49**, 738 (1993).

431. O. F. Schall, K. Robinson, J. L. Atwood, and G. W. Gokel, "Self-Assembling Nickel Clusters form Binding Sites for Alkali Metal Cations," *J. Am. Chem. Soc.*, **115**, 5962 (1993).

432. D. Lorcy, K. D. Robinson, Y. Okuda, J. L. Atwood, and M. P. Cava, "Novel Electron Acceptors Derived from Isothianaphthlene," *J. Chem. Soc., Chem. Commun.*, 345 (1993).

433. J. L. Atwood, G. W. Orr, S. G. Bott, and K. D. Robinson, "Supramolecular Complexes of Flexible, Extended Cavity Calix[4]arenes - Structural Characterization of a Molecular Venus's Flytrap," *Angew. Chem. Int. Ed. Engl.*, **32**, 1093 (1993).

434. J. L. Atwood, G. W. Orr, K. D. Robinson, and F. Hamada, "Calixarenes as Enzyme Models," *Supramol. Chem.*, **2**, 309 (1993).

435. F. M. Elms, M. G. Gardiner, G. A. Koutsantonis, C. L. Raston, J. L. Atwood, and K. D. Robinson, "Tertiary Phosphine Adducts of Alane and Gallane," *J. Organomet. Chem.*, **449**, 45 (1993).

436. F. Hamada, G. W. Orr, H. Zhang, and J. L. Atwood, "Crystal Structure of cyanocalix[4]arene methyl ether," *J. Cryst. Spec. Res.*, **23**, 681 (1993).

437. M. V. Lakshmikantham, M. P. Cava, W. H. H. Gunther, P. N. Nugara, K. A. Belmore, J. L. Atwood, and P. Cragg, "Synthesis of 1,2-Ditellurolane Derivatives," *J. Am. Chem. Soc.*, **115**, 885 (1993).

438. J. L. Atwood, G. W. Orr, R. K. Juneja, S. G. Bott, and F. Hamada, "Supramolecular Assemblies Based on Calixarenes," *Pure & Appl. Chem.*, **65**, 1471 (1993).

439. R. K. Juneja, K. D. Robinson, C. P. Johnson, and J. L. Atwood, "Synthesis and Characterization of Rigid, Deep-Cavity Calix[4]arenes," *J. Am. Chem. Soc.,* **115**, 3818

(1993).

440. J. L. Atwood, K. W. Butz, M. G. Gardiner, C. Jones, G. A. Koutsantonis, C. L. Raston, and K. D. Robinson, "Mixed-Donor and Monomeric N-Donor Adducts of Alane," *Inorg. Chem.*, **32**, 3482 (1993).

441. D. A. Atwood, A. H. Cowley, R. D. Hernandez, R. A. Jones, L. L. Rand, S. G. Bott, and J. L. Atwood, "Synthesis and Structural Characterization of a Homoleptic Bismuth Arenethiolate," *Inorg. Chem.*, **32**, 2972 (1993).

442. A. Razavi and J. L. Atwood, "Preparation and Crystal Structures of the Complexes(η^5-C$_5$H$_4$CPh$_2$-η^5-C$_{13}$H$_8$)MCl$_2$ (M = Zr, Hf) and the Catalytic Formation of High Molecular Weight High Tacticity Syndiotactic Polypropylene," *J. Organomet. Chem.*, **459**, 117 (1993).

443. D. A. Atwood, V. O. Atwood, A. H. Cowley, H. R. Gobran, and J. L. Atwood, "Facile Transmetalation Reactions of Macrocyclic (C$_{22}$H$_{22}$N$_4$) Complexes of Germanium(II), Tin(II), and Lead(II)," *Inorg. Chem.*, **32**, 4671 (1993).

444. A. Razavi and J. L. Atwood, "Isospecific Propylene Polymerization with Unbridged Group 4 Metallocenes," *J. Am. Chem. Soc.*, **115**, 7529 (1993).

445. R. D. Schluter, A. H. Cowley, D. A. Atwood, R. A. Jones, and J. L. Atwood, "An Alkyl-substituted indium(I) Tetramer," *J. Coord. Chem.*, **30**, 25 (1993).

446. C. Scordilis-Kelley, K. D. Robinson, K. A. Belmore, J. L. Atwood, and R. T. Carlin, "Evidence for Hydrogen Bonds in 1,2-dimethyl-3-propylimidazolium Chloride and Its Chloroaluminate Molten Salts," *J. Cryst. Spec. Res.*, **23**, 601 (1993).

447. A. K. Singh, R. K. Juneja, J. L. Atwood, and R. J. Bridges, "Para-sulfonatocalixarenes are Potent Blockers of Colonic Chloride Channels," *Biophys. J.*, **64**, A17 (1993).

448. A. K. Singh, R. K. Juneja, R. Wang, J. L. Atwood, and R. J. Bridges, "TS-TM-Calix[4]arene: A Subnanomolar Blocker of ORCC," *Ped. Pulm.*, **9**, 227 (1993).

449. P. C. Junk and J. L. Atwood, "On the Crystal Structure of Hexathia-18-crown-6," *Supramol. Chem.*, **3**, 241 (1994).

450. A. Harton, M. K. Nagi, M. M. Glass, P. C. Junk, J. L. Atwood, and J. B. Vincent, "Synthesis and Characterization of Symmetric and Asymmetric Oxo-bridged Trinuclear Chromium Benzoate Complexes: Crystal and Molecular Structure of

$[Cr_3O(O_2CPh)_6(py)_3]ClO_4$," *Inorg. Chim. Acta*, **217**, 171 (1994).

451. J. L. Atwood, G. W. Orr, and K. D. Robinson, "First structural authentication of third-sphere coordination: [p-sulfonatocalix[4]arene]$^{5-}$ as a third-sphere ligand for Eu^{3+}," *Supramol Chem.*, **3**, 89 (1994).

452. J. L. Atwood, S. M. Lawrence, and C. L. Raston, "N,N'-Di-t-Butylethylenediamine/$Cl_nH_{3-n}AlNMe_3$ Derivatives,"*J. Chem. Soc., Chem. Commun.*, 73 (1994).

453. J. L. Atwood, G. A. Koutsantonis, F.-C. Lee, and C. L. Raston, "A Thermally Stable Alane - Secondary Amine Adduct: [$H_3Al(2,2,6,6$-Tetramethylpiperidine)]," *J. Chem. Soc., Chem. Commun.*, 91 (1994).

454. J. L. Atwood,. F.-C. Lee, C. L. Raston, and K. D. Robinson, "Bimetallic Aluminum and Gallium Derivatives of 1,1,1,5,5,5-Hexafluoropentane-2,4-dione via Selective Metallation/Hydrometallation," *J. Chem. Soc., Dalton Trans.*, 2019 (1994).

455. J. L. Atwood, P. C. Junk, M. T. May, and K. D. Robinson, "Synthesis and X-ray Structure of [H_3O^+·18-crown-6][Br-Br-Br]; a Compound Containing both H_3O^+ and a Linear and Symmetrical Br_3^- Ion Crystallized from Aromatic Solution," *J. Chem. Cryst.*, **24**, 243 (1994).

456. P. C. Junk and J. L. Atwood, "Synthesis and X-ray Structures of [H_3O^+·18-crown-6]$_n$[MCl_4^{n-}]; (M = Fe, n = 1; M = Co, n = 2); Compounds which Form Liquid Clathrates with Aromatic Solutions," *J. Chem. Cryst.*, **24**, 247 (1994).

457. J. L. Atwood, G. A. Koutsantonis, and C. L. Raston, "High Purity Fullerene-60 via Molecular Recognition," *Nature*, **368**, 229 (1994).

458. J. W. Steed, P. C. Junk, J. L. Atwood, M. J. Barnes, C. L. Raston, and R. S. Burkhalter, "Ball and Socket Nano-Structures: New Supramolecular Chemistry Based on Cyclotriveratrylene," *J. Am. Chem. Soc.*, **116**, 10346 (1994).

459. J. W. Steed, R. K. Juneja, R. S. Burkhalter, and J. L. Atwood, "Synthesis of Cationic Organometallic Calixarene Hosts by Direct Metallation of the Outer Face," *J. Chem. Soc., Chem. Commun.*, 2205 (1994).

460. J. L. Atwood, R. K. Juneja, P. C. Junk, and K. D. Robinson, "Structure of p-tert-Butylcalix[5]arene.Ethyl Acetate. A Polymeric Array of Neighbor-Included Calixarenes," *J. Chem. Cryst.*, **24**, 573 (1994).

461. Z. Hu, J. L. Atwood, and M. P. Cava, "A Simple Route to Sulfur Bridged Annulenes," *J. Org. Chem.*, **59**, 8071 (1994).

462. J. L. Atwood, S. G. Bott, S. Harvey, and P. C. Junk, "Cationic, Neutral, and Anionic Organoaluminum Species in [AlMe$_2$·18-crown-6·AlMe$_2$X][AlMeX$_3$], (X = Cl, I)," *Organometallics*, **13**, 4151 (1994).

463. D. A. Atwood, V. O. Atwood, A. H. Cowley, R. A. Jones, J. L. Atwood, and S. G. Bott, "Synthesis and Structural Characterization of Homoleptic Gallium Amides," *Inorg. Chem.*, **33**, 3251 (1994).

464. J. W. Steed, R. K. Juneja, and J. L. Atwood, "A Water-Soluble "Bear Trap" Exhibiting Strong Anion Complexation Properties," *Angew. Chem. Int. Ed. Engl.*, **33**, 2456 (1994).

465. J. L. Atwood, S. G. Bott, P. C. Junk, and M. T. May, "Liquid Clathrate Media Containing Transition Metal Halocarbonyl Anions," *J. Organomet. Chem.*, **487**, 7 (1995).

466. H. Zhang, J. W. Steed, and J. L. Atwood, "Inclusion Chemistry of Cyclotetraveratrylene," *Supramol. Chem.*, **4**, 185 (1995).

467. A. Razavi and J. L. Atwood, "Preparation and crystal structure of the complexes (η^5-C$_5$H$_3$MeCMe$_2$-η^5-C$_{13}$H$_8$)MCl$_2$ (M = Zr, Hf). Mechanistic aspects of catalytic formation of a syndio-iso-stereoblock type polypropylene," *J. Organomet. Chem.*, **497**, 105 (1995).

468. P. C. Blake, M. F. Lappert, R. G. Taylor, J. L. Atwood, W. E. Hunter, and H. Zhang, "Synthesis, Spectroscopic Properties, and X-ray Structures of [MCp"$_2$Cl$_2$] [M = Th or U; Cp" = η-C$_5$H$_3$(SiMe$_3$)$_2$-1,3], [UCp"$_2$X$_2$] (X= Br, I or BH$_4$," *J. Chem. Soc., Dalton Trans.*, 3335 (1995).

469. L. J. Barbour, J. W. Steed, and J. L. Atwood, "Inclusion Chemistry of Cyclotetracatechylene," *J. Chem. Soc., Perkin Trans. 2* , 857 (1995).

470. J. L. Atwood, L. J. Barbour, P. C. Junk, and G. W. Orr, "Structure of the Water Soluble p-Sulfonatocalix[4]arene which Acts as a Receptor for Tetramethylammonium Ions," *Supramol. Chem.*, **5**, 105 (1995).

471. K. T. Holman, M. M. Halihan, J. W. Steed, S. S. Jurisson, and J. L. Atwood, "Hosting a Radioactive Guest: Binding of ^{99}TcO$_4^-$ by a Metallated

Cyclotriveratrylene," *J. Am. Chem. Soc.*, **117**, 7848 (1995).

472. J. L. Atwood and P. C. Junk, "Synthesis and X-ray Structure of $[H_5O_2^+\cdot21$-Crown-7][WOCl$_5^-$]; a Complex in Which the 21-Crown-7 Molecule Adopts a Rigid, Bowlic Conformation," *Chem. Comm.*, 1551 (1995).

473. P. C. Junk, M. T. May, K. D. Robinson, L. MacGillivray, and J. L. Atwood, "Synthesis and X-ray Structure of [H$_3$O$^+\cdot$18-crown-6][I$_7^-$]: A New Infinite Saw-Horse Geometry for I$_7^-$ Crystallized from a Liquid Clathrate Medium," *Inorg. Chem.*, **34**, 5395 (1995).

474. L. R. MacGillivray and J. L. Atwood, "Proton Induced Chirality: Proton Complexation in the Chiral Cryptand [222-2H$^+$] Dication Isolated from a Liquid Clathrate Medium," *J. Org. Chem.*, **60**, 4972 (1995).

475. J. W. Steed, C. P. Johnson, C. L. Barnes, R. K. Juneja, J. L. Atwood, S. Reilly, R. L. Hollis, P. H. Smith, and D. L. Clark, "Supramolecular Chemistry of p-sulfonatocalix[5]arene: A Water Soluble, Bowl Shaped Host with a Large Molecular Cavity," *J. Am. Chem. Soc.*, **117**, 11426 (1995).

476. A. Razavi, L. Peters, L. Nafpliotis, K. D. Daw, J. L. Atwood, and U. Thewald, "The Geometry of the Site and Its Relevance for Chain Migration and Stereospecificity," *Macromol. Symp.*, **89**, 345-67 (1995).

477. A. Razavi, D. Vereecke, L. Petyers, K. D. Daw, L. Nafpliotis, and J. L. Atwood, "Manipulation of the Ligand Structure as an Effective and Versatile Tool for Modification of Active Site Properties in Homogeneous Ziegler-Natta Catalyst Systems," *Ziegler Catal.*, 111-47 (1995).

478. J. W. Steed, H. Zhang, and J. L. Atwood, "Inclusion Chemistry of Cyclotriveratrylene and Cyclotricatechylene," *Supramol. Chem.*, **7**, 37 (1996).

479. L. J. Barbour, L. R. MacGillivray, and J. L. Atwood, "Crystal and Molecular Structure of [H$_3$O·18-crown-6]$_2$[ReCl$_6$] Isolated from a Liquid Clathrate Medium," *J. Chem. Cryst.*, **26**, 59 (1996).

480. J. W. Steed, C. P. Johnson, R. K. Juneja, and J. L. Atwood "Anion Inclusion Within the Cavity of π-Metalated p-tert-butylcalix[5]arene," *Supramol. Chem.*, **6**, 235 (1996).

481.   J. L. Atwood, S. G. Bott, P. C. Junk, and M. T. May, "Anionic Coordination Complexes of Mo and W which Crystallize from Liquid Clathrate Media with

Oxonium Ion-Crown Ether Cations," *J. Coord. Chem.*, **37**, 89 (1996).

482. J. L. Atwood, "An Introduction to the Crystallography of Supramolecular Compounds," in *Crystallography of Supramolecular Compounds*, Eds: G. Tsoucaris, J. L. Atwood, and J. Lipkowski, Kluwer, Dordrecht, 1996, pp. 1-6.

483. J. L. Atwood, "Structural Models of Biological Significance from Supramolecular Systems," in *Crystallography of Supramolecular Compounds*, Eds: G. Tsoucaris, J. L. Atwood, and J. Lipkowski, Kluwer, Dordrecht, 1996, pp. 355-365.

484. L. J. Barbour, L. R. MacGillivray, and J. L. Atwood, "Structural Consequences of M-Cl...H-N Hydrogen Bonds in Substituted Pyridinium Salts of the Cobalt(II)tetrachloride Anion Isolated from Liquid Clathrate Media," *Supramol. Chem.*, **7**, 167 (1996).

485. L. R. MacGillivray and J. L. Atwood, "Insight into the Mechanism of the Protonation of Cryptand 222 within a Liquid Clathrate Medium: Synthesis and X-ray Crystal Structure of $[H_3O][222\text{-}2H][(CoCl_3)_2(\mu\text{-}Cl)]$," *J. Chem. Soc., Chem. Commun.*, 735 (1996).

486. C. P. Johnson, J. L. Atwood, J. W. Steed, C. B. Bauer, and R. D. Rogers, "Transition Metal Complexes of p-Sulfonatocalix[5]arene," *Inorg. Chem.*, **35**, 2602 (1996).

487. L. J. Barbour, A. Damon, G. W. Orr, and J. L. Atwood, "Inclusion of Protonated Organic Species by p-Sulfonatocalix[4]arene anions. Crystal and Molecular Structure of the Inclusion Compounds $(Na)_2[Cu(H_2O)_4(p\text{-}sulfonatocalix[4]arene)_2][Cu(H_2O)_4(pyridine)_2](pyridinium)_2 \cdot 10H_2O$ and $Na_4(morpholinium)[p\text{-}sulfonatocalix[4]arene] \cdot 8H_2O$," *Supramol. Chem.*, **7**, 209 (1996).

488. J. L. Atwood, "Diffraction Studies of Supramolecular Compounds," in Physical Supramolecular Chemistry, Eds.: L. Echegoyen and A. Kaifer, Kluwer, Dordrecht, 1996, pp 261-272.

489. J. L. Atwood, P. C. Junk, S. M. Lawrence, and C. L. Raston, "Zinc Dimerization of p-tert-butylcalix[4]arene," *Supramol. Chem.*, **7**, 15 (1996).

490. J. L. Atwood, M. G. Gardiner, C. Jones, C. L. Raston, B. W. Skelton, and A. H. White, "Trimethylaluminum and -gallium Derivatives of Calix[4]arenes: Cone (Mono-metallic) or Doubly Flattened Partial Cone (Tetra-metallic) Conformations," *J. Chem. Soc., Chem. Commun.*, 2487 (1996).

491. J. L. Atwood, C. Jones, C. L. Raston, and K. D. Robinson, "The First Structural Characterization of a Five Coordinate Aluminum Trichloride - Bidentate Tertiary Amine Adduct, Trichloro(1,4-dimethylpiperazine)aluminum," *Main Group Chem.*, **1**, 345 (1996).

492. J. L. Atwood, L. J. Barbour, E. S. Dawson, P. C. Junk, and J. Kienzle, "X-ray Structure of the Water Soluble Adeninium p-Sulfonatocalix[4]arene which Displays Cationic and Anionic Bilayers," *Supramol. Chem.,* **7,** 271 (1996).

493. J. L. Atwood, M. J. Barnes, M. G. Gardiner, and C. L. Raston, "Cyclotriveratrylene Polarisation Assisted Aggregation of C_{60}," *J. Chem. Soc., Chem. Commun.*, 1449 (1996).

494. C. L. Raston, J. L. Atwood, P. J. Nichols, and I. B. N. Sudria, "Supramolecular Encapsulation of Aggregates of C_{60}," *J. Chem. Soc., Chem. Commun.*, 2615 (1996).

495. J. L. Atwood, K. T. Holman, and J. W. Steed, "Laying Traps for Elusive Prey: Recent Advances in the Non-Covalent Binding of Anions," *J. Chem. Soc., Chem. Commun.*, 1401 (1996).

496. L. R. MacGillivray and J. L. Atwood, "Structural Reorganization of the $[222\text{-}2H]^{2+}$ Dication Through Cation-π and Charge-Charge Interactions: Synthesis and Structure of Its $[CoCl_4].0.5\ C_6H_5CH_3$ Salt," *Angew. Chem. Int. Ed. Engl.*, **35**, 1828 (1996).

497. K. T. Holman, M. M. Halihan, S. S. Jurisson, J. L. Atwood, R. S. Burkhalter, A. R. Mitchell, and J. W. Steed, "Inclusion of Neutral and Anionic Guests within the Cavity of π-Metallated Cyclotriveratrylenes," *J. Am. Chem. Soc.*, **118**, 9567 (1996).

498. A. D. Hunter, R. Chukwu, B. D. Santarsiero, S. G. Bott, and J. L. Atwood, "Synthesis and Characterization of Polyaromatic Azine Derivatives of (η^5-C_5H_5)Fe(CO)$_2$ and (η^5-C_9H_7)Fe(CO)$_2$," *J. Organomet. Chem.*, **526**, 1 (1996).

499. A. Razavi and J. L. Atwood, "Synthesis and Characterization of the Catalytic Isotactic-specific Metallocene $[C_4H_9\text{-}C_5H_3\text{-}C(CH_3)_2\text{-}(C_{13}H_8)ZrCl_2]$. Mechanistic Aspects of the Formation of Isotactic Polypropylene, the Stereoregulative Effect of the Distal Substituent and the Relevance of C_2 Symmetry, *J. Organomet. Chem.*, **520**, 115 (1996).

500. J. L. Atwood, P. C. Junk, M. T. May, and K. D. Robinson, "New, Simple Coordination Compounds of Cr, Mo, and W from Liquid Clathrate Media," *J. Coord. Chem.*, **40**, 247 (1996).

501. C. Li, J. C. Medina, E. Abel, J. L. Atwood, and G. W. Gokel, "Neutral Molecule Receptor Systems using Ferrocene's "Atomic Ball Bearing" Character as the Flexible Element," *J. Am. Chem. Soc.*, **119**, 1609 (1997).

502. L. R. MacGillivray and J. L. Atwood, "Molecular Recognition of the Cyclic Water Trimer in the Solid State," *J. Am. Chem. Soc.*, **119**, 2592 (1997).

503. L. R. MacGillivray and J. L. Atwood, "Ether Cleavage of [2.2.2]cryptand: Synthesis and X-ray Crystal Structure of [NH(CH$_2$CH$_2$I)$_3$][I$_5$]," *J. Chem. Cryst.*, **27**, 209 (1997).

504. K. T. Holman, J. W. Steed, and J. L. Atwood, "Intra-cavity Inclusion of [CpFe^{II}(arene)]$^+$ Guests by Cyclotriveratrylene," *Angew. Chem. Int. Ed. Engl.*, **36**, 1736 (1997).

505. L. R. MacGillivray and J. L. Atwood, "Structural Consequences of Competing Noncovalent Forces: the out-out Conformation of the Doubly Protonated [2.2.2]cryptand," *Chem. Commun.*, 477 (1997).

506. L. J. Barbour, G. W. Orr, and J. L. Atwood, "Supramolecular Intercalation of C$_{60}$ into a Calixarene Bilayer - a Well-Ordered Solid-State Structure Dominated by van der Waals Contacts," *Chem. Commun.*, 1439 (1997).

507. M. Staffilani, K. S. B. Hancock, J. W. Steed, K. T. Holman, J. L. Atwood, R. K. Juneja, and R. S. Burkhalter, "Anion Binding within the Cavity of π-Metalated Calixarenes," *J. Am. Chem. Soc.*, **119**, 6324 (1997).

508. L. R. MacGillivray and J. L. Atwood, "Rational Design of Multi-Component Calix[4]arenes and Control of Their Alignment in the Solid State," *J. Am. Chem. Soc.*, **119**, 6931 (1997).

509. K. T. Holman, J. L. Atwood, and J. W. Steed, "Supramolecular Anion Receptors," in *Advances in Supramolecular Chemistry*, Vol. 4, G. W. Gokel, Ed., JAI Publications, New York, 287 (1997).

510. L. R. MacGillivray and J. L. Atwood, "A Chiral Spherical Molecular Assembly Held Together by 60 Hydrogen Bonds," *Nature*, **389**, 469 (1997). *C&EN*, October 6, 1997, p. 12

511. L. R. MacGillivray and J. L. Atwood, "Synthesis and Structure of (H$_2$O)(12-crown-4)Co(II)(Co(II)Cl$_3$)(μ-Cl) Isolated from a Liquid Clathrate Medium," *J. Chem. Cryst.*, **27**, 453 (1997).

512. J. L. Atwood and J. W. Steed, "Structural and Topological Aspects of Anion Coordination," in *Supramolecular Chemistry of Anions*, A. Bianchi, K. Bowman-James, E. Garcia-Espana, Eds., Wiley-VCH, New York (1997).

513. J. L. Atwood and P. C. Junk, "Synthesis and X-ray Structure of Oxonium Ion Complexes of 21-Crown-7 and Dibenzo-30-crown-10," *J. Chem. Soc., Dalton Trans.*, 4393 (1997).

514. J. L. Atwood and P. C. Junk, "Use of Metal Carbonyls in the Formation of $H_5O_2^+$ in [$H_5O_2^+$·15-Crown-5][$MOCl_4(H_2O)^-$], (M=Mo, W), and a Second Sphere Coordination Complex in [*mer*-$CrCl_3(H_2O)_3$·15-Crown-5]," *J. Organomet. Chem.,* **565**, 179 (1998).

515. M. Staffilani, G. Bonvicini, J. W. Steed, K. T. Holman, J. L. Atwood, and M. R. J. Elsegood, "Bowl vs. Saddle Conformations in Cyclononatriene-based Anion Binding Hosts," *Organometallics* , **17**, 1732 (1998).

516. J. L. Atwood, L. J. Barbour, C. L. Raston, and I. B. N. Sudria, "Assemblies of C_{60} and C_{70} in the Molecular Pincer-Like Jaws of Calix[6]arene," *Angew. Chem. Int. Ed. Engl.*, **37**, 981 (1998).

517. P. C. Andrews, J. L. Atwood, L. J. Barbour, P. J. Nichols, and C. L. Raston, "Rigid Concave Surfaces: An Entry to Confinement of Globular Molecules, " *Chem. Eur. J.,* **4**, 1384 (1998).

518. K. N. Rose, L. J. Barbour, G. W. Orr, and J. L. Atwood, "Self-Assembly of Carcerand-Like Dimers of Calix[4]resorcinarene Facilitated by Hydrogen Bonded Solvent Bridges," *Chem. Commun.*, 407 (1998).

519. L. J. Barbour, G. W. Orr, and J. L. Atwood, "Supramolecular Assembly of Well-Separated, Linear Columns of Closely Spaced C_{60} Molecules Facilitated by Dipole Induction," *Chem. Commun.,* 1901 (1998).

   C&EN, Science/Technology Concentrates, September 14, 1998, p. 28.

520. A. Alvanipour, J. L. Atwood, S. G. Bott, P. C. Junk, U. H. Kynast, and H. Prinz, "Some Crown Ether Chemistry of Ti, Zr, and Hf Derived from Liquid Clathrate Media, " *J. Chem. Soc., Dalton Trans.*, 1223 (1998).

521. L. R. MacGillivray, K. T. Holman, and J. L. Atwood, "One-Dimensional Hydrogen Bonded Polymers Based on c-Methylcalix[4]resorcinarene and a Crystal

Engineering Design Strategy," *Cryst. Eng.,* **1,** 87 (1998).

522. P. C. Junk and J. L. Atwood, "Hydrogen-bonded Tetramethylethylenediammonium and Triphenylphosphonium Complexes Derived from Liquid Clathrate Media," *J. Coord. Chem.*, 46, 505   (1998).

523. L. R. MacGillivray, R. H. Groeneman, and J. L. Atwood, "Design and Self-Assembly of Cavity-Containing Rectangular Grids," *J. Am. Chem. Soc.*, **120**, 2676 (1998).

524. E. Abel, R. Castro, I. M. McRobbie, L. Barbour, J. L. Atwood, A. E. Kaifer, and G. W. Gokel, "A Redox-Switchable Molecular Receptor Based on Anthraquinone," *Supramol. Chem.*, **9**, 199 (1998).

525. K. T. Holman, G. W. Orr, J. W. Steed, and J. L. Atwood, "Deep Cavity [CpFe(arene)]$^+$-Based Anion Hosts," *Chem. Commun.*, 2109 (1998).

526. P. C. Blake, M. A. Edelman, P. B. Hitchcock, J. Hu, M. F. Lappert, S. Tian, G. Muller, J. L. Atwood, and H. Zhang, "Organometallic Chemistry of the Actinides. Part 4. The Chemistry of Some Tris(cyclopentadienyl)actinide Complexes," *J. Organometal. Chem.*, **551**, 261 (1998).

527. J. L. Atwood, L. R. MacGillivray, K. N. Rose, L. J. Barbour, K. T. Holman, and G. W. Orr, "Large Molecular Assemblies Held Together by Non-Covalent Bonds," in *Physical Methods of Characterization of Supramolecular Assemblies*, Ed.: G. Tsoucaris, Dordrecht, 7 (1998).

528. L. J. Barbour, G. W. Orr, and J. L. Atwood, "An Intermolecular $(H_2O)_{10}$ Cluster in a Solid-State Supramolecular Complex," *Nature*, **393**, 671 (1998).

529. R. H. Groeneman, L. R. MacGillivray, and J. L. Atwood, "Aromatic Inclusion within a Neutral Cavity-Containing Rectangular Grid," *Chem. Commun.*, 2735 (1998).

530. L. J. Barbour and J. L. Atwood, "RES2INS: a Graphical Interface for the SHELX Program Suite," *J. Appl. Cryst.*, **31**, 963 (1998).

531. L. R. MacGillivray, K. T. Holman, and J. L. Atwood, "Multi-Guest Inclusion within One-Dimensional Hydrogen Bonded Polymers Based on *C*-Methylcalix[4]resorcinarene," *Am. Cryst. Assoc. Trans.*, **33**, 129 (1998).

532. J. L. Atwood, L. J. Barbour, P. J. Nichols, C. L. Raston, and C. A. Sandoval, "Symmetry-Aligned Supramolecular Encapsulation of C60; [C_{60} > (L)$_2$]. L = *p*-

Benzylcalix[5]arene or *p*-Benzylhexahomooxacalix[3]arene," *Chem. Eur. J.*, **5**, 990 (1999).

533. L. R. MacGillivray and J. L. Atwood, "Structural Classification and General Principles for the Design of Spherical Molecular Hosts," *Angew. Chem., Int. Ed. Engl.,* **38**, 1018 (1999).

534. R. H. Groeneman, L. R. MacGillivray, and J. L. Atwood, "One-Dimensional Coordination Polymers Based upon Bridging Terephthalate Ions," *Inorg. Chem.*, **38**, 208 (1999).

535. P. C. Andrews, J. L. Atwood, L. J. Barbour, P. D. Croucher, P. J. Nichols, N. O. Smith, B. W. Skelton, A. H. White, and C. L. Raston, "Supramolecular Confinement of C_{60}, S_8, P_4Se_3, and Toluene by Metal(II) Macrocyclic Complexes," *J. Chem. Soc., Dalton Trans.*, 2927 (1999).

536. G. W. Orr, L. J. Barbour, and J. L. Atwood, "Controlling Molecular Self-Organization: Formation of Nanometer-Scale Spheres and Tubules," *Science*, **285**, 1049 (1999).
C&EN, News of the Week, August 16, 1999, p. 5.
Cover Illustration

537. R. H. Groeneman and J. L. Atwood, "Terephthalate Bridged Coordination Polymers Based Upon Group Two Metals," *Cryst. Eng.*, **2**, 241 (1999).

538. L. R. MacGillivray and J. L. Atwood, "Unique Guest Inclusion within Multi-Component, Extended-Cavity Resorcin[4]arenes," *Chem. Commun.*, 181 (1999).

539. L. R. MacGillivray, J. L. Reid, J. L. Atwood, and J. A. Ripmeester, "Vinyl-Group Alignment Along the Upper Rim of a *Multi*-Component Resorcin[4]arene," *Cryst. Eng.*, **2**, 47 (1999).

540. L. R. MacGillivray and J. L. Atwood, "Discrete and Infinite Host Frameworks Based upon Resorcin[4]arenes by Design," in *Crystal Engineering: From Molecules and Crystals to Materials*, Ed. A. G. Orpen and D. Braga, 407-419, Kluwer, The Netherlands, 1999.

541. L. R. MacGillivray and J. L. Atwood, "Spherical Molecular Containers: From Discovery to Design," in *Adv. Supramol. Chem.*, Vol. 6; Ed.: G. W. Gokel; JAI, 157-183 (1999).

542. J. L. Atwood, "Crystal Engineering Based on Diffraction Studies of Supramolecular Compounds," in *Crystal Engineering*, Ed. K. R. Seddon and M. Zaworotko, 371-381,

Kluwer, The Netherlands, 1999.

543. J. L. Atwood, M. J. Hardie, C. L. Raston, and C. A. Sandoval, "Convergent Synthesis of *p*-Benzylcalix[7]arene: Condensation and UHIG of *p*-Benzylcalix[6 or 8]arenes," *Organic Lett.*, **1**, 1523 (1999).

544. J. L. Atwood and P. C. Junk, "Synthesis and X-ray Crystal Structures of Novel Oxonium Ion-12-Crown-4 Complexes Isolated from Liquid Clathrate Media," *J. Coord. Chem.*, **51**, 379 (2000).

545. L. R. MacGillivray and J. L. Atwood, "Hydrogen Bonded Cavities Based upon Resorcin[4]arenes by Design," in *Calixarenes for Separations*; Ed.: G. L. Lumetta, R. D. Rogers, and A. S. Gopalan, ACS, 325-340, 2000.

546. L. R. MacGillivray and J. L. Atwood, "Cavity-Containing Materials Based Upon Resorcin[4]arenes by Discovery and Design," *J. Solid State Chem.*, **152**, 199 (2000).

547. R. A. Groeneman and J. L. Atwood, "Self-Assembly of a Novel One-Dimensional Zig-Zag Coordination Polymer," *Supramol. Chem.*, **11**, 251 (2000).

548. L. R. MacGillivray and J. L. Atwood, "The 'Boat' Conformation of a Resoprcin[4]arene Self-assembles as a 'T-Shaped' Building Block in the Solid State to Form a Linear 1D Hydrogen-Bonded Array," *Supramol. Chem.*, **11**, 293 (2000).

549. L. R. Barbour, G. W. Orr, and J. L. Atwood, "Characterization of a Well Resolved Supramolecular Ice-Like $(H_2O)_{10}$ Cluster in the Solid State," *Chem. Comm.*, 859 (2000).

550. Z. Chen, J. Wang, V. S. Gopalaratnam, B. Orr, and J. L. Atwood, "Thermal Measurement Associated with Material Failure Using Thermochromic Coatings," *Experimental Techniques*, **24**, 29 (2000).

551. J. L. Atwood and P. C. Junk, "Formation and Crystal Structures of Novel Seven-coordinate 15-crown-5 Complexes of Manganese(II), Iron(II) and Cobalt(II) *Polyhedron*, **19**, 85 (2000).

552. E. Elisabeth, L. J. Barbour, G. W. Orr, K. T. Holman, and J. L. Atwood, "Synthesis and Structure of a One Dimensional Coordination Polymer Based Upon Tetracyanocalix[4]arene in the Cone Conformation," *Supramol. Chem.*, **12**, 317 (2000).

553. M. S. Selvan, M. D. McKinley, R. H. Dubois, and J. L. Atwood, "Liquid-Liquid Equilibria for Toluene plus Heptane + 1-Ethyl-3-methylimidazolium Triiodide and

Toluene plus Heptane + 1-Butyl-3-methylimidazolium Triiodide," *J. Chem. Eng. Data*, **45**, 841 (2000).

554. L. R. MacGillivray and J. L. Atwood, "Spherical Molecular Assemblies: A Class of Hosts for the Next Millennium," in *Chemistry for the 21st Century.*; Ed.: E. Keinan and I. Schechter, Wiley-VCH, 130-150, 2001.

555. A. M. Bond, W. Miao, C. L. Raston, T. J. Ness, M. J. Barnes, and J. L. Atwood, "Electrochemical and Structural Studies on Microcrystals of the $(C_{60})_x$(CTV) Inclusion Complexes (x = 1, 1.5; CTV = Cyclotriveratrylene)," *J. Phys. Chem. B,* **105**, 1687 (2001).

556. R. H. Groeneman and J. L. Atwood, "Controlling Aromatic Inclusion within NonAqueous Copper Iodide Coordination Polymers," *Supramol. Chem.*, **12**, 353 (2001).

557. J. L. Atwood, L. J. Barbour, M. J. Hardie, C. L. Raston, M. N. Statton, and H. R. Webb, "Hetero-bimetallic Cage Molecules: Solvated Na_2M_2(p-sulfonatocalix[4]arene)$_2$, M = Y, Eu," *Cryst. Eng. Comm.*, **4**, 1 (2001).

558. J. L. Atwood, L. J. Barbour, M. J. Hardie, and C. L. Raston, "Metal Sulfonatocalixarene Complexes: Bi-layers, Capsules, Spheres, Tubular Arrays and Beyond," *Coord. Chem. Rev.*, **222**, 3 (2001).

559. J. L. Atwood, L. J. Barbour, and A. Jerga, "Hydrogen-Bonded Molecular Capsules are Stable in Polar Media," *Chem. Comm.*, 2376 (2001).

560. J. L. Atwood, L. J. Barbour, M. J. Hardie, E. Lygris, C. L. Raston, and H. R. Webb, "Inclusion Complexes of 18-Crown-6 and (Na^+.[2.2.2]cryptand) in [*C*-Methylcalix[4]resorcinarene-H_n], n = 0, 1," *Cryst. Eng. Comm.*, 10 (2001).

561. J. L. Atwood, L. J. Barbour, T. J. Ness, C. L. Raston, and P. L. Raston, "A Well Resolved Ice-Like $(H_2O)_8$ Cluster in an Organic Supramolecular Complex," *J. Am. Chem. Soc.*, **123**, 7192 (2001).

562. K. N. Rose, M. J. Hardie, J. L. Atwood, and C. L. Raston, "Oxygen-center Laden C_{2h} Symmetry Resorcin[4]arenes," *J. Supramol. Chem.*, **1**, 35 (2001).

563. L. J. Barbour and J. L. Atwood, "Non-covalent Interactions Exert Extraordinary Influence Over Conformation and Properties of a Well-Known Supramolecular Building Block," *Chem. Comm.*, 2020 (2001).

564. J. L. Atwood, L. J. Barbour, and A. Jerga, "On the Synthesis and Structure of the Very Large Spherical Capsules Derived from Hexamers of Pyrogallol[4]arenes," *J. Supramol. Chem.*, **1**, 131 (2001).

565. L. R. MacGillivray, K. T. Holman, and J. L. Atwood, "Hydrogen Bonds Assist the Organization of Up to 11 Guests within Self-Assembling Cavities of Nanometer Dimensions," *J. Supramol. Chem.*, **1**, 125 (2001).

566. J. L. Atwood, T. Ness, P. J. Nichols, and C. L. Raston, "Confinement of Amino Acids in Tetra-*p*-sulfonated Calix[4]arene Bi-layers," *Cryst. Growth & Design*, **2**, 171 (2002).

567. J. L. Atwood, L. J. Barbour, and C. L. Raston, "Supramolecular Organization of C_{60} into Linear Columns of Five-Fold, Z-Shaped Strands," *Cryst. Growth & Design*, **2**, 3 (2002).

568. J. L. Atwood, L. J. Barbour, and A. Jerga, "Organization of the Interior of Molecular Capsules by Hydrogen Bonding," *Proc. Natl. Acad. Sci.*, **99**, 4837 (2002).

569. J. L. Atwood, L. J. Barbour, and A. Jerga, "Supramolecular Stabilization of $N_2H_7^+$," *J. Am. Chem. Soc.*, **124**, 2122 (2002).

570. J. L. Atwood, L. J. Barbour, and A. Jerga, "Storage of Methane and Freon by Interstitial van der Waals Confinement," *Science*, **296**, 2367 (2002).
Science Express, May 9, 2002, www.sciencexpress.org, *C&EN*, July 8, 2002, p. 27, *C&EN*, Chemistry Highlights 2002, December 22, 2003, p. 47, Highlights, *Angew. Chem. Int. Ed. Engl.*, 42, 1686 (2003).

571. J. L. Atwood, L. J. Barbour, S. Dalgarno, C. L. Raston, and H. R. Webb, "Supramolecular Assemblies of *p*-Sulfonatocalix[4]arene with Aquated Trivalent Lanthanide Ions," *Dalton Trans.*, 4351 (2002).

572. J. L. Atwood and A. Szumna, "Hydrogen Bonds Seal Single-Molecule Molecular Capsules," *J. Am. Chem. Soc.*, **124**, 10646 (2002).

573. J. L. Atwood, L. J. Barbour, A. Jerga, and B. L. Schottel, "Guest Transport in a Non-Porous Organic Solid via Dynamic van der Waals Cooperativity," *Science*, **298**, 1000 (2002).
Science Perspectives, J. W. Steed, 298, 976 (2002)
C&EN, November 4, 2002, p. 8
C&EN, Chemistry Highlights 2002, December 22, 2003, p. 47.

574. J. L. Atwood, "Kagome Lattice: A Molecular Toolkit for Magnetism," *Nature*

Materials, **1**, 91 (2002).

575. J. L. Atwood, L. J. Barbour, and A. Jerga, "Polymorphism of Pure p-tert-Butylcalix[4]arene: Conclusive Identification of the Phase Obtained by Desolvation," *Chem. Comm.*, 2952 (2002).

576. J. A. Gawenis, K. T. Holman, J. L. Atwood, and S. S. Jurisson, "Extraction of Pertechnetate and Perrhenate from Water with Deep-Cavity [CpFe(arene)]$^{+}$-Derivatized Cyclotriveratrylenes," *Inorg. Chem.*, **41**, 6028 (2002).

577. J. L. Atwood, L. J. Barbour, M. W. Heaven, and C. L. Raston, "Synthesis of 2-Imino-5-phenylimidazolidin-4-one and the Structure of Its Trifluoroacetate Salt," *J. Chem. Cryst.*, **33**, 175 (2003).

578. J. L. Atwood and A. Szumna, "Cation-π Interactions in Neutral Resorcin[4]arenes," *J. Supramol. Chem.*, **2**, 421 (2003).

579. J. L. Atwood and L. J. Barbour, "Molecular Graphics: From Science to Art," *Cryst. Growth Des.*, **3**, 3 (2003).
      Cover Illustration (Cover design used for all 2003 issues.)

580. Z. Chen, J. L. Atwood, and Y.-W. Mai, "Rate-Dependent Transition from Thermal Softening to Hardening in Elastomers," *J. Applied Mechanics*, **70**, 611 (2003).

581. J. L. Atwood and A. Szumna, "Anion-Sealed Single-Molecule Capsules," *Chem. Comm.*, 940 (2003).
      C&EN, News of the Week, April 14, 2003, p. 11.
      C&EN, Chemistry Highlights 2003, December 22, 2003, p. 47.

582. J. L. Atwood, L. J. Barbour, M. W. Heaven, and C. L. Raston, "Association and Orientation of C$_{70}$ Complexation with Calix[5]arene," *Chem. Comm.,* 2270 (2003).

583. M. W. Heaven, L. J. Barbour, J. L. Atwood, and C. L. Raston, "Controlling the van der Waals Connectivity of Fullerene C$_{60}$," *Angew. Chem. Int. Ed. Engl.*, **42**, 3254 (2003).

584. J. L. Atwood, L. J. Barbour, and A. Jerga, "A New Class of Material for the Recovery of Hydrogen from Gas Mixtures," *Angew. Chem. Int. Ed. Engl.*, **43**, 2948 (2004).
      C&EN, News of the Week, May 31, 2004, p. 7.
      Science News, June 12, 2004, pp. 380-381.

585. J. L. Atwood, S. J. Dalgarno, M. J. Hardie, and C. L. Raston, "Hydrogen-Bonded Arrays of a Ytterbium(III) p-sulfonatocalix[6]arene Complex," *New J. Chem.*, **28**, 326 (2004).

586. K. S. Chichak, S. J. Cantrill, A. R. Pease, S.-h. Chiiu, G. W. V. Cave, J. L. Atwood, and J. F. Stoddart, "Molecular Borromean Rings," *Science*, **304**, 1308 (2004).
C&EN, News of the Week, May 31, 2004, p. 5.
C&EN, Chemistry Highlights 2004, December 20, 2004, p. 60-61.

587. S. J. Dalgarno, M. J. Hardie, J. L. Atwood, and C. L. Raston, "Bilayers, Corrugated Bilayers, and Coordination Polymers of *p*-Sulfonatocalix[6]arene,"*Inorg. Chem.*, **43**, 6351 (2004).

588. J. L. Atwood, L. J. Barbour, S. J. Dalgarno, M. J. Hardie, C. L. Raston, and H. R. Webb, "Toward Mimicking Viral Geometry with Metal-Organic Systems," *J. Am. Chem. Soc.*, **126**, 13170 (2004).

589. G. W. V. Cave, J. Antesberger, L. J. Barbour, R. M. McKinlay, and J. L. Atwood, "Inner Core Structure Responds to Communication between nanocapsule Walls," *Angew. Chem. Int. Ed. Engl.*, **43**, 5263 (2004).
Cover Illustration
C&EN, Science & Technology, January 3, 2005, 30-32

590. J. L. Atwood, L. J. Barbour, G. O. Lloyd, and P. K. Thallapally, "Polymorphism of Pure *p-tert*-Butylcalix[4]arene: Subtle Thermally-Induced Modifications," *Chem. Comm.*, 922 (2004).

591. G. W. V. Cave, M. C. Ferrarelli, and J. L. Atwood, "A Supramolecular Approach to Deepening the Pyrogallol[4]arene Cavity: Nano-Cups," *Chem. Comm.*, 2787 (2005).

592. J. L. Atwood, L. J. Barbour, P. K. Thallapally, and T. B. Wirsig, "A Crystalline Organic Substrate Absorbs Methane under STP Conditions," *Chem. Comm.*, 51 (2005).
Materials Research Society Bulletin, 30, 2005, 154-155

593. S. J. Dalgarno, M. J. Hardie, J. L. Atwood, J. E. Warren, and C. L. Raston, "A Complex 3-D 'wavy brick wall' Coordination Polymer Based on p-Sulfonatocalix[8]arene," *New. J. Chem.*, **29**, 649 (2005).

594. J. Antesberger, G. W. V. Cave, M. C. Ferrarelli, M. W. Heaven, C. L. Raston, and J. L. Atwood, "Solvent-free, direct synthesis of supramolecular nano-capsules," *Chem. Comm.*, 892 (2005).

595. G. O. Lloyd, J. L. Atwood, and L. J. Barbour, "Water-assisted self-assembly of harmonic single and triple helices in a polymeric coordination complex," *Chem. Comm.*, 1845 (2005).

596. J. L. Atwood, S. J. Dalgarno, M. J. Hardie, and C. L. Raston, "Selective single crystal complexation of L- or D-leucine by *p*-sulfonatocalix[6]arene," *Chem. Comm.*, 337 (2005).

597. J. L. Atwood, G. W. V. Cave, and R. M. McKinlay, "A Supramolecular Blueprint Approach to Metal-Coordinated Capsules," *PNAS*, **102**, 5944 (2005).

598. P. K. Thallapally, G. O. Lloyd, T. B. Wirsig, M. W. Bredenkamp, J. L. Atwood, and L. J. Barbour, "Organic Crystals Absorb Hydrogen Gas under Mild Conditions,"*Chem. Comm.*, 5272 (2005).

599. P. K. Thallapally, G. O. Lloyd, J. L. Atwood, and L. J. Barbour, "Diffusion of Water in a Nonporous Hydrophobic Crystal," *Angew. Chem. Int. Ed. Engl.*, 44, 3848 (2005). Editors' Choice, *Science*, **308**, 1521 (2005).

600. R. M. McKinlay, P. K. Thallapally, G. W. V. Cave, and J. L. Atwood, "Hydrogen Bonded Supramolecular Assemblies as Robust Templates in the Synthesis of Large Metal-Coordinated Capsules," *Angew. Chem. Int. Ed. Engl.*, **44**, 5733 (2005).

601. P. K. Thallapally, T. B. Wirsig, L. J. Barbour, and J. L. Atwood, "Crystal Engineering of Non-porous Organic Solids for Methane Sorption," *Chem. Comm.*, 4420 (2005).

602. S. J. Dalgarno, D. B. Bassil, S. A. Tucker, and J. L. Atwood, "Fluorescent Probe Molecules Report Ordered Inner Phase of Nano-Capsules in Solution," *Science*, **309**, 2037 (2005).

603. S. J. Dalgarno, J. L. Atwood, and C. L. Raston, "Host-Guest Complexes with *p*-Sulfonatocalix[4,5]arenes, Charged crown Ethers and Lanthanides: Factors Affecting Molecular Capsule Formation," *Cryst. Growth Des.*, **6**, 174 (2006).

604. S. J. Dalgarno, G. W. V. Cave, and J. L. Atwood, "Toward the Isolation of Functional Organic Nano-tubes," *Angew. Chem. Int. Ed. Engl.*, **45**, 570 (2006).

605. P. K. Thallapally, L. Dobrzanska, T. R. Gingrich, T. B. Wirsig, L. J. Barbour, and J. L. Atwood, "Acetylene Absorption and Binding in a Nonporous Crystal Lattice," *Angew. Chem. Int. Ed. Engl.*, **45**, 6506 (2006).

606. M. W. Heaven, G. W. V. Cave, R. M. McKinlay, J. Antesberger, S. J. Dalgarno, P. K.

Thallapally, and J. L Atwood, "Hydrogen Bonded Hexamers Self-Assemble as Spherical and Tubular Superstructures on the Sub-Micron Scale," *Angew. Chem. Int. Ed. Engl.*, **45**, 6221 (2006).

607. S. J. Dalgarno, J. L. Atwood, and C. L. Raston, "Sulfonatocalixarenes: Molecular Capsule and 'Russian Doll' Arrays to Structures Mimicking Viral Geometry," *Chem. Comm.*, 4567 (2006).

608. S. J. Dalgarno, N. P. Power, J. Antesberger, R. M. McKinlay, and J. L. Atwood, "Synthesis and Structural Characterisation of Lower Rim Halogenated Pyrogallol[4]arenes: Bi-layers and Hexameric Nano-capsules," *Chem. Comm.*, 3803 (2006).

609. S. J. Dalgarno, D. B. Bassil, S. A. Tucker, and J. L. Atwood, "Cocrystallization and Encapsulation of a Fluorophore with Hexameric Pyrogallol[4]arene Nano-capsules: Structural and Fluorescence Studies," *Angew. Chem. Int. Ed. Engl.*, **45**, 7019 (2006).

610. P. K. Thallapally, S. J. Dalgarno, and J. L. Atwood, "Frustrated Organic Solids Display Unexpected Gas Sorption," *J. Amer. Chem. Soc.,* **128**, 15060 (2006). *C&EN*, News of the Week, November 13, 2006, 14

611. R. M. McKinlay and J. L. Atwood, "Hexameric *C*-alkylpyrogallol[4]arene Molecular Capsules Sustained by Metal-ion Coordination and Hydrogen Bonds," *Chem. Comm.*, 2956 (2006).

612. P. K. Thallapally and J. L. Atwood, "Sorption of Nitrogen Oxides (NOx's) in a Nonporous Crystal Lattice," *Chem. Comm.*, 1521 (2007). *Chemistry World*, Chemical Sciences, March 28, 2007

613. S. J. Dalgarno, J. L. Atwood, and C. L. Raston, "Synthesis and Structural Characterisation of Two Polynuclear Hafnium (IV) Complexes," *Inorg. Chim. Acta*, **360**, 1344 (2007).

614. P. K. Thallapally, K. A. Kirby, and J. L. Atwood, "Comparison of Porous and Nonporous Materials for Gas Storage," *New J. Chem.*, **31**, 629 (2007).

615. S. J. Dalgarno, P. K. Thallapally, L. J. Barbour, and J. L. Atwood, "Engineering Void Space in Organic van der Waals Crystals: Calixarenes Lead the Way", *Chem. Soc. Rev.*, **36**, 236 (2007).

616. N. P. Power, S. J. Dalgarno, and J. L. Atwood, "Robust and Stable Pyrogallol[4]arene Molecular Capsules Facilitated via an Octanuclear Zinc

Coordination Belt," *New J. Chem.*, **31**,17 (2007).
Cover Illustration

617. S. J. Dalgarno, J. L. Atwood, and C. L. Raston, "Structural Versatility in Praseodymium Complexes of *p*-Sulfonatocalix[4]arene," *Cryst. Growth Des.*, **7**, 1762 (2007).

618. R. M. McKinlay and J. L. Atwood, "Hydrogen-Bonded Hexameric Nanotoroidal Assembly," *Angew. Chem. Int. Ed. Engl.*, **46**, 2394 (2007).

619. R. M. McKinlay, S. J. Dalgarno, P. J. Nichols, S. Papadopoulos, J. L. Atwood, and C. L. Raston, "Icosahedral Galloxane Clusters," *Chem. Comm.*, 2393 (2007).

620. S. J. Dalgarno, N. P. Power, and J. L. Atwood, "Ionic Dimeric Pyrogallol[4]arene Capsules," *Chem. Comm.*, 3447 (2007).

621. P. K. Thallapally, B. P. McGrail, J. L. Atwood, C. Gaeta, C. Tedesco, and P. Neri, "Carbon Dioxide Capture in a Self-Assembled Organic Nanochannel," *Chem. Mat.*,**19**, 3355 (2007).
Cover Illustration

622. S. J. Dalgarno, J. Antesberger, R. M. McKinlay, and J. L. Atwood, "Water as a Building Block in Solid-State Acetonitrile-Pyrogallol[4]arene Assemblies: Structural Investigations," *Chem. Eur. J.*, **13**, 8248 (2007).

623. D. B. Bassil, S. J. Dalgarno, G. W. V. Cave, J. L. Atwood, and S. A. Tucker, "Spectroscopic Investigations of ADMA Encapsulated in Pyrogallol[4]arene Nanocapsules," *J. Phys. Chem. B*, **111**, 9088 (2007).

624. N. P. Power, S. J. Dalgarno, and J. L. Atwood, "Guest and Ligand Behavior in Zinc-Seamed Pyrogallol[4]arene Molecular Capsules," *Angew. Chem. Int. Ed. Engl.*, **46**, 8601 (2007).
Inside Cover Illustration

625. J. L. Daschbach, P. K. Thallapally, J. L. Atwood, B. P. McGrail, and L. X. Dang, "Free Energies of CO_2/H_2 Capture by p-tert-Butylcalix[4]arene: A Molecular Dynamics Study," *J. Chem. Phys.*, **127**, 104703-1-104703-4 (2007).

626. J. L. Atwood, T. E. Clark, S. J. Dalgarno, M. Makha, C. L. Raston, J. Tian, and J. E. Warren, "Calix[5]arene: A Versatile Sublimate that Displays Gas Sorption Properties," *Chem. Comm.*, 4848 (2007).
Cover illustration

627. T. E. Clark, M. Makha, A. N. Sobolev, S. J. Dalgarno, J. L. Atwood, and C. L. Raston, "Structural Diversity of Methyl-Substituted Inclusion Complexes of Calix[5]arene," *Cryst. Growth Des.*, 7, 2059 (2007).

628. S. J. Dalgarno, J. E. Warren, J. Antesberger, T. E. Glass, and J. L. Atwood, "Large Diameter Non-covalent Nanotubes Based on the Self-assembly of *para*-Carboxylatocalix[4]arene," *New J. Chem.*, **31**, 1891 (2007).
Inside Cover Illustration

629. S. J. Dalgarno, N. P. Power, J. E. Warren, and J. L. Atwood, "Rapid Formation of Metal-Organic Nano-Capsules Gives New Insight into the Self-Assembly Process," *Chem. Comm.*, 1539 (2008).

630. S. J. Dalgarno, N. P. Power, and J. L. Atwood, "Organic Nanocapsules," *Organic Nanostructures*, Ed. J. W. Steed and J. L. Atwood, Wiley, 317-346 (2008).

631. P. K. Thallapally, B. P. McGrail, H. T. Schaef, S. J. Dalgarno, J. Tian, and J. L. Atwood, "Gas-Induced Transformation and Expansion of a Non-Porous Organic Solid," *Nature Mat.*, **7**, 146 (2008).

632. S. J. Dalgarno, N. P. Power, and J. L. Atwood, "Metallo-Supramolecular Capsules," *Coord. Chem. Rev.*, **252**, 825 (2008).

633. S. J. Dalgarno, K. M. C. Bosque, J. E. Warren, T. E. Glass, and J. L. Atwood, "Interpenetrated Nano-capsule Networks Based on the Alkali Metal Assisted Assembly of *p*-Carboxylatocalix[4]arene-*O*-methyl Ether," *Chem. Comm.*, 1410 (2008).

634. T. E. Clark, M. Makha, A. N. Soblev, D. Su, H. Rohrs, M. L. Gross, J. L. Atwood, and C. L. Raston, "Self-organised nano-arrays of *p*-phosphonic acid functionalised higher order calixarenes," *New J. Chem.*, **32**, 1478 (2008).

635. S. J. Dalgarno, P. K. Thallapally, J. Tian, and J. L. Atwood, "*Pseudo*-polymorphism in the Toluene Solvate of p-*tert*-Butylcalix[5]arene: Structural and Gas Sorption Investigations," *New J. Chem.*, **32**, 2095 (2008).

636. G. W. V. Cave, S. J. Dalgarno, J. Antesberger, M. C. Ferrarelli, R. M. McKinlay, and J. L. Atwood, "Investigations into Chain Length Control Over Solid-State Pyrogallol[4]arene Nanocapsule Packing," *Supramol. Chem.*, **20**, 157 (2008).

637. T. E. Clark, M. Makha, A. N. Sobolev, H. Rohrs, J. L. Atwood, and C. L. Raston, "Engineering Nano-Rafts of Polyphosphonates," *Chem. Eur. J.*, 3931 (2008).

68

638. K. S. Iyer, M. Norret, S. J. Dalgarno, J. L. Atwood, and C. L. Raston, "Loading Molecular Hydrogen Cargo within Viruslike Nanocontainers," *Angew. Chem. Int. Ed. Engl.*, 47, 6362 (2008).

639. P. K, Thallapally, P. B. McGrail, S. J. Dalgarno, and J. L. Atwood, "Gas/Solvent-Induced Transformation and Expansion of a Nonporous Solid to 1:1 Host Guest Form," *Cryst. Growth & Des.*, **8**, 2090 (2008).

640. S. J. Dalgarno, J. E. Warren, J. L. Atwood, and C. L. Raston, "Versatility of *p*-sulfonatocalix[5]arene in Building up Multicomponent Bilayers," *New J. Chem.*, **32**, 2100 (2008).

641. P. K. Thallapally, J. Tian, M. R. Kishan, C. A. Fernandez, S. J. Dalgarno, P. B. McGrail, J. E. Warren, and J. L. Atwood, "A Flexible (Breathing) Interpenetrated Metal-Organic Frameworks for CO_2 Separation Applications," *J. Am. Chem. Soc.*, **130**, 16842 (2008).

642. P. Jin, S. J. Dalgarno, C. Barnes, S. J. Teat, and J. L. Atwood, "Ion Transport to the Interior of Metal-Organic Pyrogallol[4]arene Nano-Capsules," *J. Am. Chem. Soc.*, **130**, 17262 (2008).

643. P. Jin, S. J. Dalgarno, J. E. Warren, S. Teat, and J. L. Atwood, "Enhanced Control over Metal Composition in Mixed Ga/Zn and Ga/Cu Coordinated Pyrogallol[4]arene Nano-Capsules," *Chem. Comm.*, 3348 (2009).

644. J. Tian, P. K. Thallapally, S. J. Dalgarno, P. B. McGrail, and J. L. Atwood, "Amorphous Molecular Organic Solids for Gas Adsorption," *Angew. Chem. Int. Ed. Engl.*, **48**, 5492 (2009).

645. S. J. Dalgarno, T. Szabo, A. Siavosh-Haghighi, C. A. Deakyne, J. E. Adams, and J. L. Atwood, "Exploring the Limits of Encapsulation within Hexameric Pyrogallol[4]arene Nano-Capsules," *Chem. Comm.*, 1339 (2009).

646. J. Tian, S. J. Dalgarno, P. K. Thallapally, and J. L. Atwood, "Increased Control Over the Desolvation of p-tert-Butylcalix[5]arene," *Cryst. Eng. Comm.*, **11**, 33 (2009).

647. J. Tian, P. K. Thallapally, S. J. Dalgarno, and J. L. Atwood, "Free Transport of Water and CO_2 in Nonporous Hydrophobic Clarithromycin Form II Crystals," *J. Am. Chem. Soc.*, **131**, 13216 (2009).
Chemical & Engineering News, News of the Week, September 7, 2009, p. 14.

648. C. Tedesco, L. Erra, V. Cipolletti, C. Gaeta, P. Neri, M. Brunelli, A. N. Fitch, and

J. L. Atwood, "Methane Adsorption in a Supramolecular Organic Zeolite," *Chem. Eur. J.*, **16**, 2371 (2010).

649. A. K. Maerz, H. Thomas, N. P. Power, C. A. Deakyne, and J. L. Atwood, "Dimeric Nanocapsule Induces Conformational Change," *Chem. Comm.*, 1235 (2010).

650. J. L. Atwood., E. K. Brechin, S. J. Dalgarno, R. Inglis, L. F. Jones, A. V. Mossine, M. J. Paterson, N. P. Power, S. J. Teat, "Magnetism in Metal-Organic Capsules," *Chem. Comm.*, 3484 (2010).

651. M. R. Kishan, J. Tian, P. K. Thallapally, C. A. Fernandez, S. J. Dalgarno, J. E. Warren, B. P. McGrail, and J. L. Atwood, "Flexible Metal-Organic Supramolecular Isomers for Gas Separation," *Chem. Comm.* 538 (2010).
Cover Illustration

652. P. Jin, S. J. Dalgarno, and J. L. Atwood, "Mixed Metal-Organic Nanocapsules," *Coord. Chem. Rev.*, **254**, 1760 (2010).

653. J. L. Whetstine, K. K. Kline, D. A. Fowler, C. Barnes, J. L. Atwood, and S. A. Tucker, "Spectroscopic Investigations of Pyrene Butanol Encapsulated in *C*-hexylpyrogallol[4]arene Nanocapsules," *New J. Chem.*, **34**, 2587 (2010).

654. K. T. Holman, S. D. Drake, J. W. Steed, G. W. Orr, and J. L. Atwood, "Aryl-Extended Cyclotriguaiacylenes and an Aryl Bridged Cryptophane that Provides Snapshots of a Molecular Gating Mechanism, *Supramol. Chem.*, **22**, 870 (2010).

655. J. Tian, P. K. Thallapally, and J. L. Atwood, "Gas-Induced Solid State Transformation of an Organic Lattice: From Nonporous to Nanoporous," *Chem. Comm.*, 701 (2011).

656. J. Tian, S. J. Dalgarno, and J. L. Atwood, "A New Strategy of Transforming Pharmaceutical Crystal Forms," *J. Am. Chem. Soc.*, **133**, 1399 (2011).
Chemical & Engineering News, News of the Week, January 17, 2011, p. 8.

657. A. K. Maerz, D. A. Fowler, C. M. Beavers, S. J. Teat, S. J. Dalgarno, C. A. Deakyne, and J. L. Atwood, "Solid-State Investigation into Conformational Control of Zinc(II) Dimeric Nanocapsules Using *C*-4-propoxyphenylpyrogallol[4}arenes," *Chem. Comm.*, submitted.

658. A. V. Mossine, H. Kumari, D. A. Fowler, A. Shih, S. R. Kline, C. L. Barnes, and J. L. Atwood, "Ferrocene as a Hydrophobic Temblating Agent with Pyrogallol[4]arenes," *J. Am. Chem. Soc.*, submitted.

659. P. Jin, S. J. Dalgarno, S. J. Teat, and J. L. Atwood, "Structural Alteration of the Metal-Organic Pyrogallol[4]arene Nano-Capsule Motif by Incorporation of Large Metal Centres," *Chem. Comm.*, submitted.

660. D. A. Fowler, J. Tian, C. L. Barnes, S. J. Teat, and J. L. Atwood, "Cocrystallization of *C*-Butylpyrogallol[4]arene and *C*-Propan-3-olpyrogallol[4]arene with Gabapentin," *Cryst. Eng. Comm.*, **13**, 1446 (2011).

661. S. J. Dalgarno, J. L. Atwood, and C. L. Raston, "Structural Diversity in Lanthanide Diaza-Crown Ether Complexes of *p*-sulfonatocalix[4 or 5]arenes: 'Molecular Capsule' versus 'Alternative Bi-Layer' Arrays," *Dalton Trans.*, submitted.

662. S. J. Dalgarno, K. S. Iyer, J. L. Atwood, and C. L. Raston, "Hydrogen-Bonded Molecular Capsules," *Nanoscale*, submitted.

663. R. K. Motkuri, P. K. Thallapally, B. P. McGrail, and J. L. Atwood, "A Metal-Organic Framework with Pore Expansion (Breathing) Using Polar and Non-Polar Solvents," *J. Am. Chem. Soc.*, submitted.

664. D. A. Fowler, A. V. Mossine, S. J. Teat, S. J. Dalgarno, and J. L. Atwood, "Formation of 1-D Polymer Chains of Dimeric Pyrogallol[4]arene Capsules," *J. Am. Chem. Soc.*, submitted.

665. M. Lusi, J. L. Atwood, L. R. Macgillivray, and L. J. Barbour, "Isostructural Coordination Polymers: Epitaxis vs. Solid Solution," *Chem. Eng. Comm.*, in press.

666. K. Jucke, K. M. Anderson, M. H. Filby, J. A. K. Howard, J. W. Steed, M. Henry, M. J. Gutmann, J. Wright, S. A. Mason, L. J. Barbour, C. Oliver, A. W. Coleman, and J. L. Atwood, "The Structure of Water: Behaviour in p-Sulfonatocalix[4]arene, a Highly Hydrated Clay-Mimic," *J. Am. Chem. Soc.*, submitted.

667. A. K. Maerz, D. A. Fowler, A. V. Mossine, M. Mistry, H. Kumari, C. L. Banes, C. A. Deakyne, and J. L. Atwood, "Solvent Mediated Self-Assembly of Organic Nanostructures," *New J. Chem.*, accepted.

668. L. Erra, C. Tedesco, V. Cipolletti, L. Annunziata, C. Gaeta, M. Brunelli, A. Fitch, C. Knofel, P. Llewellyn, J. L. Atwood, and P. Neri, "Acetylene and Argon Adsorption in a Supramolecular Organic Zeolite," *Chem. Mat.*, submitted.

PATENTS

1.　　"Liquid Clathrates"
　　　U. S. Patent 4,024,170 (1977).

2.　　"Coal Liquefaction Using Liquid Clathrates"
　　　U. S. Patent 4,321,127 (1982).

3.　　"Multidentate Macromolecular Complex Salt Clathrates"
　　　U. S. Patent 4,496,744 (1985).

4.　　"Calixarene Chloride-Channel Blockers"
　　　with R. J. Bridges, R. K. Juneja, and A. K. Singh,
　　　U. S. Patent 5,489,612 (1996).

5.　　"Separation of Fullerenes by Complexation"
　　　with C. L. Raston, U. S. Patent 5,711,927 (1998).

6.　　"Substantially Spherical Molecular and Ionic Assemblies"
　　　with L. R. MacGillivray, U. S. Patent 7,169,957 (2007).

7.　　"Formation of Nanometer-Scale Structures"
　　　with G. W. Orr and L. J. Barbour, U. S. Patent 6,495,669 (2002).

8.　　"Hexameric Complexes and Their Preparation"
　　　U. S. Patent 7,014,868 (2006).

9.　　"Self-Assembled Calixarene Based Guest-Host Assemblies for Guest Storage by   van der
　　　Waals Confinement" with L. J. Barbour and A. Jerga, U. S. Patent 7,132,571 (2006).

10.　　"Calixarene-Based Guest-Host Assemblies for Guest Storage and Transfer,"
　　　with L. J. Barbour and A. Jerga
　　　U. S. Patent 7,217,846 (2007).

11.　　"Material for the Recovery of Hydrogen from Gas Mixtures"
　　　with L. J. Barbour and A. Jerga
　　　filed April 19, 2004.

12.　　"Processes for the Preparation of Calixarene Derivatives"
　　　with C. L. Raston
　　　filed June 13, 2008.

13.　　"New Strategy for Transforming Pharmaceutical Solids"
　　　with J. Tian and S. J. Dalgarno
　　　to be filed.

EXHIBIT C

Uses of X-Ray Powder Diffraction In the Pharmaceutical Industry

Igor Ivanisevic, Richard B. McClurg, and Paul J. Schields

SSCI, a Division of Aptuit, West Lafayette, IN

1   INTRODUCTION

Among the many experimental techniques available for the identification of solid forms, including polymorphs, solvates, salts, cocrystals and amorphous forms, X-ray powder diffraction (XRPD) stands out as a generally accepted "gold standard." While this does not mean that XRPD should be used to the exclusion of other experimental techniques when studying solid forms, X-ray diffraction (XRD) has applications throughout the drug development and manufacturing process, ranging from discovery studies to lot release. The utility of X-ray diffraction becomes evident when one considers the direct relationship between the measured X-ray diffraction pattern and the structural order and/or disorder of the solid. XRPD provides information about the structure of the underlying material, whether it exhibits long-range order as in crystalline materials, or short-range order as in glassy or amorphous materials. This information is unique to each structure—whether crystalline or amorphous—and encoded in the uniqueness of the XRPD pattern collected on a well-prepared sample of the material being analyzed.

One must draw a distinction between crystalline materials, which give rise to XRPD patterns with numerous well-defined sharp diffraction peaks, and glassy or amorphous

TABLE 1 Types of Solid Forms Described by the Wunderlich (1) Classification System

Solid Form	Translation	Orientation	Conformation
Crystal	Long range	Long range	Long range
Condis crystal (glass)	Long range	Long range	Short range
Plastic crystal (glass)	Long range	Short range	Short range
Liquid crystal (glass)	Short range	Long range	Short range
Amorphous (glass)	Short range	Short range	Short range

materials whose XRPD patterns contain typically three or less broad maxima (X-ray amorphous halos). In practice, using XRPD, one can usually measure a sequence of progressively more disordered crystalline materials that ultimately result in glass. A classification system has been proposed by Wunderlich (1), Table 1, to describe the type of structural order and molecular packing present in molecular organic solid forms using three order parameter classes: translation, orientation, and conformation.

Solid forms of a given molecule exhibiting long-range crystalline order (e.g., polymorphs, solvates, co-crystals, and salts) can be identified and characterized using XRPD by their unique combination of order parameters. Amorphous solid forms do not exhibit any long-range order but are identifiable and characterized by their unique local molecular order, apparent in the X-ray amorphous diffraction pattern (2).

Knowing that X-ray powder diffraction is sensitive to structural order, some of its typical applications in the analysis of solid-state properties of a drug substance or product include:

- Identification of existing forms of the active pharmaceutical ingredient (API).
- Characterization of the type of order present in the API (crystalline and/or amorphous).
- Determination of physical and chemical stability.
- Identification of the solid form of the API in the drug product.
- Identification of excipients present in a drug product.
- Monitoring for solid form conversion upon manufacturing.
- Detection of impurities in a drug product.
- Quantitative analysis of a drug product.

Where appropriate data are available, XRPD analysis can determine the solid-form structure and crystal-packing relationship among individual molecules in the solid. This information is essential to the understanding of solid-state chemistry of drugs and important from the regulatory perspective.

2 X-RAY DIFFRACTION THEORY

When dealing with organic samples, a common simplification called the first Born approximation (3,4) is useful in explaining the X-ray diffraction process. Solid forms
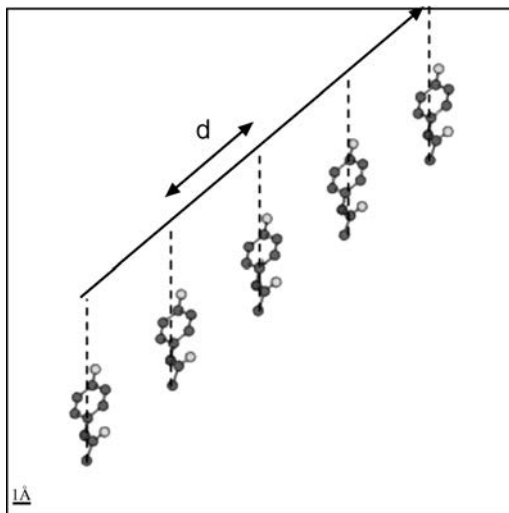
FIGURE 1   *A simple periodic array of molecules with a single orientation and conformation and constant spacing, d.*

of organic materials are expected to interact weakly with incident X-rays (generally true provided the crystallite size is not too large). This means that the amplitude of doubly and multiply scattered radiation will be very small and negligible when compared to the singly scattered radiation (4). In the presence of crystal defects, grain boundaries or disordered systems (i.e., typical laboratory samples and not large, perfect single crystals), the multiply scattered radiation becomes even less significant.

Respecting the limits of these assumptions, we can model the diffraction process as a Fourier transform of the electron density within the sample. Figure 1 shows a simple example containing a periodic array of molecules separated by a constant spacing, d, and with a single orientation and conformation. While each atom is considered a point source of scattering (5), the molecules themselves can be reduced to point sources of scattering under the assumption that the electron density distribution of a collection of atoms is the sum of the electron density distributions attributed to individual centered atoms (4). Note that atoms in a molecule are not necessarily the same as isolated, free atoms, though they are often approximated as such. The latter approximation allows us to substitute values for the Fourier transform of electron density of each individual atom using the tables of atomic scattering factors (6).

During the diffraction process, the ordered arrangement of point scattering centers in real space produces a set of diffraction events in reciprocal space corresponding to sharp peaks. A spacing of d between the point centers (molecules) in real space will correspond to a peak spacing of $2\pi/d$ in reciprocal space (also called Q-space). This simple Fourier identity, illustrated in Fig. 2, will apply to any molecular-translational order existing within a solid form (4).

Therefore, diffracted peak positions can be expressed in terms of d-space, Q-space or, most commonly, 2θ, the angle between diffracted and undeviated X-ray waves (5).
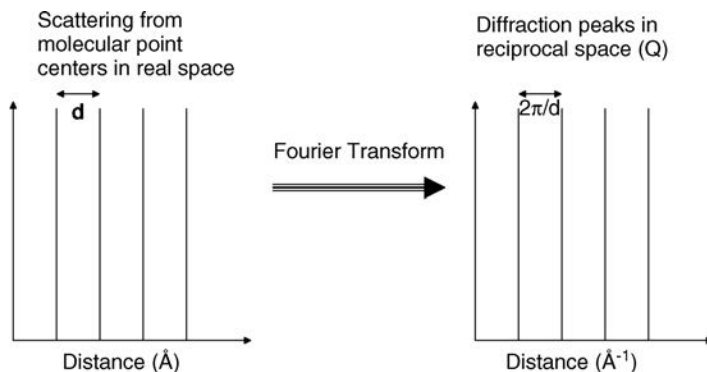
FIGURE 2   *A Fourier transform relates a periodic array of molecular point scattering centers in real space to a family of diffraction peaks in reciprocal space.*

Bragg's law can be used to relate the X-ray half-scattering angle θ to the aforementioned spacing parameter, d, as seen in Eq. 1.

$$n\lambda = 2d\sin\theta \tag{1}$$

The parameter λ is the wavelength of the incident X-ray radiation, with a typical value of approximately 1.54 Å for a Cu X-ray radiation source. n is an integer and can best be understood through the explanation of why Bragg's law holds. Consider a case of many parallel scattering planes—each of which is a collection of previously introduced point-scattering centers—reflecting incoming X-ray radiation of wavelength λ at the angle θ, as seen in Fig. 3 (5). The two diffracted waves in Fig. 3 will interfere with each other either constructively (adding together to produce stronger peaks) or destructively (subtracting from each other to some extent), depending on whether they are in phase or out of phase, respectively (4). Since the wave diffracted by the bottom plane in Fig. 3 travels a greater distance (greater by exactly $a + b$) than the wave diffracted by the top plane, that extra distance must be equal to an integer multiple of λ for points to remain in phase and total constructive reinforcement to
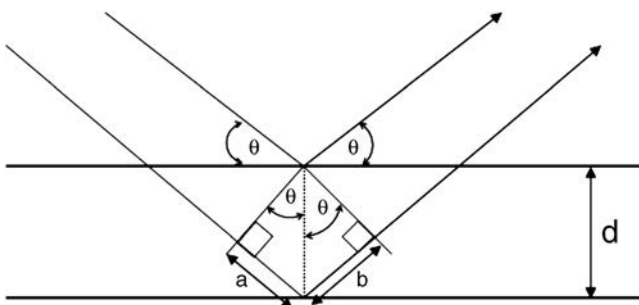
FIGURE 3   *Bragg's law for parallel planes.*

occur between the scattering from these planes (Eq. 2).

$$n\lambda = a + b \tag{2}$$

a and b can be expanded using the law of sines as $\sin\theta = a/d = b/d$. Simple substitution then transforms Eq. 2 into Bragg's law (1). The integer n refers to the order of the diffraction. For additional readings on X-ray diffraction theory, see for example References (4–8).

3   X-RAY DIFFRACTION EXPERIMENTAL PROCEDURES

XRPD patterns display diffracted intensity as a function of the experimental parameter 2θ (angle between diffracted and undeviated X-ray waves). Intensity is typically expressed in counts or counts per second while peaks are listed as positions in $°2\theta$ or d-spacings (usually measured in Å or nm).

3.1   Crystalline Materials

For materials exhibiting long-range (crystalline) order, XRPD patterns will contain sharp peaks, Fig. 4, whose shape and width will depend on the type of instrument on which the data were collected. Measurement ranges for crystalline materials depend on the type of study. For example, in a common application of XRPD—small-molecule polymorphism study—1–40$°2\theta$ is a typical measurement range used, since
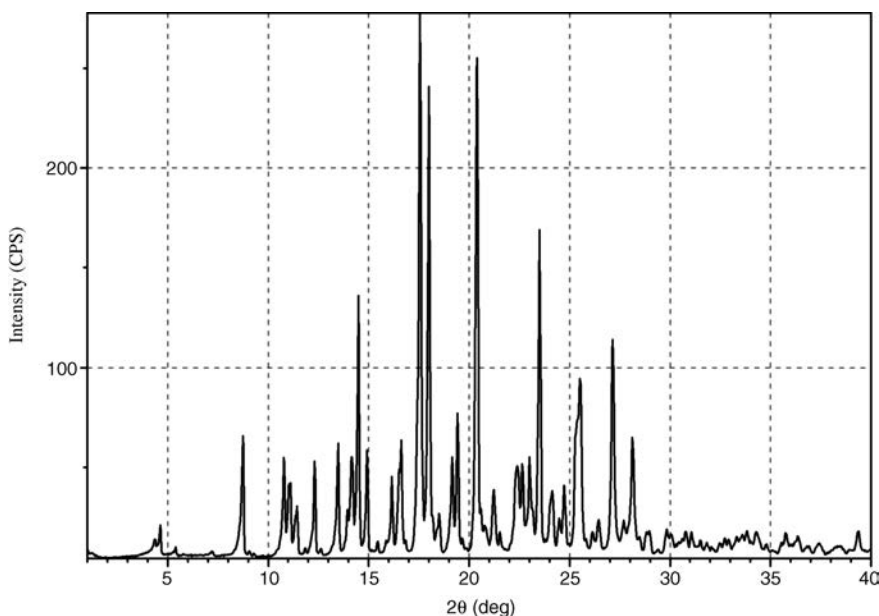
FIGURE 4   *XRPD pattern of crystalline itraconazole.*

peaks above approximately $30°2\theta$ become too numerous and overlapped to be useful in differentiating between polymorphs. When working with large molecules (e.g., biologicals), it is advantageous to measure to as low an angle as allowed by the geometry of the instrument (approximately $0.5°2\theta$ is achievable in typical laboratory settings with modern instruments, sub $0.5°2\theta$ using a synchrotron or with a dedicated small-angle scattering instrument). Certain computational methods may require measurements to significantly higher 2θ angles, up to $100°2\theta$.

Collection time varies per application but, for polymorphism studies, good patterns of crystalline material on modern instruments can be obtained in 2–10 min. In high throughput configurations for well plates, collection times of less than a minute per pattern can readily be achieved. Depending on the instrument geometry and application, 2–20 mg of crystalline sample may be required, and the sample can be reused afterwards as XRPD is typically non-destructive.

XRPD suffers from two common sample-related effects that can play a significant role when characterizing or identifying crystalline material. Ideal XRPD samples have large numbers of randomly oriented crystallites. The reproducibility of an XRPD pattern is dependent on particle-orientation statistics, while preferred orientation limits the degree to which a pattern accurately represents the structure, as opposed to a particular sample preparation. For those reasons, one must assess the particle statistics and degree of preferred orientation before one can be confident the peak identifications made from a particular pattern are representative of the material.

The effect of non-random (preferred) orientation of crystallites in a sample is to increase the relative intensities of some peaks and decrease the relative intensities of others. The variation in peak intensity is proportional to the degree of preferred orientation. In extreme cases, it can cause peaks to disappear completely while exaggerating otherwise faint peaks. Even in mild cases, a different set of relative intensities would result from diffractometers with different sample geometries.

Poor particle statistics are displayed by samples where a relatively small number of crystallites contribute to the integrated XRPD patterns. Since the small population of large crystallites cannot represent all possible orientations, the measured relative intensities are not reproducible. Irreproducible peak intensities lead to the expectation that the pattern may differ dramatically if the same experiment was repeated on a different sample of the same material even using the same diffractometer.

Both preferred orientation and poor particle statistics can be reduced to some extent in laboratory samples by spinning the sample in a holder (9, 10). Diffractometers allow the sample to be spun around one or two axes. In addition, a simple way of assessing the degree of preferred orientation or particle statistics in a sample is to analyze it on two different diffractometers with different spinning geometries. A summary of methods to minimize preferred orientation can be found in References (11–14). Bish (5) includes a detailed discussion on sample preparation and related problems.

3.2   X-Ray Amorphous Materials

In the case of X-ray amorphous (disordered, glassy or amorphous) materials, there will be no sharp peaks observed in the XRPD pattern, only broad halos (Fig. 5).
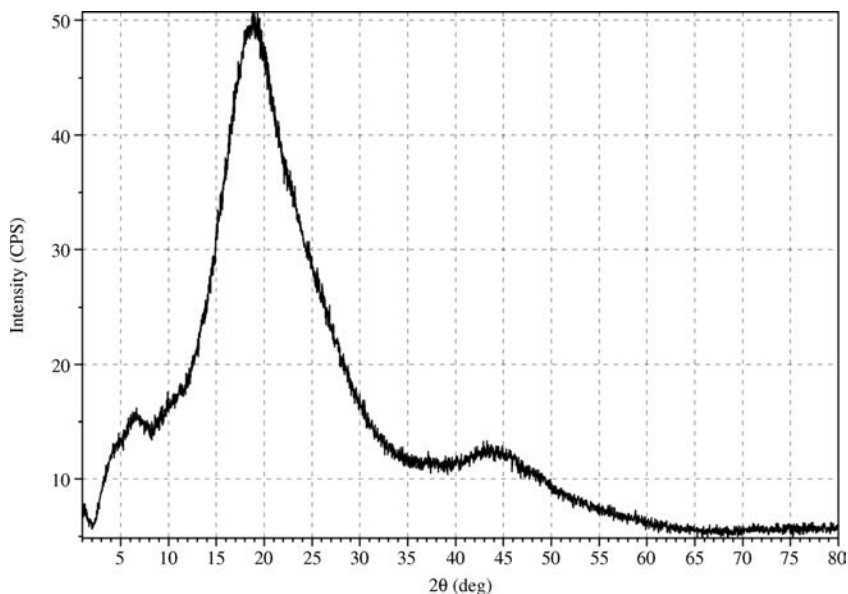
FIGURE 5   *XRPD pattern of amorphous itraconazole.*

Nevertheless, as we shall see later on, it is possible to extract structural information from these types of patterns using computational methods. Many of the computational methods used to analyze disordered materials require that the data are collected over a broad range, typically from 1 to $100°2\theta$. Furthermore, because the signal-to-noise ratio in X-ray amorphous patterns is typically poor, longer collection times are often used. 30–60 min is not uncommon for a single pattern. Finally, a greater amount (50–100 mg) of amorphous sample is typically warranted to obtain a good XRPD pattern.

XRPD patterns of both crystalline and X-ray amorphous materials contain some experimental artifacts, for example, instrument-background functions, sample-holder fingerprints, incoherent (Compton) scattering, polarization and Lorentz effects, and air scatter (5). The relatively low signal generated from X-ray amorphous samples means those artifacts will represent a much greater portion of the overall diffracted intensity. Therefore, computational methods used to analyze X-ray amorphous materials (15–17) are very sensitive to experimental artifacts and care must be taken to minimize their presence. Instrument intensity-correction functions can be determined using known standards and computationally modeled thereafter. Sample holders that produce significant X-ray scattering of their own in the relevant regions (e.g., glass capillaries) should be avoided when working with amorphous materials. Instead, samples can be sandwiched between thin polymer films with low X-ray background (e.g., Etnom®). Given the chemical formula of the material, Compton scattering can be calculated from atom-scattering tables (6) and subtracted from the overall signal. Air scatter can be largely eliminated using custom-built enclosures for a helium atmosphere.
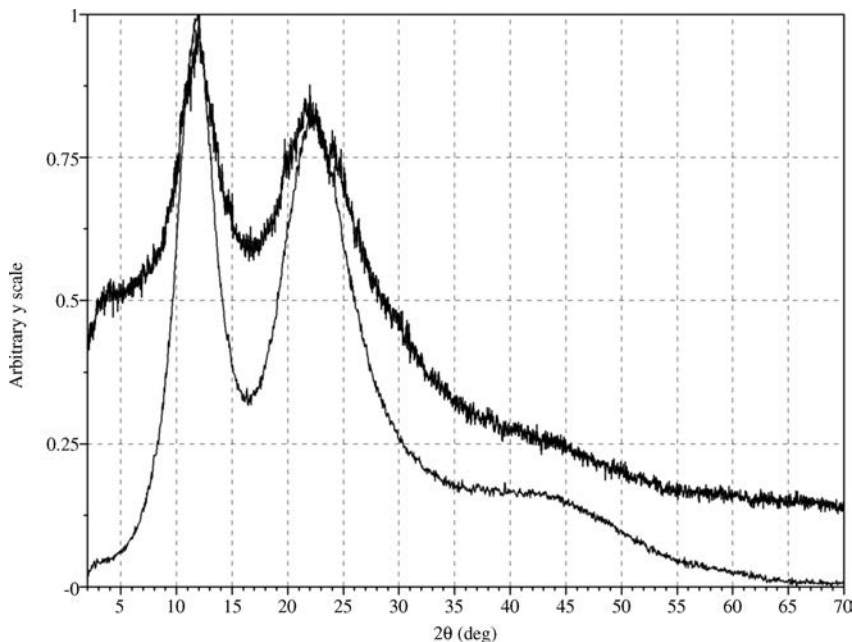
FIGURE 6   *The effects of experimental artifacts on amorphous X-ray patterns. Both patterns were collected from the same sample of amorphous nifedipine. The top pattern was collected from approximately 10 mg of material packed in a glass capillary under ambient conditions. The collection time was 5 min. The bottom pattern was collected from approximately 100 mg of material sandwiched between two thin sheets of Etnom® film in a He-purged enclosure. The collection time was 1 h.*

Figure 6 shows an X-ray amorphous pattern of nifedipine collected on a standard instrument with no special considerations and the sample packed in a glass capillary, compared to the same sample collected on a specially configured instrument using a low background sample holder, He atmosphere, and longer collection time. Note the patterns in this figure have not been offset but normalized to top intensity. As seen in the bottom pattern of Fig. 6, the low angle air scatter contribution is largely eliminated through the use of He. Furthermore, the broad glass scattering around $25°2\theta$ which causes a shift in the position of the second amorphous halo in the top pattern is not evident in the bottom pattern. Typically, in screening applications, no more than a few milligrams of material are available, resulting in patterns where the glass/air scatter signal overwhelms the signal from the material itself and little structure is evident.

Certain types of analyses involving crystalline materials (e.g., quantitative studies or indexing) may also benefit from careful experimental setups but the most common applications (i.e., polymorph detection or identification (18)) generally do not require the specialized setups or longer collection times used for amorphous materials.

3.3   Instrumentation

Laboratory X-ray diffractometers typically consist of an X-ray source, sample chamber and detector. The most commonly used X-ray source in laboratory experiments with organics is Cu, though instruments typically allow different sources to be used with some configuration. Slits and optics are used to focus the incident and diffracted radiation on the sample and detector, respectively. Specimens usually can be rotated to alleviate some of the intensity artifacts discussed earlier. Detectors can be point, line or area, with the latter offering advantages in both speed of acquisition and ability to assess the particle statistics and preferred orientation in a sample through examination of Debye rings (19). Synchrotron sources are sometimes used for specialized measurements to collect high quality data. Detailed descriptions of X-ray instrumentation can be found, for example in Reference (5).

The alignment of a diffractometer is maintained through the use of calibration standards, such as silicon, to verify the position calibration (5). Regular calibrations are accepted industry practice (cGMP), with the frequency of calibration ranging from every X number of samples to set time periods (e.g., daily), depending on how much data one is willing to risk invalidating due to a failed calibration. When a silicon standard is used, the Si 111 peak position is typically verified using a short scan in the appropriate region (around $28.4°2\theta$). Other standards may be used, for example, to verify low angle alignment.

Diffractometers can typically be operated in either reflection or transmission configurations. Reflection is by far the more common and also referred to as Bragg-Brentano geometry (Fig. 7). In reflection measurements, incoming X-rays are "reflected" off the sample surface and focused by the instrument optics onto the detector. Errors due to sample transparency to X-rays are common for organic samples (5,14). The X-rays penetrate many atomic layers below the surface meaning the average diffracting surface lies somewhat beneath the surface of the sample. This type of error can lead to peak position errors in measured patterns of as much as a tenth of a degree. Therefore, low absorbing samples are often prepared as thin films using
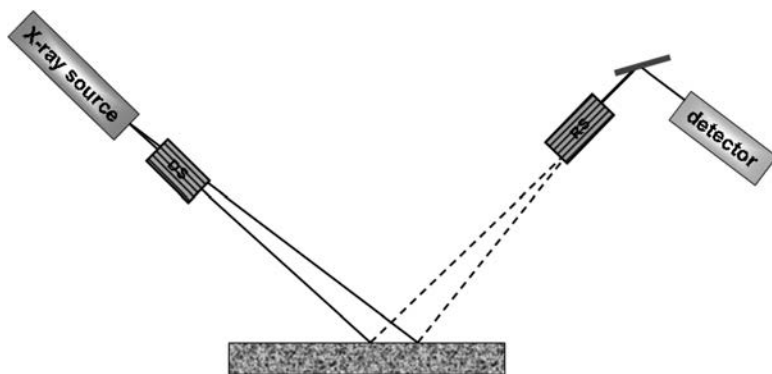
FIGURE 7   *Bragg-Brentano diffractometer geometry.*

a low background holder, to reduce the penetration effect. Displacement errors arise from the difficulty of preparing samples such that the surface of the sample is level with the surface of the holder (where the instrument is focused). Sample-displacement errors can result in significant, systematic shifts in measured peak positions, on the order of several tenths of a degree in particularly bad cases. Experience in preparing samples such that they are level with the surface of the holder is the only solution to this problem, although computational methods can be used to shift the pattern and correct peak positions, where the error is recognized. A further limitation of reflection measurements is the inability to measure to very low angles—typically $2.5°2\theta$ is a practical limit—making this type of measurement less useful for the analysis of large molecules which are expected to have peaks in the 0–$2.5°2\theta$ range.

Transmission mode analysis overcomes many of the limitations of reflection mode when carefully configured. In transmission measurements, the incident X-rays pass through the sample and are diffracted not only on the surface but throughout the sample. This type of analysis is possible for organics due to their relative transparency to X-rays. The sample no longer needs to be level with the holder but thickness of the sample is important and can cause peak displacement errors (when the sample is too thick). Transmission configurations generally allow lower angle measurements than reflection, making them useful for large molecules. However, it becomes essential that the holder containing the sample is as X-ray transparent as possible, because its "fingerprint" will be part of the X-ray pattern collected on each sample. Disposable, low background thin polymer films are commonly used to hold the sample in transmission measurements. In addition, it is common practice to regularly collect blanks (X-rays of the holder material itself) to ensure its signature does not change between different lots. Nevertheless, the extra effort required to operate instruments in transmission mode is well worth the improvement in data quality, especially when working with X-ray amorphous materials.

4   APPLICATIONS OF X-RAY DIFFRACTION IN DRUG DEVELOPMENT AND MANUFACTURING

XRD has a broad range of applications in various stages of drug development and manufacturing. This section will address many of the common XRPD uses from a practical standpoint. In the broadest terms, these applications can be divided between API characterization and identification. While there is some overlap in both categories, the former is more commonly applied during drug development (before the drug is on the market) while the latter is directed more toward manufacturing, regulatory aspects and intellectual property.

4.1   API Characterization

Guidelines from regulatory authorities regarding the need for characterization of a drug substance under development have been clearly stated. Below is an example relating to the issue of polymorphism (20):

"Polymorphic forms of a drug substance can have different chemical and physical properties, including melting point, chemical reactivity, apparent solubility, dissolution rate, optical and mechanical properties, vapor pressure, and density. These properties can have a direct effect on the ability to process and/or manufacture the drug substance and the drug product, as well as on drug product stability, dissolution, and bioavailability. Thus, polymorphism can affect the quality, safety, and efficacy of the drug product."

While there are a number of methods to characterize polymorphs of a drug substance (21), the two broadly accepted methods of providing unequivocal proof of polymorphism recognized by the above source are single crystal X-ray diffraction and X-ray powder diffraction (20). Other techniques (e.g., thermal or spectroscopic methods) can be helpful in further characterizing drug products but only X-ray provides the necessary structural information to uniquely identify different polymorphs. Therefore, in early drug development, X-ray powder diffraction is often used as a primary experimental technique and a means of differentiating between the experimentally generated materials. Fully characterizing any material requires the use of complementary techniques (thermal or spectroscopic) but X-ray is typically done first because it is fast, non-destructive, requires little material, and provides the necessary structural information.

Synchrotron X-ray diffraction has frequently been used to characterize pharmaceutical materials in applications where additional sensitivity not provided by laboratory X-ray diffractometers may be required (e.g., crystallization monitoring (22,23)). The tradeoff is the greater expense and time investment typically associated with such measurements. Since such applications tend to be specialized, this section will focus primarily on laboratory XRPD methods.

4.1.1 *Qualitative Analysis of Materials (Phase Identification)* Every structurally different crystalline material will exhibit a unique XRPD pattern upon analysis (14). Therefore, the use of XRPD for phase identification was recognized early and remains the most common application of XRPD to pharmaceuticals. This so-called qualitative analysis typically refers either to the initial characterization of material previously not analyzed by XRPD or to the identification of a phase or phases in a sample of material by comparison to reference patterns. Reference patterns are previously collected XRPD patterns of the same material. Where available, XRPD patterns calculated from, for example, single crystal structures can be substituted but one should remember that the temperature at which the pattern is calculated can have a significant effect on the calculated XRPD profile. When dealing with mixtures of phases, qualitative analysis can provide an estimate of the relative proportions of different phases in the sample, usually based on the comparison of peak intensities for characteristic peaks of the different phases. Due to sample artifacts such as preferred orientation and poor particle statistics, this type of analysis should never be confused with quantitative analysis of mixtures, addressed later in this chapter. Databases of known XRPD patterns for various pharmaceutical materials are published annually by the Centre for Diffraction Data (ICDD) and the Cambridge Crystallographic Data Centre (CSD).

12   *USES OF X-RAY POWDER DIFFRACTION IN THE PHARMACEUTICAL INDUSTRY*

XRPD patterns are typically compared by overlaying and aligning the data from different samples. This procedure is typically done electronically, either using the software provided by the XRPD instrument vendor or using custom-developed software. The primary assessment might include determining whether each sample is X-ray amorphous or crystalline based on the absence or presence of crystalline peaks, respectively. When comparing XRPD data of crystalline samples, one notes any differences in peak positions (to within a certain precision, e.g., 0.1 °2θ (24)) which correspond to structural differences between the samples. Intensities are generally not relied upon for qualitative analysis due to previously mentioned instrument and sample artifacts, although they have to be used to some degree to allocate the peak positions (based on local maxima).

It is not uncommon for two patterns to share some but not all of the peak positions. This can be a coincidence or it can be due to one of the samples being a mixture of multiple phases, including the phase in the other sample. Experience and data from complementary experimental techniques are needed to resolve such ambiguous cases. It should also be noted that, at higher 2θ values, peaks of most organic materials become considerably overlapped and determining their exact positions becomes difficult. Therefore, free-standing peaks at low angles are the primary means of differentiating structures and XRPD data above approximately 30 °2θ are rarely useful for qualitative analysis.

Figure 8 shows XRPD patterns of two crystalline polymorphs of sulfamerazine. The patterns in Fig. 8 were collected from material crystallized in glass capillaries during a polymorphism screen. A polymorphism screen is typically run early in the
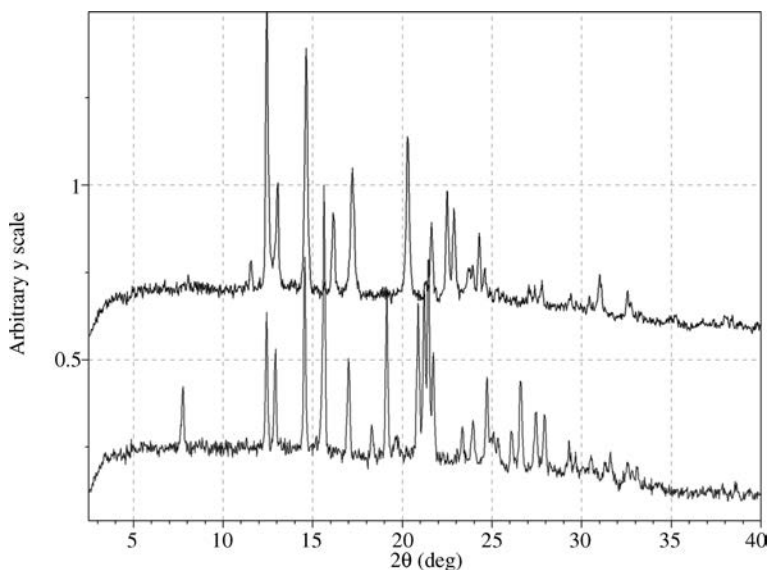
FIGURE 8   *Two polymorphs of sulfamerazine. Patterns offset for clarity.*

drug development process to identify and (partially) characterize the different polymorphs of a drug substance. Assuming XRPD was the first analytical technique used on the samples, the data in Fig. 8 could be used to make a qualitative assessment regarding the probable nature of the material generated during crystallization experiments. Therefore, one could designate the first of the patterns crystalline "Pattern A" and the other crystalline "Pattern B," noting the sharp peaks and lack of diffuse halos as a sign of crystallinity and the structural differences, as evidenced by the different peak positions in each pattern. There is insufficient information at this stage to designate either pattern as a polymorph of the material (e.g., they could be a solvate, hydrate, or a mixture of two or more polymorphs). However, it is clear that both materials are crystalline and structurally different. Further characterization using for example, thermal methods (TGA, DSC) would confirm these materials are not solvates or mixtures but actual polymorphs and aid in determining the thermodynamically stable polymorph. XRPD provides information about the structure of materials, not thermodynamics, although variable-temperature XRPD has been used to study changes in structure at different temperatures.

One can envision a large number of different crystallization experiments (using different solvents or conditions) performed on the API, some possibly in automated fashion, with the resulting material characterized initially by XRPD. This is in fact a common approach to polymorphism, salt, and cocrystal screening and perhaps the most common application of XRPD in the drug development process. The latter two screens are usually performed when the polymorph(s) of the drug candidate itself are not sufficiently bioavailable, in an effort to produce a formulation that addresses the bioavailability problem. An XRPD pattern is taken of the API and the guest material (e.g. acid) and the mixture of the two. If a salt or cocrystal was formed, the XRPD pattern of the mixture should be more than just a sum of the reference patterns of the API and the guest.

Therefore, the first application for XRPD during drug development is typically to identify the materials generated using different experimental methodologies, often in automated high throughput screening environments (25–27). To simplify this pattern recognition problem that often involves hundreds or thousands of experimental data sets per screen, people have developed various computational approaches to recognize, sort, and classify unknown XRPD patterns, either through comparison to a known database of materials (28) or simply within the experimental set of unknown patterns (18, 29, 30). The latter often uses an approach called hierarchical clustering (31, 32).

XRPD data are often catalogued in databases using the so called Hanawalt system (33–34). In this system, the data are stored as d versus I/I_{max} pairs. The use of d-space eliminates the need to specify the radiation source wavelength and allows comparison between laboratories using different instrumentation. A similar system is often used for intellectual property filings, as discussed later in this chapter.

However, as we shall see in following sections, there is considerable structural information available in a typical XRPD pattern that can be used to characterize the material. Making use of this information usually requires high quality laboratory data and the use of advanced computational methods.

4.1.2 Structural Analysis of Crystalline Forms XRPD patterns of crystalline materials have sharp peaks due to constructive interference of diffracted radiation. As mentioned previously, XRPD patterns can be used to identify particular substances by comparison with reference patterns, analogous to the use of fingerprints to identify people. For example, the experimental XRPD pattern of Mannitol in Fig. 9 (bottom pattern) compares best with the simulated pattern of the beta form (second pattern) indicating that the sample is likely form beta, and not form alpha or delta. The positions of the reflections in XRPD patterns are functions of the size and shape of the crystallographic unit cell. Reflection intensities are functions of the atomic positions within the unit cell. A variety of instrumental and sample preparation artifacts influence the intensities, and to a lesser extent, the positions of the reflections. A first step in the further characterization of an XRPD pattern of a crystalline sample is to rationalize the reflection positions using a process called indexing.

4.1.2.1 Indexing Indexing is the process of determining the size and shape of the unit cell given the peak positions in a diffraction pattern. The term gets its name from the assignment of Miller index labels to individual peaks. For most applications, the index labels are less important than are the unit cell length and angle parameters that provide the link between crystal properties and the diffraction pattern.
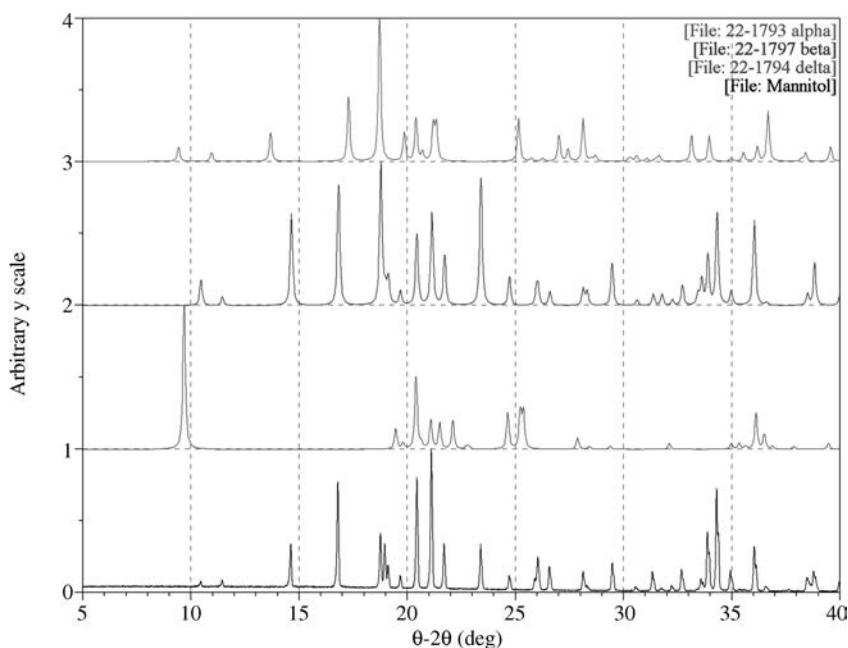
FIGURE 9   *Comparison of simulated (top three) and measured (bottom) XRPD patterns of Mannitol. The legend provides ICDD reference codes and form designations for the simulated patterns.*

Indexing plays a role in single crystal and powder diffraction pattern analysis, but there are qualitative differences between indexing single crystal and powder diffraction data. For single crystal diffraction, reflections are recorded as a function of the three-dimensional orientation of a crystal relative to the incident radiation. Each reflection in single crystal diffraction corresponds to a solution of the Laue equations, or equivalently the vector form of the Bragg equation. For powder diffraction, the (ideally) isotropic distribution of particle orientations leads to cylindrical symmetry in the diffracted radiation. Therefore, each reflection in powder diffraction corresponds to a solution of the scalar form of the Bragg equation (35). As a result of the loss of information regarding the relative orientations of diffracting crystallites, indexing of XRPD data is more challenging than single crystal diffraction data.

There are a variety of methods available for indexing XRPD patterns, some of which are in the public domain and others that are sold commercially. Examples include ITO (36), TREOR (37), N-TREOR (38), singular value decomposition (39), X-CELL (40), and DICVOL (41). The methods differ in their methods for identifying and refining potential solutions, ability to determine low symmetry solutions, efficiency, and sensitivity to extraneous and/or missing peaks. Development of novel methods and refinement of existing methods continues to be an area of active research. When applying these automated methods, it is important to be aware that multiple solutions can appear to adequately index a XRPD pattern. These degenerate solutions are called lattice metric singularities (42). In such cases, it is common practice to accept the higher symmetry solution unless there is other evidence supporting the lower symmetry solution.

Successful XRPD indexing serves several purposes. If all of the peaks in a pattern are indexed using a single unit cell, this is strong evidence that the sample contains a single crystalline phase. Given the indexing solution, the unit cell volume may be calculated directly. The difference in molar volume between an anhydrous crystal form and the molar volume of hydrates, solvates, and co-crystals can be useful for determining their stoichiometries. If the chemical composition of a crystal is known, then indexing provides the means of determining very accurate true densities. Indexing is also a robust description of a crystalline form. Common practice is to characterize forms using a list of XRPD peak positions for selected intense peaks, but the intensities of individual peaks are sensitive to changes in temperature, defect density, and preferred orientation effects as a result of sample preparation. Also, the positions of peaks are sensitive to temperature, strain, and changes in hydration state. Although unit cell parameters change as a result of these effects, the changes are less pronounced when comparing indexing solutions than when comparing peak lists based on particular selection criteria. Indexing can be used to show that a XRPD pattern is consistent with the structure of a crystal determined via single crystal diffraction. Also, indexing is a preliminary step for other analyses including structure determination from XRPD data and Rietveld refinement.

Data   Not all XRPD patterns are amenable to indexing. XRPD patterns must have sufficient signal-to-noise and peak resolution to provide enough peak positions to uniquely define the indexing solution. Signal-to-noise can be improved by eliminating sources of diffuse scattering such as glass sample holders and by collecting the pattern

for a longer time. Peak width is a convolution of instrumental and sample contributions. Therefore, a diffractometer with adequate monochromatization is necessary, but not sufficient to ensure good peak resolution. Samples containing nanoscale crystalline regions or defective crystals display broadened peaks in their XRPD patterns. In the extreme, these broadened peaks can overlap and produce a pattern that appears to contain only amorphous halos as discussed elsewhere in this chapter.

Wilson showed that centrosymmetric crystal structures (those containing an inversion center) are more likely to have very weak and very strong reflections than are non-centrosymmetric crystal structures (lacking an inversion center) which tend to have a narrower distribution of peak intensities (43). Ordered crystals containing only one enantiomer (or diastereomer) of a chiral molecule cannot crystallize in space groups with mirror planes, glide planes, or inversion centers since those operations change the chirality of the molecule. Therefore, crystals containing non-chiral molecules or racemic mixtures of chiral molecules may adopt a centrosymmetric structure whose XRPD pattern has a large fraction of very weak reflections. Since these weak reflections are often important for successful indexing of the XRPD pattern, care should be taken to optimize peak sensitivity when collecting XRPD data for indexing, particularly for non-chiral molecules or racemic mixtures. This can be accomplished by reducing sources of background scattering and by increased collection times, for example.

The bottom XRPD pattern in Fig. 9 is an experimental XRPD pattern of Mannitol, form beta. Since Mannitol is chiral, it is expected to crystallize in a non-centrosymmetric structure and the corresponding XRPD pattern should have relatively few extremely weak or strong reflections. There is relatively little diffuse background scattering and the signal-to-noise ratio appears to be very good in the pattern. Also, the peaks are quite sharp leading to good peak resolution. All of these observations suggest that the XRPD pattern is amenable to indexing under the assumption that the pattern represents a single crystalline phase.

Results   A successful indexing solution for the Mannitol XRPD pattern from Fig. 9 is illustrated in Fig. 10. The bars in Fig. 10 correspond to positions of allowed reflections based on Bragg's Law. All of the observed peaks in the XRPD pattern are indexed by one or more of the allowed reflections. Also, there are relatively few allowed reflections that are not observed. In some cases, the reflections are too weak to be evident at the scale shown in Fig. 10, but are evident using an expanded scale. If the allowed reflections did not account for all of the observed reflections, then the solution
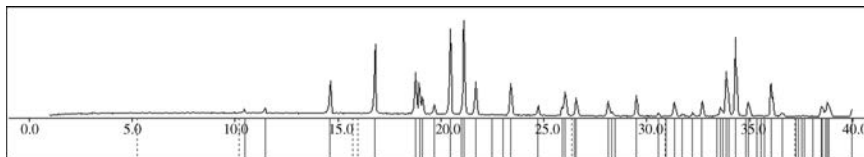
FIGURE 10   *Indexed XRPD pattern of Mannitol form beta. Green bars indicate allowed reflections based on the unit cell dimensions and assigned space group $P2_12_12_1$ (no. 19). Dashed bars indicate extinct reflections.*

would have been rejected as unable to fully describe the observed pattern. If there were a large number of allowed but unobserved peaks, then the solution would be rejected in favour of a smaller volume and/or higher symmetry solution. Since the illustrated solution falls into neither category, it is accepted as a good description of the observed pattern. This confirms that the XRPD pattern is of a single crystalline phase.

There are some allowed reflections, marked with dashed bars in Fig. 10, that are not observed. These systematic extinctions are the result of space group symmetry elements of the contents of the unit cell. Systematic extinctions are the result of centered unit cells, screw axes, and/or glide planes. Rules indicating which reflections are extinct based on their Miller indices are tabulated (35). Given the observed systematic extinctions in a pattern, an extinction symbol may be assigned (44). In the illustrated case, the extinction symbol $(P2_12_12_1)$ corresponds to only one space group, $P2_12_12_1$ (no. 19). In many other cases, there are two or more space groups corresponding to the observed extinction symbol and additional analysis is needed to fully determine the space group.

The solution illustrated in Fig. 10 is orthorhombic with length parameters given in Table 2. Given the length parameters, the unit cell volume is readily calculated. The number of asymmetric units in the unit cell for a given space group is tabulated in Reference (44). For space group $P2_12_12_1$ there are four asymmetric units in the unit cell $(Z = 4)$. Assuming that there is one Mannitol molecule per asymmetric unit $(Z' = 1)$, then the molar volume and density are readily calculated. The density is a bit higher than typical organic molecules, but is as expected for sugars such as Mannitol. A reasonable density confirms that the correct number of molecules per asymmetric unit was assumed.

Having successfully indexed the XRPD pattern, determined the extinction symbol, and calculated the density, the analysis of peak positions in the Mannitol XRPD pattern is complete. Additional information regarding the Mannitol sample can be derived from the peak shapes and intensities using the Rietveld method.

TABLE 2   Indexing Results and Derived Quantities

Substance and Form	Mannitol Form Beta
Composition	$C_6H_{14}O_6$
MW (amu/molecule)	182.172
Family and space group	Orthorhombic $P2_12_12_1$ (no. 19)
a (Å)	8.6790
b (Å)	16.8980
c (Å)	5.5502
α (deg)	90
β (deg)	90
γ (deg)	90
V (Å^3)	813.65
Z' (molecules/unit)	1
Z (units/cell)	4
V/Z (Å^3/unit)	203.41
ρ (g/cm^3)	1.487

4.1.2.2 Rietveld Analysis   The Rietveld method is a computational tool for extracting structural and microstructural information about a crystalline solid from its powder-diffraction pattern. This computational method was pioneered by Hugo Rietveld in the late 1960s (45, 46). The ability to obtain structural information from polycrystalline materials from which a crystal suitable for single-crystal analysis was either unavailable or practically impossible to obtain was a significant achievement. Initially the method was mostly used to refine the atomic positions and lattice parameters of crystal structures. Use of the Rietveld method proliferated with the increased accessibility of digital data in the 1980s and is now routinely used for quantitative analysis of phase mixtures for a wide range of materials and applications from cement and minerals to pharmaceuticals. This method is also used to characterize crystal defects and the microstructural properties of polycrystalline solids, such as preferred orientation, microstrain, and crystal size.

The Rietveld method computes a powder pattern using information describing the crystal structure and the instrumental technique used to collect the diffraction pattern. An iterative algorithm refines the structural and instrumental parameters used in the computation to minimize the difference (residual) between the observed and calculated diffraction intensity at each scattering angle (2θ). The success of a Rietveld analysis depends on building an appropriate model for the algorithm so the best fit (global minimum) to the experimental pattern can be efficiently discovered while avoiding false minima. Many freeware computer programs available for Rietveld analysis are listed and described on the website (47); many programs are also commercially available. To set up a model for a system of interest and obtain reliable information, each program requires a skilled user with understanding of diffraction theory and experiment. A recommended way to learn and assess the reliability of a Rietveld program is by refining patterns of well-characterized powders. α Al_2O_3 NIST SRM 676 is a very good standard because it has no preferred orientation, two refinable atomic positions determined by single-crystal analysis (48), and two lattice parameters. The accuracy of the measured intensity and 2θ combined with the skill of the Rietveld analyst and the accuracy of the Rietveld refinement algorithm determines the accuracy of the refined parameters. The applicable theoretical corrections used to compute the diffraction pattern for a particular data-collection technique require the user to judiciously construct the appropriate models (49, 50).

The minimum information needed to calculate a diffraction pattern is the atomic positions, space group, and lattice parameters of the crystal structure. The Rietveld program calculates the position and intensity of the diffraction peaks and assigns them a 2θ-dependent profile determined by the instrumental model. The parameters describing the profile are obtained from the results of a Rietveld analysis of a pattern of NIST SRM 660a LaB6 profile standard. This standard can also be used to check the accuracy of the lattice-parameter refinement and to refine the wavelength intensity ratio if more than one X-ray wavelength was used for data collection. For example, the ratio of Cu Kα2 to Kα1 is ~ 0.5 and can vary several hundredths depending on the type and alignment of the monochromator of the instrument used to collect the powder pattern. Standardizing the profile function allows microstrain and size (51) to be more

accurately refined as well as improving the fit of the calculated pattern to the experimental pattern.

Several quantitative and qualitative ways of assessing the "goodness of fit" between the experimental and calculated patterns are available. The qualitative assessment is a careful visual examination of the fit and the residual intensity. Visual assessment is essential and compliments the quantitative measures of the fit. The quantitative measures of the fit include the weighted pattern residual (R_w) and the ratio of R_w to the expected residual (R_w/R_{exp}). This ratio indicates how close the fit is to the theoretically best residual calculated using the number of data points in the observed pattern, the number of refined variables, and the uncertainty of the observed intensity intrinsic to counting photons.

The refinement is usually done in several stages (52) with only some of the refinable parameters being refined in each stage. The scale factor for the incident-beam intensity is always refined, and the background is usually refined in the first stage. The background is best minimized in the experimental pattern by use of antiscatter slits and helium; reducing background also improves the detection limit. Background is usually modeled with a polynomial and, if the background cannot be adequately fit, it can be artificially minimized by subtracting an appropriate blank pattern collected with identical collection parameters as the specimen of interest. Subsequent stages depend on the goal of interest. None of the refinable parameters will usually be refined well the first time; therefore, several iterations are used to find the global minimum.

A successful Rietveld refinement requires the user to know if the pattern of interest displays artifacts from inadequate orientation statistics (OS) and preferred orientation. These artifacts affect relative peak intensities and can generate significantly inaccurate structure refinements. If preferred orientation is well understood, it can be corrected by a variety of models available in many Rietveld programs. OS artifacts are manifest in random fluctuations of relative intensity for each preparation of the sample and cannot be corrected. The spiky peaks generated by OS artifacts can be difficult to detect by visual examination of the one-dimensional XRPD pattern. Fortunately, they can be readily detected by collecting a two-dimensional pattern with an area detector. If the Debye rings in the two-dimensional pattern are spotty, then OS is a potential problem depending on how the pattern of interest is collected. Both PO and OS artifacts can be practically eliminated by collecting the pattern in transmission geometry using a Gandolfi spinner and by comminution of the sample. Unfortunately comminution is often not a viable option because many samples, especially organics, are susceptible to stress-induced phase transformation.

We provide an example of the limitations of refining a pattern displaying a slight amount of PO. Rietveld refinement using Maud (version 1.999) was applied to a pattern of β mannitol collected with a laboratory diffractometer in transmission geometry. To correct PO we used a March-Dollase model on the 130 hkl (Fig. 11). The atomic positions were compared to those from a single-crystal structure determination by Kaminsky et al. (53). The thermal parameters were bound to be the same for all atoms and set to be isotropic; hydrogen was not included. Without using PO corrections, the fit to the measured pattern was poor (Fig. 12).
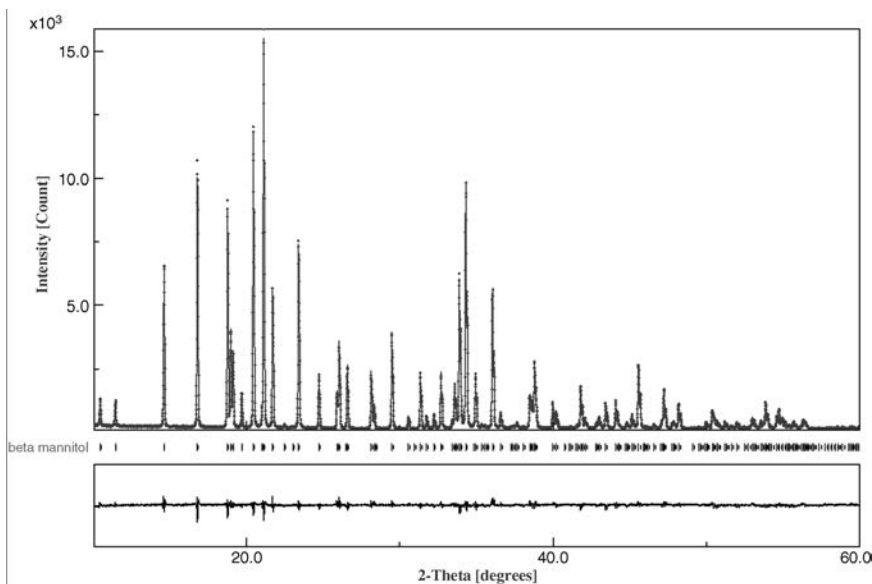
FIGURE 11   *Overlay of a Rietveld refinement of* β *mannitol with* $R_w = 7.19\%$ *and* $R_w/R_e = 1.6$ used to investigate the use of spherical harmonics to facilitate the refinement of the lattice parameters and thermal factor.
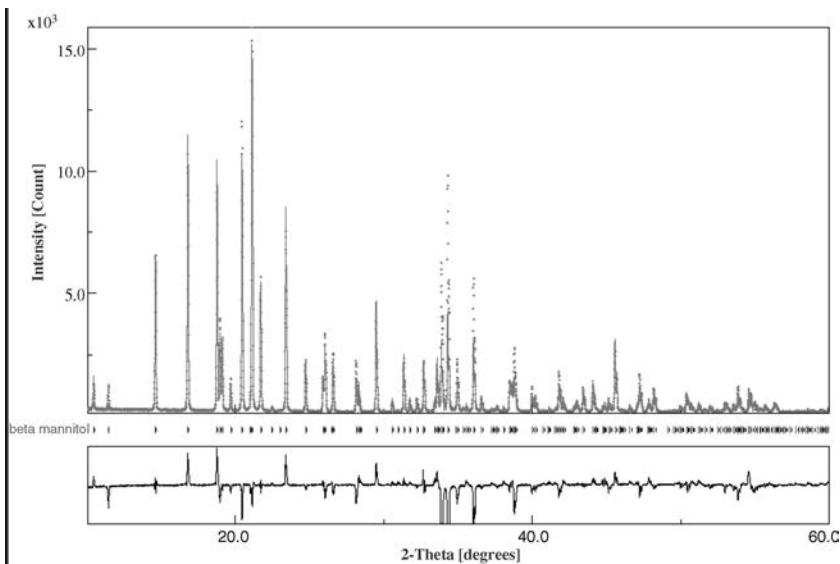
FIGURE 12   *Rietveld refinement of* β *mannitol without spherical harmonics,* $R_w = 26.3\%$ *and* $R_w/R_e = 5.9$.

TABLE 3   Bond Distances for β-Mannitol from a Rietveld Refinement of a Pattern with Orientation-Statistics Artifacts Compared to Those from a Single-Crystal Analysis by Kaminsky et al. (53) and a Rietveld Refinement by Botez et al. (54)

Bond Distance	Kaminsky et al. 1997 (Å)	Botez et al. 2003 (Å)	Difference (Å)	This Study (Å)	Difference (Å)
C1-C2	1.517 (2)	1.545 (17)	0.028	1.585	0.068
C2-C3	1.539(2)	1.546 (15)	0.007	1.543	0.004
C3-C4	1.523 (2)	1.515 (16)	−0.008	1.555	0.032
C4-C5	1.539 (2)	1.592 (14)	0.053*	1.618	0.079
C5-C6	1.521 (2)	1.552 (16)	0.031	1.569	0.048
C1-O1	1.425(2)	1.416 (17)	−0.016	1.485	0.053
C2-O2	1.440 (2)	1.443 (16)	0.016	1.444	0.017
C3-O3	1.433(2)	1.390 (17)	−0.042	1.431	−0.001
C4-O4	1.448(2)	1.434 (15)	−0.004	1.356	−0.082*
C5-O5	1.445(2)	1.439 (16)	0.011	1.461	0.033
C6-O6	1.436(2)	1.431 (18)	0.004	1.460	0.033
Standard deviation			0.026	n/a	0.040
Sum			0.080	n/a	0.284

*Maximum deviation.

The bond distances, Table 3, from our refinement had a 0.04 Å standard deviation relative to the single-crystal values and a maximum absolute error as high as 0.08 Å. This uncertainty is ten times larger than the uncertainty of the single-crystal bond distances and slightly higher than those refined by Botez et al. (54) using a pattern collected with a synchrotron. Our bond distances also have a positive bias. These relatively high uncertainties reflect the intensity inaccuracies from not completely correcting the PO. The inaccuracies of atomic positions will increase as the magnitude of PO and OS artifacts increase. The calculated bond angles also will be more significantly more uncertain than the reliable single-crystal values.

The magnitude of thermal displacements above those commonly measured by single-crystal analysis indicates the amount of static-displacement defects in the crystal. The refined thermal parameter (B) was 2.4 Å^2, and the single-crystal values for carbon and oxygen ranged from 1.64 to 2.81 Å^2. This result indicates the 2θ-dependent intensity corrections provided by the Debye-Scherrer geometry and the curved position-sensitive detector models are reasonably accurate. The intensity fluctuations from slight PO are not expected to significantly affect the thermal parameter if enough of the pattern was refined, but, depending on the magnitude of the PO artifacts, a reasonably accurate B value might not always be obtained unless an accurate PO correction is applied.

The orthorhombic lattice parameters were refined to $a = 8.6790 \text{ Å}$, $b = 16.8980 \text{ Å}$, and $c = 5.5502 \text{ Å}$, and the zero offset was $0.0004°$. These lattice parameters are within 0.01% of those refined by Botez et al. (54). The negligible offset indicates the diffractometer was very well aligned.

The beginning Rietveld analyst must have a good understanding of experimental and theoretical diffraction physics and the Rietveld model to assess the goodness of fit. The β mannitol example described here demonstrates a fairly good fit to the observed

pattern using PO corrections does not necessarily mean the refined parameters are reliable and accurate; the bond distance and angles must be compared to known ranges from reliable single-crystal determinations to see if the results are reasonable. Values of bond distance and angle for moieties on organic molecules can be found in the Cambridge Crystal Structure database. Although patterns containing intensity artifacts can be analyzed using Rietveld analysis to provide useful structural information, the use of appropriate data-collection techniques is always the best way to obtain the most reliable results.

4.1.3   Structural Analysis of Disordered Crystalline Forms   Highly crystalline forms of APIs are preferred in the drug development process because of their high level of purity and resistance to physical and chemical instabilities under ambient conditions (34). Unfortunately, most organic crystals are generally imperfect, containing different types of defects in the structure of the crystal lattice (4). The defective regions in a crystal introduce disorder into what is otherwise an ordered system, and correspond to sites with higher levels of energy in the solid (55). In many cases, defects can eventually lead to the formation of glass or amorphous (supercooled liquid) materials. Defects are typically formed through kinetic processes, for example, milling or dehydration, as opposed to thermodynamic processes. Whereas defects can offten be reversed, the formation of amorphous material creates a different solid state that can agglomerate or recrystallize into a different crystalline form. Pharmaceutical interest in the study of defects arises from the demonstrated role that these high energy sites can play in affecting a number of important physical and chemical phenomena. The presence of defects can, for example, produce higher dissolution rates (56, 57), greater chemical instability (58, 59), altered mechanical properties (60–62), and enhanced hygroscopicity (63, 64).

XRPD combined with computational methods can be used to study crystalline defects (4, 15), even quantitate kinetic disorder parameters (e.g., crystal strain). Random defects within a crystal structure will generate diffuse X-ray scattering similar to X-ray amorphous scattering, though with halo positions and widths that are typically different from those measured from the amorphous (supercooled liquid) phase (15). This rule can be broken when defects in the material form a kinetic glass but it is possible to monitor the agglomeration of defects starting with perfect crystals all the way through glass, using XRPD. Such a study was reported in Reference (15) and is summarized below as an example application of XRPD to the study of crystalline defects.

In this study, defects were introduced into Raffinose pentahydrate through dehydration over time. XRPD measurements were taken at regular time intervals, Fig. 13, to monitor per cent crystallinity (65) and total diffraction methodology was used to model both the coherent long range crystalline contributions and incoherent short range disorder components together as a single system (66, 67). Rietveld methods were used for structure modeling (68, 69) and to track the structural phase changes in crystalline material. In addition, methods built around the use of the Pair Distribution Function (PDF) (8, 11, 70–75), $G(r)$ in Eq. 3, were employed to confirm the Rietveld results. Finally, it was shown that the introduction of defects through
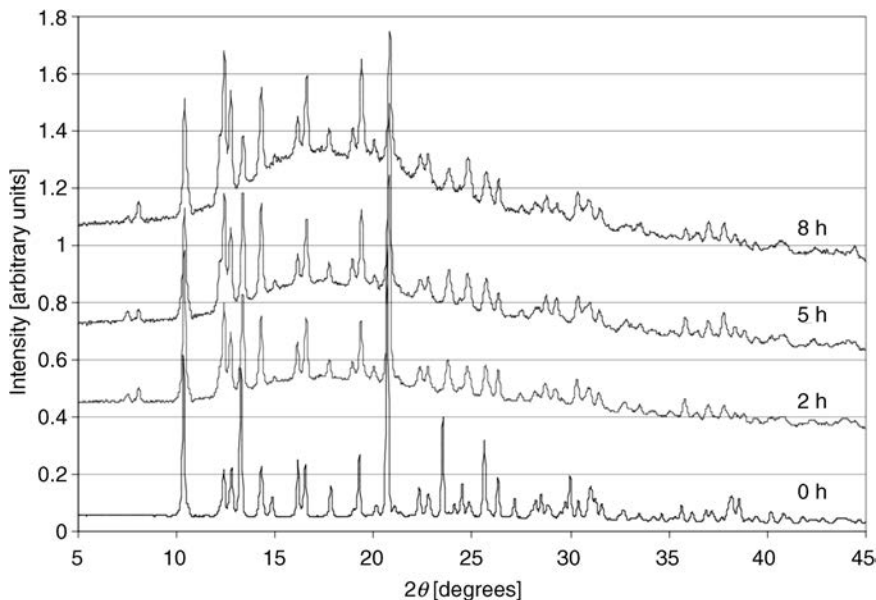
FIGURE 13   XRPD patterns collected in transmission mode for raffinose pentahydrate dried at 60° C under vacuum for (from bottom to top): 0, 2, 5, and 8 h, respectively.

dehydration of an organic crystal hydrate eventually leads to the formation of amorphous material.

$$G(r) = 4\pi r[\rho(r) - \rho_0] \tag{3}$$

Where ρ_0 is the average number density of the structure and $\rho(r)$ is the atom pair density for X-ray scattering (76) (Eq. 4).

$$\rho(r) = \left(\frac{1}{4}\pi r^2\right) \sum_{p,q} \left(\frac{f_p f_q}{\langle f \rangle^2}\right) \delta(r - r_{pq}) \tag{4}$$

The terms in Eq. 4 include $f_{p,q}$, the individual atomic form factors; $\langle f \rangle$, the mean atomic form factor of the structure; and the distance r_{pq}, corresponding to the atom pair separation. $\rho(r)$ represents the probability of finding an atom pair separated by the distance r, weighted by the atomic form factors and averaged over all atom pairs in the structure. The calculation needs to be evaluated over a crystal structure large enough to give the atom pair relationships for a distance of interest.

The PDF is a generally useful computational tool when analyzing X-ray amorphous or disordered systems. PDF analysis unlocks information present (but not obvious) in XRPD patterns, providing a measure of inter-atomic distances that define a solid form (70). From these distances, one can draw conclusions regarding the relationship between ordered and disordered forms of a material. By convention (71),
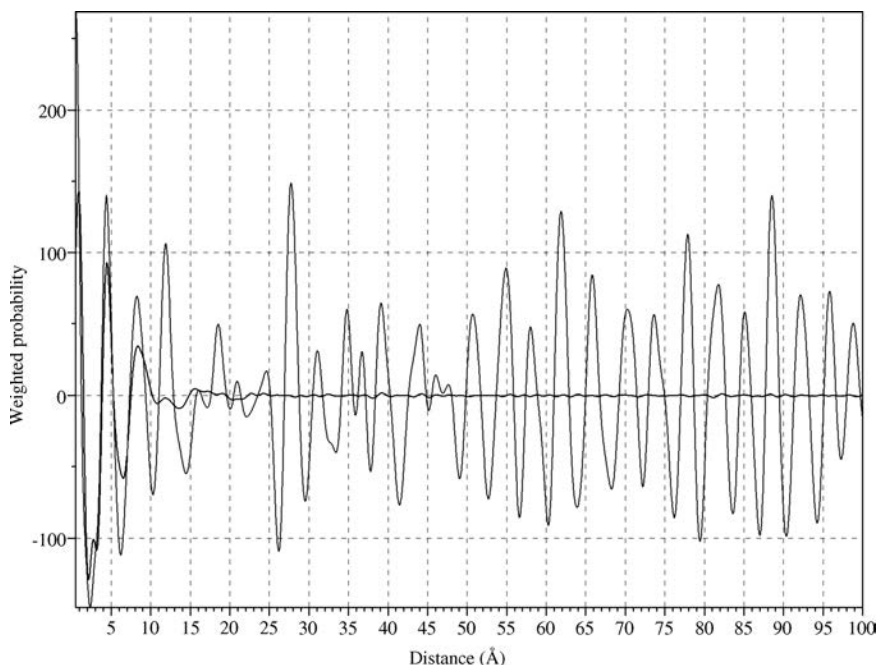
FIGURE 14   *PDF traces of crystalline (lighter, with many peaks) and amorphous (darker, with few initial peaks) felodipine. The crystalline sample shows long-range order as evidenced by peaks in the PDF up to and exceeding 100 Å. The amorphous sample shows only short-range order with PDF peaks disappearing after approximately 20 Å. Note that both samples have similar short-range order with peaks in the PDF overlapping below 10 Å.*

the PDF trace is typically plotted as distance (in Å) vs. (weighted) probability of finding two atoms with that separation. Peaks in the PDF correspond to inter-atomic distances that are common to the material in question, with the product of the peak area and distance giving the number of atom units with that specific separation. Figure 14 illustrates a PDF trace of amorphous felodipine superimposed against a PDF trace of crystalline felodipine. Both traces show similar short-range order (below 10 Å) but whereas the amorphous trace has no peaks in the PDF trace above approximately 20 Å (and therefore no long-range order), the crystalline trace contains peaks up to and exceeding 100 Å (indicating long-range order). Differences between defective crystalline (X-ray amorphous) and amorphous (supercooled liquid) materials can be seen in the PDFs calculated from XRPD data (15).

4.1.4   *Structural Analysis of Organic Amorphous Materials*   Amorphous organic solids, also referred to as disordered systems (77, 78), are characterized by a lack of long-range order that is observed in crystalline structures (2). They are often described as supercooled liquids, turned solid by the removal of thermal energy or a solvent without inducing crystallization (65, 78). Many of the early stage drug candidates currently under development exhibit very poor aqueous solubility (2, 79).

Higher molecular weights than were common in the past and greater hydrophobicity are thought to contribute to the decrease in aqueous solubility of organic compounds. With data to suggest that the dissolution rate is the rate-limiting step in oral absorption, it is expected that reduced solubility will lead to reduced oral bioavailability (80).

Amorphous organic compounds tend to have significantly higher initial aqueous solubilities (non-equilibrium) and dissolution rates as well as greater compressibility and different hygroscopicity, as compared to crystalline forms of the same compound (65, 81). Therefore, in compounds where the crystalline forms are poorly soluble, the amorphous form often presents an attractive formulation option (82). Dozens of APIs and excipients currently on the market are listed as being amorphous (65). Because crystalline forms are more thermodynamically stable than amorphous forms, there is a driving force for crystallizing the amorphous state. Therefore, amorphous materials are inherently unstable (both physically and chemically) and, once crystallized, the material loses the solubility advantage provided by the amorphous form. The inherent instability coupled with a lack of developed characterization tools has limited the commercial potential of working with amorphous materials at present (65, 83).

A common method used by formulation scientists to overcome the instabilities associated with amorphous materials is to prepare a composition of the amorphous API with pharmaceutically acceptable excipients that provide a barrier to crystallization of an amorphous drug product upon storage. Such compositions are often referred to as "dispersions" or "solid dispersions." Stabilizers are often selected from a variety of polymers, a commonly used one being polyvinylpyrrolidone (PVP). Intimate mixing (mixing at the molecular level) between such excipients and the amorphous API is an important factor in compositions resistant to crystallization (84). To provide a barrier to structural changes, the excipient needs to be intimately mixed (e.g., in a solution) with the API, which is often difficult to accomplish or even identify.

As noted earlier, XRPD is a useful technique in the analysis of amorphous materials. In its simplest application, XRPD is used to identify X-ray amorphous materials and classify them separately from crystalline materials (18). It can also be used to further differentiate between (supercooled liquid) amorphous material and kinetic glassy material (15, 85) or to monitor the conversion of crystalline material into amorphous material upon processing (e.g., grinding) (85) (Fig. 15). In the latter application, note the steady peak broadening and loss of intensity at higher angles in the XRPD patterns, Fig. 15, as the material becomes progressively disordered. However, some materials may immediately collapse into a binary amorphous-crystalline mixture and eventually pure amorphous material, without any broadening of the crystalline peaks that would be indicative of disorder in the crystalline phase (85).

Finally, in the analysis of multi-component amorphous mixtures, XRPD along with computational methods (16) have emerged as techniques that can be used to identify the so-called "miscible" dispersions, as compared to the phase separated physical mixtures where intimate mixing was not achieved. XRPD is often accom-
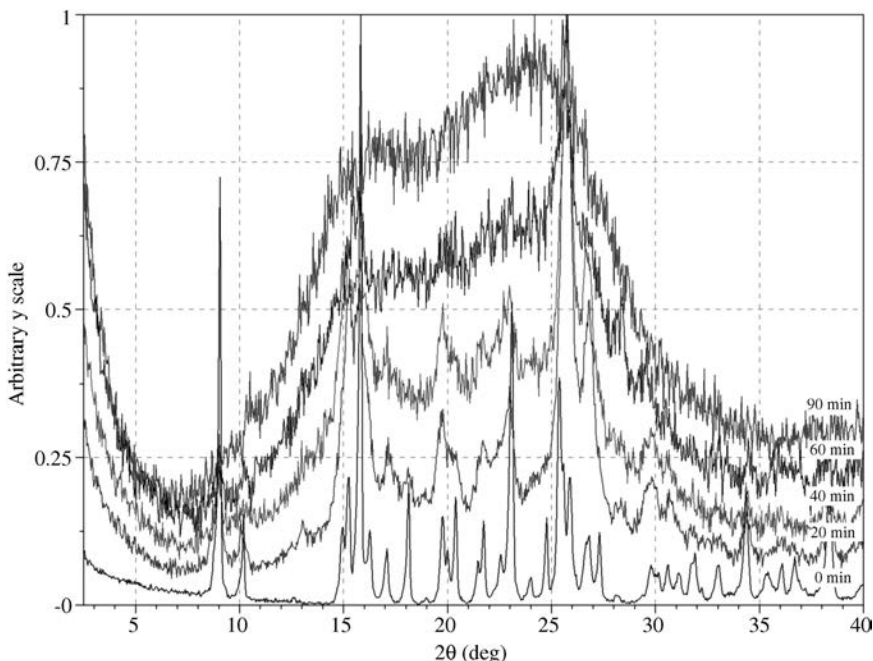
FIGURE 15   *Monitoring of cryo-grinding experiments on piroxicam form II using XRPD. Bottom-to-top, starting pattern, after 20, 40, 60, 90 min of grinding, respectively.*

panied by the use of complementary experimental techniques in this type of amorphous mixture analysis. Traditionally, thermal methods such as DSC have been used to measure glass transition temperatures when evaluating miscibility (86) and, while those methods have been shown to have limitations (16), their use is still recommended when analyzing amorphous mixtures (in addition to XRPD).

An example of this type of XRPD and computational analysis was reported in Reference (16). Solid dispersions of three different systems were analyzed initially using thermal measurements. Glass transition temperatures were identified from thermal data. For the system where two glass transition temperatures were identified, phase separation was indicated. The other two systems had a single glass transition temperature, suggesting miscibility and therefore stability to crystallization. XRPD data were collected on all three systems and the patterns were then analyzed using computational methods. Linear combinations of measured XRPD patterns and calculated PDFs were used to model the systems to determine the level of interaction between the two components in each system. The conclusions derived from thermal data were confirmed by XRPD for two of the three systems. However, the third system was identified as a so-called nano-suspension with domain sizes smaller than the resolution of thermal methods. Therefore, a prediction was made that this system is in fact phase separated despite the single glass transition temperature, and would re-crystallize. This prediction was confirmed elsewhere in the literature (87).
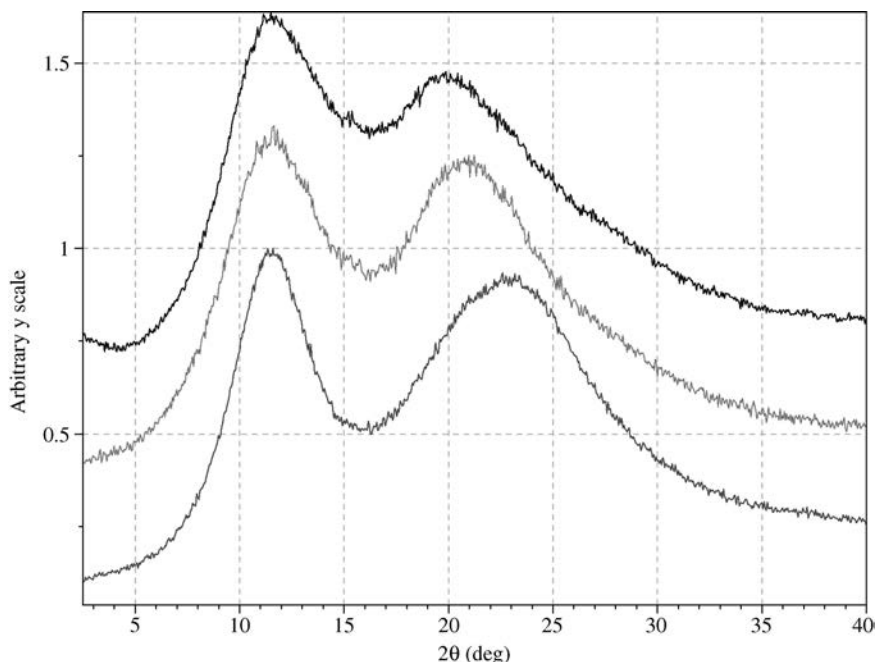
FIGURE 16   *XRPD patterns of, top-to-bottom, amorphous PVP, a solid dispersion of PVP and felodipine (70% PVP, 30% felodipine by weight), and amorphous felodipine.*

Figure 16 shows example XRPD patterns of a pharmaceutically acceptable excipient (PVP, top pattern), amorphous drug product (felodipine, bottom pattern), and a solid dispersion of the two (70% PVP and 30% felodipine by weight, middle pattern). Despite the lack of long-range order (and therefore crystalline peaks), one can observe clear differences in the structure of these amorphous materials from these XRPD patterns, using the position and width of the two broad halos in each pattern. For example, the second halo in the dispersion is located in between the second halos for the excipient and the drug product, suggesting it is a mixture of the two materials. Additional computational analysis could be applied (16) to determine the level of miscibility of the two components in the dispersion.

4.1.5   Characterization of Multi-Component Mixtures   A common application for X-ray powder diffraction is in the characterization of multi-component mixtures. The technique is highly effective when used for this application provided the materials are structurally different (88) and fall within the limit of detection of XRPD. With good laboratory instrumentation and sample preparation methods and typical counting times, the limit of detection for XRPD can be on the order of 2–3% by weight, or even lower when detecting the presence of crystalline materials in an amorphous-crystalline mixture. In multi-component crystalline mixtures the limit of detection can become significantly worse, especially if the component being detected has no unique peaks as compared to

the other components in the mixture. The detection of low levels of amorphous material mixed with a predominately crystalline sample can be difficult and is a subject of ongoing research (65). XRPD can also be used to quantify the amount of (crystalline or amorphous) component in the mixture as the diffracted intensity in the pattern is related to the weight percentage of the component in the mixture.

4.1.5.1 Characterization of Crystalline Mixtures (Quantitative Analysis) Quantitative analysis of crystalline mixtures typically refers to the determination of the relative amounts of different phases in a sample containing multiple phases (i.e., in a mixture), using experimental XRPD data. In broad terms, quantitative methods can be separated into those requiring the use of internal or external standards and ones based around the use of the full diffraction pattern (5,11, 14, 89, 90). The application of standards to this problem is not new, dating back to the 1930s (91). When using standards, it is essential to work with a randomly oriented fine powder specimen to avoid problems with preferred orientation or poor particle statistics and to be confident that the sample is representative of the material being analyzed (5, 14). In addition, there are a number of structure, instrument, and measurement-sensitive factors (14) that affect quantitative analysis.

The internal standard method (92, 93) (also called the RIR method, for reference intensity ratio) is the most general and the most commonly used of any XRPD quantitative phase analysis methods in the past. It requires that a known weight percentage of a standard material be homogeneously mixed with the sample whose phase composition one is trying to determine. The method is based on dividing the intensity of a line (peak) of the phase whose ratio in the composition is being determined by the intensity of the line for the internal standard used. As such, it is important to choose an internal standard that has peaks that do not overlap with any found in the mixture itself. Examples of standards include corundum, silicon, and SRM 676 (Al_2O_3) (5). The latter is particularly good at minimizing preferred orientation problems. For a detailed discussion on the RIR method see for example, (5, 14), in recent years it has been increasingly replaced by full pattern methods because of difficulties in ensuring random orientation of all components in the mixture.

The full pattern methods can be traced to quantitative work performed on cements in the 1960s (94–98). The same principles apply to pharmaceuticals with some modifications, the most important of which is the need to normalize the total diffracted intensity across different patterns before using the full pattern method. The simplest of such full pattern methods rely on fitting entire observed or calculated patterns of reference materials to an observed pattern of the mixture (5, 99). If not previously available, XRPD patterns of the reference (standard) materials must be first collected, meaning one must know the composition of the mixture beforehand. The references must be analyzed under the same conditions and instrumental settings as the mixture. When possible, the instrumental background and noise should be removed by data processing (100). Provided the same sample preparation techniques were used to

make the reference materials and the mixture(s), sample artifacts should not present as big a problem as for internal standard methods as the full pattern methods do not rely on single peaks. The weighted sum of the selected reference patterns is fit using least-squares minimization (e.g., (101)) to the unknown mixture. In this procedure, each point in the pattern is treated as an independent observation and a single weight is applied to each pattern, giving its ratio in the mixture. The best calculated fit is reported along with the weights used to obtain this pattern (5, 98, 99).

A second commonly used full pattern quantitative method is based on the use of the Rietveld method (5, 14, 102). In this method, the refinement is done by minimizing the sum of weighted, squared differences between measured and calculated intensities at every 2θ position in the pattern. The Rietveld method does require the knowledge of the crystal structure for every component (of interest) in the mixture. This method is applicable even in the presence of overlapping peak lines and is less sensitive to preferred orientation problems. However, the requirement to have at least approximate crystal structures of every component can be problematic for APIs under development. Some examples of Rietveld applications to quantitative analysis include (103–105). Freely available software, for example, TOPAS (106) or GSAS (107), can be used for Rietveld quantitative analysis.

Finally, novel quantitative approaches using full pattern fitting are still an active area of research. Recent example include References (89, 108).

4.1.5.2 Characterization of Crystalline-Amorphous Mixtures (Per cent Crystallinity)   Degree (or per cent) of crystallinity is perhaps the most common quantitative application of XRPD in the drug development process. When the amorphous phase is present or suspected, XRPD can be used to characterize the material and determine the ratio of crystalline to amorphous material in the sample. Most X-ray methods used for this purpose are based on total sample scattering (i.e., scattering from both the amorphous and crystalline phases). In addition, the total diffracted area in each measurement needs to be normalized between samples to account for example, weight or absorption differences across samples. Once the patterns are normalized, per cent crystallinity can be easily calculated as a fraction of crystalline content in the total diffracted intensity measured from a sample (109). Several methods exist to estimate the crystalline content in an XRPD pattern (65, 110):

   i. Measuring the integrated peak area under the crystalline peaks and dividing by the X-ray intensity scattered by the entire sample (65). This is a common approach that works well except when many overlapping crystalline peaks are present. Examples of this type of analysis can be found in, References (110–122).

   ii. Measuring the maximum intensity of a subset of characteristic peaks (109). This method can only be applied if all the samples are analyzed under the same conditions, there is no peak broadening due to disorder or particle size issues, and a reproducible ratio of intensity can be demonstrated for the chosen peaks across multiple samples. Typically, the use of internal standards is recommended for this method (65,109) to ensure the above conditions are met. Such

internal standards can include lithium fluoride, silicon metal powder, or zinc oxide. A variation on this method uses peak area rather than height (123). Examples of these types of studies include References (123–129).

iii. Quantification of the amorphous content using a region where no crystalline peaks appear in the mixture pattern (130). Since the diffraction in such regions is caused by short-range ordering of amorphous materials, it can be used to estimate the amorphous content present in the sample. The method may be more robust and sensitive than peak intensity measurements (110) though it is limited to mixtures where crystalline peaks are not present in the entire range of amorphous diffraction.

Other methods for the determination of per cent crystallinity have been reported in literature, for example, using specialized instrument optics (131). If both amorphous and crystalline reference patterns are available, full pattern quantitative or semi-quantitative methods used in crystalline mixture analysis can be applied here as well. Such an example is shown in Fig. 17. Physical mixtures of amorphous and crystalline sucrose were prepared with known weight ratios (0%, 20%, 40%, 60%, 80%, and 100% crystalline). The pure amorphous and pure crystalline patterns were then linearly fitted using Brent minimization (101) to each mixture. A single weight was used per reference pattern (applied to all intensity points) and the sum of squared differences at each intensity point was used as the error metric. All patterns were first
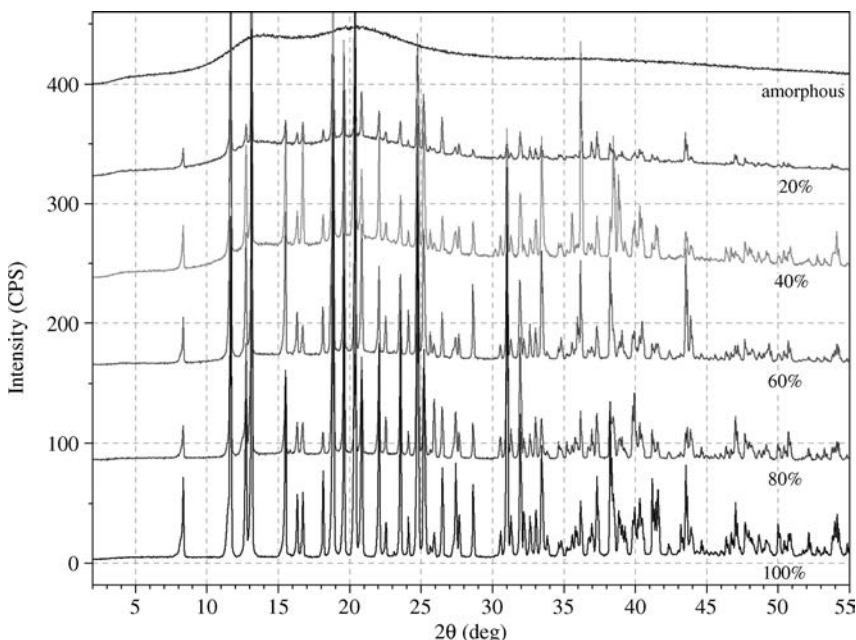

FIGURE 17 *XRPD quantitative analysis of physical mixtures of amorphous and crystalline sucrose. Top-to-bottom, amorphous sucrose, 20, 40, 60, 80 and 100% crystalline sucrose.*

normalized to same total diffracted intensity. The calculated per cent crystallinity values for the 20/40/60/80 mixtures were 17.2%, 40.7%, 64.4%, 84.3%, respectively. In practice, this approach coupled with good XRPD data consistently yields results within 5% of actual values for mixtures ranging from 10 to 90% crystalline.

4.1.5.3 Re-Crystallization of Amorphous Materials   XRPD can also be used to monitor re-crystallization of amorphous materials. A typical application of this kind would be to characterize the extent of crystallinity during processing steps (e.g., scale-up of bulk material, formulation, manufacturing) or simply upon storage over the intended shelf life of the drug product, to ensure safety and efficacy (132). As noted earlier, amorphous materials will have different performance than crystalline counterparts (65,133), including for example sensitivity to moisture (134–136), reduced chemical stability (113,126,137), postcompression hardness (112), and enhanced dissolution rate (81,138).

Figure 18 shows the monitoring of recrystallization of amorphous felodipine by XRPD over a 7 day period. The top pattern is pure amorphous felodipine, the remaining patterns were collected on the same sample stored under ambient conditions (25°C and 50% RH) after a period of 2, 3, 5, and 7 days, respectively. The aforementioned computational methods were used to determine per cent crystallinity in each pattern, with the first and last patterns used as reference amorphous and crystalline material, respectively. Given those assumptions, the pattern collected after
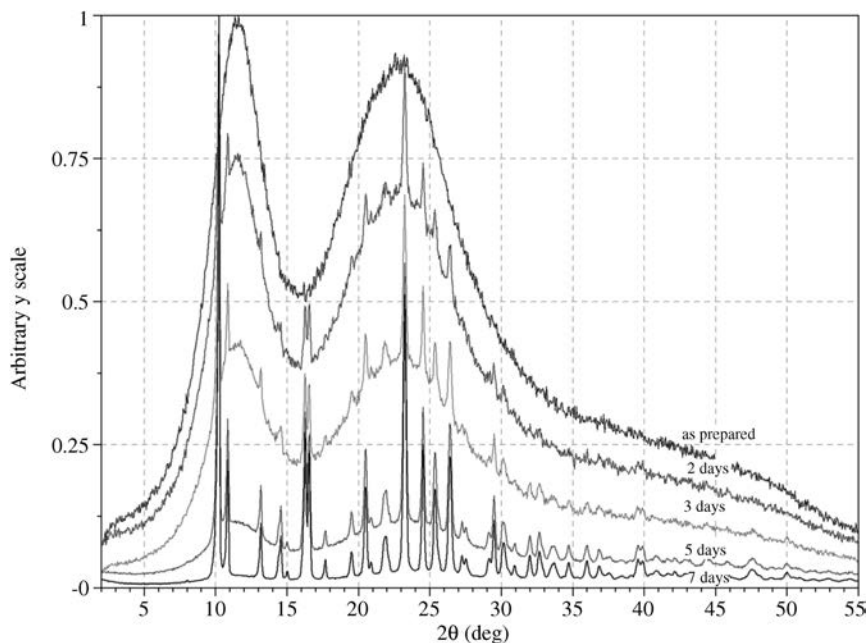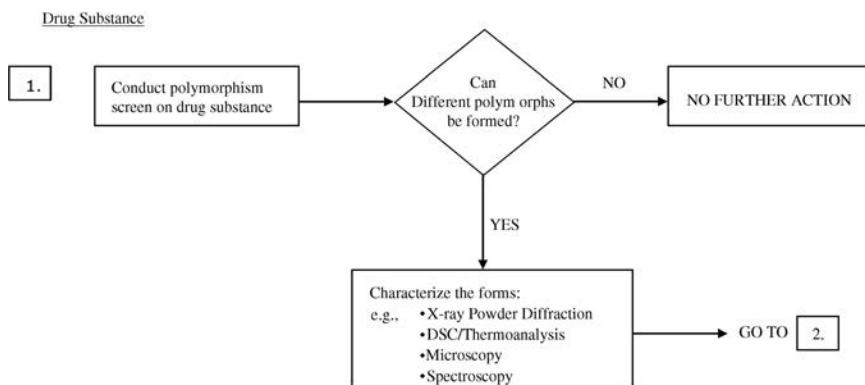

FIGURE 18   *Recrystallization of amorphous felodipine monitored by XRPD. Top-to-bottom, amorphous felodipine, same sample after 2, 3, 5, and 7 days in ambient conditions, respectivelly.*

2 days is approximately 5% crystalline, followed by 11% after 3 days and 45% after 5 days. After 7 days the sample is almost completely crystalline.

4.1.6 Regulatory Considerations   The Food and Drug Administration's (FDA) New Drug Application (NDA) guideline (139) states that "appropriate" analytical procedures should be used to detect polymorphic, solvated (including hydrated), or amorphous forms of a drug substance. Likewise, the guideline states that it is the applicant's responsibility to control the crystal form of the drug substance. If bioavailabilty is affected by the change in crystal form, the applicant must demonstrate the suitability of the control methods. This highlights the importance of controlling the crystal form of the drug substance and, as shown in previous sections, the use of XRPD can provide essential structural information on crystalline and amorphous forms of a drug substance.

The ICH Q6A document (139) provides clear guidelines on how X-ray information should be used in the NDA. As noted in the section on API characterization, XRPD is one of two broadly accepted methods of providing unequivocal proof of polymorphism by the regulatory authorities (20), the other being single crystal X-ray diffraction. Characterization of the API by X-ray and/or some other method is required by the NDA guidelines as different solid forms may have different properties (20,140). An often-cited example is ritonavir (141), whose amorphous form is up to 20 times more bioavailable than the crystalline form, and which crystallized into a new less soluble form after 2 years on the market. XRPD is directly mentioned in the ICH decision trees as part of the drug application process, Fig. 19 (140,142). Some NDA submissions include XRPD methods on the drug substance.

It is often necessary to establish a specification or test (e.g., XRPD or IR) to ensure that the proper drug form is manufactured. Failure to do so may result in the manufacture of different polymorphs with different properties, potentially altering the dosage form performance (as in the case of ritonavir). Regulatory authorities are aware of such challenges and expect the manufacturer to demonstrate control over the

FIGURE 19   *ICH Q6A decision tree directing characterization of the forms by X-ray powder diffraction (adapted by author from Reference (140)).*

crystalline or amorphous form in the manufacturing process. Production scale-up requires a process be developed that can reproducibly make the desired polymorph. Where mixtures of forms cannot be avoided, quantitative control (e.g., using XRPD as outlined earlier) is typically required to ensure that the ratios between forms are maintained. Furthermore, this requirement may extend beyond the manufacturing process and through the retest date of the drug substance and potentially throughout the shelf life of the product, which can be a difficult requirement if the forms interconvert. Quantitative XRPD techniques are typically validated by following the ICH Q2A and Q2B guidance (139). It is therefore advantageous to select the most stable solid polymorph for production, determined using a process called polymorph screening in which XRPD plays a major role as outlined earlier. (The use of the most stable form would ensure that there would be no conversion into other forms).

Certain USP monographs require the use of XRPD on the drug substance. One example is the carbamazepine monograph which states that the X-ray diffraction pattern conforms to that of USP carbamazepine RS, similarly determined (140). The exact method of certification used by the USP in the reference standard is not known. In addition, USP recommends the precision to use when comparing peak positions between different XRPD patterns, that is, a peak in one XRPD pattern that falls within the USP-specified range of a peak in the other pattern is to be considered the same. That precision has varied from 0.1 to 0.2 °2θ, depending on the year of USP issue (24).

XRPD has been identified as a unique tool for drug substance and/or product analysis that can directly contribute to FDA's "quality by design" initiative. In addition, this tool can help improve the time to market by providing information regarding the structure of the molecule early on in the development process. Finally, XRPD methods can be used to ensure the drug product and/or substance is consistent and has the same identity, purity, and potency (140).

4.2 API Identification

4.2.1 Analysis of a Drug Product   XRD is frequently applied to the analysis of a drug product. A simple XRD method used for this purpose might involve the following steps (140):

1. Determination of the XRD patterns of all solid components in the drug product.
2. Selection of a region or regions in 2θ where only the polymorph of interest (analyte) diffracts.
3. Preparation of reference physical mixtures containing all API forms as well as excipients.
4. Development of computational/mathematical methods.
5. Validation of the method following the ICH Q2A and Q2B methods.
6. Application of the method.

Chemometric (PLS) methods (143–146) may also be used to increase sensitivity and lower the detection limit. Such analytical XRD methods can have a variety of

applications ranging from online process monitoring to support in litigation of drug product counter-fitting.

One example of the above approach that also includes quantitative analysis of the active ingredient is the XRD method developed by Suryanarayanan (147). The method was applied to intact tablets and required preparation of mixtures containing various weight fractions of the drug and excipient. The quantitative analysis relied on identifying integrated intensities of several diffraction lines for each compound and calculating their ratios as a function of the weight loading of the drug in the tablet. The reported error for the method was less than 10% for a drug loading of 40% weight-in-tablet.

4.2.2 *Monitoring Effects of Processing and Manufacturing on the API* XRD has been used to study the effects of processing and manufacturing on the solid form of an API. Many of the previously mentioned XRPD methods used for API characterization can also be applied for this purpose.

For example, the antiviral drug MCC-478, known to exist in several anhydrous polymorphic forms as well as a hydrate, was studied in tablet formulation using XRD (148). The XRD patterns of the tablets containing the various forms of the MCC-478 revealed at least one peak unique to each form—generally a prerequisite for this type of work. A semi-quantitative method was developed to characterize the physical form of the API in intact film-coated tablets despite the relatively low weight loading of the API ($<20\%$) in the tablet that also contained a highly crystalline excipient, mannitol, in much greater proportion (60%). The use of this method confirmed that the aqueous film-coating process did not change the form of the API. Furthermore, the same method was used to verify that the API form remained stable (unchanged) over 6 months under accelerated aging conditions (40°C/75% RH). Therefore, the XRD method found application not only for process control during manufacturing, but also for the quality control of the final product.

With increased emphasis by regulatory authorities on understanding and controlling production processes, the implementation of online XRD methods as part of Process Analytical Technology (PAT) is gaining momentum (140). Production processes that are well understood and controlled are considered to be lower risk than those that have not been subject to PAT. It should be noted that spectroscopic methods (NIR, IR, Raman) are also frequently used to monitor polymorphic conversion during processing. Each method has its advantages and disadvantages but typically XRD methods are capable of analyzing the largest sample volume simultaneously and have been used extensively for this purpose in the cement, gypsum and catalyst industries.

An example application of XRD online monitoring was a study of polymorphic conversion during wet granulation (140,149). Wet granulation is a size enlargement process that uses a binder and water to form larger agglomerates, potentially causing phase transformations during the water addition step. Two enantiotropically related forms of flufenamic acid were monitored with a transition temperature of 42°C. XRD was able to identify the form present at various steps of the process.

Online XRD methods used to monitor crystallization of a drug substance have been the subject of extensive research (e.g., Reference (150)). Online processing cells have

been developed for the examination of temperature-dependant polymorphic changes in pharmaceutical materials using *in situ* XRD. Such cells can recirculate the crystallizing solution and monitor the changes by XRD.

4.2.3   Intellectual Property Considerations   XRPD is frequently used to identify and/or characterize new materials in patent application filings. Typically, a list of XRPD peak positions is provided, listing 2θ and/or *d*-space position and relative (to maximum) intensity of crystalline peaks. Estimated experimental errors in position (2θ and/or *d*-space) may be provided, often adopted from the USP (24). It is important to remember that aforementioned instrumental and sample artifacts can and do affect peak positions and intensities. Therefore, providing strict limits on peak positions or relying on intensity information in patent claims yields data that are too narrowly defined. A skilled patent practitioner should therefore be consulted on how best to incorporate solid-state data into a patent application.

The XRPD peak listings may include a list of all observed peaks that can be visually identified above the noise level in the pattern (typically determined through an intensity threshold). However, since it is unlikely that all such peaks will be reproduced in every XRPD pattern of the material, a subset of low angle, non-overlapping peaks with strong intensity (10% or more of maximum observed peak intensity) may be included as peaks "representative" of the material. In this case, it is helpful to have access to XRPD data collected on more than one type of diffractometer geometry in order to assess the reproducibility of peak intensities, which can frequently be affected by for example, preferred orientation and poor particle statistics in a sample.

Where materials exhibit polymorphism and multiple forms are found, it is typical to provide a listing of characteristic (unique) peaks that differentiate one form of a material from all the other known forms of the same material. For different salts or co-crystals where the material can be differentiated chemically, this consideration may be less important but it still applies to polymorphs of a given salt/cocrystal.

REFERENCES

1. Wunderlich B. A classification of molecules and transitions as recognized by thermal analysis. Thermochim Acta 1999; 340/41: 37–52.
2. Yu L. Amorphous pharmaceutical solids: preparation, characterization and stabilization. Adv Drug Deliv Rev 2001; 48: 27–42.
3. Sakurai JJ. Modern quantum mechanics. Reading, MA: Addison Wesley; 1994.
4. Cowley JM. Diffraction physics. 2nd revised edition. Amsterdam: Elsevier Science; 1990.
5. Bish DL, Post JE.In: Ribbe PH, editor. Modern powder diffraction. Reviews in mineralogy. Vol. 20. Washington, DC: Mineralogical Society of America; 1989.
6. Cowley, JM. International Tables for X-ray Crystallography, Vol. C, Part 4.3., pp. 259–429, International Union of Crystallography, ISBN 978-1-4020-4969-9.

7. James RW. The optical principles of the diffraction X-rays. Ithaca, NY: Cornell University Press; 1965.

8. Warren BE. X-ray diffraction. New York: Dover Publications; 1990.

9. de Wolff PM, Taylor JM, Parrish W. Experimental study of effects of crystallite size statistics on X-ray diffractometer intensities. J Appl Phys 1959; 30: 63–69.

10. Parrish W, Huang TC. Accuracy and precision of intensities in X-ray polycrystalline diffraction. Adv X-ray Anal 1983; 26: 35–44.

11. Klug HP, Alexander LE. X-ray diffraction procedures for polycrystalline and amorphous materials. New York: Wiley; 1974.

12. Smith DK, Barett CS. Special handling problems in X-ray diffractometry. Adv X-ray Anal 1979; 22: 1–12.

13. Bunge HJ. Texture analysis in material science. 2nd ed. Gottingen: Cuvillier Verlag; 1993.

14. Jenkins R, Snyder RL. Introduction to X-ray powder diffractometry. In: Winefordner JD, editor. Chemical analysis. Vol. 138. New York: John Wiley & Sons; 1996.

15. Bates S, Kelly R, Ivanisevic I, Shields P, Zografi G, Newman A. Assessment of defects and amorphous structure produced in raffinose pentahydrate upon dehydration. J Pharm Sci 2007; 96 (5): 1418–1433.

16. Newman A, Engers D, Bates S, Ivanisevic I, Kelly R, Zografi G. Characterization of API: polymer mixtures using X-ray powder diffraction. J Pharm Sci 2008; 97 (11): 4840.

17. Billinge SJL, Kanatzidis MG. Beyond crystallography: the study of disorder, nanocrystallinity and crystallographically challenged materials using pairwise distribution functions. Chem Commun 2004; 749–760.

18. Ivanisevic I, Bugay DE, Bates S. On pattern matching of X-ray powder diffraction data. J Phys Chem B 2005; 109 (16): 7781–7787.

19. Bergese P, Bontempi E., Colombo I, Depero LE. Micro X-ray diffraction on capillary powder samples: a novel and effective technique for overcoming preferred orientation. J Appl Cryst 2001; 34: 663–665.

20. *Guidance for Industry: ANDAs: Pharmaceutical Solid Polymorphism Chemistry, Manufacturing, and Controls Information*. U.S. Department of Health and Human Services Food and Drug Administration Center for Drug Evaluation and Research (CDER); 2007.

21. Brittain H. Polymorphism in pharmaceutical solids. New York: Marcel Dekker, Inc; 1999.

22. Varshney DB, Kumar S, Shalaev EY, Kang S-W, Gatlin LA, Suryanarayanan R. Solute crystallization in frozen systems–use of synchrotron radiation to improve sensitivity. Pharm Res 2006; 23 (10): 2368–2374.

23. Blagden N, Davey R, Song M, Quayle M, Clark S, Taylor D, Nield A. A novel batch cooling crystallizer for in situ monitoring of solution crystallization using energy dispersive X-ray diffraction. Cryst. Growth Des 2002; 3 (2): 197–201.

24. United States Pharmacopeia. X-ray diffraction. Natl Formulary 2008; 31 (26): 374.

25. Hertzberg RP, Pope AJ. High-throughput screening: new technology for the 21st century. Curr Opin Chem Biol 2000; 4: 445–451.

26. Barberis A. Cell-based high-throughput screens for drug discovery. Eur Biopharm Rev 2002; (Winter).

27. Johnston PA. Cellular platforms for HTS: three case studies. Drug Discov Today 2002; 7: 353–363.

28. Marquart RG. Katsnelson I, Milne GWA, Heller SR, Jnr GGJ, Jenkins R. A search-match system for X-ray powder diffraction data. J. Appl. Cryst. 1979; 12 (6): 629–634.

29. Gurley K, Kijewski T, Kareem A. First- and higher-order correlation detection using wavelet transforms. J Engr Mech 2003; 129 (2): 188–201.

30. Gilmore CJ, Barr G, Paisley J. High-throughput powder diffraction. I. A new approach to qualitative and quantitative powder diffraction pattern analysis using full pattern profiles. J Appl Cryst 2004; 37: 231–242.

31. Johnson SC. Hierarchical clustering schemes. Psychometrika 1967; 2: 241–254.

32. Borgatti SP. How to explain hierarchical clustering. Connections 1994; 17 (2): 78–80.

33. Hanawalt JD, Rinn HW, Frevel LK. Chemical analysis by X-ray diffraction-classification and use of X-ray diffraction patterns. Ind Eng Chem, Anal Ed 1938; 10: 457–512.

34. Byrn SR, Pfeiffer RR, Stowell JG. Solid-state chemistry of drugs. 2nd ed. West Lafayette, IN: SSCI Inc; 1999.

35. Massa W. Crystal structure determination. 2nd ed. Berlin: Springer; 2004.

36. Visser JW. A fully automatic program for finding the unit cell from powder data. J Appl Cryst 1969; 2: 89–95.

37. Werner P-E, Eriksson L, Wetdahl M. TREOR, a semi-exhaustive trial-and-error powder indexing program for all symmetries. J Appl Cryst 1985; 18: 367–370.

38. Altomare A, Giacovazzo C, Guagliardi A, Moliterni AGG, Rizzi R, Werner P-E. New techniques for indexing: N-TREOR in EXPO. J Appl Cryst 2000; 33: 1180–1186.

39. Coelho AA. Indexing of powder diffraction patterns by iterative use of singular value decomposition. J Appl Cryst 2003; 36: 86–95.

40. Neumann MA. X-cell: a novel indexing algorithm for routine tasks and difficult cases. J Appl Cryst 2003; 36: 356–365.

41. Boultif A, Louer D. Powder pattern indexing with the dichotomy method. J Appl Cryst 2004; 37: 724–731.

42. Mighell AD. Lattice metric singularities and their impact on the indexing of powder patterns. Powder Diffr 2000; 15 (2): 82–85.

43. Wilson AJC. Determination of absolute from relative X-ray intensity data. Nature 1942; 150: 151–152.

44. Looijenga-Vos A, Buerger MJ. International tables for crystallography. Vol. A. 5th ed. International Union of Crystallography; 2005. ISBN 978-1-4020-4969-9 (Online tables).

45. Rietveld HM. Line profiles of neutron powder-diffraction peaks for structure refinement. Acta Crystallogr 1967; 22: 151–152.

46. Rietveld HM. The early days: a retrospective view (Chapter 2). In: Young RA,editor. The rietveld method. Oxford, UK: Oxford University Press; 1993.

47. http://www.ccp14.ac.uk/solution/rietveld_software/index.html.

48. Lewis J, Schwarzenbach D, Flack HD. Electric field gradients and charge density in corundum, alpha-Al2O3. Acta Crystallogr 1982; A38: 733–739.

49. Taylor JC. Rietveld made easy: a practical guide to the understanding of the method and successful phase quantifications. Canberra: Sietronics Pty Ltd; 2001.

50. McCusker LB, Von Dreele RB, Cox DE, Louër D, Scardi P. Rietveld refinement guidelines. J Appl Cryst 1999; 32: 36–50.

51. Schields PJ, Bates S, McClurg RB, Gendron C. Comparison of simulated and experimental XRPD patterns of silver with twin faults using MAUD and DIFFaX. Adv X-ray anal 2008; 51: D076.

52. Will G. Powder diffraction: the Rietveld method and the two stage method to determine and refine crystal structures from powder diffraction data. Berlin, Heidelberg: Springer; 2006.

53. Berman HM, Jeffrey GA, Rosenstein RD. The crystal structures of the alpha and beta forms of D-mannitol. Acta Crystallogr 1968; B24 (3): 442–449.

54. Botez CE. Stephens PW, Nunes C, Suryanarayan R. Crystal structure of anhydrous delta-D-mannitol. Powder Diffr 2003; 18 (3): 214–218.

55. Zhang J. Ebbens S, Chen X, Jin Z, Luk S, Madden C, Patel N. Roberts C. Determination of surface free energy of crystalline and amorphous lactose by atomic force microscopy adhesion measurement. Pharm Res 2006; 23 (2): 401–407.

56. Burt HM, Mitchell AG. Crystal defects and dissolution. Int J Pharm 1981; 9: 137–152.

57. Prasad KVR, Ristic RI, Sheen DB, Sherwood JN. Dissolution kinetics of paracetamol single crystals. Int J Pharm 2002; 238 (1–2): 29–41.

58. Huttenrauch R, Fricke S, Zielke P. Mechanical activation of pharmaceutical systems. Pharm Res 1985; 2 (6): 302–306.

59. Shalaev E, Shalaeva M, Zografi G. The effect of disorder on the chemical reactivity of an organic solid, tetraglycine methyl ester: change of the reaction mechanism. J Pharm Sci 2002; 91 (2): 584–593.

60. Hiestand E, Smith DP. Indices of tableting performance. Powder Tech 1984; 38: 145–159.

61. Wildfong PLD, Hancock BC, Moore MD, Morris KR. Towards an understanding of the structurally based potential for mechanically activated disordering of small molecule organic crystals. J Pharm Sci 2006; 95 (12): 2645–2656.

62. Huttenrauch R, Keiner I. Rekristallisation aktivierter feststoffe beim verpressen. Pharmazie 1977; 32: 129–130.

63. Huttenrauch R. Abhangigkeit der hygroscopizitat von der kristallinitat. Pharmazie 1977; 32: 240–244.

64. Ahlneck C, Zografi G. The molecular basis of moisture effects on the physical and chemical stability of drugs in the solid state. Int J Pharm 1990; 62: 87–95.

65. Shah B, Kakumanu VK, Bansal AK. Analytical techniques for quantification of amorphous/crystalline phases in pharmaceutical solids. J Pharm Sci 2006; 95 (8): 1641–1665.

66. Wellberry TR, Butler BD. Interpretation of diffuse X-ray scattering via models of disorder. J Appl Cryst 1994; 27 (3): 205–231.

67. Keen DA, Dove MT. Total scattering studies of silica polymorphs: similarities in glass and disordered crystalline local structures. Mineral Mag 2000; 64 (3): 447–455.

68. Ferrari M, Lutterotti L. Method for the simultaneous determination of anisotropic residual stresses and texture by X-ray diffraction. J Appl Phys 1994; 76 (11): 7246–7255.

69. Matthies S, Lutterotti L, Wenk HR. Advances in texture analysis from diffraction spectra. J Appl Cryst 1997; 30: 31–42.

70. Billinge SJL, Thorpe MF. Local structure from diffraction. New York: Plenum Press; 1998.

71. Debye P. Scattering from noncrystalline substances. Ann Phys 1915; 46: 809–823.

72. Proffen T. Analysis of occupational and displacive disorder using atomic pair distribution function: a systematic investigation. Z Kristallogr 2000; 215: 1–8.

73. Proffen T, Billinge SJL, Egami T, Louca D. Structural analysis of complex materials using the atomic pair distribution function—a practical guide. Z Kristallogr 2003; 218: 132–143.

74. Bishop M, Bruin C. The pair correlation function: a probe of molecular order. Am J Phys 1984; 52 (12): 1106–1108.

75. Guinier A. X-ray diffraction in crystals, imperfect crystals, and amorphous bodies. New York: Dover Publications; 1994.

76. Peterson PF. Bozin ES, Proffen T, Billinge SJL. Improved measures of quality for the atomic pair distribution function. J Appl Cryst 2003; 36: 53–64.

77. Kauzmann W. The nature of the glassy state and the behavior of liquids at low temperatures. Chem Rev 1948; 43: 219–256.

78. Hancock BC. Disordered drug delivery: destiny, dynamics and the deborah number. J Pharm Pharmacol 2002; 54: 737–746.

79. Angell CA. The old problems of glass and the glass transition, and the many new twists. Proc Natl Acad Sci USA 1995; 92: 6675–6682.

80. Yalkowsky SH. Solubility and solubilization in aqueous media. Oxford: Oxford University Press; 1999.

81. Hancock BC, Parks M. What is the true solubility advantage for amorphous solids? Pharm Res 2000; 17 (4): 397–404.

82. Pouton CW. Formulation of poorly water-soluble drugs for oral administration: physicochemical and physiological issues and the lipid formulation classification system. Eur J Pharm Sci 2006; 29 (3–4): 278–287.

83. Kaushal AM, Gupta P, Bansal AK. Amorphous drug delivery systems: molecular aspects, design and performance. Crit Rev Ther Drug Carrier Syst 2004; 21: 133–193.

84. Serajuddin ATM. Solid dispersion of poorly water soluble drugs: early promises, subsequent problems, and recent breakthroughs. J Pharm Sci 1999; 88 (10): 1058–1066.

85. Bates S, Zografi G, Engers D, Morris K, Crowley K, Newman A. Analysis of amorphous and nanocrystalline solids from their X-Ray diffraction patterns. Pharm Res 2006; 23 (10): 2333–2348.

86. Taylor LS, Zografi G. Spectroscopic characterization of interactions between PVP and indomethacin in amorphous molecular dispersions. Pharm Res 1997; 14 (12): 1691–1698.

87. Vasanthavada M, Tong W.-Q, Joshi Y, Kislalioglu MSS. Phase behavior of amorphous molecular dispersions I: determination of the degree and mechanism of solid solubility. Pharm Res 2004; 21 (9): 1598–1606.

88. Cincic D, Friscic T, Jones W. Isostructural materials achieved by using structurally equivalent donors and acceptors in halogen-bonded cocrystals. Chem Eur J 2008; 14: 747–753.

89. Dong W, Gilmore CJ, Barr G, Dallman C, Feeder N, Terry S. A quick method for the quantitative analysis of mixtures. I. Powder X-ray diffraction. J Pharm Sci 2008; 97 (6): 2260–2276.

90. Zevin LS, Kimmel G. Quantitative X-ray diffracometry. New York: Springer-Verlag; 1995.

91. Clark GL, Reynolds DH. Quantitative analysis of mine dusts. Ind Eng Chem, Anal Ed 1936; 8: 36–42.

92. Chung FH. Quantitative interpretation of X-ray diffraction patterns. I. Matrix-flushing method of quantitative multicomponent analysis. J Appl Cryst 1974; 7: 519–525.

93. Chung FH. Quantitative interpretation of X-ray diffraction patterns. II. Adiabatic principle of X-ray diffraction analysis of mixtures. J Appl Cryst 1974; 7: 526–531.

94. Berger RL, Frohnsdorff GJC, Harris PH, Johnson PD. Application of X-Ray diffraction to routine mineralogical analysis of portland cement. *Highway Research Board Special Report*, Vol. 90; 1966. p 234–253.

95. Ballantyne C.M. Quantitative automatic determination of cement compound composition using X-ray diffraction techniques. *Cement and Concrete Association Report*, 1968.

96. Gutteridge WA. Quantitative X-ray powder diffraction in the study of some cementitive materials. Br Ceram Proc 1984; 35: 11–23.

97. Smith DK, Johnson GG, Wims AM. Use of full diffraction spectra. Both experimental and calculated in quantitative powder diffraction analysis. Aust J Phys 1988; 41: 311–321.

98. Stutzman PE, Pattern fitting for quantitative X-ray powder diffraction analysis of portland cement and clinker. In: 18th international conference on cement microscopy. Houston, TX: International Cement Microscopy Association; 1996.

99. Smith DK, Scheible A, Wims AM, Johnson JL, Ullmann G. Quantitative X-ray powder diffraction method using the full diffraction pattern. Powder Diffr 1987; 2: 73–77.

100. Savitzky A, Golay MJE. Smoothing and differentiation of data by simplified least squares procedures. Anal Chem 1964; 36: 1627–1639.

101. Brent RP. Algorithms for minimization without derivatives. Englewood Cliffs, NJ: Prentice-Hall; 1973.

102. Rietveld HM. A profile refinement method for nuclear and magnetic structures. J Appl Cryst 1969; 2: 65–71.

103. Hill RJ, Howard CJ. Quantitative phase analysis from neutron powder diffraction data using the Rietveld method. J Appl Cryst 1987; 20: 467–474.

104. Bish DL, Chipera SJ. Problems and solutions in quantitative analysis of complex mixtures by X-ray powder diffraction. Adv X-ray Anal 1988; 31: 295–308.

105. Bish DL, Howard SA. Quantitative phase analysis using the Rietveld method. J Appl Cryst 1988; 21: 86–91.

106. Coelho AA. TOPAS user manual. Karlsruhe, Germany: Bruker AXS GmbH; 2003.

107. Larson AC, Von Dreele RB.General Structure Analysis System (GSAS), Los Alamos National Laboratory LAUR, Vol. 86; 2000. p 748.

108. Chipera SJ, Bish DL. FULLPAT: a full-pattern quantitative analysis program for X-ray powder diffraction using measured and calculated patterns. J Appl Cryst 2002; 35 (6): 744–749.

109. Suryanarayan R. X-ray powder diffractometry. In: Brittain HG,editor. Physical characterization of pharmaceutical solids. New York: Marcel Dekker Inc; 1995. p 187–221.

110. Byard SJ. Jackson SL, Smail A, Bauer M, Apperly DC. Studies on the crystallinity of a pharmaceutical development drug substance. J Pharm Sci 2005; 94 (6): 1321–1335.

111. Matsunaga Y, Bando N, Yuasa H, Kanaya Y. Effects of grinding and tabletting on physicochemical stability of an anticancer drug, TAT-59. Chem Pharm Bull 1996; 44: 1931–1934.

112. Nakai Y, Yamamoto K, Terada K, Kajiyama A. Relationships between crystallinity of β-cyclodextrin and tablet characteristics. Chem Pharm Bull 1985; 33: 5110–5112.

113. Pikal MJ, Lukes AL, Lang JE, Gaines K. Quantitative crystallinity determinations for β-lactam antibiotics by solution calorimetry: correlation with stability. J Pharm Sci 1978; 67: 767–772.

114. Black DB, Lowering EG. Estimation of the degree of crystallinity in digoxin by X ray and infrared methods. J Pharm Pharmacol 1977; 29: 684–687.

115. Kamat MS, Osawa T, Deangelis RJ, Koyama Y, DeLuca PP. Estimation of the degree of crystallinity of cefazolin sodium by X-ray and infrared methods. Pharm Res 1988; 5 (7): 426–429.

116. Saleki-Gerhardt A, Stowell JG, Byrn SR, Zografi G. Hydration and dehydration of crystalline and amorphous forms of raffinose. J Pharm Sci 1995; 84 (3): 318–323.

117. Thompson KC, Draper JP, Kaufman MJ, Brenner GS. Characterization of the crystallinity of drugs: B02669, a case study. Pharm Res 1994; 11 (9): 1362–1365.

118. Ohta M, Buckton G. Determination of the changes in surface energetics of cefditoren pivoxil as a consequence of processing induced disorder and equilibration to different relative humidities. Int J Pharm 2004; 269: 81–88.

119. Nakai Y, Fukuoka E, Nakajima S, Hasegawa J. Crystallinity and physical characteristics of microcrystalline cellulose. Chem Pharm Bull 1977; 25: 96–101.

120. Otsuka M, Kaneniwa N. Effects of grinding on the crystallinity and chemical stability in the solid state of cephalothin sodium. Int J Pharm 1990; 62: 65–73.

121. Gubskaya AV, Lisnyak YV, Blagoy YP. Effect of cryogrinding on physico-chemical properties of drugs. I. Theophylline evaluation of particle sizes and the degree of crystallinity, relation to dissolution parameters. Drug Dev Ind Pharm 1995; 21: 1953–1964.

122. Nakai Y, Fukuoka E, Nakajima S, Morita M. Physico-chemical properties of crystalline lactose. I. Estimation of the degree of crystallinity and the disorder parameter by an X-ray diffraction method. Chem Pharm Bull 1982; 30: 1811–1818.

123. Saleki-Gerhardt A, Ahlneck C, Zografi G. Assessment of disorder in crystalline solids. Int J Pharm 1994; 101: 237–247.

124. Suryanarayan R. Evaluation of two concepts of crystallinity using calcium gluceptate as a model compound. Int J Pharm 1985; 24: 1–17.

125. Clas SD, Faizer R, O'Connor RE, Vadas EB. Quantification of crystallinity in blends of lyophilized and crystalline MK-0591 using X-ray powder diffraction. Int J Pharm 1994; 121 (1): 73–79.

126. Otsuka M, Kaneniwa N. Effect of grinding on the degree of crystallinity of cephalexin powder. Chem Pharm Bull 1983; 31: 4489–4495.

127. Matsuda Y. Otsuka M, Onoe M, Tatsumi E. Amorphism and physicochemical stability of spray-dried frusemide. J Pharm Pharmacol 1992; 44: 627–633.

128. Imaizumi H, Nambu N, Nagai T. Stability and several physical properties of amorphous and crystalline indomethacin. Chem Pharm Bull 1980; 28: 2565–2569.

129. Livingston RA, Stutzman PE, Schumann I. Quantitative X-ray diffraction analysis of handmolded brick. In: Baer NS, Fritz S, Livingston RA,editors. Foam conservation of historic brick structures. Shafesbury, UK: Donhead Publishing Ltd; 1998. p 105–116.

130. Crocker LS, McCauley JA. Comparison of the crystallinity of imipenem samples by X-ray diffraction of amorphous material. J Pharm Sci 1995; 84 (2): 226–227.

131. Chen C, Bates S, Morris K. Quantifying amorphous content of lactose using parallel beam X-ray powder diffraction and whole pattern fitting. J Pharm Biomed Anal 2001; 26: 63–72.

132. Seyer JJ, Luner PE, Kemper MS. Application of diffuse reflectance near-infrared spectroscopy for the determination of crystallinity. J Pharm Sci 2000; 89 (10): 1305–1316.

133. Craig DQM, Royall PG, Kett VL, Hopton ML. The relevance of the amorphous state to pharmaceutical dosage forms: glassy drugs and freeze dried systems. Int J Pharm 1999; 179: 179–207.

134. Fukuoka E, Makita M, Yamamura S. Some physicochemical properties of glassy indomethacin. Chem Pharm Bull 1986; 34: 4314–4321.

135. Yoshioka M, Hancock BC, Zografi G. Crystallization of indomethacin from the amorphous state below and above its glass transition temperature. J Pharm Sci 1994; 83 (12): 1700–1705.

136. Hancock BC, Shamblin SL, Zografi G. Molecular mobility of amorphous pharmaceutical solids below their glass transition temperature. Pharm Res 1995; 12: 799–806.

137. Oberholzer ER, Brenner GS. Cefoxitin sodium: solution and solid state chemical stability studies. J Pharm Sci 1979; 68 (7): 836–866.

138. Mullins J, Macek T. Some pharmaceutical properties of novobiocin. J Am Pharm Assoc Sci Ed 1960; 49: 245–248.

139. http://www.fda.gov/cder

140. Byrn SR, Bates S, Ivanisevic I. Regulatory aspects of X-ray powder diffraction part II. Am Pharm Rev 2005; 8 (5): 137–141.

141. Law D, Schmitt EA, Marsh KC, Everitt EA, Wang W, Fort JJ, Krill SL, Qiu Y. Ritonavir-PEG 8000 amorphous solid dispersions: in vitro and in vivo evaluations. J Pharm Sci 2004; 93 (3): 563–567.

142. Byrn SR, Bates S, Ivanisevic I. Regulatory aspects of X-ray powder diffraction, part I. Am Pharm Rev 2005; 8 (3): 55–59.

143. Höskuldsson A. Prediction methods in science and technology. Vol. 1. Copenhagen: Thor Publishing; 1996.

144. Höskuldsson A. PLS regression methods. J Chemom 1988; 2: 211–228.

145. Wold S, Johansson E, Cocchi M. PLS—partial least squares projections to latent structures. In: Kubinyi H,editor. 3D QSAR in drug design, theory, methods and applications. Leiden: ESCOM Science Publishers; 1993.

146. Eriksson L, Johansson E, Kettaneh-Wold N, Wold S. Multi- and megavariate data analysis—principles and apllications. Umeå, Sweden: Umetrics; 2001.

147. Suryanarayanan R, Herman CS. Quantitative analysis of the active tablet ingredient by powder X-ray diffractometry. Pharm Res 1991; 8 (3): 393–399.

148. Yamada H, Suryanarayanan R. X-ray powder diffractometry of intact film coated tablets—an approach to monitor the physical form of the active pharmaceutical ingredient during processing and storage. J Pharm Sci 2007; 96 (8): 2029–2036.

149. Davis T, *Ph.D. Thesis*, Purdue University, West Lafayette; 2003.

150. MacCalman ML, Roberts KJ, Kerr C, Hendriksen B. On-line processing of pharmaceutical materials using in situ X-ray diffraction. J Appl Cryst 1995; 28: 620–622.

EXHIBIT D

Basic
Solid State
Chemistry

Second Edition

Anthony R. West

Basic
Solid State Chemistry

Second Edition

ANTHONY R. WEST

Department of Engineering Materials
Sheffield University
formerly of Department of Chemistry
University of Aberdeen

Other Wiley Editorial Offices

John Wiley & Sons Inc., 111 River Street, Hoboken, NJ 07030, USA

Jossey-Bass, 989 Market Street, San Francisco, CA 94103-1741, USA

Wiley-VCH Verlag GmbH, Boschstr. 12, D-69469 Weinheim, Germany

John Wiley & Sons Australia Ltd, 33 Park Road, Milton, Queensland 4064, Australia

John Wiley & Sons (Asia) Pte Ltd, 2 Clementi Loop #02-01, Jin Xing Distripark, Singapore 129809

John Wiley & Sons Canada Ltd, 22 Worcester Road, Etobicoke, Ontario, Canada M9W 1L1

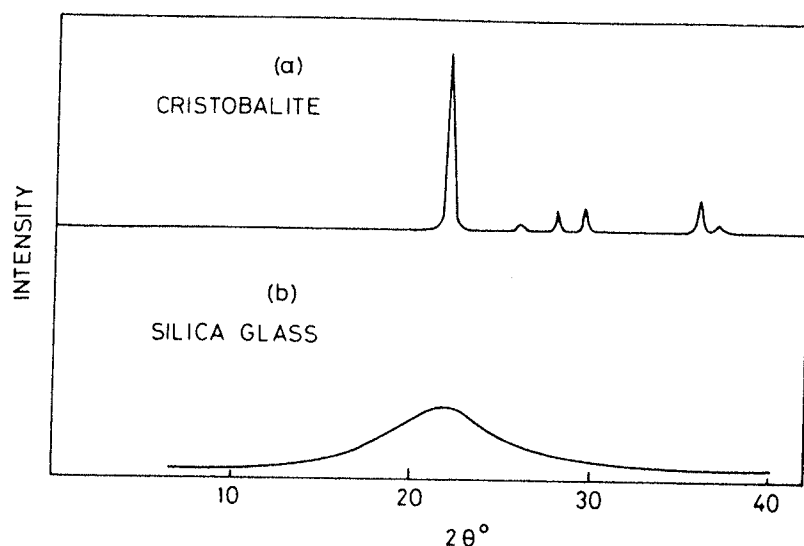**Fig. 3.11** X-ray powder diffraction pattern of (a) cristobalite and (b) glassy SiO_2, $CuK\alpha$ radiation

Samples for diffractometry take various forms: they include thin layers of fine powder sprinkled onto a glass slide smeared with vaseline and thin flakes pressed onto a glass slide. The objective is always to obtain a sample which contains a random arrangement of crystal orientations. If the crystal arrangement is not random, then *preferred orientation* exists and can introduce errors, sometimes very large, into the measured intensities. Preferred orientation is a serious problem for materials that crystallize in a characteristic, very non-spherical shape, e.g. clay minerals which usually occur as thin plates or some cubic materials which crystallize as cubes and, on crushing, break up into smaller cubes. In a powder aggregate of such materials, the crystals tend to sit on their faces, resulting in a non-random average orientation.

g)   Focusing of X-rays: theorem of a circle

A big disadvantage of Debye–Scherrer cameras is that incident and diffracted beams are, inevitably, divergent and of low intensity. In diffractometers and modern focusing cameras, a convergent X-ray beam is used; this gives a dramatic improvement in resolution and, because much more intense beams may be used, exposure times are greatly reduced. It is not possible to focus or converge X-rays using the X-ray equivalent of an optical lens; instead, use is made of certain geometric properties of the circle in order to obtain a convergent X-ray beam. These properties are illustrated in Fig. 3.12(a). The arc XY forms part of a circle and all angles subtended on the circumference of this circle by the arc XY are equal, i.e. $XCY = XC'Y = XC''Y = \alpha$. Suppose that X

is the reference position on the film. The mark is made by removing the beam stop for a fraction of a second while the X-rays are switched on. If required, a scale may be printed onto the film and the positions of the lines, relative to A, may be measured with a travelling microscope or, better, by microdensitometry; 2θ values and d-spacings may then be computed or obtained from tables.

The Guinier method is capable of giving accurate d-spacings with results comparable to those obtained by diffractometry. Intensities are either estimated visually or measured using microdensitometry. Sample sizes are small, $\lesssim 1$ mg, and exposure times vary between 5 min and 1 hr, depending on factors such as the crystallinity of the sample and the presence or absence of heavy elements which absorb X-rays.

j)   A powder pattern of a crystalline phase is its 'fingerprint'

There are two main factors which determine powder patterns: (a) the size and shape of the unit cell and (b) the atomic number and position of the atoms in the cell. Thus, two materials may have the same crystal structure but almost certainly will have distinct powder patterns. For example, KF, KCl and KI all have the rock salt structure and should show the same set of lines in their powder patterns, but, as can be seen from Table 3.3, both the positions and intensities of the lines are different in each. The positions or d-spacings vary because the unit cells are of different size and, therefore, the a parameter in the d-spacing formula varies. Intensities differ because different anions with different atomic numbers and therefore different scattering powers are present in the three materials, even though the atomic coordinates are the same for each (i.e. cations at corner and face centre positions, etc.). KCl is a rather extreme example because the intensities of 111 and 311 reflections are too small to measure, but it serves to illustrate the importance of scattering power of the atoms present. Intensities are discussed in more detail in the next section.

A powder pattern has two characteristic features, therefore: the d-spacings of the lines and their intensity. Of the two, the d-spacing is more useful and capable of precise measurement. The d-spacings should be reproducible from sample to sample unless impurities are present to form a solid solution. Intensities are more difficult to measure quantitatively and often vary from sample

Table 3.3   *X-ray powder diffraction patterns for potassium halides*

(hkl)	KF, $a = 5.347$ Å		KCl, $a = 6.2931$ Å		KI, $a = 7.0655$ Å	
	d(Å)	I	d(Å)	I	d(Å)	I
111	3.087	29		—	4.08	42
200	2.671	100	3.146	100	3.53	100
220	1.890	63	2.224	59	2.498	70
311	1.612	10	—	—	2.131	29
222	1.542	17	1.816	23	2.039	27
400	1.337	8	1.573	8	1.767	15

to sample especially if preferred orientation is present. Thus, the differences in tabulated intensities for, say, the (220) reflection of the three materials in Table 3.3 are probably not absolute, quantitatively.

The likelihood of two materials having the small cell parameters and d-spacings decreases considerably with decreasing crystal symmetry. Thus, cubic materials have only one variable, a, and there is a fair chance of finding two materials with the same a value. On the other hand, triclinic powder patterns have six variables, a, b, c, α, β and γ, and so accidental coincidences are far less likely. Problems of identification, if they occur, are most likely to be experienced with high symmetry, especially cubic, materials or in cases where similar-sized ions may replace each other in a particular structure.

k)   Intensities

Intensities of X-ray reflections are important for two main reasons. First, quantitative measurements of intensity are necessary in order to solve crystal structures. Second, qualitative or semi-quantitative intensity data are needed in using the powder fingerprint method to characterize materials and especially in using the *Powder Diffraction File* to identify unknowns. Although this book is not concerned with the methods of structure determination, it is important that the factors which control the intensity of X-ray reflections be understood. The topic falls into two parts: the intensity scattered by individual atoms and the resultant intensity scattered from the large number of atoms in a crystal.

i)   Scattering of X-rays by an atom: atomic scattering factors

Atoms diffract or scatter X-rays because an incident X-ray beam, which can be described as an electromagnetic wave with an oscillating electric field, sets each electron of an atom into vibration. A vibrating charge such as an electron emits radiation which is in phase or *coherent with* the incident X-ray beam. The electrons therefore act as secondary point sources of X-rays. Coherent scattering may be likened to an elastic collision between the wave and the electron: the wave is deflected by the electron without loss of energy and, therefore, without change of wavelength. The intensity of the radiation scattered coherently by 'point source' electrons is given by the *Thomson equation*:

$$I_{\mathrm{p}} \propto \frac{1}{2}(1 + \cos^2 2\theta) \qquad (3.5)$$

where I_{p} is the scattered intensity at any point, P, and 2θ is the angle between the directions of the incident beam and the diffracted beam that passes through P. From this equation, the scattered beams are most intense when parallel or antiparallel to the incident beam and are weakest when at 90° to the incident beam. The Thomson equation is also known as the *polarization factor* and is one of the standard angular correction factors that must be applied when processing intensity data for use in structure determination.

EXHIBIT E

QV
738
AA1
P5u
1995

Contents

USP 23

as the cur-

ppropriate
ig of water,
ample may
the analyte
e the water

d, dissolve
rous meth-
·ortion into

er may be
iich an ap-
ed into the
ue may be

or transfer
the coulo-
l the water
istrument's
in the sub-

ENE

i by means
joints (see

ratus are as
internal di-
: condenser,
m in length
ving tube E
to 156 mm
at the error
ted volume.
ith rheostat
ask and the

hromic acid
d dry in an
with a small
listilling the

Procedure—Place in the dry flask a quantity of the substance, weighed accurately to the nearest centigram, which is expected to yield 2 to 4 mL of water. If the substance is of a pasty character, weigh it in a boat of metal foil of a size that will just pass through the neck of the flask. If the substance is likely to cause bumping, add enough dry, washed sand to cover the bottom of the flask, or a number of capillary melting-point tubes, about 100 mm in length, sealed at the upper end. Place about 200 mL of toluene in the flask, connect the apparatus, and fill the receiving tube E with toluene poured through the top of the condenser. Heat the flask gently for 15 minutes and, when the toluene begins to boil, distil at the rate of about 2 drops per second until most of the water has passed over, then increase the rate of distillation to about 4 drops per second. When the water has apparently all distilled over, rinse the inside of the condenser tube with toluene while brushing down the tube with a tube brush attached to a copper wire and saturated with toluene. Continue the distillation for 5 minutes, then remove the heat, and allow the receiving tube to cool to room temperature. If any droplets of water adhere to the walls of the receiving tube, scrub them down with a brush consisting of a rubber band wrapped around a copper wire and wetted with toluene. When the water and toluene have separated completely, read the volume of water, and calculate the percentage that was present in the substance.

METHOD III (GRAVIMETRIC)

Procedure for Chemicals—Proceed as directed in the individual monograph preparing the chemical as directed under *Loss on Drying* ⟨731⟩.

Procedure for Biologics—Proceed as directed in the individual monograph.

Procedure for Vegetable Drugs—Place about 10 g of the drug, prepared as directed (see *Vegetable Drugs—Methods of Analysis* ⟨561⟩) and accurately weighed, in a tared evaporating dish. Dry at 105° for 5 hours, and weigh. Continue the drying and weighing at 1-hour intervals until the difference between two successive weighings corresponds to not more than 0.25%.

⟨941⟩ X-RAY DIFFRACTION

Every crystal form of a compound produces its own characteristic X-ray diffraction pattern. These diffraction patterns can be derived either from a single crystal or from a powdered specimen (containing numerous crystals) of the material. The spacings between and the relative intensities of the diffracted maxima can be used for qualitative and quantitative analysis of crystalline materials. Powder diffraction techniques are most commonly employed for routine identification and the determination of relative purity of crystalline materials. Small amounts of impurity, however, are not normally detectable by the X-ray diffraction method, and for quantitative measurements it is necessary to prepare the sample carefully to avoid preferred orientation effects.

The powder methods provide an advantage over other means of analysis in that they are usually nondestructive in nature (specimen preparation is usually limited to grinding to ensure a randomly oriented sample, and deleterious effects of X-rays on solid pharmaceutical compounds are not commonly encountered). The principal use of single-crystal diffraction data is for the determination of molecular weights and analysis of crystal structures at the atomic level. However, diffraction established for a single crystal can be used to support a specific powder pattern as being truly representative of a single phase.

Solids—A solid substance can be classified as being crystalline, noncrystalline, or a mixture of the two forms. In crystalline materials, the molecular or atomic species are ordered in a three-dimensional array, called a lattice, within the solid particles. This ordering of molecular components is lacking in noncrystalline material. Noncrystalline solids sometimes are referred to as glasses or amorphous solids when repetitive order is nonexistent in all three dimensions. It is also possible for order to exist in only one or two dimensions, resulting in mesomorphic phases (liquid crystals). Although crystalline materials are usually considered to have well-defined visible external morphologies (their habits), this is not a necessity for X-ray diffraction analysis.

The relatively random arrangement of molecules in noncrystalline substances makes them poor coherent scatterers of X-rays, resulting in broad, diffuse maxima in diffraction patterns. Their X-ray patterns are quite distinguishable from crystalline specimens, which give sharply defined diffraction patterns.

Many compounds are capable of crystallizing in more than one type of crystal lattice. At any particular temperature and pressure, only one crystalline form (polymorph) is thermodynamically stable. Since the rate of phase transformation of a metastable polymorph to the stable one can be quite slow, it is not uncommon to find several polymorphs of crystalline pharmaceutical compounds existing under normal handling conditions.

In addition to exhibiting polymorphism, many compounds form crystalline solvates in which the solvent molecule is an integral part of the crystal structure. Just as every polymorph has its own characteristic X-ray patterns, so does every solvate. Sometimes the differences in the diffraction patterns of different polymorphs are relatively minor, and must be very carefully evaluated before a definitive conclusion is reached. In some instances, these polymorphs and/or solvates show varying dissolution rates. Therefore, on the time scale of pharmaceutical bioavailability, different total amounts of drug are dissolved, resulting in potential bioinequivalence of the several forms of the drug.

Fundamental Principles—A collimated beam of monochromatic X-rays is diffracted in various directions when it impinges upon a rotating crystal or randomly oriented powdered crystal. The crystal acts as a three-dimensional diffraction grating to this radiation. This phenomenon is described by Bragg's law, which states that diffraction (constructive interference) can occur only when waves that are scattered from different regions of the crystal, in a specific direction, travel distances differing by integral numbers (n) of the wavelength (λ). Under such circumstances, the waves are in phase. This condition is described by the Bragg equation:

$$\frac{n\lambda}{2 \sin \theta} = d_{hkl},$$

in which d_{hkl} denotes the interplanar spacings and θ is the angle of diffraction.

A family of planes in space can be indexed by three whole numbers, usually referred to as Miller indices. These indices are the reciprocals, reduced to smallest integers, of the intercepts that a plane makes along the axes corresponding to three non-parallel edges of the unit cell (basic crystallographic unit). The unit cell dimensions are given by the lengths of the spacings along the three axes, a, b, c, and the angles between them, α, β, and γ. The interplanar spacing for a specific set of parallel planes hkl is denoted by d_{hkl}. Each such family of planes may show higher orders of diffraction where the d values for the related families of planes nh, nk, nl are diminished by the factor $1/n$ (n being an integer: 2, 3, 4, etc.). Every set of planes throughout a crystal has a corresponding Bragg diffraction angle associated with it (for a specific λ).

The amplitude of a diffracted X-ray beam from any set of planes is dependent upon the following atomic properties of the crystal: (1) position of each atom in the unit cell; (2) the respective atomic scattering factors; and (3) the individual thermal motions. Other factors that directly influence the intensities of the diffracted beam are: (1) the intensity and wavelength of the incident radiation; (2) the volume of crystalline specimen; (3) the absorption of the X-radiation by the specimen; and (4) the experimental arrangement utilized to record the intensity data. Thus, the experimental conditions are especially important for measurement of diffraction intensities.
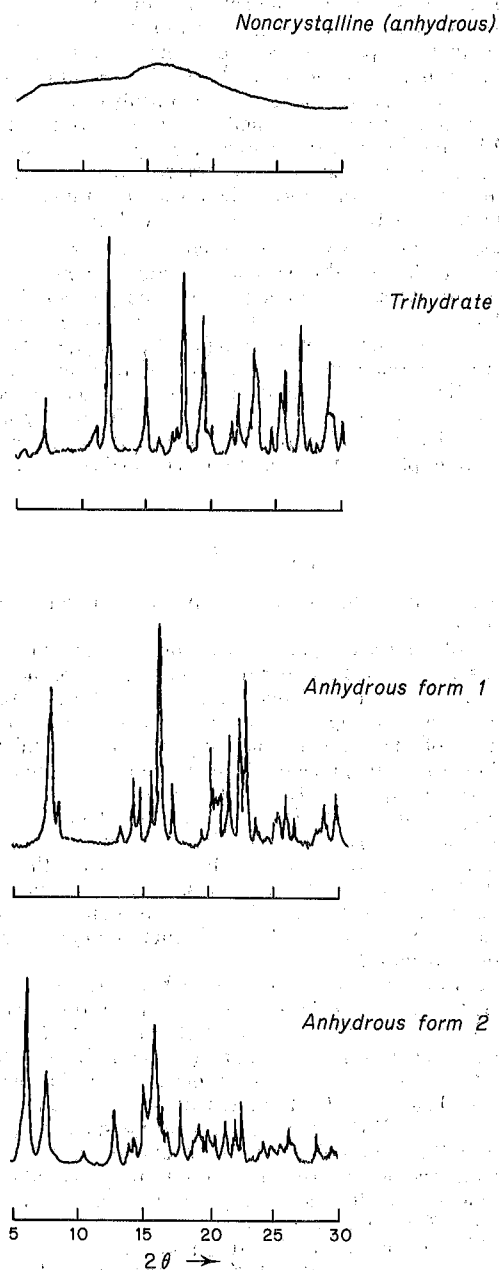
Only a limited number of Bragg planes are in a position to diffract when monochromatized X-rays pass through a single crystal. Techniques of recording the intensities of all of the possible diffracting hkl planes involve motion of the single crystal and the recording media. Recording of these data is accomplished by photographic techniques (film) or with radiation detectors.

A beam passing through a very large number of small, randomly oriented crystals produces continuous cones of diffracted rays from each set of lattice planes. Each cone corresponds to the diffraction from various planes having a similar interplanar spacing. The intensities of these Bragg reflections are recorded by either film or radiation detectors. The Bragg angle can be measured easily from a film, but the advent of radiation detectors

has made possible the construction of diffractometers that read this angle directly. The intensities and *d* spacings are more conveniently determined with powder diffractometers employing radiation detectors than by film methods. Microphotometers are frequently used for precise intensity measurements of films.

An example of the type of powder patterns obtained for four different solid phases of ampicillin are shown in the accompanying figure. These diffraction patterns were derived from a powder diffractometer equipped with a Geiger-Müller detector; nickel-filtered Cu *Kα* radiation was used.

Noncrystalline (anhydrous)

Trihydrate

Anhydrous form 1

Anhydrous form 2

5   10   15   20   25   30
2θ →

Typical Powder Patterns Obtained for Four Solid Phases of Ampicillin

Radiation—The principal radiation sources utilized for X-ray diffraction are vacuum tubes utilizing copper, molybdenum, iron, and chromium as anodes; copper X-rays are employed most commonly for organic substances. For each of these radiations there is an element that will filter off the *Kβ* radiation and permit the *Kα* radiation to pass (nickel is used, in the case of copper radiation). In this manner the radiation is practically monochroma-

tized. The choice of radiation to be used depends upon the absorption characteristics of the material and possible fluorescence by atoms present in the specimen.

Caution—Care must be taken in the use of such radiation. Those not familiar with the use of X-ray equipment should seek expert advice. Improper use can result in harmful effects to the operator.

Test Preparation—In an attempt to improve randomness in the orientation of crystallites (and, for film techniques, to avoid a grainy pattern), the specimen may be ground in a mortar to a fine powder. Grinding pressure has been known to induce phase transformations; therefore, it is advisable to check the diffraction pattern of the unground sample.

In general, the shapes of many crystalline particles tend to give a specimen that exhibits some degree of preferred orientation in the specimen holder. This is especially evident for needle-like or plate-like crystals where size reduction yields finer needles or platelets. Preferred orientation in the specimen influences the relative intensities of various reflections.

Several specialized handling techniques may be employed to minimize preferred orientation, but further reduction of particle size is often the best approach.

Where very accurate measurement of the Bragg angles is necessary, a small amount of an internal standard can be mixed into the specimen. This enables the film or recorder tracing to be calibrated. If comparisons to literature values (including compendial limits) of *d* are being made, calibrate the diffractometer. NIST standards are available covering to a *d*-value of 0.998 nm. Tetradecanol[1] may be used (*d* is 3.963 nm) for larger spacing.

The absorption of the radiation by any specimen is determined by the number and kinds of atoms through which the X-ray beam passes. An organic matrix usually absorbs less of the diffracted radiation than does an inorganic matrix. Therefore, it is important in quantitative studies that standard curves relating amount of material to the intensity of certain *d* spacings for that substance be determined in a matrix similar to that in which the substance will be analyzed.

In quantitative analyses of materials, a known amount of standard usually is added to a weighed amount of specimen to be analyzed. This enables the amount of the substance to be determined relative to the amount of standard added. The standard used should have approximately the same density as the specimen and similar absorption characteristics. More important, its diffraction pattern should not overlap to any extent with that of the material to be analyzed. Under these conditions a linear relationship between line intensity and concentration exists. In favorable cases, amounts of crystalline materials as small as 10% may be determined in solid matrices.

Identification of crystalline materials can be accomplished by comparison of X-ray powder diffraction patterns obtained for known[2] materials with those of the unknown. The intensity ratio (ratio of the peak intensity of a particular *d* spacing to the intensity of the strongest maxima in the diffraction pattern) and the *d* spacing are used in the comparison. If a reference material (e.g., USP Reference Standard) is available, it is preferable to generate a primary reference pattern on the same equipment used for running the unknown sample, and under the same conditions. For most organic crystals, it is appropriate to record the diffraction pattern to include values for 2θ that range from as near zero degrees as possible to 40 degrees. Agreement between sample and reference should be within the calibrated precision of the diffractometer for diffraction angle (2θ values should typically be reproducible to ±0.10 or 0.20 degrees), while relative intensities between sample and reference may vary up to 20 percent. For other types of samples (e.g., inorganic salts), it may be necessary to extend the 2θ region scanned to well beyond 40 degrees. It is generally sufficient to scan past the ten strongest reflections identified in the Powder Diffraction File.[2]

---

[1] Brindley, GW and Brown, G, eds., *Crystal Structures of Clay Minerals and their X-ray Identification*, Mineralogical Society Monograph No. 5, London, 1980, pp. 318 ff.
[2] The International Centre for Diffraction Data, Newtown Square Corporate Campus, 12 Campus Boulevard, Newtown Square, PA 19073, maintains a file on more than 60,000 crystalline materials, both organic and inorganic, suitable for such comparisons.

EXHIBIT E

UNITED STATES PATENT AND TRADEMARK OFFICE

APR 2 1 2008

Commissioner for Patents
United States Patent and Trademark Office
P.O. Box 1450
Alexandria, VA 22313-1450
www.uspto.gov

Mary K. VanAtten
Patent Department
Bristol-Myers Squibb Company
P.O. Box. 4000
Princeton, NJ 08543-4000

In Re: Patent Term Extension
        Application for
        U.S. Patent No. 6,596,746

NOTICE OF FINAL DETERMINATION

A determination has been made that U.S. Patent No. 6,596,746, which claims the human drug product Sprycel® (dasatinib), is eligible for patent term extension under 35 U.S.C. § 156. The period of extension has been determined to be 76 days.

A single request for reconsideration of this final determination as to the length of extension of the term of the patent may be made if filed within underline one month of the date of this notice. Extensions of time under 37 CFR § 1.136(a) are not applicable to this time period. In the absence of such request for reconsideration, the Director will issue a certificate of extension, under seal, for a period of 76 days.

The period of extension, if calculated using the Food and Drug Administration determination of the length of the regulatory review period published in the Federal Register of May 25, 2007 (72 Fed. Reg. 29334), would be 628 days. Under 35 U.S.C. § 156(c):

$$\text{Period of Extension} = \tfrac{1}{2}\,(\text{Testing Phase}) + \text{Approval Phase}$$
$$= \tfrac{1}{2}\,(1{,}000 - 110) + 183$$
$$= 628 \text{ days (1.7 years)}$$

Since the regulatory review period began April 4, 2003, before the patent issued (July 22, 2003), only that portion of the regulatory review period occurring after the date the patent issued has been considered in the above determination of the length of the extension period 35 U.S.C. § 156(c). (From April 4, 2003, to and including July 22, 2003, is 110 days; this period is subtracted for the number of days occurring in the testing phase according to the FDA determination of the length of the regulatory review period.) No determination of a lack of due diligence under 35 U.S.C. § 156(c)(1) was made.

However, the 14 year exception of 35 U.S.C. § 156(c)(3) operates to limit the term of the extension in the present situation because it provides that the period remaining in the term of the patent measured from the date of approval of the approved product plus any patent term extension cannot exceed fourteen years. The period of extension calculated above, 628 days, would extend the patent from April 13, 2020 to January 1, 2022, which is beyond the 14-year limit (the approval date is June 28, 2006, thus the 14 year limit is June 28, 2020). The period of extension is thus limited to 76 days, by operation of 35 U.S.C. § 156(c)(3). Accordingly, the period of extension is the number of days to extend the term of the patent from its original expiration date, April 13, 2020, to and including June 28, 2020, or 76 days.

The limitations of 35 U.S.C. 156(g)(6) do not operate to further reduce the period of extension determined above.

Upon issuance of the certificate of extension, the following information will be published in the Official Gazette:

U.S. Patent No.:   6,596,746

U.S. Patent No. 6,596,746   Page 2

expiration date, April 13, 2020, to and including June 28, 2020, or 76 days.

The limitations of 35 U.S.C. 156(g)(6) do not operate to further reduce the period of extension determined above.

Upon issuance of the certificate of extension, the following information will be published in the Official Gazette:

U.S. Patent No.:	6,596,746
Granted:	July 22, 2003
Original Expiration Date[1]:	April 13, 2020
Applicant:	Jagabandhu Das, et al.
Owner of Record:	Bristol-Myers Squibb Company
Title:	Cyclic Protein Tyrosine Kinase Inhibitors
Product Trade Name:	Sprycel® (dasatinib)
Term Extended:	76 days
Expiration Date of Extension:	June 28, 2020

---

[1]Subject to the provisions of 35 U.S.C. § 41(b).
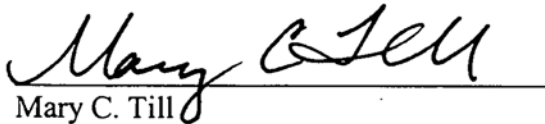
U.S. Patent No. 6,596,746   Page 3

Any correspondence with respect to this matter should be addressed as follows:

By mail: Mail Stop Hatch-Waxman PTE   By FAX: (571) 273-7755
            Commissioner for Patents
            P.O. Box 1450
            Alexandria, VA 22313-1450.

Telephone inquiries related to this determination should be directed to the undersigned at (571) 272-7755.

Mary C. Till

Mary C. Till
Legal Advisor
Office of Patent Legal Administration
Office of the Deputy Commissioner
 for Patent Examination Policy

cc: Office of Regulatory Policy   RE: Sprycel® (dasatinib)
       Food and Drug Administration   FDA Docket No.: 2006E-0516
       10903 New Hampshire Ave., Bldg. 51, Rm. 6222
       Silver Spring, MD 20993-0002

       Attention: Beverly Friedman

EXHIBIT F

VOGEL's

Vogel, Arthur Israel

TEXTBOOK OF
PRACTICAL ORGANIC CHEMISTRY

FIFTH EDITION
Revised by former and current members of
The School of Chemistry,
Thames Polytechnic, London

Brian S. Furniss

Antony J. Hannaford

Peter W. G. Smith

Austin R. Tatchell

QD261
V6
1989

before such air displacement, and before sealing. Care must be exercised when sealed ampoules, particularly those which have been stored for some time, are reopened, and the precautions outlined in Section 2.3.2, p. 38 should be noted.

DETERMINATION OF PHYSICAL CONSTANTS

2.33 DETERMINATION OF MELTING POINT – MIXED MELTING POINTS

A pure crystalline organic compound has, in general, a definite and sharp melting point; that is, the melting point range (the difference between the temperature at which the collapse of the crystals is first observed and the temperature at which the sample becomes completely liquid) does not exceed about 0.5 °C. The presence of small quantities of miscible, or partially miscible, impurities will usually produce a marked increase in the melting point range and cause the commencement of melting to occur at a temperature lower than the melting point of the pure substance. The melting point is therefore a valuable criterion of purity for an organic compound.

A sharp melting point is usually indicative of the high purity of a substance. There are, however, some exceptions. Thus a eutectic mixture of two or more compounds may have a sharp melting point, but this melting point may be changed by fractional crystallisation from a suitable solvent or mixture of solvents. The number of exceptions encountered in practice is surprisingly small, hence it is reasonable to regard a compound as pure when it melts over a range of about 0.5 °C (or less) and the melting point is unaffected by repeated fractional crystallisation.

The experimental method in most common use is to heat a small amount (about 1 mg) of the substance in a capillary tube inserted into a suitable melting point apparatus and to determine the temperature at which melting occurs. The *capillary melting point tubes are prepared* either from soft glass test tubes or from wide glass tubing (*c.* 12 mm diameter).* A short length of glass tubing or glass rod is firmly fused to the closed end of the test tube. The test tube (or wide glass tubing) must first be thoroughly washed with distilled water to remove dust, alkali and products of devitrification which remain on the surface of the glass, and then dried. The closed end of the test tube is first heated while being slowly rotated in a small blowpipe flame; the glass rod or tube is simultaneously heated in the same manner. When the extremities of both pieces of glass are red hot, they are firmly fused togeher, twisting of the joint being avoided, and then removed momentarily from the flame until the seal is just rigid enough that no bending occurs. The test tube is then immediately introduced into a large 'brush' flame, so that a length of about 5 cm is heated, and the tube is rotated uniformly in the flame. When the heated portion has become soft and slightly thickened as the result of the heating, the tube is removed from the flame and, after a second or two, drawn, slowly at first and then more rapidly, as far apart as the arms will permit (or until the external diameter of the tube has been reduced to 1–2 mm).

---

* Pyrex glass is preferable, but this requires an oxygen-gas blowpipe for manipulations. Suitable melting point tubes may be purchased from dealers in scientific apparatus or chemicals. It is, however, excellent practice for the student to learn to prepare his own capillary tubes.

EXHIBIT G

Mission

REF.

2004

USP 27

THE UNITED STATES PHARMACOPEIA

NF 22

THE NATIONAL FORMULARY

By authority of the United States Pharmacopeial Convention, Inc., meeting at Washington, D.C., April 12–16, 2000. Prepared by the Council of Experts and published by the Board of Trustees.

Official from January 1, 2004

The designation on the cover of this publication, "USP NF 2004," is for ease of identification only. The publication contains two separate compendia: The Pharmacopeia of the United States Twenty-seventh Revision, and the National Formulary, Twenty-second Edition.

⟨881⟩ TENSILE STRENGTH

Devices for measurement of tensile strength used in the United States may be calibrated in the English units of measure. The following directions are given in metric units with the understanding that the corresponding English equivalents may be used.

Surgical Suture

Determine the tensile strength of surgical suture on a motor-driven tensile strength testing machine having suitable clamps for holding the specimen firmly and using either the principle of constant rate of load on specimen or the principle of constant rate of elongation of specimen, as described below. The apparatus has two clamps for holding the strand. One of these clamps is mobile. The clamps are designed so that the strand being tested can be attached without any possibility of slipping. Gauge length is defined as the interior distance between the two clamps. For gauge lengths of 125 to 200 mm, the mobile clamp is driven at a constant rate of elongation of 30 ±5 cm per minute. For gauge lengths of less than 125 mm, the rate of elongation per minute is adjusted to equal 2 times the gauge length per minute. For example, a 5-cm gauge length has a rate of elongation of 10 cm per minute.

Determine the tensile strength of the suture, whether packaged in dry form or in fluid, promptly after removal from the container, without prior drying or conditioning. Attach one end of the suture to the clamp at the load end of the machine, pass the other end through the opposite clamp, applying sufficient tension so that the specimen is taut between the clamps, and engage the second clamp. Perform as many breaks as are specified in the individual monograph. If the break occurs at the clamp, discard the reading on the specimen.

Procedure for a machine operating on the principle of constant rate of load on specimen—This description applies to the machine known as the Incline Plane Tester.

The carriage used in any test is of a weight such that when the break occurs, the position of the recording pen on the chart is between 20% and 80% of the capacity that may be recorded on the chart. The friction in the carriage is low enough to permit the recording pen to depart from the zero line of the chart at a point not exceeding 2.5% of the capacity of the chart when no specimen is held in the clamps.

For surgical sutures of intermediate and larger sizes, the clamp for holding the specimen is of the roll type, with a flat gripping surface. The roll has a diameter of 19 mm and the flat gripping surface is not less than 25 mm in length. The length of the specimen, when inserted in the clamps, is at least 127 mm from nip to nip. The speed of inclination of the plane of the tester is such that it reaches its full inclination of 30° from the horizontal in 20 ± 1 seconds from the start of the test.

For surgical sutures of small sizes, the suitable clamp has a flat gripping surface of not less than 13 mm in length. The speed of inclination of the plane is such that it reaches its full inclination of 30° from the horizontal in 60 ± 5 seconds from the start of the test.

Except where straight pull (no knot required) is indicated in the suture monograph, tie the test suture into a surgeon's knot with one turn of suture around flexible rubber tubing of 6.5-mm inside diameter and 1.6-mm wall thickness. The surgeon's knot is a square knot in which the free end is first passed twice, instead of once, through the loop, and pulled taut, then passed once through a second loop, and the ends are drawn taut so that a single throw is superimposed upon a double throw. Start the first knot with the left end over the right end, exerting sufficient tension to tie the knot securely. Where the test specimen includes a knot, place the specimen in the testing device with the knot approximately midway between the clamps. Leave the flexible rubber tubing in place for the duration of the test.

Procedure for a machine operating on the principle of constant rate of elongation of specimen—This description applies to any suitable tensile testing machine that operates on the principle of constant rate of elongation of specimen.

Except where straight pull (no knot required) is indicated in the suture monographs, tie the test suture into a simple knot formed by placing one end of a strand held in the right hand over the other end held in the left hand, passing one end over the strand and through the

loop so formed, and pulling the knot tight. The specimen is placed in the testing device with the knot approximately midway between the clamps.

Textile Fabrics and Films

Determine the tensile strength of textile fabrics, including adhesive tape, on a constant-speed or pendulum-type of testing machine of the following general description.

The clamps for holding the specimen are smooth, flat, parallel jaws that are not less than 25 mm in length in the dimension parallel to the direction of application of the load. When the width of the strip being tested does not exceed 19 mm, the jaws of the clamp should be at least 25 mm wide. If the width of the strip is greater than 19 mm and not greater than 44 mm, the width of the jaws of the clamp should be at least 50 mm. If the width of the specimen is greater than 44 mm, cut a 25-mm strip, and use a clamp with jaws not less than 50 mm wide. Round all edges that might have a cutting action on the specimen to a radius of 0.4 mm. The jaws are 76.2 mm apart at the beginning of the test, and they separate at the rate of 30.5 cm ± 13 mm per minute. The machine is of such capacity that when the break occurs, the deviation of the pendulum from the vertical is between 9° and 45°.

⟨891⟩ THERMAL ANALYSIS

Precisely determined thermodynamic events, such as a change of state, can indicate the identity and purity of drugs. Compendial standards have long been established for the melting or boiling temperatures of substances. These transitions occur at characteristic temperatures, and the compendial standards therefore contribute to the identification of the substances. Because impurities affect these changes in predictable ways, the same compendial standards contribute to the control of the purity of the substances.

Thermal analysis in the broadest sense is the measurement of physical-chemical properties of materials as a function of temperature. Instrumental methods have largely supplanted older methods dependent on visual inspection and on measurements under fixed or arbitrary conditions, because they are objective, they provide more information, they afford permanent records, and they are generally more sensitive, more precise, and more accurate. Furthermore, they may provide information on crystal perfection, polymorphism, melting temperature, sublimation, glass transitions, dehydration, evaporation, pyrolysis, solid-solid interactions, and purity. Such data are useful in the characterization of substances with respect to compatibility, stability, packaging, and quality control. The measurements used most often in thermal analysis, i.e., transition temperature, thermogravimetry, and impurity analysis, are described here.

Transition Temperature—As a specimen is heated, its uptake (or evolution) of heat can be measured [differential scanning calorimetry (DSC)] or the resulting difference in temperature from that of an inert reference heated identically [differential thermal analysis (DTA)] can be measured. Either technique provides a record of the temperature at which phase changes, glass transitions, or chemical reactions occur. In the case of melting, both an "onset" and a "peak" temperature can be determined objectively and reproducibly, often to within a few tenths of a degree. While these temperatures are useful for characterizing substances, and the difference between the two temperatures is indicative of purity, the values cannot be correlated with subjective, visual "melting-range" values or with constants such as the triple point of the pure material.

A complete description of the conditions employed should accompany each thermogram, including make and model of instrument; record of last calibration; specimen size and identification (including previous thermal history); container; identity, flow rate, and pressure of gaseous atmosphere; direction and rate of temperature change; and instrument and recorder sensitivity.

It is appropriate to make a preliminary examination over a wide range of temperature (typically room temperature to decomposition temperature or about 10° to 20° above the melting point) and over a wide range of heating rates (2° to 20° per minute), which may reveal unexpected effects; then a single examination or replicate examinations over a narrow range, bracketing the transition of interest at one

USP 27

or more lower heating rates, can be made. In examining pure crystalline materials, rates as low as 1° per minute may be appropriate, whereas rates of up to 10° per minute are more appropriate for polymeric and other semi-crystalline materials. As the reliability of the measurements varies from one substance to another, statements of the number of significant figures to be used in the reporting of intralaboratory repeatability and of interlaboratory reproducibility cannot be given here, but should be included in the individual monograph.

Thermogravimetric Analysis—Thermogravimetric analysis involves the determination of the mass of a specimen as a function of temperature, or time of heating, or both, and when properly applied, provides more useful information than does loss on drying at fixed temperature, often for a fixed time and in what is usually an ill-defined atmosphere. Usually, loss of surface-absorbed solvent can be distinguished from solvent in the crystal lattice and from degradation losses. The measurements can be carried out in atmospheres having controlled humidity and oxygen concentration to reveal interactions with the drug substance, between drug substances, and between active substances and excipients or packaging materials.

While the details depend on the manufacturer, the essential features of the equipment are a recording balance and a programmable heat source. Equipment differs in the ability to handle specimens of various sizes, the means of sensing specimen temperature, and the range of atmosphere control. Calibration is required with all systems, i.e., the mass scale is calibrated by the use of standard weights; calibration of the temperature scale, which is more difficult, involving either variations in positioning of thermocouples and their calibration; or in other systems, calibration involves the use of standard materials because it is assumed that the specimen temperature is the furnace temperature.

Procedural details are specified in order to provide, for valid interlaboratory comparison of results. The specimen weight, source, and thermal history are noted. The equipment description covers dimensions and geometry, the materials of the test specimen holder, and the location of the temperature transducer. Alternatively, the make and model number of commercial equipment are specified. In all cases, the calibration record is specified. Data on the temperature environment include the initial and final temperatures and the rate of change or other details if nonlinear. The test atmosphere is critical; the volume, pressure, composition, whether static or dynamic, and if the latter, the flow rate and temperature are specified.

Eutectic Impurity Analysis—The basis of any calorimetric purity method is the relationship between the melting and freezing point depression, and the level of impurity. The melting of a compound is characterized by the absorption of latent heat of fusion, ΔH_f, at a specific temperature, T_o. In theory, a melting transition for an absolutely pure crystalline compound should occur within an infinitely narrow range. A broadening of the melting range, due to impurities, provides a sensitive criterion of purity. The effect is apparent visually by examination of thermograms of specimens differing by a few tenths percent in impurity content. A material that is 99% pure is about 20% molten at 3° below the melting point of the pure material (see accompanying figure).
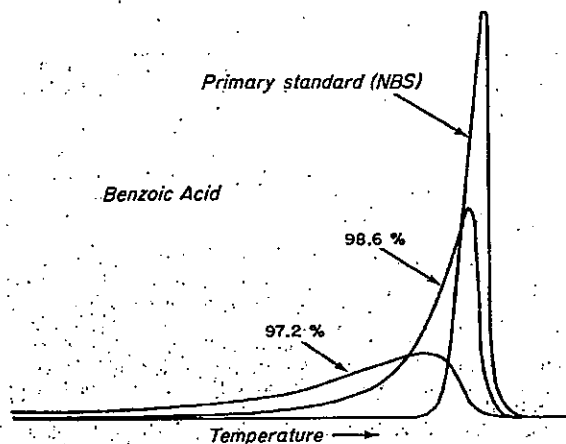
Superimposed Thermograms Illustrating the Effect of Impurities on DSC Melting Peak Shape

The parameters of melting (melting range, ΔH_f, and calculated eutectic purity) are readily obtained from the thermogram of a single melting event using a small test specimen, and the method does not require multiple, precise actual temperature measurements. Thermogram units are directly convertible to heat transfer, millicalories per second.

The lowering of the freezing point in *dilute solutions* by molecules of nearly equal size is expressed by a modified van't Hoff equation:

$$\frac{dT}{dX_2} = \frac{RT^2}{\Delta H_f} \cdot (K - 1), \qquad (1)$$

in which T = absolute temperature in degrees Kelvin (°K), X_2 = mole fraction of minor component (solute; impurity), ΔH_f = molar heat of fusion of the major component, R = gas constant, and K = distribution ratio of solute between the solid and liquid phases.

Assuming that the temperature range is small and that no solid solutions are formed ($K = 0$), integration of the van't Hoff equation yields the following relationship between mole fraction of impurity and the melting-point depression:

$$X_2 = \frac{(T_o - T_m)\Delta H_f}{RT_o^2}, \qquad (2)$$

in which T_o = melting point of the pure compound, in °K, and T_m = melting point of the test specimen, in °K.

With no solid solution formation, the concentration of impurity in the liquid phase at any temperature during the melting is inversely proportional to the fraction melted at that temperature, and the melting-point depression is directly proportional to the mole fraction of impurity. A plot of the observed test specimen temperature, T_s, versus the reciprocal of the fraction melted, $1/F$, at temperature T_s, should yield a straight line with the slope equal to the melting-point depression $(T_o - T_m)$. The theoretical melting point of the pure compound is obtained by extrapolation to $1/F = 0$:

$$T_s = T_o - \frac{RT_o^2 X_2(1/F)}{\Delta H_f}. \qquad (3)$$

Substituting the experimentally obtained values for $T_o - T_m$, ΔH_f, and T_o in Equation 2 yields the mole fraction of the total eutectic impurity,

which, when multiplied by 100, gives the mole percentage of total eutectic impurities.

Deviations from the theoretical linear plot also may be due to solid solution formation ($K \neq 0$), so that care must be taken in interpreting the data.

To observe the linear effect of the impurity concentration on the melting-point depression, the impurity must be *soluble* in the liquid phase or melt of the compound, but *insoluble* in the solid phase, i.e., no solid solutions are formed. Some chemical similarities are necessary for solubility in the melt. For example, the presence of ionic compounds in neutral organic compounds and the occurrence of thermal decomposition may not be reflected in purity estimates. The extent of these theoretical limitations has been only partially explored.

Impurities present from the synthetic route often are similar to the end product, hence there usually is no problem of solubility in the melt. Impurities consisting of molecules of the same shape, size, and character as those of the major component can fit into the matrix of the major component without disruption of the lattice, forming solid solutions or inclusions; such impurities are not detectable by DSC. Purity estimates are too high in such cases. This is more common with less-ordered crystals as indicated by low heats of fusion.

Impurity levels calculated from thermograms are reproducible and probably reliable within 0.1% for ideal compounds. Melting-point determinations by scanning calorimetry have a reproducibility with a standard deviation of about 0.2°. Calibration against standards may allow about 1° accuracy for the melting point, so that this technique is comparable to other procedures.

Compounds that exist in polymorphic form cannot be used in purity determination unless the compound is completely converted to one form. On the other hand, DSC and DTA are inherently useful for detecting, and therefore monitoring, polymorphism.

Procedure—The actual procedure and the calculations to be employed are dependent on the particular instrument used. Consult the manufacturer's literature and/or the thermal analysis literature for the most appropriate technique for a given instrument. In any event, it is imperative to keep in mind the limitations of solid solution formation, insolubility in the melt, polymorphism, and decomposition during the analysis.

⟨905⟩ UNIFORMITY OF DOSAGE UNITS

NOTE—In this chapter, *unit* and *dosage unit* are synonymous. The uniformity of dosage units can be demonstrated by either of two methods, weight variation or content uniformity. The requirements of this chapter apply both to dosage units containing a single active ingredient and to dosage units containing two or more active ingredients; unless otherwise specified in the individual monograph, they apply individually to each active ingredient in the product. *Content Uniformity* requirements may be applied in all cases. The test for *Content Uniformity* is required for:

(1) coated tablets, other than film-coated tablets containing 50 mg or more of an active ingredient that comprises 50% or more (by weight) of one tablet;
(2) transdermal systems;
(3) suspensions in single-unit containers or in soft capsules;
(4) inhalations (other than solutions for inhalation packaged in glass or plastic ampuls, intended for use in nebulizers) packaged in premetered dosage units. (For inhalers and premetered dosage units labeled for use with a named inhalation device, also see *Aerosols, Metered-Dose Inhalers, and Dry Powder Inhalers* ⟨601⟩);
(5) solids (including sterile solids) that are packaged in unit-dose containers and that contain active or inactive added substances, except that the test for *Weight Variation* may be applied in the special situations stated below; and
(6) suppositories.

When the test for *Content Uniformity* is not required, the test for *Weight Variation* may be applied in any of the following situations:
(1) products containing 50 mg or more of an active ingredient comprising 50% or more, by weight, of the dosage unit or, in the

case of hard capsules, the capsule contents, except that uniformity of other active ingredients present in lesser proportions is demonstrated by meeting *Content Uniformity* requirements;
(2) liquid-filled soft capsules other than soft capsules containing suspensions;
(3) solids (including sterile solids) that are packaged in single-unit containers and contain no added substances, whether active or inactive;
(4) solids (including sterile solids) that are packaged in single-unit containers, with or without added substances, whether active or inactive, that have been prepared from true solutions and freeze-dried in the final containers and are labeled to indicate this method of preparation; and
(5) solutions for inhalation packaged in glass or plastic ampuls, intended for use in nebulizers, oral solutions, and syrups when these articles are packaged in single-unit containers.

WEIGHT VARIATION

For the determination of dosage-unit uniformity by weight variation, select not fewer than 30 units, and proceed as follows for the dosage form designated. [NOTE—Specimens other than these test units may be drawn from the same batch for *Assay* determinations.]

Uncoated and Film-Coated Tablets—Weigh accurately 10 tablets individually. From the result of the *Assay*, obtained as directed in the individual monograph, calculate the content of active ingredient in each of the 10 tablets, assuming homogeneous distribution of the active ingredient.

Hard Capsules—Weigh accurately 10 capsules individually, taking care to preserve the identity of each capsule. Remove the contents of each capsule by a suitable means. Weigh accurately the emptied shells individually, and calculate for each capsule the net weight of its contents by subtracting the weight of the shell from the respective gross weight. From the results of the *Assay*, obtained as directed in the individual monograph, calculate the content of active ingredient in each of the capsules, assuming homogeneous distribution of the active ingredient.

Soft Capsules—Determine the net weight of the contents of individual capsules as follows. Weigh accurately the 10 intact capsules individually to obtain their gross weights, taking care to preserve the identity of each capsule. Then cut open the capsules by means of a suitable clean, dry cutting instrument such as scissors or a sharp open blade, and remove the contents by washing with a suitable solvent. Allow the occluded solvent to evaporate from the shells at room temperature over a period of about 30 minutes, taking precautions to avoid uptake or loss of moisture. Weigh the individual shells, and calculate the net contents. From the results of the *Assay*, obtained as directed in the individual monograph, calculate the content of active ingredient in each of the capsules, assuming homogeneous distribution of the active ingredient.

Solids (Including Sterile Solids) in Single-Unit Containers—Proceed as directed for *Hard Capsules*, treating each unit as described therein.

Solutions for Inhalation Packaged in Glass or Plastic Ampuls, Intended for Use in Nebulizers—Proceed as directed for *Hard Capsules*, treating each unit as described therein.

Oral Solutions and Syrups Packaged in Single-Unit Containers—Weigh accurately the amount of liquid that drains in not more than 5 seconds from each of 10 individual containers. If necessary, compute the equivalent volume after determining the apparent density. From the result of the *Assay*, obtained as directed in the individual monograph, calculate the content of active ingredient in the liquid drained from each of the 10 units.

CONTENT UNIFORMITY

For the determination of dosage-unit uniformity by assay of individual units, select not fewer than 30 units, and proceed as follows for the dosage form designated.

UNCOATED AND COATED TABLETS, HARD AND SOFT CAPSULES, SUPPOSITORIES, TRANSDERMAL SYSTEMS, ORAL SOLUTIONS IN SINGLE-UNIT CONTAINERS, SUSPENSIONS IN SINGLE-UNIT CONTAINERS, SYRUPS IN SINGLE-UNIT CONTAINERS, INHALATIONS PACKAGED IN PREMETERED

EXHIBIT H

Preparation, characterization and in vitro release kinetics of clozapine solid lipid nanoparticles

Vobalaboina Venkateswarlu*, Kopparam Manjunath

NDDS Laboratory, University College of Pharmaceutical Sciences, Kakatiya University, Warangal-506 009, Andhra Pradesh, India

Abstract

Clozapine, a lipophilic antipsychotic drug, has very poor oral bioavailability ($<27\%$) due to first pass effect. Solid lipid nanoparticle (SLN) delivery systems of clozapine have been developed using various triglycerides (trimyristin, tripalmitin and tristearin), soylecithin 95%, poloxamer 188 and charge modifier stearylamine. Hot homogenization of melted lipids and aqueous phase followed by ultrasonication at temperature above the melting point of lipid was used to prepare SLN dispersions. Particle size and zeta potential were measured by photon correlation spectroscopy (PCS) using Malvern Zetasizer. Process and formulation variables have been studied and optimized. Differential scanning calorimetry (DSC) and powder X-ray diffraction (PXRD) studies were performed to characterize state of drug and lipid modification. In vitro release studies were performed in 0.1 N HCl, double-distilled water and phosphate buffer, pH 7.4, using modified Franz diffusion cell. Stable SLN formulations of clozapine having mean size range of $60–380$ nm and zeta potential range of -23 to $+33$ mV were developed. More than 90% clozapine was entrapped in SLN. DSC and PXRD analysis showed that clozapine is dispersed in SLN in an amorphous state. The release pattern of drug is analyzed and found to follow Weibull and Higuchi equations.
© 2004 Elsevier B.V. All rights reserved.

Keywords: Solid Lipid Nanoparticles; Clozapine; DSC; PXRD; Release kinetics

1. Introduction

Since a decade, trials are being made to utilize solid lipid nanoparticles (SLN) as alternative drug delivery system to colloidal drug delivery systems such as lipid emulsions, liposomes and polymeric nanoparticles. SLN combines the advantages of different colloidal carriers and also avoids some of their disadvantages. SLN can be used to improve the bioavailability of drugs, e.g. cyclosporine A [1], and to obtain sustained release of lipophilic drugs like camptothecin [2]. It was reported that Idarubicin-loaded SLN acted as a prolonged release system after duodenal administration to rats [3]. Clozapine is described as an atypical antipsychotic agent because it is effective in the treatment of both positive and negative symptoms of schizophrenia and has low extrapyramidal side effects. However, the use of clozapine has been severely limited by the occurrence of agranulocytosis in a small percentage of population. Clozapine, a lipophilic drug, is rapidly absorbed orally with a bioavailability of 0.27 [4].

DSC and PXRD analysis are used to investigate the crystalline structure of the SLN and drug. Characterization of degree of lipid crystallization and lipid

---

* Corresponding author. Tel.: +91-870-2446259 (office), 2438752 (residence); fax: +91-870-2438844.

E-mail address: vobala@yahoo.com (V. Venkateswarlu).

modification are helpful in understanding the drug incorporation and release pattern. Fewer data are available on drug release from SLN in the literature [2,5–8]. In vitro drug release studies are important to understand the in vivo performance of the dosage form. Drug release studies help in evaluation of sustained and prolonged release dispersion systems. In the present work, clozapine solid lipid nanoparticles are developed and characterized for crystallinity of drug and lipids. Effect of lipids, percentage of poloxamer 188 and charge modifier, stearylamine, on drug release are studied. Much attention is given to investigate release kinetics of clozapine from SLN.

2. Materials and methods

2.1. Materials

Clozapine was a kind gift from SPARC, Baroda, India. Trimyristin (TM) (Dynasan 114), tripalmitin (TP) (Dynasan 116) and tristearin (TS) (Dynasan 118) were generously supplied by Sasol Germany. Soy phosphatidylcholine 95% (Epikuron 200) was donated by Degussa Texturant Systems, Deutschland, Hamburg. Poloxamer 188 (Pluronic F 68) and dialysis membrane-70 were purchased from HiMedia, India. Stearylamine and dicetyl phosphate were obtained from Sigma (St. Louis, MO, USA). Centrisart filters (molecular weight cutoff 20,000) were purchased from Sartorius, Goettingen, Germany. The other chemicals were of analytical reagent grade.

2.2. Partitioning behaviour of clozapine in various lipids

Ten milligrams of clozapine was dispersed in a mixture of melted lipid (1 g) and 1 ml of hot distilled water and shaken for 30 min in a hot water bath. Aqueous phase was separated after cooling by ultracentrifugation with the help of Centrisart and analyzed for drug content by HPLC.

2.3. Preparation of clozapine solid lipid nanoparticles by hot homogenization technique

Clozapine (40 mg), triglyceride (400 mg) and phosphatidylcholine 95% (200 mg) were dissolved in 10 ml of mixture of chloroform and methanol (1:1). Organic solvents were completely removed using Buchi rotoevaporator (400 mbar, 60 °C). Nitrogen was blown on to the lipid layer for 30 min to remove traces of vapors of organic solvents if any. Drug embedded lipid layer was melted by heating at 5 °C above melting point of the lipid. An aqueous phase was prepared by dissolving poloxamer 188 (200 mg) in double-distilled water (sufficient to produce 20 ml of the preparation) and heated to same temperature of the molten lipid phase. Hot aqueous phase was added to molten lipid phase and homogenization was carried out (at 6000 rpm and temperature maintained 5 °C above the melting point of the lipid) with the help of Diax 900 homogenizer (Heidolph, Germany) for 3 min. Coarse hot oil in water emulsion so obtained was ultrasonicated (12T-probe) using Sonopuls ultrahomogenizer (Bandelin, Germany) for 25 min. Clozapine solid lipid nanoparticles (CLZ) were obtained by allowing hot nanoemulsion to cool to room temperature. Stearylamine or dicetyl phosphate was used as surface charge modifier of CLZ and was incorporated along with lipids. Blank solid lipid nanoparticles (BL) were prepared in a similar way without drug. Blank and clozapine solid lipid nanoparticles prepared with trimyristin, tripalmitin and tristearin are abbreviated as BL-TM, BL-TP, BL-TS, CLZ-TM, CLZ-TP and CLZ-TS, respectively.

2.4. Measurement of size and zeta potential of SLN

Size and zeta potential of SLN were measured by photon correlation spectroscopy (PCS) using Malvern Zetasizer. Samples were diluted appropriately with the aqueous phase of the formulation for the measurements.

2.5. Assay and entrapment efficiency

Formulation (0.2 ml) was diluted to 10 ml with chloroform/methanol (1:1). Final dilution was made with mobile phase and clozapine content was determined by HPLC.

2.5.1. Entrapment efficiency
The entrapment efficiency of the drug was determined by measuring the concentration of free drug in

the dispersion medium. Ultracentrifugation was carried out using Centrisart, which consist of filter membrane (molecular weight cutoff 20,000 Da) at the base of the sample recovery chamber. About 1 ml of undiluted sample of CLZ was placed in the outer chamber and the sample recovery chamber placed on top of the sample. The unit was centrifuged at 3500 rpm for 15 min. The solid lipid nanoparticles along with encapsulated drug remained in the outer chamber and aqueous phase moved into the sample recovery chamber through filter membrane. The amount of the clozapine in the aqueous phase was estimated by HPLC.

2.5.2. Statistical analysis

Size and entrapment efficiency of SLNs with and without stearylamine were compared using the Student's *t*-test. Statistical analyses were performed using statistical package for social sciences (SPSS version 11.0).

2.5.3. HPLC analysis of clozapine

The chromatographic system consisted of a Shimadzu LC-10AT solvent delivery pump equipped with a 20-μl loop and rheodyne sample injector. Wakosil II 5C18RS (SGE) (25 cm × 4.6 mm ID) analytical column was used. Detector used was SPD-10A VP dual wavelength UV–Visible detector (Shimadzu) operated at 254 nm. Mobile phase was methanol/water/triethylamine (65:35:0.5); pH was adjusted to 6.5 with glacial acetic acid and flow rate was kept at 1 ml/min. The data was recorded using Winchrome software.

2.6. Stability studies

Clozapine SLNs of different triglycerides with and without stearylamine (1% poloxamer 188) were stored at 25 °C for 6 months and average size and entrapment efficiency were determined.

2.7. Effect of sterilization

To see the effect of sterilization on particle size, zeta potential and entrapment efficiency, BL and CLZ dispersions (with and without charge modifier, stearylamine, in the formulation) were autoclaved at 121 °C for 20 min.

2.8. Characterization by differential scanning calorimetry

DSC analysis was performed using Mettler DSC 822e/200 (Mettler Toledo). The instrument was calibrated with indium (calibration standard, purity >99.999%) for melting point and heat of fusion. A heating rate of 10 °C/min was employed in the range of 20–220 °C. Analysis was performed under a nitrogen purge (50 ml/min). A standard aluminum sample pans (40 μl) were used. About 10 mg sample was taken for analysis. An empty pan was used as reference.

Preparation of mixtures of SLN components for thermal analysis:

(i) Physical mixtures (PM) of clozapine and triglycerides (trimyristin, tripalmitin and tristearin).
(ii) Mixtures obtained by solvent evaporation (SM)— clozapine and triglyceride were dissolved in a mixture of chloroform and methanol (1:1) and the solvents were removed by rotoevaporation.

The ratios of clozapine to triglyceride were similar to that of weight ratios in SLN formulation. PM, SM, lyophilized CLZ, clozapine and triglycerides were subjected to same thermal cycles.

2.9. Powder X-ray diffractometry (PXRD)

Powder X-ray diffractometer, Siemen's D-5000 (Germany), was used for diffraction studies. PXRD studies were performed on the samples by exposing them to CuK$_\alpha$ radiation (40 kV, 30 mA) and scanned from 2° to 70°, 2θ at a step size of 0.045° and step time of 0.5 s. Samples used for PXRD analysis were same as those of DSC analysis.

2.10. In vitro release kinetics of clozapine from SLN

In vitro release studies were performed using modified Franz diffusion cell. Dialysis membrane having pore size 2.4 nm, molecular weight cutoff between 12,000–14,000, was used. Membrane was soaked in double-distilled water for 12 h before mounting in a Franz diffusion cell. CLZ formulation (1 ml) was placed in the donor compartment and the receptor compartment was filled with dialysis medium

V. Venkateswarlu, K. Manjunath / Journal of Controlled Release 95 (2004) 627–638

(0.1 N HCl or phosphate buffer, pH 7.4, or double-distilled water of pH 7.0) (12 ml). At fixed time intervals, 100 µl of the sample was withdrawn from receiver compartment through side tube. Fresh double-distilled water was placed to maintain constant volume. Samples were analyzed by HPLC method as described above.

3. Results and discussions

3.1. Partitioning behaviour of clozapine

Calibration curve ($y = 305827x - 44681$, $R^2 = 0.9989$) of clozapine was used to calculate the concentration of clozapine in the aqueous phase. Partition coefficients (ratio of the amount of clozapine in lipid to the amount of clozapine in aqueous phase) obtained were 28.4 ± 1.91, 66.1 ± 4.65, 77.0 ± 1.47, 224.9 ± 6.7, 274.6 ± 9.4 and 283.5 ± 8.2 for glycerol monostearate (imwitor 900), stearicacid, tribehenin (compritol 888), TM, TS and TP, respectively. Triglycerides (TM, TS and TP) in which clozapine exhibited higher partition coefficients were selected for preparation of SLN. Highest partition coefficient was observed with TP.

3.2. Preparation of SLN

SLN have been prepared by various researchers using different methods [9–12]. In the present study, we have developed an economical, simple and reproducible method for the preparation of SLN, i.e. homogenization followed by ultrasonication at above the melting point of the lipid. To disperse the clozapine homogeneously in the lipid, solvent system chloroform/methanol (1:1) was used. Homogenization time was optimized to 3 min. There was no decrease in particle size with further increase in homogenization time. To reduce the particle size below 1 µm, probe ultrasonicator was used. A 25-min sonication was necessary to obtain solid lipid nanoparticles in the range of 60–380 nm with narrow size distribution.

3.3. Measurement of size and zeta potential

Sizes of drug-loaded SLN of different triglycerides, with different percentages of poloxamer 188, were shown in Fig. 1. In all the formulations, optimum size (224.8–266.3 nm) was obtained at 1% poloxamer concentration. In the presence of stearylamine (0.05%), the particle size range was still reduced, i.e. 60.4–103.1 nm in case of BL and 96.7–163.3 nm in case of CLZ (Table 1).

Size and zeta potential of BL and CLZ, with and without stearylamine, were shown in Table 1. BL possess negative zeta potential whereas zeta potential shifted to positive sign in CLZ. This might be due to orientation of clozapine (having four basic nitrogen atoms in its structure) on to the surface of SLN. To alter the zeta potential, stearylamine and dicetyl phosphate were included in the formulation individually. As the concentration of stearylamine increased from 0.05% to 0.3%, zeta potential was increased from 33.2 ± 0.6 to 39.6 ± 0.3 in case of CLZ-TM. Addition of stearylamine (0.05%) in BL and CLZ altered zeta potential to positive sign in all three lipid-based SLNs (Table 1). It clearly indicates the participation of stearlyamine around the SLN along with the phosphatidlycholine and poloxamer 188. BL containing dicetylphosphate was stable (size 109 ± 8.2 nm and zeta potential -30.3 ± 4.2 mV). CLZ containing 0.05–0.1% of dicetylphosphate became gel within 2 days whereas 0.2–0.3% dicetylphosphate formulations became gel within 12 h. This may be due to ionic interaction between clozapine and dicetylphos-
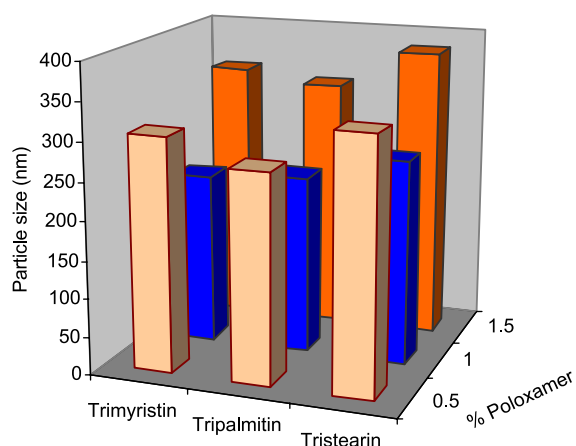

Fig. 1. Effect of poloxamer 188 concentration (0.5%, 1.0% and 1.5%) on particle size of clozapine SLNs of different triglycerides (trimyristin, tripalmitin and tristearin).

Table 1
Average size and zeta potential of SLNs of different triglycerides with and without stearylamine (1% poloxamer 188) (mean ± S.D., $n = 3$)

Triglyceride	Size (nm)				Zeta potential (mV)			
	Without stearylamine		With stearylamine		Without stearylamine		With stearylamine	
	BL	CLZ	BL	CLZ	BL	CLZ	BL	CLZ
Trimyristin	145.1 ± 4.3	224.8 ± 4.2	103.1 ± 7.5*	150.2 ± 1.5**	− 23.7 ± 1.5	1.1 ± 0.4	4.3 ± 3.8	33.2 ± 0.6
Tripalmitin	111.8 ± 0.8	233.3 ± 13.4	60.4 ± 6.6**	163.3 ± 0.7**	− 29.0 ± 6.0	0.2 ± 0.1	4.5 ± 0.4	23.2 ± 0.9
Tristearin	152.0 ± 4.0	266.3 ± 8.9	70.8 ± 5.4**	96.7 ± 3.8**	− 22.9 ± 1.0	4.1 ± 0.3	6.3 ± 0.4	21.3 ± 1.3

Statistical significances with stearylamine versus without stearylamine are **$p < 0.001$, *$p < 0.01$.

phate leading to gelation. This gel formation is specific to drug.

3.4. Assay and entrapment efficiency

Assay results showed that concentration of clozapine in the total system ranges from 1.92 to 1.98 mg/ml for different formulations. As shown in Table 2 and Fig. 2, as the percentage of poloxamer 188 increased entrapment efficiency was decreased marginally. This may be due to increased solubility of clozapine in the aqueous phase as the percentage of poloxamer 188 increased.

3.5. Stability data

After 6 months storage at 25 °C, increase in size of SLN ranged from 40.3 to 78.9 nm. Entrapment efficiencies of SLNs of different triglycerides with and without stearylamine were lowered by 1.4–3.5%

Table 2
Entrapment efficiency of clozapine SLNs of different triglycerides with and without stearylamine (mean ± S.D., $n = 3$)

SLN	Percentage of poloxamer	Entrapment efficiency (%)	
		Without stearylamine	With stearylamine
CLZ-TM	0.5	97.2 ± 0.16	–
	1.0	94.2 ± 0.32	98.8 ± 0.13**
	1.5	89.7 ± 0.45	–
CLZ-TP	0.5	95.5 ± 0.22	–
	1.0	93.6 ± 0.31	98.5 ± 0.15**
	1.5	93.4 ± 0.20	–
CLZ-TS	0.5	95.1 ± 0.19	–
	1.0	94.1 ± 0.26	96.5 ± 0.23**
	1.5	93.4 ± 0.35	–

Statistical significances with stearylamine versus without stearylamine are **$p < 0.001$.

after 6 months of storage at 25 °C (Table 3). Transitions of dispersed lipid from metastable forms to stable form might occur slowly on storage due to small particle size and the presence of emulsifier that may lead to drug expulsion from solid lipid nanoparticles [13–15]. Therefore lowered entrapment efficiency observed on storage may be due to drug expulsion during lipid modification.

3.6. Effect of sterilization

Effect of sterilization on particle size, zeta potential and entrapment efficiency was shown in Table 4. In all three lipid-based SLNs, size of the particles increased almost two to three times after sterilization. Zeta potential was shifted from positive to negative in all the SLNs. In the literature it was shown that
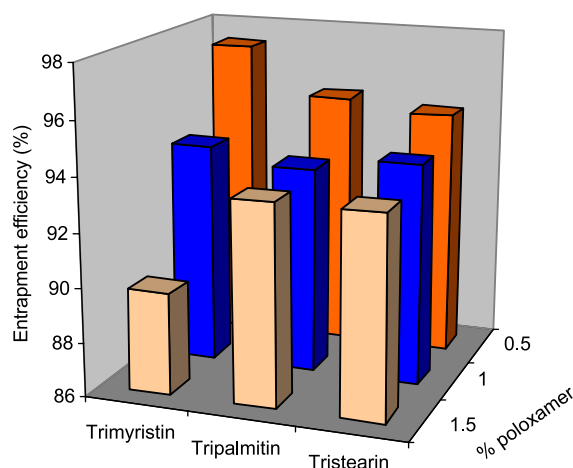

Fig. 2. Effect of poloxamer 188 concentration (0.5%, 1.0% and 1.5%) on entrapment efficiency of clozapine SLNs of different triglycerides (trimyristin, tripalmitin and tristearin).

V. Venkateswarlu, K. Manjunath / Journal of Controlled Release 95 (2004) 627–638

Table 3
Effect of time of storage (at 25 °C) on particle size and entrapment efficiency of SLNs of different triglycerides (trimyristin, tripalmitin and tristearin) with and without stearylamine (1% poloxamer) (mean $\pm$ S.D., $n = 3$)

SLN	Size (nm)			Entrapment efficiency (%)	
	0 day	1 month	6 months	Zero day	6 months
Without stearylamine					
CLZ-TM	224.8 $\pm$ 4.2	232.9 $\pm$ 8.0	265.1 $\pm$ 9.5	94.2 $\pm$ 0.32	92.4 $\pm$ 0.41
CLZ-TP	233.3 $\pm$ 13.4	249.8 $\pm$ 4.4	289.4 $\pm$ 10.4	93.6 $\pm$ 0.31	91.2 $\pm$ 0.29
CLZ-TS	266.3 $\pm$ 8.9	291.5 $\pm$ 7.1	326.5 $\pm$ 12.1	94.1 $\pm$ 0.26	90.6 $\pm$ 0.33
With stearylamine (0.05%)					
CLZ-TM	150.2 $\pm$ 1.5	164.5 $\pm$ 5.7	198.5 $\pm$ 7.4	98.8 $\pm$ 0.13	97.3 $\pm$ 0.24
CLZ-TP	163.3 $\pm$ 0.7	178.9 $\pm$ 8.6	224.3 $\pm$ 11.2	98.5 $\pm$ 0.15	96.4 $\pm$ 0.29
CLZ-TS	96.7 $\pm$ 3.8	123.5 $\pm$ 9.7	175.6 $\pm$ 23.4	96.5 $\pm$ 0.23	93.7 $\pm$ 0.36

autoclaving was possible in case of lecithin stabilized SLNs. However, autoclaving was not suitable for SLNs stabilized with poloxamer series (sterically stabilizing polymers) due to partial collapse of polymer adsorption layer during autoclaving leading to particle aggregation [16]. We have prepared SLNs stabilized with 95% phosphatidlycholine and poloxamer 188 whose particle size was increased two to three times after autoclaving, still they were in nanometer range. It was found that sterilization by autoclaving has least effect on entrapment efficiency (Table 4). Therefore, sterilization by autoclaving can be performed for SLNs of triglycerides (TM, TP and

TS) stabilized with phosphatidylcholine and poloxamer 188.

3.7. Differential scanning calorimetry

Fig. 3a shows DSC curves of clozapine, trimyristin, PM and SM of clozapine with trimyristin and lyophilized CLZ-TM. The thermograms of the lyophilized CLZ-TM and SM did not show the melting peak for the clozapine around 184 °C. This shows that clozapine was not in crystalline state. However, this was confirmed by the presence of melting peak of clozapine in the PM. Endother-

Table 4
Effect of sterilization on particle size, zeta potential and entrapment efficiency of SLNs with and without stearylamine (1% poloxamer) (mean $\pm$ S.D., $n = 3$)

| SLN	Size (nm)		Zeta potential (mV)		Entrapment efficiency (%)	
	Before	After	Before	After	Before	After
Without stearylamine						
BL-TM	145.1 $\pm$ 4.3	362.7 $\pm$ 4.6	$-$ 23.7 $\pm$ 1.5	$-$ 29.2 $\pm$ 0.8	–	–
CLZ-TM	224.8 $\pm$ 4.2	515.7 $\pm$ 29.4	1.1 $\pm$ 0.4	$-$ 3.9 $\pm$ 0.7	94.2 $\pm$ 0.32	89.8 $\pm$ 0.45
BL-TP	111.8 $\pm$ 0.8	282.8 $\pm$ 4.7	$-$ 29.0 $\pm$ 6.0	$-$ 29.1 $\pm$ 0.4	–	–
CLZ-TP	233.3 $\pm$ 3.4	535.7 $\pm$ 30.4	0.2 $\pm$ 0.1	$-$ 5.7 $\pm$ 1.8	93.6 $\pm$ 0.31	88.1 $\pm$ 0.39
BL-TS	152.0 $\pm$ 4.0	310.0 $\pm$ 3.8	$-$ 22.9 $\pm$ 1.0	$-$ 25.7 $\pm$ 0.3	–	–
CLZ-TS	266.3 $\pm$ 8.9	615.6 $\pm$ 35.4	4.1 $\pm$ 0.3	$-$ 4.3 $\pm$ 1.8	94.1 $\pm$ 0.26	90.2 $\pm$ 0.47
With stearylamine						
BL-TM	103.1 $\pm$ 7.5	240.2 $\pm$ 9.5	4.3 $\pm$ 3.8	$-$ 9.4 $\pm$ 0.4	–	–
CLZ-TM	150.2 $\pm$ 1.5	289.0 $\pm$ 10.3	33.2 $\pm$ 0.6	$-$ 6.0 $\pm$ 0.1	98.8 $\pm$ 0.13	94.8 $\pm$ 0.32
BL-TP	60.4 $\pm$ 6.6	174.5 $\pm$ 5.6	4.5 $\pm$ 0.4	$-$ 1.3 $\pm$ 0.1	–	–
CLZ-TP	163.0 $\pm$ 5.4	353.7 $\pm$ 3.1	23.2 $\pm$ 0.9	0.7 $\pm$ 0.6	98.5 $\pm$ 0.15	91.7 $\pm$ 0.41
BL-TS	70.8 $\pm$ 5.4	190.8 $\pm$ 16.6	6.3 $\pm$ 1.6	$-$ 4.9 $\pm$ 0.4	–	–
CLZ-TS	96.7 $\pm$ 3.8	287.4 $\pm$ 10.5	21.3 $\pm$ 1.3	$-$ 7.2 $\pm$ 0.9	96.5 $\pm$ 0.23	92.6 $\pm$ 0.46
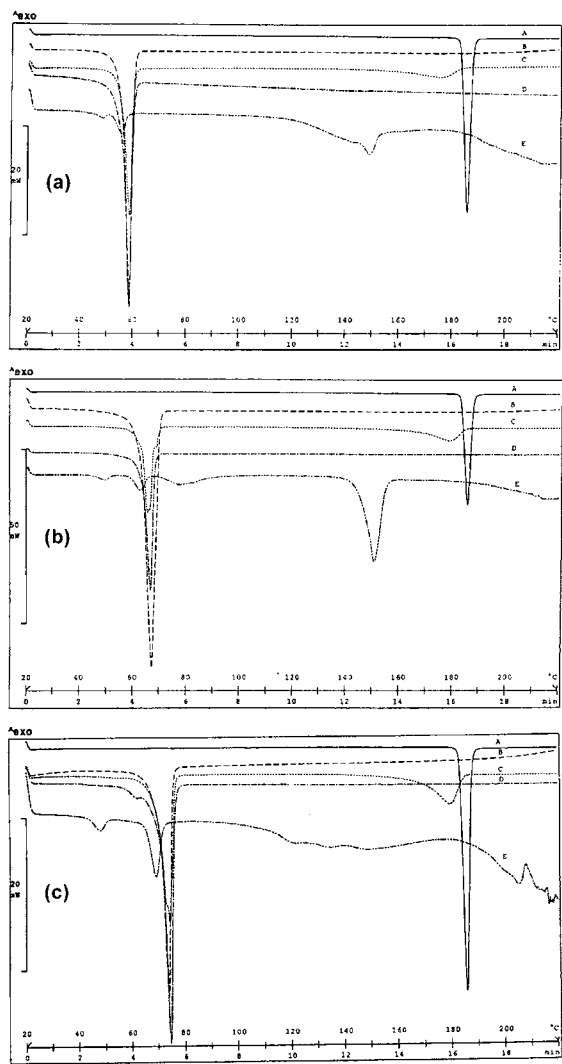
Fig. 3. Overlaid DSC thermograms: clozapine (A), (a) trimyristin (B), physical mixture of clozapine and trimyristin (C), solvent evaporated mixture of clozapine and trimyristin (D) and lyophilized clozapine SLN of trimyristin (E). (b) Tripalmitin (B), physical mixture of clozapine and tripalmitin (C), solvent evaporated mixture of clozapine and tripalmitin (D) and lyophilized clozapine SLN of tripalmitin (E). (c) Tristearin (B), physical mixture of clozapine and tristearin (C), solvent evaporated mixture of clozapine and tristearin (D) and lyophilized clozapine SLN of tristearin (E).

mic peak of glucose used as cryoprotectant was observed at 148.5 °C in CLZ-TM curve. There was no melting peak for clozapine in lyophilized CLZ-TP and CLZ-TS also. This suggests that clozapine was not in crystalline state but it is in amorphous

state. Similar results were reported by Cavalli et al. [17,18] stating that rapid quenching of the microemulsion does not allow the drug to crystallize. DSC analysis of camptothecin SLN prepared by high pressure homogenization showed that camptothecin was in amorphous state [20]. In our method, lipids and clozapine were dissolved in a mixture of solvents and, subsequently, solvents were evaporated. This allowed homogeneous dispersion of drug in the lipid. Furthermore, method of preparation (homogenization followed by ultrasonication) and the presence of surfactants could not allow the drug to crystallize. Thermodynamic stability of lipid nanoparticles depends upon their existing lipid modification. Polymorphic transitions after crystallization of triglyceride nanoparticles are slower for longer chain triglycerides than for shorter chain triglycerides [21], whereas these transitions are faster for small size of crystallites [22]. The type of surfactant and storage time affects the crystallinity of SLN and, consequently, degradation velocity [1]. Degree of crystallinity of lyophilized SLN was

Table 5
Melting peaks, enthalpies and crystallinity of bulk tryglycerides, PMs, SMs and lyophilized SLN

	Parameter	Bulk	PM	SM	Lyophilized SLN
Trimyristin	Melting peak (°C)	57.56	57.92	57.45	55.46
	Enthalpy (J/g)	174.85	156.67	154.41	6.58
	Crystallinity (%)	100	99.5	98.12	64.3
Tripalmitin	Melting peak (°C)	65.08	65.09	65.66	62.83
	Enthalpy (J/g)	209.26	185.91	164.45	8.20
	Crystallinity (%)	100	98.71	87.3	66.9
Tristearin	Melting peak (°C)	72.94	72.69	73.43	68.76
	Enthalpy (J/g)	192.28	170.8	157.83	11.10
	Crystallinity (%)	100	98.69	91.2	98.6

Physical mixture (PM) and solvent evaporated mixture (SM) contain 90% triglyceride; Lyophilized SLN contains 5.85% triglyceride. Degree of crystallinity of PM, SM and lyophilized SLN was calculated by comparing their enthalpy with enthalpy of bulk triglycerides.

V. Venkateswarlu, K. Manjunath / Journal of Controlled Release 95 (2004) 627–638

calculated by comparing enthalpy of SLN with enthalpy of bulk lipid according to Mulhen et al. [7] and Freitas and Muller [23]. Enthalpy of bulk lipid is being taken as 100%. Enthalpy of SLN was calculated on the basis of total weight taken. Crystallinity of SLNs was in the following order: CLZ-TS (98.6%)>CLZ-TP (66.9%)>CLZ-TM (64.3%). Melting points of triglycerides TM, TP and TS in SLN form were depressed when compared to melting points of corresponding bulk triglycerides (Table 5). This suggests that triglycerides in SLNs might be in the β form. Mulhen et al. [7] reported that compritol in SLN was β or βI form. This melting point depression might be due to small particle size (nanometer range), their high specific surface area and the presence of surfactant. This was confirmed by PMs and SMs where such type of melting point depression was not found.

This melting point depression can be attributed to the Kelvin effect [24].

3.8. Powder X-ray diffractometry (PXRD)

Overlaid PXRD patterns of clozapine, triglyceride, PM and SM of clozapine with triglycerides and lyophilized CLZ of triglyceride were shown in Fig. 4a and b. PXRD pattern of clozapine exhibits sharp peaks at 2θ scattered angles 10.5, 17.4, 19.4, 19.7 and 23.7 indicates crystalline nature. In PMs and SMs of all three types of triglycerides, decreased peak intensities were observed at 2θ scattered angles 10.5 and 17.4 for clozapine. This shows that degree of crystallinity of clozapine reduced in PMs and SMs. However, there were no characteristic peaks for clozapine in lyophilized CLZ of triglycerides. This suggests that clozapine was not in crystalline form in SLNs. PXRD
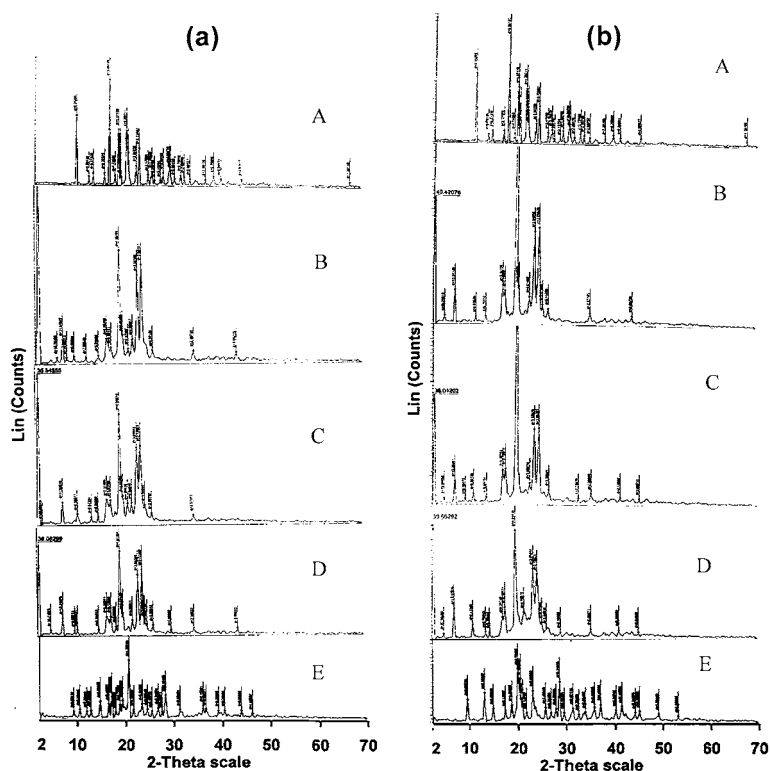

Fig. 4. Overlaid PXRD patterns: clozapine (A), (a) trimyristin (B), physical mixture of clozapine and trimyristin (C), solvent evaporated mixture of clozapine and trimyristin (D) and lyophilized clozapine SLN of trimyristin (E). (b) Tripalmitin (B), physical mixture of clozapine and tripalmitin (C), solvent evaporated mixture of clozapine and tripalmitin (D) and lyophilized clozapine SLN of tripalmitin (E).
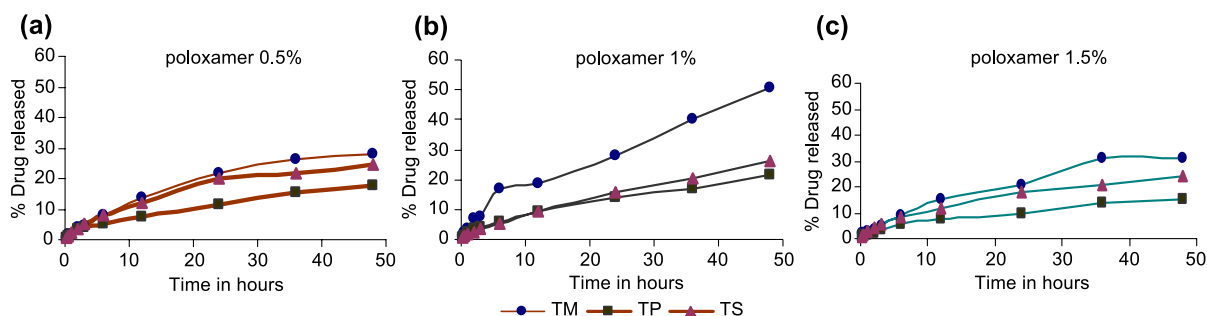
Fig. 5. Effect of triglycerides (trimyristin (TM), tripalmitin (TP) and tristearin (TS)) on in vitro release of clozapine from SLNs of different triglycerides at three different concentrations of poloxamer 188, (a) 0.5%, (b) 1.0% and (c) 1.5%, in the formulation of SLN. Double-distilled water was used as dialysis medium.

pattern of TM shows sharp peaks at 2θ scattered angles 2.6, 34.4, 42.8 and 47.8; these characteristic peaks were observed in PM, SM and lyophilized CLZ-TM indicating that TM was in crystalline state. Similarly, TP and TS were present in crystalline state in PMs, SMs and lyophilized clozapine SLNs. Degree of crystallinity was compared on the basis of peak intensity. Degree of crystallinity of triglycerides of TM, TP and TS was more in case of PM than corresponding SM. Similar trend was observed in DSC studies (Table 5).

3.9. In vitro release kinetics of clozapine from SLN

Many research groups used vertical or flow-through Franz diffusion cells and dialysis bag/tubes for the study of drug release from solid lipid and polymeric nanoparticles and niosomes [19,24–29,31]. Modified Franz diffusion cells with dialysis membrane (pore size

2.4 nm) were used in our study. Dialysis membrane retained nanoparticles and allowed the transfer of the drug immediately into the receiver compartment. Fig. 5a shows the percentage release of clozapine from CLZ-TM, CLZ-TP and CLZ-TS (with 0.5% of poloxamer 188 in the formulations). Similarly, Fig. 5b and c shows clozapine release with 1% and 1.5% poloxamer 188, respectively. Percentage of clozapine released from SLNs up to 48 h were in the following order: CLZ-TP (17.65, 21.42 and 15.32 for 0.5%, 1% and 1.5% of poloxamer 188, respectively) < CLZ-TS (24.5, 26.38 and 24.04) < CLZ-TM (27.83, 50.95 and 31.09). There exists an inverse relation between the percent drug released and partition coefficient of clozapine. SLNs containing 1% poloxamer 188 (possess more surface area due to small particle size, Fig. 1) showed highest percent release than SLNs containing 0.5% and 1.5% poloxamer 188. The slow release of clozapine from SLN suggests that clozapine homogeneously
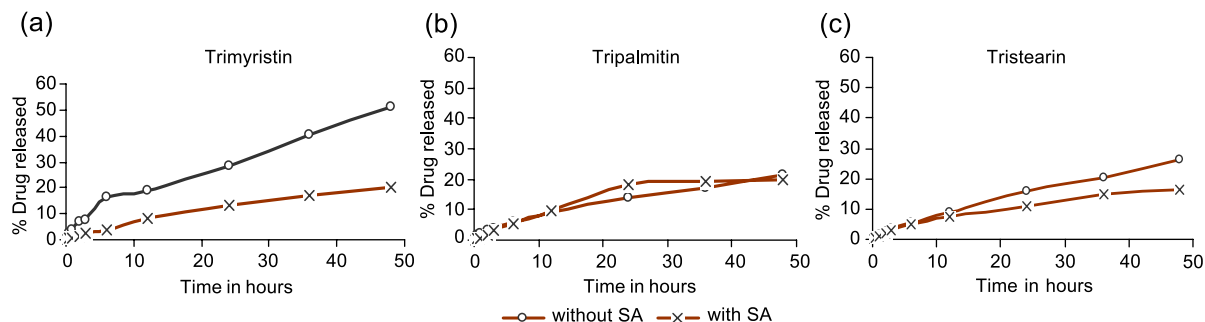

Fig. 6. In vitro release of clozapine from SLNs without and with stearylamine (0.05%) in case of (a) trimyristin SLN, (b) tripalmitin SLN and (c) tristearin SLN. Double-distilled water was used as dialysis medium.

V. Venkateswarlu, K. Manjunath / Journal of Controlled Release 95 (2004) 627–638

Table 6
Nonlinear fits of clozapine released from SLNs with and without stearylamine

SLN	Percentage of poloxamer	Equations			R^2		
		First order, $\ln(Q_0 - Q)$ vs. t	Higuchi, Q vs. $\sqrt{t}$	Weibull, $\ln \ln\{1/(1-Q)\}$ vs. $\ln t$	First order	Higuchi	Weibull
Without stearylamine							
CLZ-TM	0.5	$y = -0.0071x + 0.1441$	$y = 0.054x - 0.2560$	$y = 0.7241x - 3.5917$	0.9525	0.9915	0.9920
	1.0	$y = -0.0138x + 0.1139$	$y = 0.0852x - 0.0433$	$y = 0.7343x - 3.092$	0.9860	0.9804	0.9904
	1.5	$y = -0.008x + 0.2066$	$y = 0.0415x - 0.0180$	$y = 0.5914x - 3.5500$	0.9642	0.9799	0.9575
CLZ-TP	0.5	$y = -0.0074x + 0.3368$	$y = 0.0682x - 0.0382$	$y = 0.8472x - 3.6913$	0.9281	0.9799	0.9906
	1.0	$y = -0.0047x + 0.2999$	$y = 0.0432x - 0.0159$	$y = 0.6285x - 3.5356$	0.9837	0.9954	0.9989
	1.5	$y = -0.0033x + 0.4934$	$y = 0.0386x - 0.0113$	$y = 0.6214x - 3.6057$	0.9573	0.9916	0.9887
CLZ-TS	0.5	$y = -0.006x + 0.3960$	$y = 0.0604x - 0.0249$	$y = 0.7818x - 3.5659$	0.9380	0.9906	0.9850
	1.0	$y = -0.0062x + 0.3511$	$y = 0.0563x - 0.0392$	$y = 0.7219x - 3.6868$	0.9964	0.9815	0.9917
	1.5	$y = -0.0055x + 0.4793$	$y = 0.0607x - 0.0139$	$y = 0.6724x - 3.1819$	0.9527	0.9982	0.9926
With stearylamine							
CLZ-TM	1.0	$y = -0.0049x + 0.7711$	$y = 0.0709x - 0.0562$	$y = 0.9083x - 3.9865$	0.9823	0.9904	0.9927
CLZ-TP	1.0	$y = -0.0052x + 0.7090$	$y = 0.0733x - 0.0513$	$y = 0.9676x - 4.0416$	0.9136	0.9701	0.9896
CLZ-TS	1.0	$y = -0.0038x + 0.7599$	$y = 0.0564x - 0.0326$	$y = 0.8420x - 3.9012$	0.9616	0.9969	0.9901

Q_0 = drug to be released at zero time (mg).
Q = amount of drug released at time t (mg).
t = time in hours.

dispersed in the lipid matrix. SLNs with charge modifier (stearylamine) released lesser percent drug (20.33, 20.06, and 16.18 for CLZ-TM, CLZ-TP and CLZ-TS, respectively) than SLNs without charge modifier (50.95, 21.42 and 26.38) up to 48 h (Fig. 6). Stearylamine contains lipophilic hydrocarbon chain (18 carbons), which is accommodated in the lipid core projecting the amine group into aqueous phase, and induces positive charge [30]. Positively charged clozapine which is entrapped in the nanoparticles experiences repulsion near the interface due to the presence of

stearylamine and thus slow release is observed. Chen et al. [31] fitted release data of paclitaxel from SLN into Higuchi and Weibull equations to study drug release behavior. Thus the obtained release data was fitted into first order, Higuchi and Weibull equations. Release of drug from almost all the SLNs followed Weibul and Higuchi equations better than first-order equation (Table 6). Clozapine which is in amorphous form (confirmed by DSC and PXRD studies) dissolves in lipid, diffuses to the surface and undergoes partitioning between lipid and aqueous phase. Soluble clozapine is
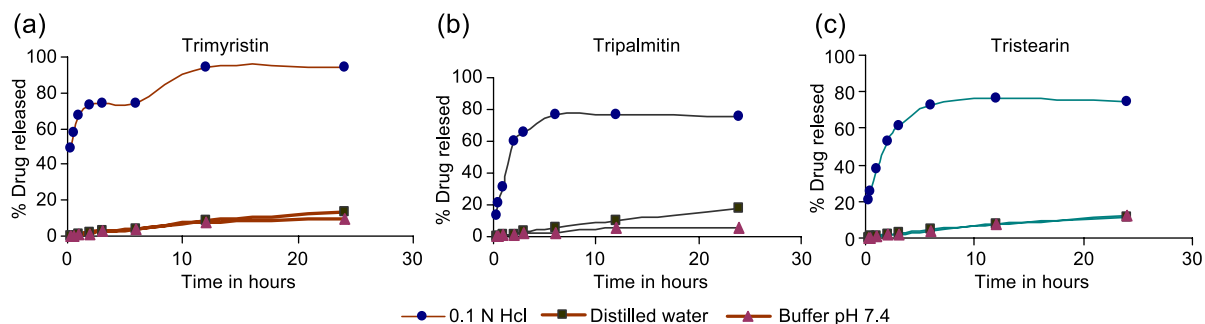

Fig. 7. Effect of pH of dialysis medium on in vitro release of clozapine from SLNs of different triglycerides: (a) trimyristin, (b) tripalmitin and (c) tristearin. Three different dialysis media, 0.1 N HCl, double-distilled water and phosphate buffer, pH 7.4, were used.

partitioned into aqueous phase from which it is dialyzed into the dialysis medium.

3.9.1. Effect of PH of dialysis media on in vitro release of clozapine

Percentage of clozapine released in different dialysis media from SLNs of different triglycerides is shown in Fig. 7a–c. Burst release was obtained when 0.1 N HCl is used as dialysis medium. About 73.33%, 59.72% and 52.38% of clozapine was released within 2 h from CLZ-TM, CLZ-TP and CLZ-TS, respectively, in 0.1 N HCl, whereas slow release was observed in double-distilled water and phosphate buffer, pH 7.4. This study was designed to know whether the clozapine SLN dispersions could be administered orally to improve the oral bioavailability. When lipid formulations of drugs (particle size ranges from 10 to 100 nm) were administered orally, lymphatic transport of SLN through Peyer's patches of intestine is observed [32]. Clozapine released rapidly from these SLN dispersions in acidic environment indicating a need to protect SLN from acidic environments if improved bioavailability has to be achieved via lymphatic transport. These SLN dispersions can be converted into powder form by lyophilization and then suitably compressed to a tablet form. Bioavailability can be improved by applying enteric coat to the tablets of CLZ (work is in progress).

4. Conclusions

Homogenization followed by ultrasonication method is suitable to produce SLN of 60–380 nm size ranges. Lipophilic drugs like clozapine can be successfully loaded in the triglycerides (TM, TP and TS). Sterilization by autoclave method can be used for sterilization of SLN prepared with triglycerides, nontoxic surfactants like poloxamer 188 and phosphatidlycholine. Stearylamine induced optimum zeta potential to CLZ-SLN and also particle size. DSC and PXRD analysis showed amorphous state of clozapine in SLN. Positively charged SLN with stearylamine showed slower release of clozapine. In vitro release of clozapine followed Weibull and Higuchi equations better than first-order equation. This system is most suitable for exploiting lymphatic transport pathway for improving oral bioavailability of clozapine.
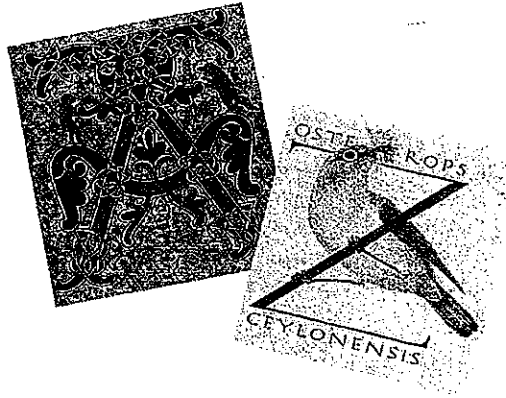
References

[1] C. Olbrich, O. Kayser, R.H. Muller, Lipase degradation of Dynasan 114 and 116 solid lipid nanoparticles (SLN)—effect of surfactants, storage time and crystallinity, Int. J. Pharm. 237 (2002) 119–128.

[2] S. Yang, J. Zhu, Y. Lu, B. Liang, C. Yang, Body distribution of camptothecin solid lipid nanoparticles after oral administration, Pharm. Res. 16 (5) (1999) 751–757.

[3] G.P. Zara, A. Bargoni, R. Cavelli, A. Fundaro, D. Vighetto, M.R. Gasco, Pharmacokinetics and tissue distribution of idarubicin-loaded solid lipid nanoparticles after duodenal administration to rats, J. Pharm. Sci. 91 (5) (2002) 1324–1333.

[4] M.W. Jann, Clozapine, Pharmacotherapy 11 (3) (1991) 179–195.

[5] A. zur Muhlen, W. Mehenert, Drug release and release mechanisms of prednisolone loaded solid lipid nanoparticles, Pharmazie 53 (1998) 552–555.

[6] R. Cavalli, E. Peira, O. Caputo, M.R. Gasco, Solid lipid nanoparticles as carriers of hydrocartisone and progesterone complexes with β-cyclodextrins, Int. J. Pharm. 182 (1999) 59–69.

[7] A. zur Muhlen, C. Schwarz, W. Mehenert, Solid lipid nanoparticles (SLN) for controlled drug delivery—drug release and release mechanisms, Eur. J. Pharm. Biopharm. 45 (1998) 149–155.

[8] S.C. Yang, L.F. Lu, Y. Cai, J.B. Zhu, B.W. Liang, C.Z. Yang, Body distribution in mice of intravenously injected camptothecin solid lipid nanoparticles and targeting effect on brain, J. Control. Release 59 (1999) 299–307.

[9] M.R. Gasco, Method for producing solid lipid microspheres having narrow size distribution, U.S. Patent 5,250,236, 1993.

[10] R.H. Muller, W. Mehenert, J.S. Lucks, A. Schwarz, M.H. Zur, C. Weyhers, D.R. Freitas, Solid lipid nanoparticles (SLN)—an alternative colloidal carrier system for controlled drug delivery, Eur. J. Pharm. Biopharm. 41 (1995) 62–69.

[11] A. Dingler, S. Gohla, Production of solid lipid nanoparticles (SLN): scaling up feasibilities, J. Microencapsul. 19 (1) (2002) 11–16.

[12] F.Q. Hu, H. Yuan, H.H. Zhang, M. Fang, Preparation of solid lipid nanoparticles with clobetasol propionate by a novel sol-

vent diffusion method in aqueous system and physicochemical characterization, Int. J. Pharm. 239 (1–2) (2002) 121–128.

[13] W. Mehnert, K. Mader, Solid lipid nanoparticles production, characterization and applications, Adv. Drug Deliv. Rev. 47 (2001) 165–196.

[14] K. Westesen, B. Siekmann, M.H.J. Koch, Investigations on the physical state of the lipid nanoparticles by synchrotron radiation X-ray diffraction, Int. J. Pharm. 93 (1993) 189–199.

[15] H. Bunjes K. Westesen, Do nanoparticles prepared from lipids solids at room temperature always possess a solid lipid matrix? Int. J. Pharm. 115 (1995) 129–131.

[16] R.H. Muller, K. Mader, S. Gohla, Solid lipid nanoparticles (SLN) for controlled drug delivery—a review of the state of the art, Eur. J. Pharm. Biopharm. 50 (2000) 161–177.

[17] R. Cavalli, D. Aquilano, M.E. Carrlotti, M.R. Gasco, Study by X-ray powder diffraction and differential scanning calorimetry of two model drugs, phenothiazine and nifedipine, incorporated into lipid nanoparticles, Eur. J. Pharm. Biopharm. 41 (1995) 329–333.

[18] R. Cavalli, O. Caputo, M.E. Carlotti, M. Trotta, C. Scarnecchia, M.R. Gasco, Sterilization and freeze–drying of drug-free and drug-loaded solid lipid nanoparticles, Int. J. Pharm. 148 (1997) 47–54.

[19] R. Cavalli, O. Caputo, M.R. Gasco, Preparation and characterization of solid lipid nanospheres containing paclitaxel, Eur. J. Pharm. Sci. 10 (2000) 305–309.

[20] S.C. Yang, J.B. Zhu, Preparation and characterization of camptothecin solid lipid nanoparticles, Drug Dev. Ind. Pharm. 28 (3) (2002) 265–274.

[21] H. Bunjes, K. Westesen, M.H.J. Koch, Crystallization tendency and polymorphic transitions in triglyceride nanoparticles, Int. J. Pharm. 129 (1996) 159–173.

[22] K. Westesen, H. Bunjes, M.H.J. Koch, Physicochemical characterization of lipid nanoparticles and evaluation of their drug loading capacity and sustained release potential, J. Control. Release 48 (1997) 223–236.

[23] C. Freitas, R.H. Muller, Correlation between long-term stability of solid lipid nanoparticles (SLN™) and crystallinity of the lipid phase, Eur. J. Pharm. Biopharm. 47 (1999) 125–132.

[24] V. Jenning, A.F. Thunemann, S.H. Gohla, Characterization of a novel solid lipid nanoparticle carrier system based on binary mixtures of liquid and solid lipids, Int. J. Pharm. 199 (2000) 167–177.

[25] V. Jenning, M. Schafer-Korting, S. Gohla, Vitamin A-loaded solid lipid nanoparticles for topical use: drug release properties, J. Control. Release 66 (2000) 115–126.

[26] A. Geze, M.C. Venier-Julienne, D. Mathieu, R. Filmon, R. Phan-Tan-Luu, J.P. Benoit, Development of 5-iodo-2-deoxyuridine milling process to reduce initial burst release from PLGA microparticles, Int. J. Pharm. 178 (1999) 257–268.

[27] N. Kun, P. Keun-Hong, W.K. Sung, H.B. You, Self-assembled hydrogel nanoparticles from curdlan derivatives: characterization, anti-cancer drug release and interaction with a hepatoma cell line (HepG2), J. Control. Release 69 (2000) 225–236.

[28] T.P. Maria, G. Ruxandra, M. Yoshiharu, D. Avi, L. Noah, L. Robert, PEG-coated nanospheres from amphiphilic diblock and multiblock copolymers: investigation of their drug encapsulation and release characteristics, J. Control. Release 46 (1997) 223–231.

[29] M. Maria, S. Chiara, V. Donatella, L. Giuseppe, M.F. Anna, Niosomes as carriers for tretinoin: I. Preparation and properties, Int. J. Pharm. 234 (2002) 237–248.

[30] M.P.Y. Piemi, D. Korner, S. Benita, J.-P. Marty, Positively and negatively charged submicron emulsions for enhanced topical delivery of antifungal drugs, J. Control. Release 58 (2) (1999) 177–187.

[31] D.-B. Chen, T.-Z. Yang, W.-L. Lu, Q. Zhang, In vitro and in vivo study of two types of long-circulating solid lipid nanoparticles containing paclitaxel, Chem. Pharm. Bull. 49 (11) (2001) 1444–1447.

[32] C.J.H. Porter, W.N. Charman, Intestinal lymphatic drug transport: an update, Adv. Drug Deliv. Rev. 50 (2001) 61–80.

EXHIBIT I

The
American
Heritage® Dictionary
of the English Language

FOURTH EDITION

mon•o¹ (mŏn′ō) *n. Informal* Infectious mononucleosis.

mon•o² (mŏn′ō) *adj. Informal* Monaural; monophonic. [Short for MONOPHONIC.]

mono– or **mon–** *pref.* **1.** One; single; alone: *monomorphic.* **2.** Containing a single atom, radical, or group: *monobasic.* **3.** Monomolecular; monatomic: *monolayer.* [Middle English, from Old French, from Latin, from Greek, from *monos*, single, alone. See **men-⁴** in Appendix I.]

mon•o•ac•id (mŏn′ō-ăs′ĭd) *n.* An acid having one replaceable hydrogen atom. ❖ *adj.* also **mon•o•a•cid•ic** (-ə-sĭd′ĭk) Having only one hydroxyl group to react with acids.

mon•o•am•ine (mŏn′ō-ăm′ēn, -ə-mēn′) *n.* An amine compound containing one amino group, especially a compound that functions as a neurotransmitter.

monoamine oxidase *n. Abbr.* **MAO** An enzyme in the cells of most tissues that catalyzes the oxidation of monoamines such as norepinephrine and serotonin.

monoamine oxidase inhibitor *n. Abbr.* **MAOI** Any of a class of antidepressant drugs that block the action of monoamine oxidase in the brain, thereby allowing the accumulation of monoamines such as norepinephrine.

mon•o•ba•sic (mŏn′ə-bā′sĭk) *adj.* **1.** Having only one hydrogen ion to donate to a base in an acid-base reaction; monoprotic. **2.** Having only one metal ion or positive radical.

mon•o•carp (mŏn′ə-kärp′) *n.* A monocarpic plant.

mon•o•car•pel•lar•y (mŏn′ə-kär′pə-lĕr′ē) *adj.* Consisting of only one carpel.

mon•o•car•pic (mŏn′ə-kär′pĭk) also **mon•o•car•pous** (-kär′pəs) *adj.* Flowering and bearing fruit only once.

mon•o•ce•phal•ic (mŏn′ō-sə-făl′ĭk) *adj.* Bearing one flower head, as in the scape of a dandelion.

Mo•noc•er•os (mə-nŏs′ər-əs) *n.* A constellation near Canis Major and Canis Minor. [Middle English, unicorn, from Old French, from Latin *monocerōs*, from Greek *monokerōs*, having one horn : *mono-*, mono- + *keras*, horn; see **ker-¹** in Appendix I.]

mon•o•cha•si•um (mŏn′ə-kā′zē-əm, -zhē-) *n., pl.* **-si•a** (-zē-ə, -zhē-ə, -zhə) A cyme having a single flower on each axis. [MONO– + (DI)CHASIUM.] **—mon′o•cha′si•al** *adj.*

mon•o•chord (mŏn′ə-kôrd′) *n.* An acoustic instrument consisting of a sounding box with one string and a movable bridge, used to study musical tones. [Middle English *monocorde*, from Old French, from Medieval Latin *monochordum*, from Greek *monokhordon* : *mono-*, mono- + *khordē*, string; see **CORD**.]

mon•o•chro•mat (mŏn′ə-krō′măt) *n.* A person with monochromatism.

mon•o•chro•mat•ic (mŏn′ə-krō-măt′ĭk) *adj.* **1.** Having or appearing to have only one color. **2.** Of or composed of radiation of only one wavelength: *monochromatic light.* **3.** Done in monochrome: *monochromatic prints and paintings.* **4.** Of or exhibiting monochromatism. **—mon′o•chro•mat′i•cal•ly** *adv.* **—mon′o•chro′ma•tic′i•ty** (-mə-tĭs′ĭ-tē) *n.*

mon•o•chro•ma•tism (mŏn′ə-krō′mə-tĭz′əm) *n.* The condition of being completely colorblind.

mon•o•chrome (mŏn′ə-krōm′) *n.* **1a.** A picture, especially a painting, done in different shades of a single color. **b.** The art or technique of executing such a picture. **2.** The state of being in a single color. **3.** A black-and-white image, as in photography or on television. [Medieval Latin *monochrōma*, from feminine of Greek *monokhrōmos*, of one color : *mono-*, mono- + *khrōma*, color.] **—mon′o•chrome′, mon′o•chro′mic** (-krō′mĭk) *adj.*

mon•o•cle (mŏn′ə-kəl) *n.* An eyeglass for one eye. [French, from Late Latin *monoculus*, having one eye : Greek *mono-*, mono- + Latin *oculus*, eye; see **ok*ʷ*-** in Appendix I.] **—mon′o•cled** (-kəld) *adj.*

mon•o•cline (mŏn′ə-klīn′) *n.* A geologic structure in which all layers are inclined in the same direction. **—mon′o•cli′nal** *adj.*

mon•o•clin•ic (mŏn′ə-klĭn′ĭk) *adj.* Of or relating to three unequal crystal axes, two of which intersect obliquely and are perpendicular to the third.

mon•o•cli•nous (mŏn′ə-klī′nəs) *adj.* Having pistils and stamens in the same flower. [New Latin *monoclinus* : MONO– + Greek *klīnē*, bed; see **klei-** in Appendix I.]

mon•o•clo•nal (mŏn′ə-klō′nəl) *adj.* Of, forming, or derived from a single clone: *a monoclonal population of tumor cells.* ❖ *n.* A monoclonal product, especially a monoclonal antibody.

monoclonal antibody *n.* Any of the highly specific antibodies produced in large quantity by the clones of a single hybrid cell formed in the laboratory by the fusion of a B cell with a tumor cell.

mon•o•coque (mŏn′ə-kōk′, -kŏk′) *n.* A metal structure, such as an aircraft, in which the skin absorbs all or most of the stresses to which the body is subjected. [French : *mono-*, mono- + *coque*, shell (from Old French, from Latin *coccum*, berry, from Greek *kokkos*).]

mon•o•cot (mŏn′ə-kŏt′) *n.* A monocotyledon.

mon•o•cot•y•le•don (mŏn′ə-kŏt′l-ēd′n) *n.* Any of various flowering plants, such as grasses, orchids, and lilies, having a single cotyledon in the seed. **—mon′o•cot′y•le′don•ous** *adj.*

mo•noc•ra•cy (mō-nŏk′rə-sē, mə-) *n., pl.* **-cies** Government or rule by a single person; autocracy. **—mon′o•crat′** (mŏn′ə-krăt′) *n.* **—mon′o•crat′ic** *adj.*

mo•noc•u•lar (mō-nŏk′yə-lər, mə-) *adj.* **1.** Having or relating to one eye. **2.** Of, relating to, or intended for use by only one eye: *a monocular microscope.* [From Late Latin *monoculus*, having one eye. See **MONOCLE**.] **—mo•noc′u•lar•ly** *adv.*

mon•o•cul•ture (mŏn′ə-kŭl′chər) *n.* **1.** The cultivation of a single crop on a farm or in a region or country. **2.** A single, homogeneous culture without diversity or dissension. **—mon′o•cul′tur•al** *adj.*

mon•o•cy•cle (mŏn′ə-sī′kəl) *n.* A unicycle.

mon•o•cy•clic (mŏn′ə-sī′klĭk, -sĭk′lĭk) *adj.* **1.** Having a single cycle, as of activity or development. **2.** *Biology* Having a single whorl, as certain flowers and the shells of certain invertebrates. **3.** *Chemistry* Having a molecular structure with only one ring.

mon•o•cyte (mŏn′ə-sīt′) *n.* A large, circulating, phagocytic white blood cell, having a single well-defined nucleus and very fine granulation in the cytoplasm. Monocytes constitute from 3 to 8 percent of the white blood cells in humans. **—mon′o•cyt′ic** (-sĭt′ĭk), **mon′o•cy′toid′** (-sī′toid′) *adj.*

mon•o•cy•to•sis (mŏn′ə-sī-tō′sĭs) *n., pl.* **-ses** (-sēz) An abnormal increase of monocytes in the blood, occurring in infectious mononucleosis and certain bacterial infections such as tuberculosis.

Mo•nod (mō-nō′), **Jacques Lucien** 1910–1976. French biochemist. He shared a 1965 Nobel Prize for the study of regulatory activity in body cells.

mon•o•dac•tyl (mŏn′ə-dăk′təl) *n.* An animal having only one toe, digit, or claw on each extremity. **—mon′o•dac′ty•lous** *adj.*

mon•o•dra•ma (mŏn′ə-drä′mə, -drăm′ə) *n.* A dramatic composition for one performer. **—mon′o•dra•mat′ic** (-drə-măt′ĭk) *adj.*

mon•o•dy (mŏn′ə-dē) *n., pl.* **-dies** **1.** An ode for one voice or actor, as in Greek drama. **2.** A poem in which the poet or speaker mourns another's death. **3.** *Music* **a.** A style of composition that is dominated by a single melodic line. **b.** A style of composition having a single melodic line; monophony. **c.** A composition in either of these styles. [Late Latin *monōdia*, from Greek *monōidiā* : *mono-*, mono- + *aoidē, ōidē*, song; see **wed-²** in Appendix I.] **—mo•nod′ic** (mə-nŏd′ĭk), **mo•nod′i•cal** (-ĭ-kəl) *adj.* **—mo•nod′i•cal•ly** *adv.* **—mon′o•dist** (mŏn′ə-dĭst) *n.*

mo•noe•cious also **mo•ne•cious** (mə-nē′shəs) *adj.* **1.** *Botany* Having unisexual reproductive organs or flowers, with the organs or flowers of both sexes borne on a single plant, as in corn and pines. **2.** *Biology* Relating to or exhibiting hermaphroditism; hermaphroditic. [New Latin *Monoecia*, class name : MONO– + Greek *oikiā*, dwelling; see **weik-¹** in Appendix I.] **—mo•noe′cious•ly** *adv.* **—mo•noe′cism** (mə-nē′sĭz′əm) *n.*

mon•o•es•ter (mŏn′ō-ĕs′tər) *n.* An ester having only one ester group.

mon•o•fil•a•ment (mŏn′ə-fĭl′ə-mənt) *n.* A single strand of untwisted synthetic fiber, such as nylon, used especially for fishing line.

mo•nog•a•my (mə-nŏg′ə-mē) *n.* **1.** The practice or condition of having a single sexual partner during a period of time. **2.** The practice of marrying only once in a lifetime. **3.** *Zoology* The condition of having only one mate during a breeding season or during the breeding life of a pair. **—mo•nog′a•mist** *n.* **—mo•nog′a•mous** *adj.* **—mo•nog′a•mous•ly** *adv.*

mon•o•ge•ne•an (mŏn′ə-jē′nē-ən) *n.* Any of various trematodes of the order Monogenea that typically pass the entire life cycle as ectoparasites on a single fish. [From New Latin *Monogenea*, order name : MONO– + Greek *geneā*, race; see **GENEALOGY**.] **—mon′o•ge′ne•an** *adj.*

mon•o•gen•e•sis (mŏn′ə-jĕn′ĭ-sĭs) *n.* **1.** The theory that all living organisms are descended from a single cell or organism. **2.** Asexual reproduction, as by sporulation. **—mo•nog′e•nous** (mə-nŏj′ə-nəs) *adj.*

mon•o•ge•net•ic (mŏn′ə-jə-nĕt′ĭk) *adj.* **1.** Relating to or exhibiting monogenesis. **2.** Having a single host through the course of the life cycle. **3.** Produced under a single set of continuing conditions. Used of soil.

mon•o•gen•ic (mŏn′ə-jĕn′ĭk) *adj.* **1a.** Of or relating to monogenesis; monogenetic. **b.** Relating to monogenism. **2.** Of or regulated by one gene or one of a pair of allelic genes. **3.** Producing offspring of only one sex, as some species of aphids. **—mon′o•gen′i•cal•ly** *adv.*

mo•nog•e•nism (mə-nŏj′ə-nĭz′əm) *n.* The theory that all humans are descended from a single pair of ancestors. **—mo•nog′e•nist** *n.* **—mo•nog′e•nis′tic** *adj.*

mon•o•glot (mŏn′ə-glŏt′) *n.* A person who knows only one language. ❖ *adj.* Monolingual. [MONO– + (POLY)GLOT.]

mon•o•gram (mŏn′ə-grăm′) *n.* A design composed of one or more letters, typically the initials of a name, used as an identifying mark. ❖ *tr.v.* **-grammed, -gram•ming, -grams** also **-gramed, -gram•ing, -grams** To mark with a design composed of one or more letters. [Late Latin *monogramma*, from Late Greek *monogramma*, from neuter of *monogrammos*, consisting of a single letter : Greek *mono-*, mono- + Greek *gramma*, letter; see **–GRAM**.] **—mon′o•gram•mat′ic** (-grə-măt′ĭk) *adj.*

mon•o•graph (mŏn′ə-grăf′) *n.* A scholarly piece of writing of essay or book length on a specific, often limited subject. ❖ *tr.v.* **-graphed, -graph•ing, -graphs** To write a monograph on. **—mo•nog′ra•pher** (mə-nŏg′rə-fər) *n.* **—mon′o•graph′ic** *adj.* **—mon′o•graph′i•cal•ly** *adv.*

mo•nog•y•ny (mə-nŏj′ə-nē) *n.* The practice or condition of having only one wife at a time. **—mo•nog′y•nist** *n.* **—mo•nog′y•nous** *adj.*

mon•o•hy•brid (mŏn′ō-hī′brĭd) *n.* The hybrid of parents that differ at only one gene locus, for which each parent is homozygous with a different allele.
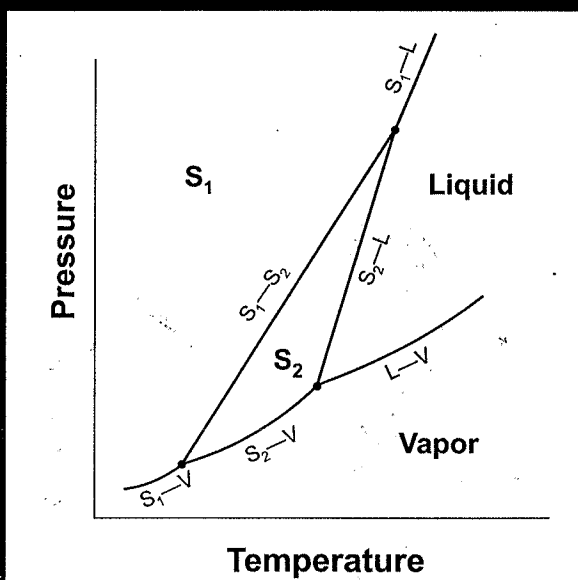
mon•o•hy•drate (mŏn′ō-hī′drāt′) *n.* A compound, such as calcium chloride monohydrate, $CaCl_2 \cdot H_2O$, that contains one molecule of water. **—mon′o•hy′drat•ed** *adj.*

EXHIBIT J

Polymorphism in Pharmaceutical Solids

edited by
Harry G. Brittain

DRUGS AND THE PHARMACEUTICAL SCIENCES

Executive Editor

James Swarbrick
AAI, Inc.
Wilmington, North Carolina

Advisory Board

Larry L. Augsburger
University of Maryland
Baltimore, Maryland

David E. Nichols
Purdue University
West Lafayette, Indiana

Douwe D. Breimer
Gorlaeus Laboratories
Leiden, The Netherlands

Stephen G. Schulman
University of Florida
Gainesville, Florida

Trevor M. Jones
The Association of the
British Pharmaceutical Industry
London, United Kingdom

Jerome P. Skelly
Copley Pharmaceutical, Inc.
Canton, Massachusetts

Hans E. Junginger
Leiden/Amsterdam Center
for Drug Research
Leiden, The Netherlands

Felix Theeuwes
Alza Corporation
Palo Alto, California

Vincent H. L. Lee
University of Southern California
Los Angeles, California

Geoffrey T. Tucker
University of Sheffield
Royal Hallamshire Hospital
Sheffield, United Kingdom

Peter G. Welling
Institut de Recherche Jouveinal
Fresnes, France

252   **Brittain**
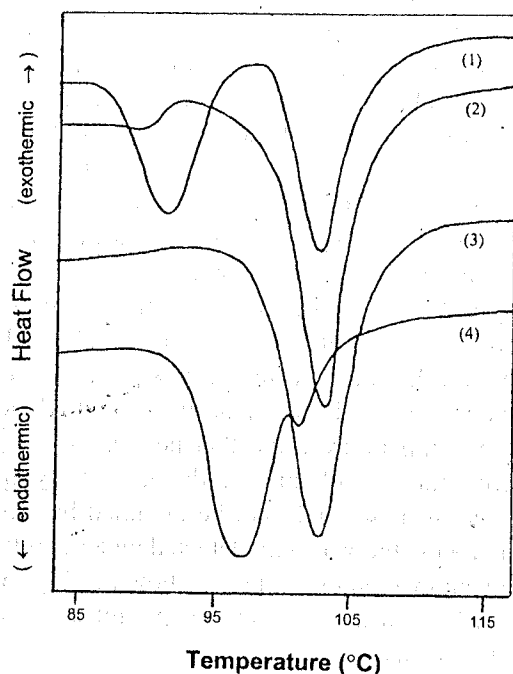
Fig. 6   Differential scanning calorimetry study of various spray-dried forms of phenylbutazone. Shown are the thermograms of (1) Form α, (2) Form β, (3) Form δ, and (4) Form ε. (The figure was adapted from data contained in Ref. 79.)

routinely on a quantitative basis, and for this reason it has become the most widely accepted method of thermal analysis for the pharmaceutical industry. The relevance of the DSC technique as a tool for pharmaceutical scientists has been amply discussed in numerous reviews [66,83–86], and a general chapter on DSC is documented in the *United States Pharmacopoeia* [87].

In the DSC method, the sample and reference materials are maintained at the same temperature, and the heat flow required to keep the equality in temperature is measured. DSC plots are therefore obtained as the differential rate of heating (in units of W/s, cal/s, or J/s) against temperature [88]. The area under a DSC peak is directly proportional to the heat absorbed or evolved by the thermal event, and integration

of these peak areas yields the heat of reaction (in units of cal/s · g or J/s · g).

Two types of DSC measurements are possible, which are usually identified as power-compensation DSC and heat-flux DSC, and the details of each have been fully described [88,89]. In power-compensated DSC, the sample and reference materials are kept at the same temperature by the use of individualized heating elements, and the observable parameter recorded is the difference in power inputs to the two heaters. In heat-flux DSC, one simply monitors the heat differential between the sample and the reference materials, with the methodology not being much different from that used for DTA.

In the DTA measurement, an exothermic reaction is plotted as a positive thermal event, while an endothermic reaction is usually displayed as a negative event. Unfortunately, the use of power-compensation DSC results in endothermic reactions being displayed as positive events, a situation counter to the latest IUPAC recommendations [90]. When the heat-flux method is used to detect the thermal phenomena, the signs of the DSC events concur with those obtained using DTA and also agree with the IUPAC recommendations.

The calibration of DSC instruments is normally accomplished through the use of compounds having accurately known transition temperatures and heats of fusion. A list of the standards currently supplied by the National Technical Information Service (NTIS) [91] is provided in Table 2. Once the DSC system is properly calibrated, it is trivial to obtain the melting point and enthalpy of fusion data for any compound upon integration of its empirically determined endotherm and application of the calibration parameters. The current state of methodology is such, however, that unless a determination is repeated a large number of times, the deduced enthalpies must be regarded as being accurate only to within approximately 5%.

As has been noted for DTA analysis, differential scanning calorimetry can also be used to establish the melting points of polymorphic species. For example, gepirone hydrochloride has been obtained in three polymorphic forms, which were found to melt at 180°C, 200°C, and 212°C [92]. In this work, it was shown that Forms I and II, and Forms I and III, were enantiotropic pair systems, but that Forms II and III were monotropic with respect to each other. The two polymorphs of phenylephrine oxazolidine each exhibited well-defined melting

EXHIBIT K

Characterization and Solid-State Transformations of the Pseudopolymorphic Forms of Sodium Naproxen

Young-soo Kim and Ronald W. Rousseau*

School of Chemical & Biomolecular Engineering, Georgia Institute of Technology, Atlanta, Georgia 30332-0100

ABSTRACT: Sodium naproxen is an antiinflammatory nonsteroidal drug used in the treatment of rheumatoid and arthritic diseases. Three pseudopolymorphic forms have been reported in the literature, along with characterizations of anhydrous and dihydrated forms. In the present work, the monohydrated form of sodium naproxen was prepared by dehydration of the dihydrated form and investigated with thermogravimetric analysis (TGA), differential scanning calorimetry (DSC), powder X-ray diffraction (PXRD) and microscopy. Characteristic properties of the monohydrated form were compared to the anhydrous and the dihydrated forms, and the transformation of higher hydrated forms to lower ones was performed in an oven or a desiccator without generating other polymorphic forms. DSC and isothermal TGA experiments determined the structural characteristics and mechanisms by which two types of water were removed from the hydrated species.

Introduction

Incorporation of solvent into the lattice of crystalline solids results in the formation of molecular adducts known as solvates. When the incorporated solvent is water, the solvates are called hydrates. A new and different unit cell, often leading to different physical properties, results with solvate formation, i.e., properties of solvates, such as density, solubility, dissolution rate, and bioavailability, are different from those of nonsolvated species. These physical property changes are analogous to those associated with polymorphism, and therefore solvates are often referred to as pseudopolymorphs to distinguish them from polymorphs.[1]

Pharmaceutical solids may come in contact with water during processing steps, such as crystallization, lyophilization, wet granulation, aqueous film-coating, or spray-drying, and they may be exposed to humid air during storage. Absorbed water molecules may reside on crystal surfaces or in crystal lattice structures, but when the absorbed water enters the lattice structure it can change the packing in the unit cell.

Naproxen ((*S*)-(+)-6-methoxy-α-methyl-2-naphthaleneacetic acid), is an antiinflammatory nonsteroidal drug used in the therapy of rheumatoid and arthritic diseases. Because the sodium salt of naproxen whose structure is shown in Figure 1, has much higher solubility in water than naproxen itself, it is of greater industrial importance.

Crystal structures have been determined for naproxen[2] and for the monohydrate[3] and anhydrate[4] of sodium naproxen. Study of the conformation of naproxen and the importance of intramolecular hydrogen-bond-like (HBL), e.g., C−H···O−C, interactions identified the four stable conformers for which HBL interactions play an important role.[5] Bansal et al.[6] observed differences in dissolution rates of hydrated tablets obtained by wet granulation from the anhydrous form,
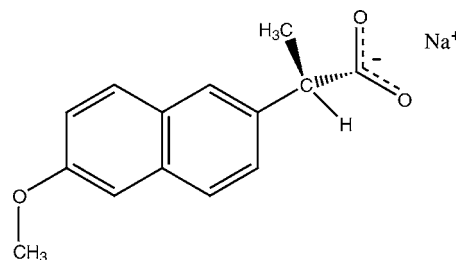
Figure 1. Schematic diagram of naproxen anion and sodium cation.

and the anhydrate and dihydrate of sodium naproxen have been characterized.[7]

Relatively little work had been done on sodium naproxen monohydrate prior to the current research. Our purpose here is 2-fold: (1) to characterize the monohydrated form, especially by comparing it to both the anhydrate and the dihydrate, and (2) to determine the energetics associated with transformation of the hydrated sodium naproxen to species of lower degrees of hydration.

Experimental Section

Materials. Naproxen sodium, supplied by Albemarle Corp., was used in experiments without further purification or processing. Cooling recrystallization was used to produce the dihydrated crystalline form of sodium naproxen; a total of 35 g of anhydrous sodium naproxen was dissolved in 100 mL of pure water (HPLC-grade purchased from Fisher Scientific) at 35 °C. The solution was cooled until recrystallization occurred. The slurry then was heated to 25 °C and filtered under vacuum, and the resulting filter cake was dried under ambient conditions. The monohydrated form of sodium naproxen was prepared by drying the dihydrate in a desiccator for 2 days. Every sample was analyzed with X-ray powder diffraction to ensure that either the anhydrate or the desired hydrate had been formed.

Thermogravimetric Analysis (TGA). The loss of mass from sodium naproxen samples was analyzed with a TG/DTA 320 instrument (Seiko Instruments Inc.). Samples of mass 10−15 mg were heated from 21−150 °C in aluminum pans that

* Corresponding author address: 311 Ferst Drive, Atlanta, GA 30332, USA. Phone: 404-894-2867, Fax: 404-385-0185. E-mail: rwr@chbe.gatech.edu.

Kim and Rousseau

were 5 mm in diameter. An empty aluminum pan was used as the reference. A heating rate of 10 °C/min was employed with a nitrogen purging rate of 90 mL/min. Open pans without lids were used and prominent peaks were observed. All TGA runs were carried out with open pans, as recommended by Di Martino et al.[7]

Differential Scanning Calorimetry (DSC). Heat flow from the samples for the dehydration and melting endotherms was measured with a DSC 220C instrument (Seiko Instruments Inc.). The temperature axis and cell constant of the DSC were calibrated with indium. The temperature range of the experiments was from 23 to 290 °C in aluminum pans that were 7 mm in diameter. DSC runs were performed at a ramping rate of 10 °C/min under nitrogen purge at a rate of 90 mL/min. Quantitative evaluation of energies associated with phase transformations required the use of open pans in the DSC experiments.[7]

Powder X-ray Diffraction (PXRD). Crystals were analyzed and identified by powder X-ray diffraction (PXRD) analysis using Philips PW1800 automatic powder diffractometer with APD 3720 analysis software. About 1 to 2 g of crystals was required. Each crystal sample was ground to a fine powder with a mortar and pestle before being pressed into the sample holder. Copper Kα radiation was used. The radiation for Copper Kα1 is 1.54056 Å. The PXRD patterns were made over a diffraction−angle (2θ) range of 1.02 to 80°, with a step size of 0.02 ° and a counting time of 1 s per step.

High-Performance Liquid Chromatography (HPLC). HPLC (Shimadzu) was used for the measurement of solution concentration, hence solubility. The chromatographic separation was performed on a reverse-phase column Varian Microsorb-MV 100-3 C18 column. A wavelength of 254 nm was used in the SPD-10AV detector. The voltage signal from the detector was interpreted by the Shimadzu CLASS−VP Chromatography Data system version 4.2 software program running on a personal computer. Two mobile phases were prepared. One was pure acetonitrile (Acros Organics) and the other was a mixture of 2% acetic acid (Sigma-Aldrich) and 98% water (volume ratio). Each mobile phase was connected to the delivery module of the HPLC. The flow rates from each reservoir were 0.5 mL/min and, totally, 1.0 mL/min. Butyrophenone (Sigma-Aldrich) was dissolved into acetonitrile and used as the internal standard.

Microscopy. Crystal samples were analyzed under the Leica DM LM microscope with the objective lens of 20×. The microscope was equipped with a Sony DKC-5000 digital camera that converted the focused light into a digital signal. This signal was visualized by Image-Pro Plus version 4.5.

Results and Discussion

Crystallization and Hydrate Transformation. Crystallization of sodium naproxen from water at the conditions described above produced a dense network of needlelike crystals. Although the mass of crystals prevented subsequent rotation of a magnetic stirrer, the residual mother liquor was easily expressed from the crystal mass during filtration. The crystals were less than 25 μm in thickness and as long as several millimeters. Unfortunately, crystals of this size were unacceptable for single-crystal X-ray diffraction analysis.

Over the range of temperatures examined in the present research, only the dihydrate of sodium naproxen was formed on crystallization from water, which is consistent with earlier work by Di Martino et al.[7] Other known pseudopolymorphs of sodium naproxen can be produced using different protocols. For example, Kim et al.[3] reported that recrystallization from a solvent comprised of pure methanol and the water absorbed from the atmosphere during the evaporation resulted in formation of monohydrated crystals. We were able
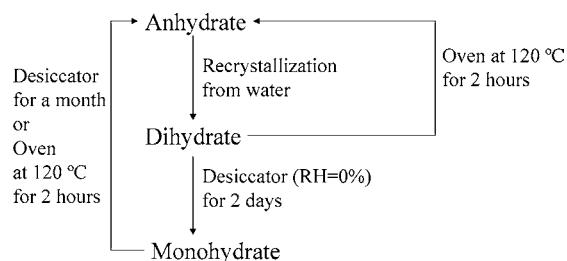
Figure 2. The path for the change between pseudopolymorphic forms of sodium naproxen.

to obtain anhydrous crystals using the procedure of Kim et al., by immediately coating the recovered crystals with oil, thereby preventing absorption of water from the atmosphere. Phan et al.[8] also reported formation of the monohydrate from a mixture of water and organic solvents. We formed the monohydrated species of sodium naproxen in our experiments by recrystallization from sodium naproxen solutions in a mixture of methanol and water (80:20, volume ratio).

The experimental procedures shown schematically in Figure 2 were developed to provide samples of the various hydrated forms of sodium naproxen. As shown, the monohydrate was obtained by placing the dihydrate in a desiccator for about 2 days at room temperature. Prepared samples of the monohydrate were analyzed with PXRD and compared to the simulated PXRD pattern of the monohydrate. The two are identical, showing that the dried samples from the dihydrate are the same as the samples recrystallized from methanol by Kim et al.[3]

The anhydrate of sodium naproxen was obtained by heating the dihydrate in an oven at 120 °C for 2 h or by leaving it in a desiccator for a month. Alternatively, the monohydrate prepared from the dihydrate could be dried in an oven or in a desiccator to produce the anhydrate. The PXRD pattern of the anhydrate obtained in any of these methods was the same as that of the original anhydrous compound obtained from Albemarle. It can be concluded, therefore, that crystallization and subsequent controlled dehydration of the dihydrate can be used to produce any of the three pseudopolymorphic forms.

The powder X-ray diffraction patterns shown in Figure 3 were generated for each of the sodium naproxen species under investigation. The peak positions and intensities show differences among the structures of the species, confirming that the three forms are distinct compounds. Obviously, the differences result from the variable water content in the crystal structures.

Thermal Analysis of the Samples. The theoretical water contents of the monohydrate and dihydrate forms of naproxen sodium are 6.666 and 12.499 wt %, respectively. Analysis of the TGA data in Figure 4 provided results quite close to the theoretical values: 0.048 ± 0.012 (mean ± SD) wt % for the anhydrate, 6.832 ± 0.286 wt % for the monohydrate, and 12.957 ± 0.655 wt % for the dihydrate.

More detailed analysis of the TGA thermograms in Figure 4 shows the existence of two separate dehydration steps for the dihydrate, whereas the monohydrate shows only one. Although the two dehydration steps for

Pseudopolymorphic Forms of Sodium Naproxen
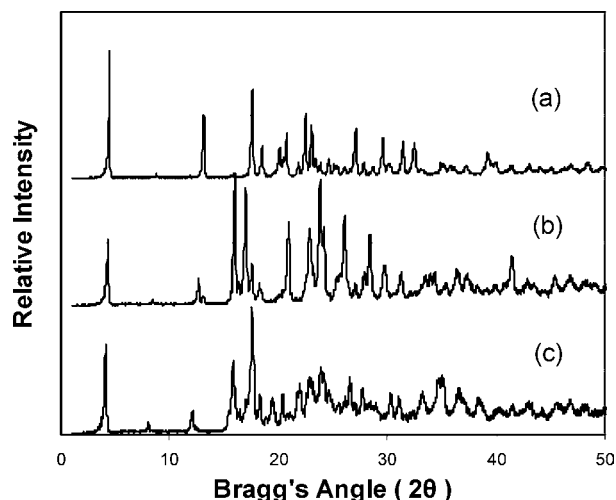
Figure 3. Powder X-ray diffraction patterns of three different pseudopolymorphic forms of sodium naproxen: (a) the anhydrate, (b) the monohydrate, and (c) the dihydrate.

Figure 5. Differential scanning calorimetry curves of three different pseudopolymorphic forms of sodium naproxen: (a) the anhydrate, (b) the monohydrate, and (c) the dihydrate.

Figure 4. TGA curves with nitrogen purge of (a) monohydrated and (b) dihydrated forms of sodium naproxen.

the dihydrate were not completely separated, the first corresponds to the removal of water that is not found in the monohydrate, while the second corresponds to that of water that is also found in the monohydrate. Because the nitrogen purge facilitates dehydration, the stabilization of the initial sample weights was carried out without nitrogen purge.

Figure 5 shows DSC thermograms for the three pseudopolymorphs of sodium naproxen. Table 1 gives the estimated energies of the transformations associated with the peaks in Figure 5. The anhydrate shows only o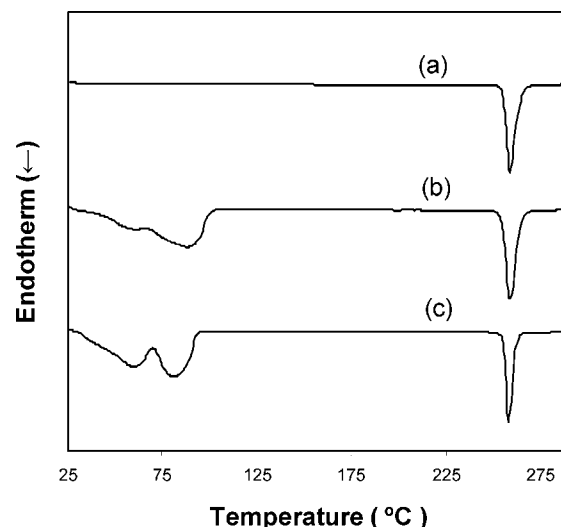ne endothermic peak, which corresponds to melting. The dihydrate has one peak for melting and two peaks corresponding to removal of two different types of water

from the unit cell. The first released water produces the first dehydration endotherm in the DSC thermogram for the dihydrate. This water is easily removed at ambient temperature, and will be discussed below. Because the peaks for the dehydration endotherms are not separated clearly, the endothermic energy for each water removed from the dihydrate could not be determined directly. Therefore, the dehydration energy for the dihydrate in Table 1 is the sum of dehydration energies for the first and second released water.

The monohydrate of sodium naproxen exhibits two peaks, one for melting and the other associated with the endotherm for dehydration. The minute peak at about 60 °C corresponds to an endotherm associated with a slight overhydration of the monohydrate sample.

The heats of dehydration in Table 1 are based on the mass of sample, in other words, 207.3 J/g of the monohydrated species and 376.8 J/g of the dihydrated species. If the anhydrous species is used as the basis, these values become 220.5 and 427.6 J/g of anhydrate, respectively. If we assume that the heat of hydration for the monohydrate is equivalent to that for removal of the second water from the dihydrate, then the heat of dehydration for removal of the first water can be found by difference: 207.1 J/g of anhydrate. Because there is less than 10% difference between the two heats of dehydration, the interactions of the first released water with the atoms that surround it in the crystal structure are energetically similar to those between the second water and its surrounding atoms.

It is expected that the heats of fusion of the three sodium naproxen species should be the same since melting occurs after removal of water and the crystal

Table 1.   Temperatures and the Endotherms for Peaks in DSC[a]

compound	first peak temp (°C)	second peak temp (°C)	heat of dehydration (J/g sample)	minimum temperature (°C)	melting temperature (°C)	heat of fusion (J/g sample)
anhydrate				258.3 ± 0.2	255.1 ± 0.1	110.7 ± 0.5
monohydrate	86.0 ± 1.5		207.3 ± 0.5	258.5 ± 0.3	254.7 ± 0.4	102.8 ± 0.9
dihydrate	60.7 ± 1.5	82.2 ± 1.3	376.8 ± 1.8	258.1 ± 0.3	255.3 ± 0.2	94.5 ± 1.3

[a] Results are means with their standard deviations.

Table 2. Converted Heats of Fusion of the Sodium Naproxen Species

compound	x_{H_2O}	$\Delta\hat{H}_{fus,n}$ (J/g)	$1/1 - x_{H_2O}$	$\Delta\hat{H}_{fus,0}$ (J/g)
anhydrate	0.00048 ± 0.00012	110.7 ± 0.5	1.00048^a	110.8^a
monohydrate	0.06832 ± 0.00286	102.8 ± 0.9	1.07333^a	110.3^a
dihydrate	0.12957 ± 0.00655	94.5 ± 1.3	1.14886^a	108.6^a

^{a} Values are calculated with means.

structures of the dehydrated species have been shown identical. However, the heats of fusion estimated in Table 1 are based on the initial sample mass, which includes whatever water had been present. These values can be converted to energy per unit mass of the anhydrous species as follows:

$$\Delta H_{fus,n} = m_n \Delta\hat{H}_{fus,n} = m_0 \Delta\hat{H}_{fus,0} \qquad (1)$$

where $\Delta H_{fus,n}$(J) is the enthalpy change with fusion measured by the DSC, $\Delta\hat{H}_{fus,n}$ is the heat of fusion per unit initial sample mass as estimated directly by the DSC, $\Delta\hat{H}_{fus,0}$ is the heat of fusion per unit mass of dehydrated sample, m is the mass of the sample, and the subscripts n and 0 denote the species with n moles of water per mole of anhydrate and the anhydrous species, respectively. Rearranging eq 1,

$$\Delta\hat{H}_{fus,0} = \frac{m_n}{m_0}\Delta\hat{H}_{fus,n} = \frac{1}{x_0}\Delta\hat{H}_{fus,n} = \left(\frac{1}{1 - x_{H_2O}}\right)\Delta\hat{H}_{fus,n} \qquad (2)$$

where x is mass fraction of the indicated species. This equation and the values of x_{H_2O} determined from TGA analyses were used to obtain the estimates of heat of fusion given in Table 2. Clearly, the converted heats of fusion for the three species are quite similar to each other and provide additional evidence that the dehydrated species have the same structure as anhydrous sodium naproxen.

Dehydration Kinetics. The DSC and TGA data on the dihydrate of sodium naproxen show the removal of two different types of water molecules from the crystal structure; these are referred to as first and second waters. The first generates the initial DSC peak and the second leads to the subsequent peak. In the following analysis, we evaluate the DSC and isothermal TGA data on both the monohydrate and dihydrate of sodium naproxen so as to elucidate the role water plays in the structures of these two species and to determine why the two waters in the dihydrate behave differently.

The rate of removal of water from a hydrated crystal can be written as

$$\frac{d\alpha}{dt} = kf(\alpha) \qquad (3)$$

where α is defined as the fraction of water removed from the hydrated crystal at time t, that is,

$$\alpha = \frac{M_T - M}{M_T} \qquad (4)$$

where M_T is the initial mass of water in the sample, and M is the mass of water in the sample at time t. The relationship between water content in a crystal sample and time is embodied in the function $f(\alpha)$, which in turn depends on the mechanism of water removal. Integration of eq 3 gives[9]

$$\int_0^1 \frac{d\alpha}{f(\alpha)} = g(\alpha) = \int_0^t k \, dt = kt \qquad (5)$$

The rate constant k may be considered to follow an Arrhenius dependency on T:

$$k = k_0 \exp\left(-\frac{\Delta E_a}{RT}\right) \qquad (6)$$

where ΔE_a is the activation energy for dehydration, R is the gas constant, and T is temperature. The activation energy can be estimated from the rate constants determined from measurements of isothermal dehydration kinetics at several temperatures, provided $g(\alpha)$ is known. Table 3 gives selected expressions from the Šesták[10] and Dong et al.[9] for $g(\alpha)$ corresponding to various solid-state processes.

Several isothermal dehydrations were performed in the TGA apparatus, and the resulting relationships between α and t were determined using the following procedure for each of the water molecules in the dihydrate and for the lone water in the monohydrate of sodium naproxen. The function in Table 3 that provided the best fit to the dehydration data was identified, and the corresponding values of k were determined. By fitting the Arrhenius expression to these values, an estimate of the activation energy of the given process was obtained.

For the first water released from the dihydrate and the lone water from the monohydrate, TGA data were fit from α at $t = 5.5$ min to $\alpha = 0.9$. (Note α is determined for each of the water molecules, and M_T in each instance is the mass associated with that specific water.) For the second water molecule removed from the dihydrate, the data were fit from $\alpha = 0.3$ to $\alpha = 0.9$. The interpretation of data on the second water removed from the dihydrate was complicated by a long transient

Table 3. Algebraic Expressions for $g(\alpha)$ Corresponding to Suggested Mechanisms of Solid-State Processes

model identifier	$g(\alpha)$	mechanism (descriptor of equation)
A2	$(-\ln(1 - \alpha))^{(1/2)}$	one-dimensional growth of nuclei (Avrami−Erofeyev equation, $n = 2$)
A3	$(-\ln(1 - \alpha))^{(1/3)}$	two-dimensional growth of nuclei (Avrami−Erofeyev equation, $n = 3$)
A4	$(-\ln(1 - \alpha))^{(1/4)}$	three-dimensional growth of nuclei (Avrami−Erofeyev equation, $n = 4$)
R1	α	one-dimensional phase boundary reaction (zero-order mechanism)
R2	$1 - (1 - \alpha)^{(1/2)}$	two-dimensional phase boundary reaction (contracting cylinder)
R3	$1 - (1 - \alpha)^{(1/3)}$	three-dimensional phase boundary reaction (contracting sphere)
D1	α^2	one-dimensional diffusion
D2	$(1 - \alpha)\ln(1 - \alpha) + \alpha$	two-dimensional diffusion
D3	$(1 - (1 - \alpha)^{(1/3)})^2$	three-dimensional diffusion (Jander's equation)
D4	$(1 - 2/3\alpha)(1 - \alpha)^{(2/3)}$	three-dimensional diffusion (Ginstling-Brounshtein equation)

Pseudopolymorphic Forms of Sodium Naproxen

Table 4. Activation Energy for the Released Water

released water	model	T (°C)	k (min^{-1})	R^2	ΔE_a (kJ/mol)	R^2
first water	R2	24.0	0.02443	0.9987	67.2	0.9850
from the		26.4	0.03214	0.9980		
dihydrate		29.5	0.04015	0.9990		
second water	D3	24.0	0.002277	0.9941	98.6	0.9383
from the		26.4	0.003712	0.9908		
dihydrate		29.5	0.004747	0.9934		
water	D3	24.1	0.000896	0.9948	92.5	0.9997
from the		26.9	0.001266	0.9958		
monohydrate		29.8	0.001804	0.9970		

The "Arrhenius plot" header spans the last two columns (ΔE_a (kJ/mol) and R^2).

Table 5. Activation Energies for Different Dehydration Reactions

| compound	activation energy (kJ/mol)	ref
cefamandole sodium monohydrate → anhydrate	71	11
neotame monohydrate → anhydrate	75 ± 9	9
theophylline monohydrate → anhydrate	140	12
sulfaguanidine monohydrate → anhydrate	67−168[a]	13
mercaptopurine monohydrate → anhydrate	191−264[b]	14

[a] These values vary depending on crystallinity of the samples as well as environmental factors. [b] These values vary depending on the method of determination.

between removal of the first and the second water molecules from the dihydrate. That is why the range of α was taken to begin at 0.3, thereby removing the transient and obtaining a higher correlation coefficient, R^2, for the resulting fits to the data. Table 4 gives the results of the analyses leading to the best fits of data for both water molecules in the dihydrate and for the water in the monohydrate.

As shown in Table 4, model R2 provided the best fit to the data involving removal of the first water from the dihydrate, but model D3 was best for the second water and for the lone water removed from the monohydrate. This implies that different resistances control the removal rate of water: a phase boundary reaction for the first water of the dihydrate and diffusion for both the second water of the dihydrate and the lone water of the monohydrate. The phase−boundary reaction is taken to be dissociation of water from the crystal lattice.

The activation energy for removal of the first water from sodium naproxen dihydrate is close to the lowest value among activation energies given in Table 5 for removal of water from several different crystal species. This is why, as shown experimentally with DSC and TGA data of the current research, the first water is very easy to remove, and it is easier to remove than the second water in sodium naproxen dihydrate. The activation energy for removal of the second water from the dihydrate was very similar to that for removing the lone water from the sodium naproxen monohydrate, and both are larger than the activation energy for removal of the first water from the dihydrate.

Dong et al.[9] postulated a dehydration mechanism for neotame monohydrate that consisted of two steps: (a) dissociation of water from the crystal lattice and then (b) diffusion of the water through channels in the crystal. Dissociation may involve breakage of hydrogen bonds or disruption of other attractive forces. It appears that a similar view is appropriate for the current system, but it is complicated by the existence of two
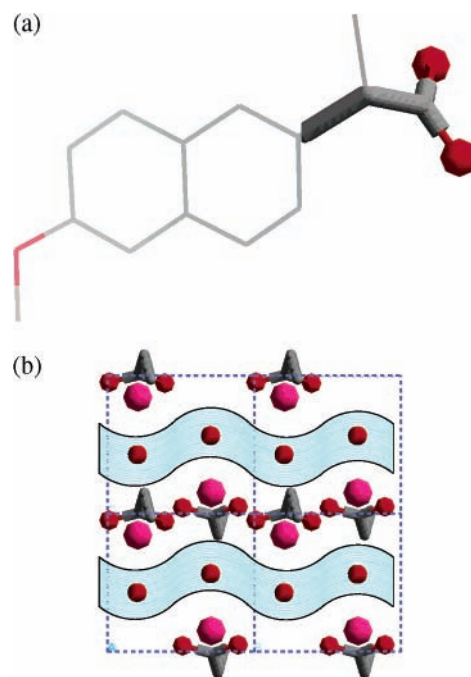
Figure 6. (a) Sodium naproxen molecule with the sodium and hydrogen atoms omitted and (b) a projection perpendicular to the [100] plane of the monohydrate. In (a), two oxygen atoms and four covalent bonds are exaggerated. For clarity, only this portion of the molecule is depicted in (b). Additionally, in (b), the smaller circles represent oxygen atoms, the larger circles represent sodium atoms, and the shaded waves show water channels in the monohydrate.

different types of behavior for the two water molecules in the dihydrate.

A packing diagram of sodium naproxen monohydrate crystals was constructed based on X-ray diffraction data,[3] and is shown in Figure 6. The diagram reveals channels for water transport within the crystals. Figure 6a shows the sodium naproxen molecule with the sodium atom omitted; in the crystal structure of Figure 6b, only the two oxygen atoms in the carboxyl group, four covalent bonds from the two oxygen atoms to the naphthyl group, a sodium atom, and an oxygen atom in the water of hydration were drawn to make it clear where water channels are in the monohydrate.

Allen et al.[15] suggested that water released at low temperature has very weak interactions with nearby molecules in the crystal lattice. Morris[16] classified hydrates as follows: (1) isolated-site hydrates, which should yield sharp DSC endotherms and narrow TGA mass losses upon dehydration, (2) channel hydrates, which have early onset temperatures of dehydration and broader DSC and TGA traces than isolated-site hydrates, and (3) ion-associated hydrates, which have strong metal−water interactions and comparatively higher dehydration temperature and molar heat of dehydration than the other hydrates. He also suggested that dehydration is affected by diffusion of water molecules from the unit cells to the crystal surface; accordingly, if there is ready access of the leaving water to channels for diffusion, dehydration occurs easily and at low temperatures. The first water removed from sodium naproxen dihydrate has an earlier onset temperature than the second water, which we show in Figure 6 to be in channels. We infer, therefore, that

since these channels exist in the monohydrate and facilitate dehydration, they must also exist in the dihydrate where removal of the first water is even easier.

Conclusion

Three different pseudopolymorphic forms of sodium naproxen were prepared by crystallization from aqueous solutions and by dehydration of higher hydrated crystalline samples. The changes in pseudopolymorphic form by dehydration in an oven and/or a desiccator imply that dehydration endotherms obtained by DSC were associated with the removal and evaporation of water incorporated in crystal structures and simultaneous transformation to lower degrees of hydration.

Analysis of TGA and DSC data demonstrated that there are two types of water molecules in the crystal structure of dihydrated sodium naproxen. Isothermal TGA data were employed to show the difference of activation energies associated with removal of these two different forms of water from the crystal structure. As expected, the first water removed from the dihydrate had a lower activation energy, explaining why it was easily removed at a low temperature. It was furthermore concluded that the relatively low activation energies and temperature ranges to remove those two different water molecules result from weak interactions with nearby molecules in the crystals lattice.

References

(1) Kuhnert-Brandstätter, M.; Gasser, P. *Microchem. J.* **1971**, *16*, 419−428.

(2) Ravikumar, K.; Rajan, S. S.; Phttabhi, V. *Acta Crystallogr.* **1985**, *C41*, 280−282.

(3) Kim, Y. B.; Park, I. Y.; Lah, W. R. *Arch. Pharm. Res.* **1990**, *13*, 166−173.

(4) Kim, Y.; VanDerveer, D.; Wilkinson, A. P.; Rousseau, R. W. *Acta Crystallogr.* **2004**, *E60*, m419−m420.

(5) Bednarek, E.; Bocian, W.; Dobrowolski, J. Cz.; Kozerski, L.; Sadlej-Sosnowska, N.; Sitkowski, J. *J. Mol. Struct.* **2001**, *559*, 369−377.

(6) Bansal, P.; Haribhakti, K.; Subramanian, V.; Plakogiannis, F. *Drug Dev. Ind. Pharm.* **1994**, *20*, 2151−2156.

(7) Di Martino, P.; Barthelemy, C.; Palmieri, G. F.; Martelli, S. *Eur. J. Pharm. Sci.* **2001**, *14*, 293−300.

(8) Phan, H. V.; Allen, R. H.; Coats, R. A. United States Patent 1999, US005874614A.

(9) Dong, Z.; Salsbury, J. S.; Zhou, D.; Munson, E. J.; Schroeder, S. A.; Prakash, I.; Vyazovkin, S.; Wight, C. A.; Grant, D. J. W. *J. Pharm. Sci.* **2002**, *91*, 1423−1431.

(10) Šesták, J. *Thermochim. Acta* **1971**, *3*, 1−12.

(11) Pikal, M. J.; Lang, J. E.; Shah, S. *Int. J. Pharm.* **1983**, *17*, 237−262.

(12) Shefter, E.; Fung, H. L.; Mok, O. *J. Pharm. Sci.* **1973**, *62*, 791−794.

(13) Sekiguchi, K.; Shirotani, K.; Sakata, O.; Suzuki, E. *Chem. Pharm. Bull.* **1984**, *32*, 1558−1567.

(14) Niazi, S. *J. Pharm. Sci.* **1978**, *67*, 488−491.

(15) Allen, P. V.; Rahn, P. D.; Sarapu, A. C.; Vanderwielen, A. J. *J. Pharm. Sci.* **1978**, *67*, 1087−1093.

(16) Morris, K. R. In *Polymorphism in Pharmaceutical Solids*; Brittain, H. G., Eds.; Marcel Dekker: New York, 1999; pp 125−181.

CG049917Q

EXHIBIT L

J|A|C|S
A R T I C L E S

Molecular Compasses and Gyroscopes with Polar Rotors: Synthesis and Characterization of Crystalline Forms

Zaira Dominguez,[†] Tinh-A. V. Khuong, Hung Dang, Carlos N. Sanrame, Jose E. Nuñez, and Miguel A. Garcia-Garibay*

Contribution from the Department of Chemistry and Biochemistry, The University of California, Los Angeles, California 90095-1569

Received March 21, 2003; E-mail: mgg@chem.ucla.edu

Abstract: We report the highly convergent synthesis and solid-state characterization of six crystalline "molecular compasses" consisting of a central phenylene rotor with polar substituents, or compass needle, and two trityl groups axially connected by acetylene linkages to the 1,4-positions. Compounds with fluoro-, cyano-, nitro-, amino-, diamino-, and nitroamino substituents are expected to emulate the parent compound which was shown to form crystals where the central phenylene can rotate about its 1,4-axis with rate constants in the $10^3 - 10^6$ s^{-1} dynamic ranges near ambient temperature, depending on crystal morphology. With data from single-crystal X-ray diffraction analysis, solid-state CPMAS ^{13}C NMR, differential scanning calorimetry (DSC), and thermogravimetric analysis (TGA), it is shown that a relatively small structural perturbation by a single polar group (F, CN, NO$_2$, NH$_2$) results in isomorphous structures with analogous properties. In analogy to the parent compound, crystals grown from benzene formed clathrate structures in the space group $P\bar{1}$ with one molecular compass and two benzene molecules per unit cell. Solvent-free crystals with the same space group obtained by a first-order phase transition between 60 and 130 °C were shown to be spectroscopically identical to those obtained by slow solvent evaporation from a mixture of CH$_2$Cl$_2$ and hexanes. A qualitative analysis of the positionally disordered phenylene groups in terms of the expected solid-state rotational dynamics suggests a nonsymmetric, 2-fold rotational potential, or a process involving full 360° turns.

1. Introduction

In search of photonic materials with electrooptic and dielectric functions based on the rotational dynamics of internal dipoles,[1,2] we recently made progress on the preparation of solids built with molecules having structures and functions that are analogous to those of macroscopic compasses and gyroscopes. Like these navigational devices, the desired structures are characterized by rigid frameworks that shield reorienting or rotating polar groups capable of responding to external electromagnetic fields and to forces causing changes in its angular momentum. We have shown that compounds with axially substituted arylene rotors linked by two acetylenes to triarylmethyl[3] and triptycyl[4] frameworks are promising candidates (Figure 1). Since rotation about alkyne−aryl single bonds in the ground state is essentially frictionless,[3−5] we expect that triarylmethanes and triptycenes with bulky substituents or bridging groups will provide the steric
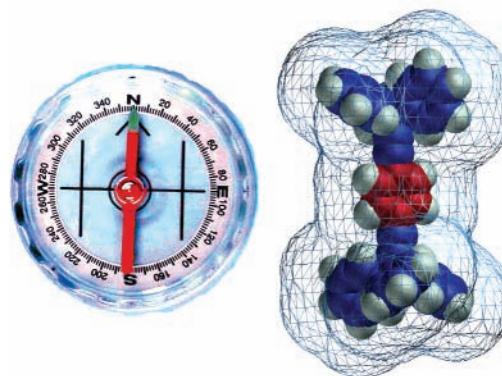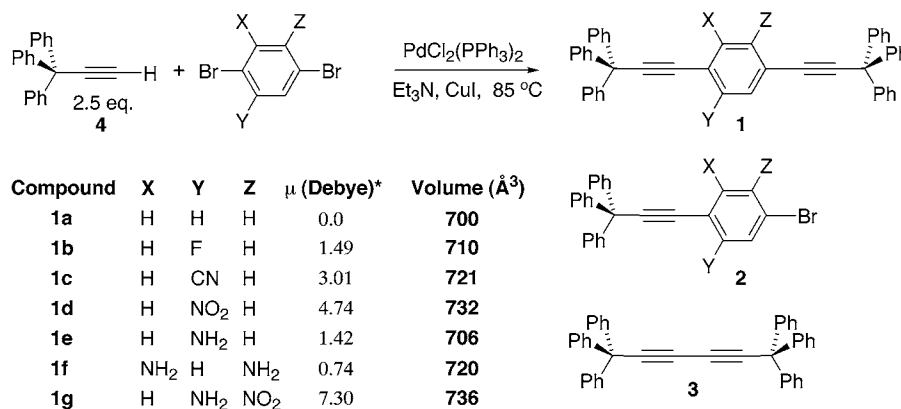

Figure 1. Suggested analogy between a macroscopic compass and 1,4-bis(triphenylpropynyl)benzene (**1a**), a molecule with a triarylmethane framework (blue) and a phenylene rotor (red). The space-filling model of **1a** is shown with a 4 Å solvent-accessible surface.

shielding required to prevent contacts between the arylene rotor and neighboring molecules in the solid state. With a combination of variable temperature ^{13}C CPMAS NMR and quadrupolar echo ^{2}H NMR line-shape analysis, we recently showed that crystals of 1,4-bis(3,3,3-triphenylpropynyl)benzene (**1a**)[6] display the

---

† Present address: Instituto de Ciencias Basicas, Universidad Veracruzana, Xalapa, Veracruz, Mexico.

(1) (a) Salech, B. E. A.; Teich, M. C. *Fundamentals of Photonics*; Wiley-Interscience: New York, 1991. (b) Weber, M. J. *Handbook of Optical Materials*; CRC Press: Boca Raton, 2002 (c) Kasap, S. O.; Kasap, S. O. *Optoelectronics and Photonics: Principles and Practices*; Prentice Hall: New York, 2001. (d) Setian, L. *Applications in Electrooptics*; Prentice Hall: New York, 2001.
(2) Hench, L. L.; West, J. K. *Principle of Electronic Ceramics*; John Wiley & Sons: New York, 1990.
(3) Dominguez, Z.; Dang, H.; Strouse, M. J.; Garcia-Garibay, M. A. *J. Am. Chem. Soc.* **2002**, *124*, 2398−2399.
(4) Godinez, C. E.; Zepeda, G.; Garcia-Garibay, M. A. *J. Am. Chem. Soc.* **2002**, *124*, 4701−4707.

(5) (a) Saebo, S.; Almolof, J.; Boggs, J. E.; Stark, J. G. *J. Mol. Struct. (THEOCHEM)* **1989**, *200*, 361−373. (b) Abramenkov, A. V.; Almenningen, A. Cyvin, B. N.; Cyvin, S. J.; Jonvik, T.; Khaikin, L. S.; Rommingin, C.; Vilkov, L. V. *Acta Chem. Scand.* **1988**, *A42*, 674−678. (c) Sipachev, V. A.; Khaikin, L. S.; Grikina, O. E.; Nikitin, V. S.; Traettberg, M. *J. Mol. Struct.* **2000**, *523*, 1−22.

Dominguez et al.

Scheme 1 [a]

Compound	X	Y	Z	μ (Debye)*	Volume (Å^3)
1a	H	H	H	0.0	700
1b	H	F	H	1.49	710
1c	H	CN	H	3.01	721
1d	H	NO$_2$	H	4.74	732
1e	H	NH$_2$	H	1.42	706
1f	NH$_2$	H	NH$_2$	0.74	720
1g	H	NH$_2$	NO$_2$	7.30	736

[a] Asterisk denotes that dipole moments and molecular volumes were calculated from structures optimized with the AM1 method as implemented by the program Spartan.

desired rotation. Despite the relatively modest shielding offered by simple triphenylmethyl (trityl) groups (Figure 1 and Scheme 1), the phenylene rotor was shown to undergo a 2-fold flipping motion in the solid state with rate constants in the MHz regime near ambient temperature. Analogous structures have been recently suggested by Glass et al.[7] as scaffolds for pinwheel fluorescence sensors in solution and by Joachim et al. for the construction of molecular "barrows" guided and driven by AFM tips on atomically smooth surfaces.[8] As a continuation of our studies on materials based on molecular compasses and gyroscopes, we report here the synthesis, characterization, and solid-state properties of several analogues of **1a** with phenylene groups possessing fluoro- (**1b**), cyano- (**1c**), nitro- (**1d**), amino- (**1e**), *o*-diamino- (**1f**), and *p*-nitroamino- (**1g**) substituents (Scheme 1). The primary goal of this work is to determine the effects of polar rotors on the crystallization of molecular compasses and gyroscopes with simple trityl frames and to test a suitable synthetic procedure. While the magnitudes of dipole moments calculated by the AM1 method for compounds **1b**−**1g** range from 0.74 to 7.30 (Scheme 1), their calculated molecular volumes differ by less than 5% from that of **1a**. Knowing that crystallization of apolar molecules is determined by weak van der Waals forces which manifest in the form of volume-filling, close-packing interactions,[9,10] one may expect homologous series such as that given by **1a**−**1g** to form isomorphous crystal structures. Noting that the introduction of polar substituents on the phenylene group of **1a** makes the analogy to macroscopic compasses closer, one may suggest that the "box" of the compass will remain constant while the nature of the "needle" inside would be systematically varied. Unless unusual dipole− dipole interactions were to be manifested, the corresponding crystals should have analogous packing arrangements. At the same time, knowing that rapid reorientation of the phenylene group occurs in crystals of **1a**, it seems possible that analogous dynamics may be observed in crystals of **1b**−**1g**. In addition to the synthesis and solution characterization of compounds **1b**−**1g**, we analyze here the relation between their various crystal

structures with a combination of X-ray diffraction, high-resolution solid-state ^{13}C CPMAS NMR, differential scanning calorimetry (DSC), and thermogravimetric analysis (TGA). The results reported in this paper confirm the expected solid-state isomorphism with various degrees of positional disorder.[9,10]
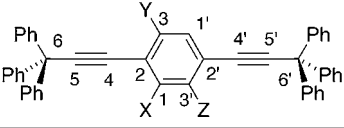
2. Results and Discussion

2.1. Synthesis. Molecular compasses **1b**−**1g** were synthesized by a double-coupling reaction with 2.5 equiv of 3,3,3-triphenyl-1-propyne and the corresponding *p*-phenylene bromide in a manner that is analogous to that reported previously for compound **1a** (Scheme 1).[3,6] Samples of 3,3,3-triphenyl-1-propyne were obtained from the reaction of trityl chloride with ethynylmagnesium bromide in benzene at ambient temperature.[7,11] Molecular compasses **1b**, **1d**, and **1e** were prepared with commercially available 2,5-diiodofluorobenzene, 2,5-dibromonitrobenzene, and 2,5-dibromoaniline, respectively. Samples of the 2-substituted 1,4-dibromophenylenes for the synthesis of molecular compasses **1c** and **1g**, and 2,3-diamino-1,4-dibromophenylene **1f**, were prepared by reported procedures (Scheme 2). 2,5-Dibromobenzonitrile was prepared by Friedel−Crafts bromination of benzonitrile as reported by Pearson et al. (Scheme 2a).[12] Our isolated yields were significantly lower than those reported by these authors (79%) but were in agreement with those recently reported by Gray et al. (12%).[13] Samples of 3,6-dibromo-1,2-phenylenediamine were prepared in good yields in a three-step procedure from *o*-phenylenediamine (Scheme 2b).[14] A clean, high-yielding, and regioselective dibromination was accomplished through a 2,1,3-benzothiadiazole obtained by condensation of the *o*-diamine with SOCl$_2$ in the presence of pyridine and subsequent reductive removal of sulfur with NaBH$_4$ regenerated the diamine. The preparation of 2,5-dibromo-4-nitroaniline was accomplished in good yields from commercial 2,5-dibromoaniline by the sequence reported by Moroni et al. (Scheme 2c).[15]

The Pd(0)-catalyzed reactions were carried out at 85 °C for 20 h with PdCl$_2$(PPh$_3$)$_2$, PPh$_3$, and CuI in Et$_3$N. The double-

(6) Dominguez, Z.; Dang, H.; Strouse, J.; Garcia-Garibay, M. A. *J. Am. Chem. Soc.* **2002**, *124*, 7719−7727.

(7) Raker, J.; Glass, T. E. *Tetrahedron* **2001**, *57*, 10233−10240.

(8) Joachim, C.; Tang, H.; Moresco, F.; Rapenne, G.; Meyer, G. *Nanotechnology* **2002**, *13*, 330−335.

(9) Kitaigorodskii, A. I. *Molecular Crystals and Molecules*; Academic Press: New York, 1973.

(10) Vainshtein, B. K.; Fridkin, V. M.; Indenbom, V. L. *Structure of Crystals*; Springer-Verlag: Berlin, 1982; Vol. II.

(11) Masson, J.-C.; Quan, M. L.; Cadiot, P. *Bull. Soc. Chim. Fr.* **1968**, *3*, 1085−1088.

(12) Pearson, D. E.; Stamper, W. E.; Suthers, B. R. *J. Org. Chem.* **1963**, *28*, 3147−3149.

(13) Gray, G. W.; Lacey, D.; Hird, M.; Toyne, K. J., PCT Int. Appl. 1989.

(14) (a) Tsubata, Y.; Suzuki, T.; Miyashi, T. *J. Org. Chem.* **1992**, *57*, 6749−6755. (b) Pilgram, K.; Zupan, M.; Skiles, R. *J. Heterocycl. Chem.* **1970**, *7*, 629−633.

(15) Moroni, M.; Le Moigne, J.; Pham, T. A.; Bigot, J. Y. *Macromolecules* **1997**, *30*, 1964−1972.

Molecular Compasses and Gyroscopes with Polar Rotors   **ARTICLES**

Table 1. ^{1}H NMR Chemical Shift Assignments of Molecular Compasses **1a−1 g**[a]

signal	1a[b]	1b Y = F (J_{HH}, Hz)	1c Y = CN (J_{HH}, Hz)	1d Y = NO$_2$ (J_{HH}, Hz)	1e Y = NH$_2$ (J_{HH}, Hz)	1f X, Z = NH$_2$	1g Y = NH$_2$ Z = NO$_2$
1	7.42	7.46 (7.6)	7.58 (8.2)	7.65 (8.2)	7.30 (7.6)	6.86	8.25
3	7.42						
1′	7.42	7.28[c]	7.80 (1.5)	8.18 (1.5)	6.86 (1.5)		6.88
3′	7.42	7.28[c]	7.67 (8.2, 1.5)	7.69 (8.2, 1.5)	6.84 (7.6, 1.5)	6.86	

[a] Spectra were measured at ambient temperature in CD$_2$Cl$_2$. [b] Reference 6. [c] Signals overlap with the *o*- and *m*-hydrogens of the trityl group.

Scheme 2

(a)

(b)

(c)
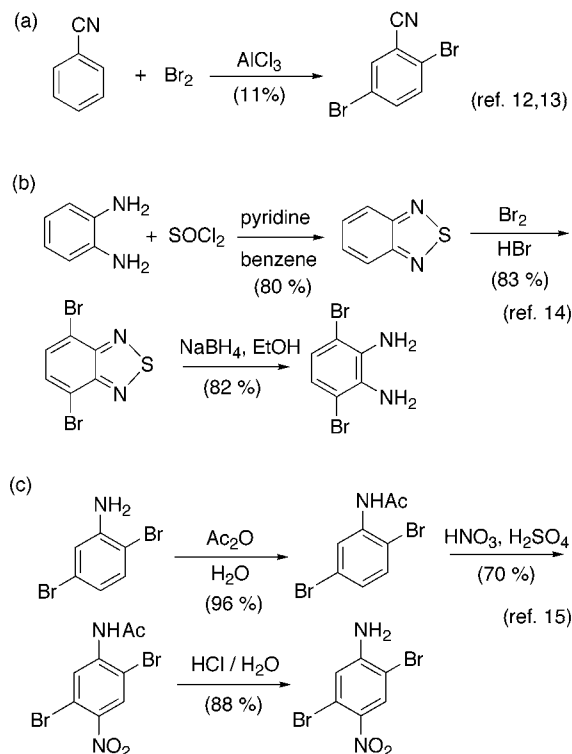
coupling reaction proceeded to completion in all cases, with the exception of those carried out with 2,5-dibromo-4-nitro-aniline (X = H, Y = NH$_2$, Z = NO$_2$) which failed to give compound **1g** under these conditions (see below). Small amounts of the known dimer **3** were also isolated along with the desired molecular compasses in the case of reactions leading to compounds **1b−1f**. Purification was carried out in all cases by column chromatography with silica gel using a mixture of CH$_2$-Cl$_2$:C$_6$H$_6$:C$_6$H$_{14}$ = 10:10:80 as the eluent. Although isolated yields under these nonoptimized conditions oscillated between 10 and 40%, molecular compasses prepared by stepwise coupling proceeded in higher overall yields (70−80%). The rate of formation of the nitroaniline molecular compass **1g** differed substantially from that of the others. Reaction conditions such as those used for the synthesis of compounds **1a−1f** yielded primarily the monocoupling product **2** (Y = NH$_2$, Z = NO$_2$) with small amounts of **1g** and alkyne dimer **3**. The regioselec-tivity of the monocoupling reaction was established by a 2D heteronuclear chemical shift correlations via multiple bond connectivities (HMBC).[16] A rapid monocoupling reaction at the

bromide that is *ortho* to the nitro group and *para* to the aniline is in agreement with expectations from the effects of substituents on similar alkyne−aryl coupling reactions.[17] However, a one-step double-coupling preparation of compound **1g** was ac-complished with an excess of 3,3,3-triphenylpropyne and longer reaction times.

2.2. Spectroscopic Characterization. The characterization of molecular compasses **1b−1g** was carried out at ambient temperature by ^{1}H NMR, ^{13}C NMR, and HMBC analyses. High-resolution mass spectra from electron impact ionization gave relatively abundant parent ions. Analysis by FT-IR revealed very weak or unobservable stretching bands for the triple bonds in all six rotors. Diffraction-quality single crystals were only obtained in the cases of the fluoro- (**1b**), cyano- (**1c**), nitro- (**1d**), and amino-susbtituted (**1e**) molecular compasses. No suitable crystals could be obtained for the diamino (**1f**) and nitroamino (**1g**) rotors.

As expected for structures that only have aromatic hydrogens, the ^{1}H NMR signals in CD$_2$Cl$_2$ appear in all cases in a very small range (less than 2 ppm). Although hydrogen signals corresponding to the trityl groups are observed as broad multiplets, signals corresponding to hydrogens of the substituted phenylenes could be assigned in most cases. A summary of chemical shift data corresponding to the ^{1}H NMR signals of the substituted phenylene groups is included in Table 1 and the corresponding ^{13}C NMR data in Table 2. The atom numbering used in Tables 1 and 2 is illustrated in the first table, which corresponds to the numbering used in a later section to describe the X-ray structures. Signals corresponding to hydrogen atoms that are *ortho* to the -F, -CN, -NO$_2$, and -NH$_2$ substituents in molecular compasses **1b**, **1c**, **1d**, and **1e** (H1′ in Table 1) occur as doublets with a small *meta* coupling constant (^4J = 1.5 Hz). Hydrogen atoms that are *meta* (C1) and *para* (C3′) to the substituent share a larger *ortho* coupling constant (^3J = 7.6−8.2 Hz). The *para* hydrogens at C3′ occur as doublet of doublets with small and large coupling constants ^4J and ^3J. The diamino compound **1f** has average mirror symmetry in solution and the two protons directly bonded to the 1,4-phenylene appear as a singlet. The spectrum of compound **1g** consists of upfield and downfield singlets corresponding to hydrogens that are *ortho* to the amine and nitro groups, respectively, which are also *para* to each other.

Since the rotational dynamics of the central phenylene in crystals of **1a** fall within a time scale that is suitable for

(16) 2D HMBC spectra are reported in the Supporting Information section.
(17) Singh, R.; Just, G. *J. Org. Chem.* **1989**, *54*, 4453−4457.

Table 2. ^{13}C Chemical Shifts of Molecular Compasses **1a**−**1g**^{a}

signal	1a^b	1b Y = F (*J*$_{CF}$, Hz)	1c Y = CN	1d Y = NO$_2$	1e Y = NH$_2$	1f X = Z = NH$_2$	1g Y = NH$_2$, Z = NO$_2$
C1	123.1	133.5 (2.0)	132.9	135.3	132.3	122.1	130.3
C2	131.3	112.3 (16)	124.3	124.6	108.4	109.6	107.6
C3	123.1	162.9 (251)	115.8	149.7	148.6	136.9	152.3
C1′	123.1	118.7 (23)	135.9	127.8	117.1	136.9	118.7
C2′	131.3	125.3 (9.5)	126.7	118.5	124.5	109.6	121.1
C3′	123.1	127.7 (4.0)	135.5	135.8	121.2	122.1	139.3
C4	84.7	84.3 (4.0)	82.0	80.9	82.5	82.8	80.1
C4′	84.7	79.0	83.4	83.3	85.8	82.8	82.2
C5, C5′	97.2	102.6 (34)	103.9	105.3	102.7	102.2	104.3, 103.6
		98.5	99.0	101.1	96.6		
C6, C6′	56.1	56.5	56.6	56.6	56.5	56.9	56.9, 57.0
		56.8	56.9	57.0	56.9		

^{a} Spectra measured at ambient temperature in CD$_2$Cl$_2$. ^{b} Values from ref 3.
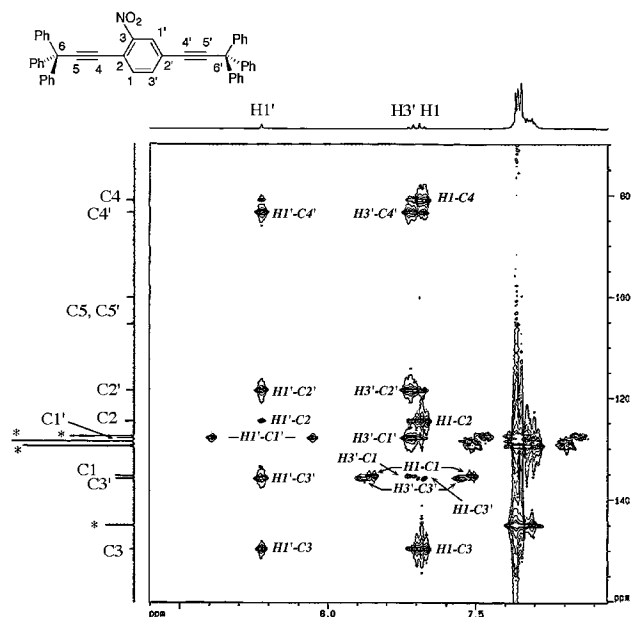
Figure 2. 500 MHz HMBC spectrum of the nitro-substituted molecular compass **1d** in CD$_2$Cl$_2$. Signals corresponding to the trityl groups appear near 7.4 ppm in the ^{1}H dimension are labeled with an asterisk (*) in the ^{13}C axis.

coalescence analysis by variable temperature ^{13}C CPMAS NMR,^{3,6} we carried out a precise assignment of ^{13}C chemical shifts corresponding to polar phenylenes in compounds **1b**−**1g**. It is well-known that assignments from solution spectra can be useful to assign signals measured in the solid state under the ^{13}C CPMAS experiments.[18] The assignment of most carbon signals was possible with HMBC measurements by taking advantage of the characteristic shielding values and coupling patterns of hydrogen atoms in the central phenylene rotors. The HMBC spectrum of compound **1d**, with a nitrophenylene rotor, is illustrated in Figure 2 as an example. Vicinal and long-range correlations between each hydrogen (H1′, H3′, and H1) and carbon nuclei of the nitrophenylene (C1−C3 and C1′−C3′) and the two alkyne carbons directly attached to the ring (C4 and C4′) allow for the unambiguous assignment of all the carbon signals.

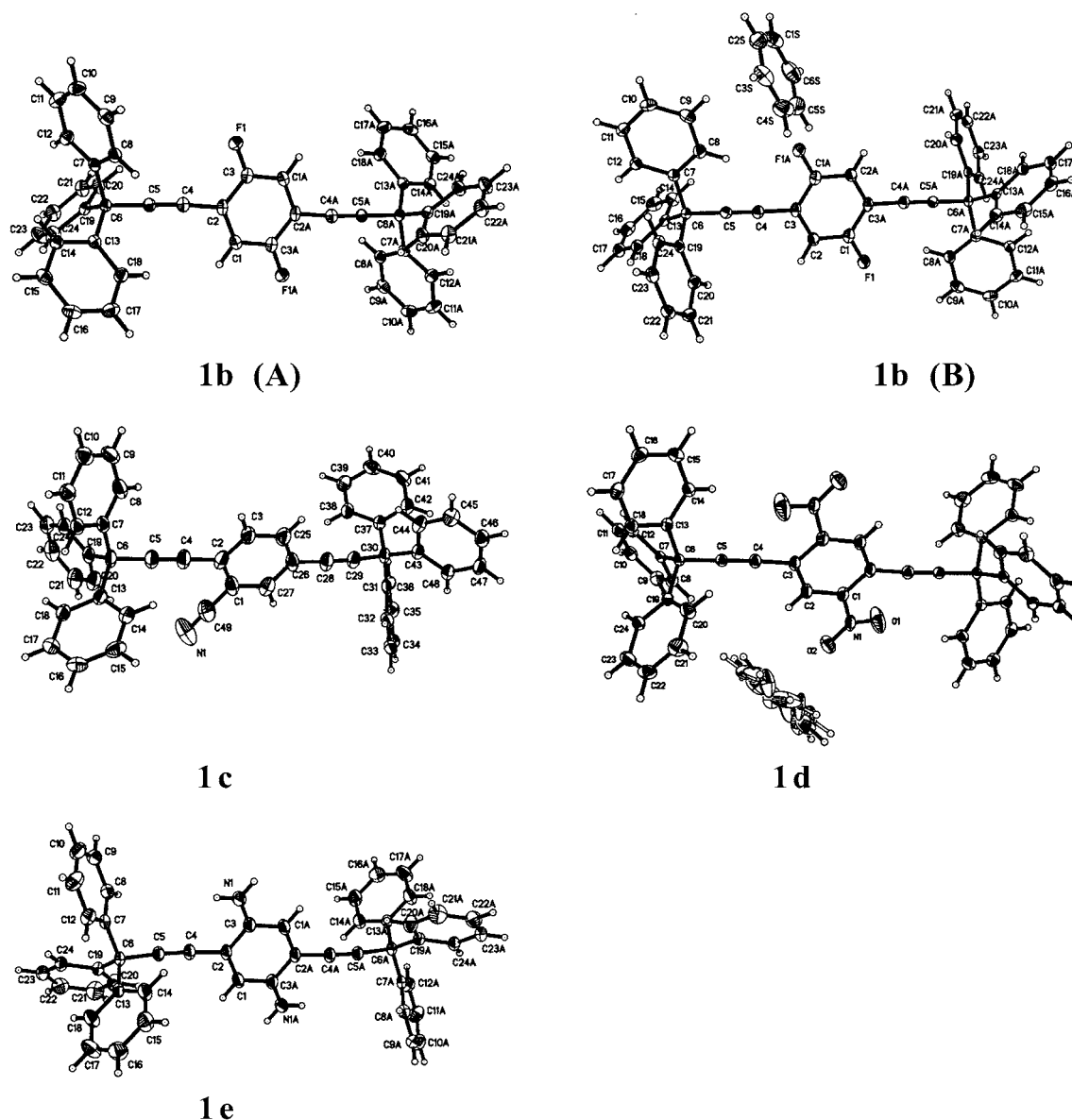A summary of the ^{13}C NMR data for compounds **1b**−**1g** is included in Table 2 along with chemical shift values for **1a**

(18) (a) Stejskal, E. O.; Memory, J. D. *High Resolution NMR in the Solid State: Fundamentals of CP/MAS*; Oxford University Press: Oxford, 1997. (b) Fyfe, C. A. *Solid State NMR for Chemists*; C.F.C Press: Guelph, Ontario, 1983.

which are included for comparison. Due to the presence of substituents that break the symmetry of the 1,4-phenylene in **1b**−**1e** and **1g**, all the carbons corresponding to the diethynylphenylenes (C1−C6 and C1′−C6′) are resolved in the ^{13}C NMR spectrum. Aromatic signals assigned to the trityl groups reveal fast conformational equilibration given by a time-averaged 3-fold symmetry that renders the three phenyl groups in each trityl group equivalent and a local 2-fold symmetry that makes each phenyl group symmetric along its 1,4-axis. Eight signals are assigned to 36 aromatic trityl carbons. Multiple bond connectivity correlations by the HMBC technique were used to assign the carbons in the 1,4-phenylene groups and the alkyne carbons directly bonded to the aromatic ring of the rotors in **1c**, **1d**, **1e**, and **1g**. The corresponding spectra are reported in the Supporting Information section. Although carbon signals of the 2-fluoro-1,4-phenylene group in **1b** were not sufficiently resolved for HMBC analyses, signals of the central phenylene and alkyne carbons could be assigned from their C−F coupling constants which range from $^1J_{CF} = 251$ Hz for the *ipso* carbon, to $^3J_{CF} = 2$ and $^4J_{CF} = 4$ Hz, respectively, for the *meta* (C1) and *para* carbons (C3′).

2.3. X-ray Studies: **Benzene Clathrates and Solvent-Free Crystals**. While polycrystalline samples could be obtained from various solvents, single crystals for structural elucidation were obtained under relatively strict conditions. Two polymorphs of **1b** could be obtained by slow evaporation from CH$_2$Cl$_2$ and from benzene. These will be referred to as **1b** (A) and **1b** (B), respectively. Crystals of **1e** were grown by slow evaporation from a mixture of hexanes and CH$_2$Cl$_2$ in a ca. 3:1 volumetric proportion. Crystals of the cyano derivative **1c** were obtained from a 3:1 mixture of hexanes and ethyl acetate and crystals from the nitro compound **1d** from saturated hot benzene solutions which were slowly cooled. We have been unable to obtain single crystals of the diamino and nitroamino compounds, **1f** and **1g**, which are suitable for X-ray diffraction analysis. Crystallographic acquisition and refinement data for compounds **1b**−**1d** are listed in Table 3 and their ORTEP structures illustrated in Figure 3. The structures of solvent-free crystals of **1b** (A) and **1e** were solved in the space group $P\bar{1}$ and have unit cell axes that differ by less the 0.12 Å and unit cell angles within 1°. Detailed analyses showed that they are closely related to the solvent-free crystals of **1a** described previously.[6] Crystals of the fluoro and nitro compounds **1b** and **1d** that are grown from benzene form triclinic structures with two solvent molecules per unit cell analogous to the benzene clathrate of **1a**.[6]

Molecular Compasses and Gyroscopes with Polar Rotors   **A R T I C L E S**

1b (A)

1b (B)

1 c

1 d

1 e

Figure 3. ORTEP diagrams of compounds **1b** (A), **1b** (B), **1c**, **1d** and **1e**. The disorder of the fluoro, amino, and nitro groups **1b**, **1e**, and **1d** is illustrated in their corresponding structures.

Table 3. Crystallographic Parameters for Molecular Compasses **1b**−**1e**

	molecular compass				
	1b (A)	**1b** (B)	**1c**	**1d**	**1e**
empir. form.	$C_{48}H_{33}F$	$C_{48}H_{33}F \cdot C_{12}H_{12}$	$C_{49}H_{33}N$	$C_{48}H_{33}NO_2 \cdot C_{12}H_{12}$	$C_{48}H_{35}N$
form. wt	627.74	627.74·156.09	645.76	655.25·156.09	625.77
crystal system	triclinic	triclinic	monoclinic	triclinic	triclinic
space group	$P\bar{1}$	$P\bar{1}$	$P2_1/c$	$P\bar{1}$	$P\bar{1}$
Z	1	1	4	1	1
size, mm^3	$0.5 \times 0.2 \times 0.5$	$0.4 \times 0.3 \times 0.1$	$0.4 \times 0.3 \times 0.2$	$0.45 \times 0.3 \times 0.2$	$0.4 \times 0.3 \times 0.05$
color, habit	colorless prism	colorless prism	colorlessprism	colorless prism	colorless prism
temp, K	100(2)	100(2)	100(2)	100(2)	298(2)
a, Å	9.1732(13)	8.644(2)	15.812(3)	8.4502(11)	9.2966(16)
b, Å	10.4607(14)	9.475(3)	20.338(4)	9.4905(12)	10.5467(18)
c, Å	10.4726(14)	14.530(4)	10.741(2)	14.6741(19)	10.5979(18)
α, degrees	62.126(2)	78.231(5)	90	79.925(2)	62.706(3)
β, degrees	85.744(3)	76.320(5)	94.226(4)	74.716(2)	71.071(3)
γ, degrees	71.673(2)	74.486(5)	90	76.347(2)	84.875(3)
V, Å^3	840.1(2)	1078.6(5)	3444.6(4)	1095.1(12)	871.3(3)
$\rho_{calc.}$, Mg/m^3	1.241	1.207	1.226	1.230	1.193
total reflections	5519	6751	15524	7345	4726
indep. reflect.	3818	4653	4962	5075	3129
R(Int)	0.0120	0.0214	0.0214	0.0147	0.0169
R1 $[I > 2\sigma(I)]$	0.0407	0.0414	0.0557	0.0534	0.0389
WR2 (all data)	0.1150	0.1013	0.1521	0.1375	0.1068

Scheme 3

Y = F, NH$_2$, NO$_2$
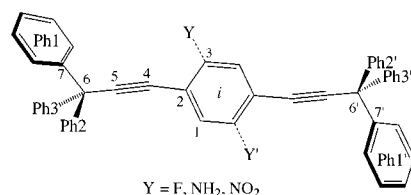
Table 4. Structural Parameters from the X-ray Structures of Compounds **1b−1e**

molecular compass	Ph1 (deg)^a	Ph2 (deg)^a	Ph3 (deg)^a	d(C6−C6′) (Å)	C7−C6−C2−C3 (deg)	C6′−C6−C4 (deg)	C6−i−C3 (deg)
1a^b	58.3	47.2	18.2	11.015	9.4	3.4	63
1a (C$_6$H$_6$)^b	29.8	45.1	50.5	11.012	1.8	0.1	57.8
1b (A)	58.7	44.1	19.5	11.028	14	2.9	63
1b (B)	27.0	50.2	50.4	11.032	1.0	0.4	57.8
1c^c	42.8	36.9	58.0	10.998	3.2	3.3	60.5
	−53.7	−56.4	−28.4		−13.4	7.9	59.7
1d (C$_6$H$_6$)$_2$	30.5	52.6	49.9	11.050	4.4	−3.2	62.4
1e	57.8	42.4	21.5	10.996	13.7	3.4	63.2

^{a} Dihedral angles given by the vector C5−C6 and the plane of each of the three phenyl groups. ^{b} Reference 6. ^{c} Compound **1c** has no average internal symmetry.

Compound **1c** crystallized in the monoclinic space group $P2_1/c$ with four molecules per unit cell. Crystals of compounds **1b**, **1d**, and **1e** showed positional disorder as the fluoro, nitro, and amino substituents have 50% occupancies in sites related by an average center of inversion in their crystal lattices. The average molecular structures resemble those of the *para*-disubstituted analogues with coincident crystallographic and molecular inversion centers (Figure 3). The crystal structure of **1c** is asymmetric and gives no indication of positional disorder.

While the X-ray-quality crystals of compounds **1a−1d** were obtained in three different packing structures, they share similar molecular conformations and structural distortions (Scheme 3). The two trityl groups in each molecule adopt chiral propeller conformations with opposite absolute configurations. Unlike gas-phase structures optimized by molecular mechanics (MM) and semiempirical (AM1) methods, which are predicted to have C_3-symmetric trityl groups (not shown), the trityl groups in **1b−1d** crystallize with their phenyl groups adopting different torsion angles which give rise to asymmetric (C_1) structures. The dihedral angles formed by the σ bond between alkyne and quaternary carbons, and the plane of each of the three rings (dihedrals C5−C6−C$_{ipso}$−C$_{ortho}$, labeled Ph1−Ph3 in Table 4) vary from ∼20° to ∼60°. The structures of compounds **1b−1d** are also characterized by having the phenyl groups projecting from the two trityl carbons in *anti* conformations (i.e., C7−C6−C6′−C7′ ≈ 180°), and by having the plane of the central arylene nearly eclipsed with one of the trityl C−Ph bonds (i.e., dihedral C7−C6−C2−C3 ≈ 0°). The structures of compounds **1b−1d** present deviations from the ideally linear geometry of a substituted triple bond. Although the center of the phenylene group (labeled "i" in Scheme 3) and the two trityl carbons (C6 and C6′) fall within a straight line, the four alkyne carbons deviate from that line. A measure of this deviation is given by the angle C6′−C6−C4 formed by the vector given by the two trityl carbons in the structure and the vector formed by the trityl carbon and the alkyne carbon C4. While an angle of 0° would be expected if the alkynes were linear, a deviation as large as 7.9° was noticed in **1c**. This distortion is accompanied by an in-plane rotation of the central phenylene so that the angle C6−

i−C3, where i is a point at the center of the substituted phenylene, takes values as large as 63.2°, when 60.0° would be expected. Structural deviations such as these have a strong effect on the rotational dynamics of macroscopic models and their potential influence on rotation of molecular compasses and gyroscopes should be kept in mind.

Packing structures of benzene-containing crystals of compounds **1b** and **1d** and solvent-free crystals of **1b** and **1c** are illustrated in Figure 4. The packing structures of benzene-grown crystals of **1b** [form B] and **1d** contain one molecular compass and two benzene molecules per unit cell. Although they are shown in Figure 4 with different choice of origin, the two structures are isomorphous with each other and with the benzene clathrate[19] of **1a** reported previously.[6] Molecular compasses reported in this study have shapes analogous to those of well-known "wheel-and-axle" and "dumbbell" structures such as 2,4-hexadiyne-1,6-diol **5**[20] and α,ω-diadamantylpolyynes **6**[21] (Scheme 4). These compounds are unable to form three-dimensional structures that satisfy the maximum-filling principle[9,10,19−21] and crystals are formed with cavities and/or channels occupied by smaller molecules. As in the previously reported benzene clathrate of **1a**,[3,6] four molecules of **1b** and **1d** make up a supramolecular cage that entraps a parallel-displaced benzene dimer (Figure 5, left). From a complementary point of view, one may describe the packing structure as having each molecular compass surrounded by six benzene dimers which form a belt around the central 1,4-diethynylphenylene (Figure 5, right). Supramolecular interactions in the structure comprise aromatic face-to-face and face-to-edge interactions[22] involving solvent molecules and phenyl groups in the two trityl units. The main difference between the benzene-containing structures of **1b** and **1d** and that of **1a** comes from the positional disorder of the fluoro and nitro groups in the former two. Additionally, the benzene-containing structure of the nitro compound **1d** displays crystallographic disorder in the solvent molecules: while the coordinates of a single benzene molecule are sufficient to describe the crystal structures of **1a**, and the form B of **1b**, the refined structure of **1d** requires two sets of overlapping benzene coordinates. The centers of mass of the two crystallographically different benzene molecules are displaced by 0.178 Å and differ by a 30° rotation with respect to the 6-fold axis and by a 2.7° angle between their mean molecular planes (not shown)
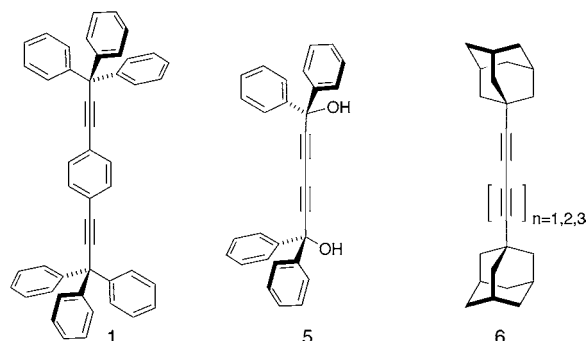
Also as expected, the packing structures of the solvent-free crystals of the fluoro and amino compounds **1b** (form A) and **1e** are isomorphous with each other and with the solvent-free structures of **1a** reported previously. The packing structure of **1e** is not shown in Figure 4 but it has been included in the Supporting Information section. Analysis of the form A of **1b**

(19) Clathrates are stoichiometric two-component crystal structures consisting of a "host" that forms a rigid lattice and a "guest" that fills interstitial positions in the same lattice. Parsonage, N. G.; Staveley, L. A. K. *Disorder in Crystals*; Oxford University Press: Oxford, 1978; Chapter 11, pp 717−798.

(20) (a) Toda, F. In *Comprehensive Supramolecular Chemistry*; McNicol, D. D., Toda, F., Bishop, R., Eds.; Pergamon: Oxford, 1996; Vol. 6.; (b) Toda, F. *Top. Curr. Chem.* **1988**, *149*, 211−238. (c) Caira, M. R.; Nassimbeni, L. R.; Toda, F.; Vujovic, D., *J. Am. Chem. Soc.* **2000**, *122*, 9367−9372. (d) Caira, M. R.; Nassimbeni, L. R.; Toda, F.; Vujovic, D. *J. Chem. Soc., Perkin Trans. 2* **2000**, 2119−2124.

(21) (a) Muller, T.; Hulliger, J.; Sechter, W.; Weber, E.; Weber, T.; Wubbenhorst, M. *Chm. Eur. J.* **2000**, *6*, 54−61. (b) Weber, E.; Nitsche, S.; Wierig, A.; Csöregh, I. *Eur. J. Org. Chem.* **2002**, 856−872.

(22) (a) Hobza, P.; Slezle, H. L.; Schag, E. W. *J. Am. Chem. Soc.* **1994**, *116*, 3500−3506. (b) Hunter, C. A.; Sanders, J. K. M., *J. Am. Chem. Soc.* **1990**, *112*, 5525−5534.

1b (B)   **1b (A)**

Loss of benzene

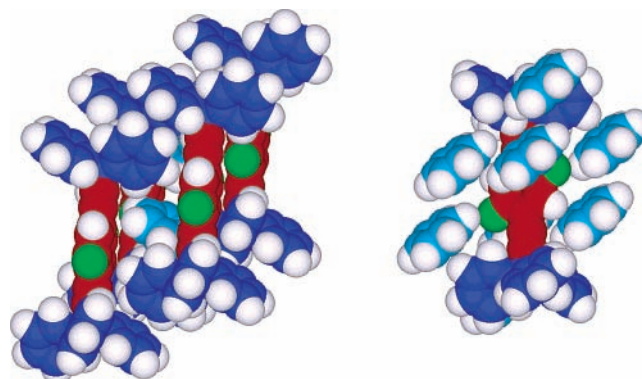**1d**   **1c**
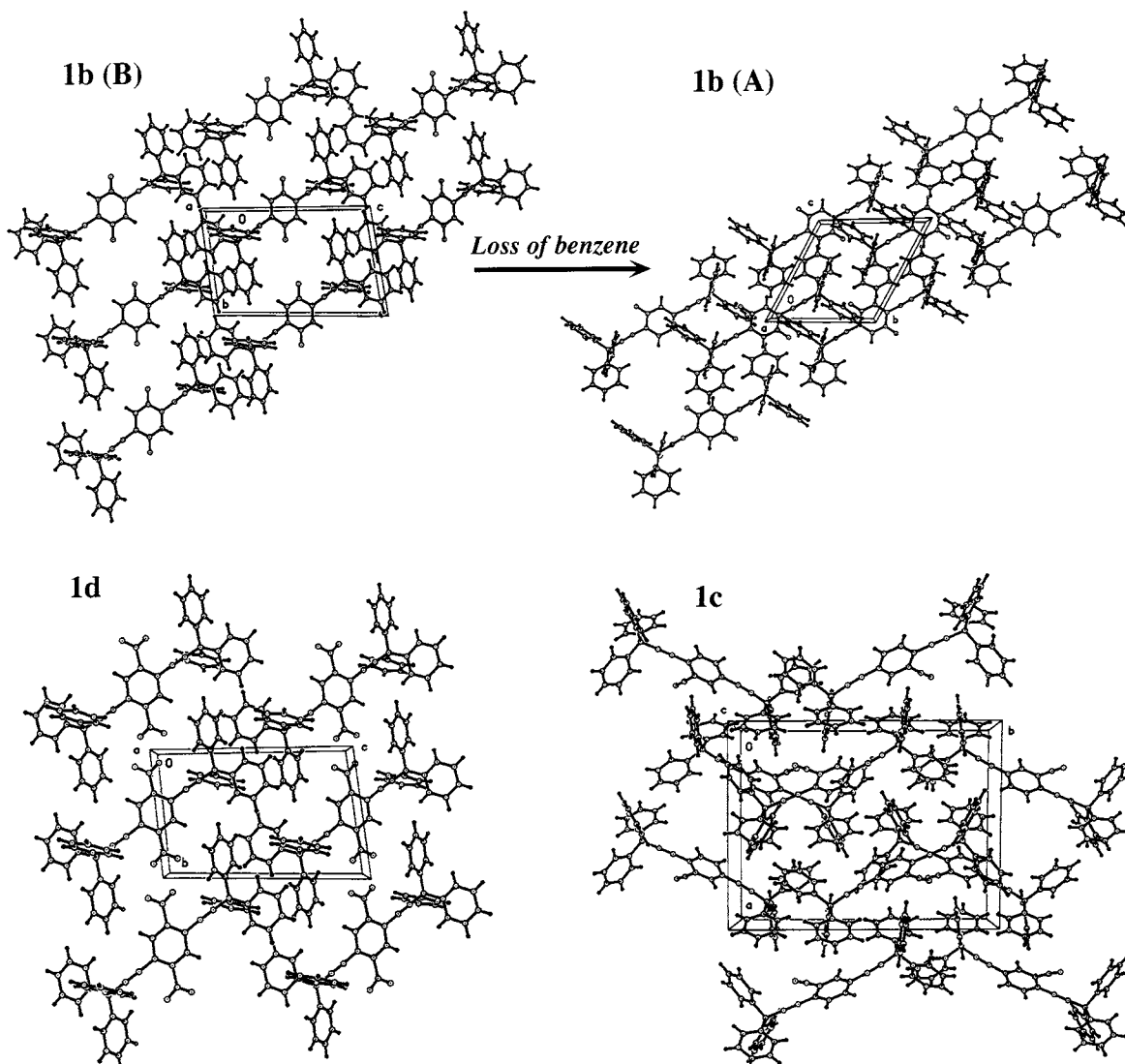
Figure 4. Top: Packing diagrams of the fluoro-substituted molecular compass **1b** its benzene clathrate, form B (right), and its solvent-free crystal, form A (left). Bottom: Packing diagram of the benzene clathrate triclinic ($P\bar{1}$) structure of the nitro-substituted molecular compass **1d** (left) and packing diagram of the solvent-free monoclinic crystal form ($P2_1/c$) of the cyano compound **1c**. Parallel-displaced benzene dimers in the structures of **1b** (B) and **1d** were removed for clarity (see Figure 5).

Scheme 4

1   5   6

n=1,2,3

Figure 5. Space-filling models of the benzene clathrate of **1b** showing trityl groups in dark blue, the 1,4-diethynyl-2-fluorophenylene group in red, the positionally disordered fluorine in green, and benzene molecules in light blue. Left: four molecular compasses make up a supramolecular cage with a benzene dimer trapped at the center. Right: Each molecular compass is surrounded by four benzene dimers around the central portion of the molecule.

illustrates a close-packed interdigitation of the dumbell-shaped molecules. Phenyl rings from trityl groups in six neighboring molecules fill-in the space around each phenylene. In analogy with the solvent-containing form **B**, molecules have their long axis aligned along the unit cell $b-c$ diagonal. As it was noticed for compound **1a**, a remarkable homology between the packing structures of the benzene clathrate and the solvent-free crystals

of **1b** help explain the first-order phase transition from one form to the other. A different packing structure was obtained in the
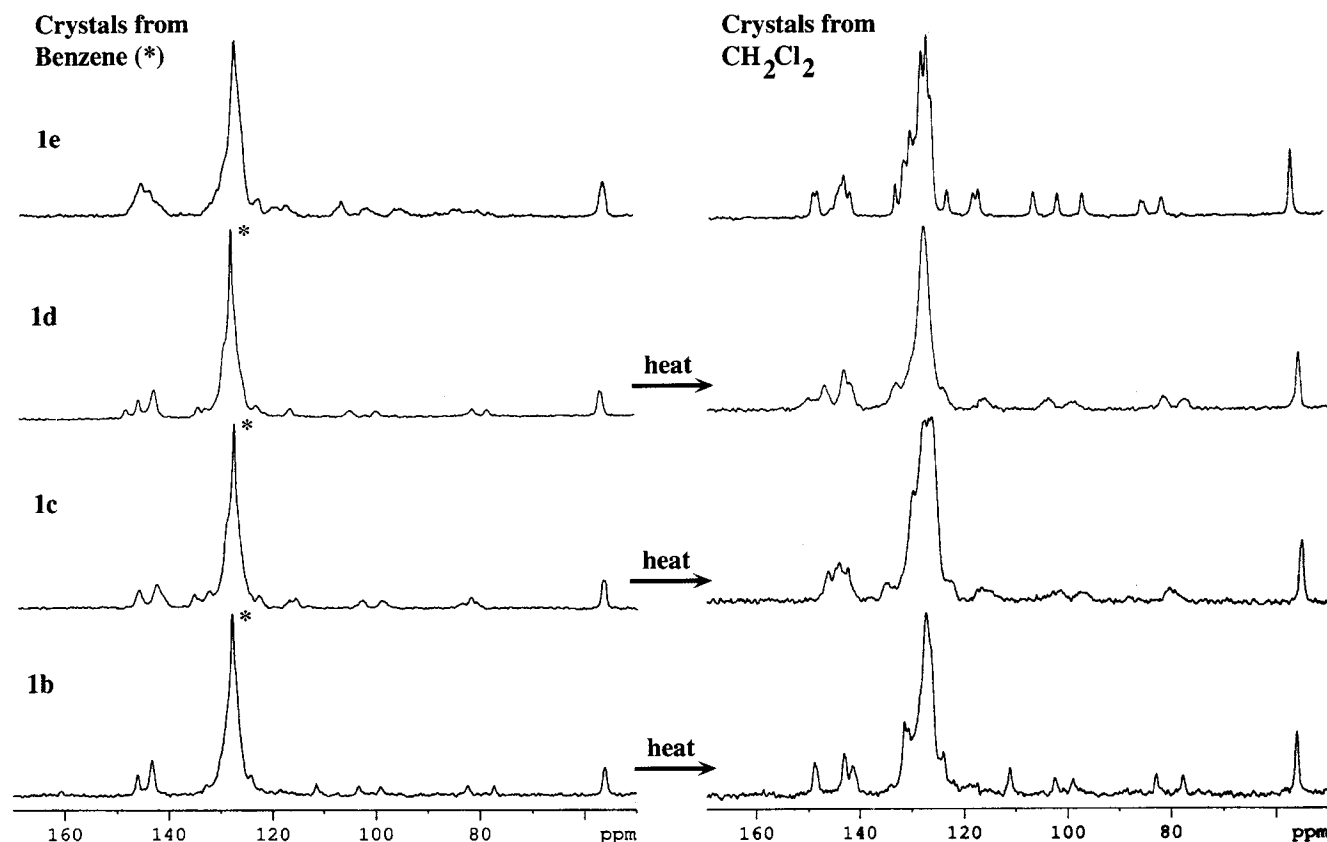
Figure 6. ^{13}C CPMAS NMR spectra measured at 300 K of crystals of **1b**−**1d** grown from benzene (left) and from CH$_2$Cl$_2$ (right). Benzene signals identified by dipolar dephasing experiments are marked with an asterisk (*). As indicated by the arrows, the spectra from benzene-containing crystals of **1b**−**1d** were transformed into the spectra obtained with crystals from CH$_2$Cl$_2$ when the samples were heated in the probe at 110 °C for 15 min. Solid samples of **1e** from benzene were solvent-free, but different from those obtained in CH$_2$Cl$_2$.

case of the cyano-substituted compound **1c** (Figure 4). Although the structure of **1c** contains no solvent of crystallization, it differs from the solvent-free crystals of **1a**, **1b**, and **1e**. Since crystals are not disordered and there is no average inversion center, one full molecule is needed to describe the asymmetric unit and four to describe the unit cell ($Z = 4$, Table 3). Although the molecular symmetry is lower (C_1) than that observed in the crystal structures of the other compounds (C_i), the symmetry of the crystal is higher, with the monoclinic space group $P2_1/c$ (Figure 4).

2.4. Solid-State ^{13}C CPMAS NMR: Characterization of Benzene Clathrate and Solvent-Free Structures. A relatively good correlation was observed between isotropic chemical shifts measured in solution and chemical shifts determined in the solid state by the ^{13}C CPMAS experiment. As illustrated in Figure 6, spectra were obtained with samples obtained from benzene and from CH$_2$Cl$_2$. Not shown in Figure 6, spectra measured with samples of **1c** from ethyl acetate were different from those obtained in benzene and in CH$_2$Cl$_2$. Signals corresponding to nonprotonated carbons, and to the highly mobile benzene molecules, could be assigned by interrupted decoupling or quaternary selection experiments.[23] In these measurements, spectra are acquired with a 50 μs interruption of the proton decoupler immediately after cross polarization and before the acquisition of the FID. Spectra measured in this manner result in the disappearance of carbon signals that experience a strong
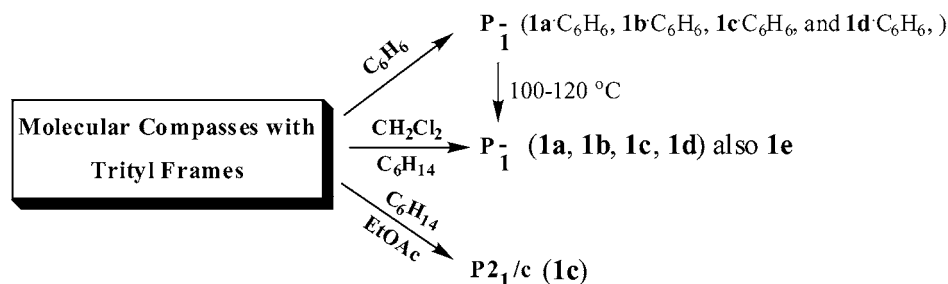
C−H dipolar interaction, such as all the static protonated carbons. Although most aromatic signals corresponding to the central phenylene rotors overlap considerably with signals corresponding to the trityl groups, some were sufficiently resolved to suggest an assignment by analogy with the solution spectra. Four well-resolved alkyne signals between 80 and 100 ppm, observed in all spectra, reflect the substantial electronic differences between the two molecular halves that are caused by the polar substituents. However, the solid-state spectra of **1b**−**1e** gave no indication of distinguishable disorder sites or local domains, which appear to manifest in the form of a rather severe line broadening. As expected from the severe overlap between trityl and phenylene carbons, spectra measured with compound **1b** as a function of temperature between 213 and 373 K showed no significant spectral changes.

The ^{13}C CPMAS spectra of crystalline samples of **1b**−**1d** grown from benzene (Figure 6, left side) displayed a sharp peak at 128 ppm, which overlaps with signals corresponding to the *ortho* and *meta* signals of the trityl groups. It was shown that benzene-grown crystals of the cyano-substituted compound **1c** do occur as a solvent clathrate. Although we have been unable to obtain diffraction-quality single crystals to solve its X-ray structure, its thermal properties are analogous to those of the benzene clathrates from compounds **1a**, **1b**, and **1d**. As previously reported for **1a**,[6] the ^{13}C CPMAS NMR spectra of crystals of **1b**−**1d** obtained from CH$_2$Cl$_2$ were identical to those obtained with benzene-grown crystals heated in situ within the NMR probe (Figure 6, right side). The monoamino derivative

---

(23) Alemany, L. B.; Grant, D. M.; Alger, T. D.; Pugmire, R. J. *J. Am. Chem. Soc.* **1983**, *105*, 6697−6704.

Molecular Compasses and Gyroscopes with Polar Rotors   **A R T I C L E S**

Scheme 5

Table 5. Thermal Analysis of Molecular Compasses **1a-1g**.

compd	mp (°C)	decomp. (°C)
1a (-H)	316 (110−130)[a]	370
1b (-F)	270 (60−100)[a]	350
1c (-CN)	218 (85−130)[a]	350
1d (-NO$_2$)	229 (110−140)[a]	370
1e (-NH$_2$)	284[b]	360
1f (2,3-NH$_2$)	283	290
1g (2-NH$_2$-5-NO$_2$)	dec	360

[a] The temperature ranges in parentheses indicate the desolvation range for the benzene clathrates determined by DSC and TGA at heating rates of 10 °C/ min. [b] No clathrate was observed.

1e was the only exception among the monosubstituted molecular compasses, as the samples obtained from benzene solution have an amorphous appearance and contain no solvent in their crystal structure (Figure 6, top left spectrum).

2.5. Thermal Analysis. As summarized in Table 5, differential scanning calorimetry (DSC) and thermogravimetric analyses (TGA) carried out with freshly recrystallized samples were consistent with the ^{13}C CPMAS results analyzed above. Endothermic peaks corresponding to crystal melting were observed between 218 and 284 °C for six of the compounds. Only the nitroaniline derivative **1g** decomposed before melting. Additionally, the DSC thermograms from samples of **1b**−**1d** grown from benzene showed a broad endothermic peak between 60 and 140 °C. That such a transition corresponds to the loss of benzene from the clathrate structure was confirmed by thermogravimetric analyses (TGA), which revealed a loss of mass corresponding to two benzene molecules per unit cell within the same temperature range. Melting transitions for crystals obtained from CH$_2$Cl$_2$, crystals from benzene desolvated in situ, and crystals grown from supercooled melts were very similar. Decomposition temperatures varied from as low as 290 °C for **1f** to as high as 370 °C for **1d**. All the monosubstituted molecular compasses **1b**−**1e** have melting points that are lower than that of the parent compound **1a**, perhaps reflecting a disruption to the packing structure caused by the polar substituent. Compounds **1b** and **1e** with the smallest substituents (F and NH$_2$) have the highest melting points and compounds **1c** and **1d** with the larger -CN and -NO$_2$ groups, respectively, have melting temperatures that are significantly lower (90−100 °C) than that of **1a**.

2.6. Crystallographic Disorder and Rotational Dynamics of Polar Phenylene Rotors. X-ray diffraction data, thermal analysis, and ^{13}C CPMAS NMR measurements as a function of temperature show that crystals of the monosubstituted fluoro (**1b**), cyano (**1c**), nitro (**1d**), and amino (**1e**) compounds crystallize in isomorphous packing structures. Crystals grown from benzene give rise to clathrate structures in the space group $P\bar{1}$ with one molecular compass and two solvent molecules per

unit cell and loss of solvent occurs by a first-order phase transition between 60 and 130 °C (Scheme 5). The solvent-free structures obtained in this manner are spectroscopically and thermally identical to those obtained by crystallization from mixtures of CH$_2$Cl$_2$ and hexanes. Not surprisingly, volume-filling, close-packing interactions determine the formation of isomorphous crystal structures with little or no influence by the polar groups.[24] In fact, a statistical analysis of crystallographic data by Whitesell et al.[25] and a study that considers packing indices and packing potential energies of crystalline carbonyls and nitriles by Gavezzotti[26] suggest that dipole−dipole interactions have little or no influence on space group symmetry and molecular orientations. However, Whitesell et al. pointed out that "this is not to say that local electrostatic interactions are not important" while Gavezzotti noted that "(dipoles) never point directly at each other, and this must be a purely electrostatic effect, since steric hindrance of the molecules would not prevent such an arrangement." Assuming that similar arguments are valid for polar groups such as those involved in this study, the formation of local domains with adjacent dipoles adopting favorable orientations should be considered (Scheme 6). While the average X-ray structures are reminiscent of the 2,6-disubstituted-1,4-diethynylphenylenes with their polar group having 50% occupancy at the two symmetry-related sites (Scheme 6a), the formation of domains (Schemes 6b and 6c) with dipoles in adjacent molecules avoiding head-to-head interactions cannot be discounted. While information on dipolar correlation between neighboring molecules is not available from the data reported in this paper, it is expected that crystallographic disorder, whether static or dynamic, will have a strong influence on the dielectric and electrooptic properties of molecular compasses and gyroscopes.

As it pertains to the dynamics of **1a**−**1e**, we previously showed that benzene-grown crystals of **1a** undergo a 2-fold phenylene flipping motion with a rate constant of 0.13×10^3 s^{-1} at 255 K and an estimated activation energy of 12.8 kcal/mol determined by variable temperature CPMAS ^{13}C NMR.[3,6] Solvent-free crystals of the same compound were shown to have a rate constant for rotation of 2.2×10^6 s^{-1} at 329 K and an activation barrier of 14.6 kcal/mol which were determined by variable temperature quadrupolar echo line-shape ^{2}H NMR analysis. With that in mind, it is of interest to ask how the various polar groups in **1b**−**1e** may affect the rotational dynamics of their corresponding phenylenes. Although variable temperature CPMAS ^{13}C NMR measurements in search of changes that could be assigned to dynamically exchanging

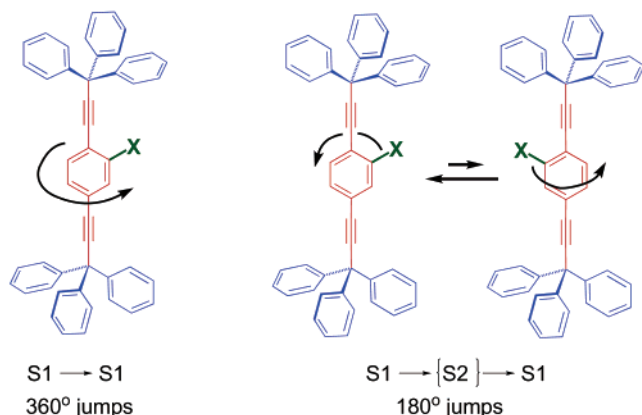(24) Claborn, K.; Kahr, B.; Kaminsky, W. *CrystEngComm* **2002**, *4*, 252−256.
(25) Whitesell, J. K.; Davies, R. E.; Saunders: L. L.; Wilson, J. R.; Feagins, J. P. *J. Am. Chem. Soc.* **1991**, *113*, 3267−3270.
(26) Gavezzotti, A. *J. Phys. Chem.* **1990**, *94*, 4319−4325.

Scheme 6

Scheme 7

S1 → S1
360° jumps

S1 → {S2} → S1
180° jumps
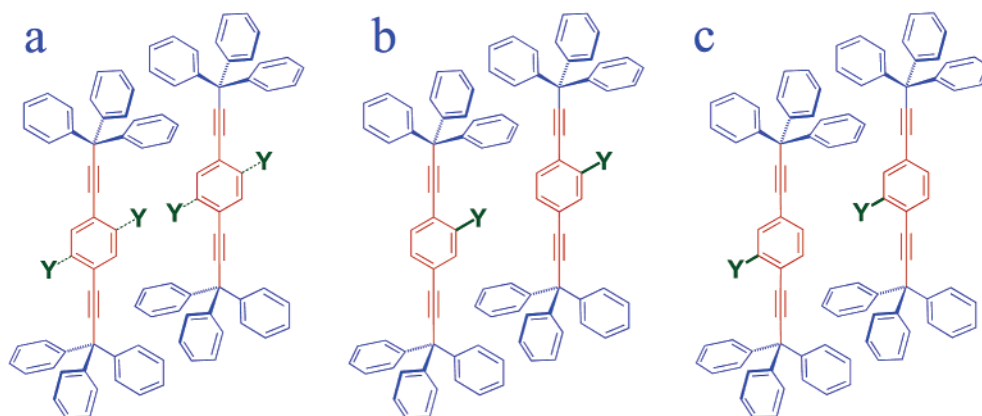
nuclei[27] gave insufficient resolution to use the method, some qualitative insight on the possible dynamics of the polar phenylenes may be deduced from the crystallographic data. Noting that the disordered sites are related by a center of inversion, one may conclude that sites occupied by the polar groups ($Y = F, CN, NO_2, NH_2$) cannot be related by a dynamic process. A dynamic interconversion would require molecular rotation along the alkyne axis and inversion of the two axially chiral trityl groups in the solid state. A static disorder implies that, on average, a given molecule can have the polar group in either one of the two centrosymmetric sites (i.e., S1 in Scheme 7), but not on both. Under these constraints, rotation must be limited to (a) full 360° rotations (S1 → S1) or (b) to two sequential 180° phenylene flips with the polar group having a very short residence time at the second site (S2) of a highly asymmetric rotational potential (i.e., S1 → S2 → S1). Dielectric spectroscopy and molecular modeling now in progress with the fluoro-derivative **1b** ($Y = F$) support the second mechanism and suggest the potential of variable temperature quadrupolar echo ^2H NMR as an additional experimental technique to confirm this dynamic process.

3. Conclusions. Molecular compasses with trityl frameworks and polar phenylene rotors can be obtained in reasonable yields by Pd(0)-coupling reactions of 1,4-dibromophenylenes and tritylacetylene. Samples were prepared with fluoro (**1b**), cyano

(27) (a) Lyerla, J. R.; Yannoni, C. S.; Fyfe, C. A. *Acc. Chem. Res.* **1982**, *15*, 208−216. (b) Horii, F.; Kaji, H.; Ishida, H.; Kuwabara, K.; Masuda, K.; Tai, T. *J. Mol. Struct.* **1998**, *441*, 303−311. (c) Frydman, L.; Olivieri, A. C.; Diaz, L. E.; Frydman, B.; Kustanovich, I.; Vega, S. *J. Am. Chem. Soc.* **1989**, *111*, 7001−7005.

(**1c**), nitro (**1d**), amino (**1e**), diamino (**1f**), and nitroamino (**1g**) susbtituents. While X-ray quality crystals of molecular compasses with two polar substituents (**1f** and **1g**) have not been obtained, samples of the monosubstituted compounds (**1b**−**1d**) crystallized from benzene gave rise to triclinic clathrate structures in the space group $P\bar{1}$ with two solvent molecules per unit cell, which can be desolvated by a first-order phase transition between 60 and 130 °C. The solvent-free structures obtained in this manner were shown to be spectroscopically and thermally identical to those obtained by crystallization from mixtures of CH_2Cl_2 and hexanes. Crystals of **1e** were only formed in the solvent-free $P\bar{1}$ modification and crystals of **1c** formed a third polymorph in the monoclinic space group $P2_1/c$. A detailed assignment of ^{13}C NMR signals in solution was used to assign the signals of the phenylene rotor in the solid state in an effort to determine whether variable temperature coalescence analysis may be used to determine the rates of gyroscopic motion in the solid state. Unfortunately, a strong spectral overlap between phenylene and trityl signals makes it impossible to apply this method. Nonetheless, ^{13}C CPMAS NMR spectra could be used to document the phase transitions between the various crystal forms which were also observed by DCS and TGA measurements. A qualitative analysis of the crystallographic data helped us formulate interesting questions regarding the formation of domains with locally aligned dipoles and the possible rotational dynamics of the central phenylene in terms of full rotations or sequential 2-fold flips along an asymmetric potential. Studies in progress to address these questions include the use of dielectric measurements as a function of frequency and temperature to determine the rates of dipolar motion in the solid state, molecular modeling, and the use of ^2H NMR line-shape analyses.

Experimental Section

General. IR spectra were obtained on a Perkin-Elmer Paragon 100 FT-IR instrument. The ^1H and ^{13}C NMR spectra were acquired on a Bruker NMR spectrometer at 500 and 125 MHz, respectively. The solvent used in all the cases was CD_2Cl_2, with TMS as an internal standard. The DSC and TGA analyses were recorded on a Perkin-Elmer Pyris Diamond DSC and TG/DTA.

Materials. All the reagents and solvents were purchased from Aldrich, except 2,5-diiodofluorobenzene, the triethylamine and the copper (I) iodide, which were obtained from Matrix Scientific, Fisher, and Acros Organics, respectively. The chemicals were used without further purification, and triethylamine was deoxygenated by sparging with Ar for at least 2 h before to use.

Molecular Compasses and Gyroscopes with Polar Rotors **A R T I C L E S**

2,5-Bis(3,3,3-triphenylpropynyl)fluorobenzene (1b). Bis(triphenylphosphine)palladium dichloride (0.024 g, 0.13 mmol), copper iodide (0.025 g, 0.13 mmol), triphenylphosphine (0.105 g, 0.4 mmol), and 2,5-diiodofluorobenzene (0.462 g, 1.3 mmol) were charged in a three-neck flask provided with a condenser and a magnetic stirrer. The flask was sparged with argon for 15 min after 30 mL of degassed triethylamine was added. The reaction mixture was heated in an oil bath to 85 °C and 3,3,3-triphenylpropyne (0.89 g, 3.32 mmol) previously dissolved in 20 mL of degassed triethylamine was added during a period of 1 h. The reaction mixture was heated an additional 18 h under argon. After cooling to room temperature, the reaction mixture was filtered and the triethylamine was evaporated. The product was purified by column crhomatography (CH$_2$Cl$_2$:benzene:hexanes 1:1:8 by volume) to afford 0.19 g of (23%) **1b** as a white solid with moderate solubility. Analysis: mp = 270 °C. ^{1}H NMR (500 MHz, CD$_2$Cl$_2$, TMS): δ 7.28 (m, 32 H, trityl unit and protons *ortho* and *para* to the F group), 7.46 (t, *J* = 7.6 Hz, 1H, *meta* to F). ^{13}C NMR (125 MHz, CD$_2$Cl$_2$, TMS): δ 56.5, 56.8, 79.0, 84.3 (d, *J* = 3.0 Hz), 98.5, 102.6 (d, *J* = 3.5), 112.3 (d, *J* = 16.0 Hz), 118.7 (d, *J* = 22.9 Hz), 125.3 (d, *J* = 9.5 Hz), 127.3, 127.4, 127.7 (d, *J* = 3.5 Hz), 128.4, 128.5, 129.4, 129.5, 133.5 (d, *J* = 2.0 Hz), 145.2, 145.3, 162.9 (d, *J* = 250.8 Hz). IR (KBr): 3084, 3059, 3019, 2367, 2330, 2229, 1595, 1544, 1491, 1442, 1445, 1182, 1117, 1080, 1032, 1002, 874, 832, 754, 720, 698, 639 cm^{-1}. MS (70 eV): *m/z* (%) 628.2 (40, M$^+$), 551.2 (13), 267.1 (100), 265.1 (55), 252.1 (30), 189.1 (19), 165.1 (72). HRMS (EI): calcd for C$_{48}$H$_{33}$F 628.2566; found 628.2562.

2,5-Bis(3,3,3-triphenylpropynyl)benzonitrile (1c). Molecular compass **1c** was obtained following the same procedure described above for compound **1b** in 10% isolated yield. Analysis: mp = 218 °C. ^{1}H NMR (500 MHz, CD$_2$Cl$_2$, TMS): δ 7.31 (m, 30 H, trityl unit), 7.58 (d, *J* = 8.2 Hz, 1H, *meta* to CN), 7.67 (dd, *J* = 8.2, 1.5 Hz, 1H, *para* to CN), 7.80 (d, *J* = 1.5 Hz, 1H, *ortho* to CN). ^{13}C NMR (125 MHz, CD$_2$Cl$_2$, TMS): δ 56.6, 56.9, 82.0, 83.4, 99.9, 103.9, 115.8, 117.5 (CN), 124.3, 126.7, 127.4, 127.5, 128.5, 129.4, 129.5, 132.9, 135.5, 135.9, 144.8, 145.0. IR (KBr): 3060, 3030, 2229, 1732, 1594, 1488, 1445, 1185, 1079, 1031, 1002, 908, 891, 842, 777, 758, 733, 662, 639 cm^{-1}. MS (70 eV): *m/z* (%) 635 (100, M$^+$), 558 (18), 544 (10), 456 (6), 368 (8), 317 (10), 293 (27), 243 (24), 165 (165), 131 (70). HRMS (EI): calcd for C$_{49}$H$_{33}$N 635.2613; found 635.2596.

2,5-Bis(3,3,3-triphenylpropynyl)nitrobenzene (1d). Molecular compass **1d** was obtained following the same procedure described above for compound **1b** in 40.2% isolated yield. Analysis: mp = 229 °C. ^{1}H NMR (500 MHz, CD$_2$Cl$_2$, TMS): δ 7.31 (m, 30 H, trityl unit), 7.65 (d, *J* = 8.2 Hz, 1H, *meta* to NO$_2$), 7.69 (dd, *J* = 8.2, 1.5 Hz, 1H, *para* to NO$_2$), 8.18 (d, *J* = 1.5 Hz, 1H, *ortho* to NO$_2$). ^{13}C NMR (125 MHz, CD$_2$Cl$_2$, TMS): δ 56.6, 57.0, 80.9, 83.3, 100.1, 105.3, 118.5, 124.6, 127.4, 127.5, 127.8, 128.5, 128.6, 129.4, 129.5, 135.3, 135.8, 144.9, 145.0, 149.7. IR (KBr): 3054, 3030, 2322, 2231, 1599, 1540, 1519, 1504, 1487, 1445, 1360, 1261, 1180, 1079, 1031, 1002, 894, 838, 807, 780, 759, 733, 702, 659, 639 cm^{-1}. MS (70 eV): *m/z* (%) 655.2 (7, M$^+$), 639.2 (17), 611.3 (53), 505.2 (34), 467.0 (17), 379.0 (63), 262.1 (45), 243.1 (36), 185.1 (79), 165.1 (100), 149.0 (26). HRMS (EI): calcd for C$_{48}$H$_{33}$NO$_2$ 655.2511; found 655.2498.

2,5-Bis(3,3,3-triphenylpropynyl)aniline (1e). Molecular compass **1e** was obtained following the same procedure described above for compound **1b** in 26% isolated yield. Analysis: mp = 284 °C. ^{1}H NMR (500 MHz, CD$_2$Cl$_2$, TMS): δ 4.17 (s, 2H, NH$_2$), 6.84 (dd, *J* = 7.6, 1.5 Hz, 1H, *para* to NH$_2$), 6.86 (d, *J* = 0.9 Hz, 1H, *ortho* to NH$_2$), 7.30 (m, 31H, trityl unit and the hydrogen *meta* to NH$_2$). ^{13}C NMR (125

MHz, CD$_2$Cl$_2$, TMS): δ 56.5, 56.9, 82.4, 85.8, 96.6, 102.7, 108.4, 117.1, 121.2, 124.5, 127.2, 127.3, 128.4, 128.5, 129.4, 129.5, 132.3, 145.5, 145.6, 148.6. IR (KBr): 3491, 3390, 3059, 3031, 2359, 2326, 2221, 1608, 1539, 1484, 1443, 1318, 1286, 1267, 1254, 1175, 1079, 1028, 816, 756, 697, 632 cm^{-1}. MS (70 eV): *m/z* (%) 625.3 (100, M$^+$), 548.2 (30), 358.2 (26), 280.1 (15), 267.1 (14), 185.1 (23), 165.1 (20). HRMS (EI): calcd for C$_{48}$H$_{35}$N 625.2769; found 625.2755.

3,6-Bis(3,3,3-triphenylpropynyl)-1,2-phenylenediamine (1f). Molecular compass **1f** was obtained following the same procedure described above for compound **1b** in 22% isolated yield. Analysis: mp = 283 °C. ^{1}H NMR (500 MHz, CD$_2$Cl$_2$, TMS): δ 3.86 (s, 4 H, NH$_2$), 6.86 (s, 2H, spacer-phenyl), 7.30 (m, 30 H). ^{13}C NMR (125 MHz, CD$_2$Cl$_2$, TMS): δ 56.88, 82.82, 102.2, 109.6, 122.1, 127.3, 128.5, 129.4, 136.9, 145.6. IR (KBr): 3418, 3340, 3062, 3027, 2353, 2327, 2219, 1616, 1598, 1445, 1207, 1180, 1072, 1031, 888, 803, 767, 752, 723, 697, 667, 637 cm^{-1}. MS (70 eV): *m/z* (%) 640.3 (100, M$^+$), 563.3 (22), 454.1 (67), 373.2 (50), 295.1 (47), 243.1 (30),185.1 (32), 182.0 (47), 165.1 (55). HRMS (EI): calcd for C$_{48}$H$_{36}$N$_2$ 640.2878; found 640.2875.

2,5-Bis(3,3,3-triphenylpropynyl)-4-nitroaniline (1g). Molecular compass **1g** was obtained in two steps. In the first of them was followed the same procedure described above for compound **1b**; however a mixture of molecular compass **1g** and 5-(3,3,3-triphenylpropynyl)-2-bromo-4-nitroaniline **2** (the product of a mono-coupling reaction) was obtained in a 1:3.5 proportion, then we added 1.5 equiv of 3,3,3-triphenyl-1-propyne to the mixture after a fast filtration by chromatographic column using as eluent the same mixture of solvent used before. The heating was continued until reaction completion (10 h); the total yield after purification in this case was 12.3%. ^{1}H NMR (500 MHz, CD$_2$Cl$_2$, TMS): δ 4.77 (s, 2H, NH$_2$), 6.88 (1, 1H, *ortho* to NH$_2$), 7.30 (m, 30 H, trityl unit), 8.25 (s, 1H, ortho to NO$_2$). ^{13}C NMR (125 MHz, CD$_2$Cl$_2$, TMS): δ 56.9, 57.0, 80.1, 82.2, 103.6, 104.3, 107.6, 118.7, 121.1, 127.4, 127.5, 128.5, 128.6, 129.3, 129.5, 130.3, 139.3, 145.0, 145.1, 152.3. IR (KBr): 3486, 3384, 3058, 3027, 2221, 1614, 1538, 1514, 1506, 1488, 1445, 1312, 1256, 1183, 1100, 1032, 854, 757, 726, 697, 628 cm^{-1}. MS (70 eV): *m/z* (%) 670.3 (47, M$^+$), 625.3 (20), 565.2 (20), 488.2 (16), 357.1 (18), 243.1 (19), 165.1 (37), 124.0 (100); 117.0 (79) HRMS (MALDI): calcd for C$_{48}$H$_{34}$N$_2$O$_2$ 670.2620; found 670.2623.

5-(3,3,3-triphenylpropynyl)-2-bromo-4-nitroaniline 2. ^{1}H NMR (500 MHz, CDCl$_3$, TMS): δ 4.57 (s, 2H, NH$_2$), 6.77 (1, 1H, *ortho* to NH$_2$), 7.26 (m, 18 H, trityl unit), 8.25 (s, 1H, ortho to NO$_2$). ^{13}C NMR (125 MHz, CDCl3, TMS): δ 56.6, 80.8, 103.4, 106.6, 118.9, 120.4, 127.0, 128.1, 129.2, 130.3, 139.3, 144.6, 148.4. IR (KBr): 3478, 3390, 3059, 3023, 2219, 1608, 1554, 1504, 1488, 1446, 1311, 1247, 1184, 1116, 1032, 891, 850, 755, 638 cm^{-1}.

Supporting Information Available: Spectroscopic data ^{1}H and ^{13}C NMR data of all compounds including HMBC spectra. X-ray diffraction data for **1b**−**1e** (CIF files) and packing diagram of **1e**. This material is available free of charge via the Internet at http://pubs.acs.org.

JA035274B

EXHIBIT M

10196A-CIP

IN THE UNITED STATES PATENT AND TRADEMARK OFFICE

IN RE APPLICATION OF "LAJEUNESSE, JEAN", ET AL
FOR: **PROCESS FOR PREPARING 2-AMINOTHIAZOLE-5-AROMATIC CARBOXAMIDES AS KINASE INHIBITORS**
APPLICATION NO: **11/192867**
PATENT NO: **7491725**
ART UNIT: **1626**
CONFIRMATION NO: **8441**

APPLICATION DATE: **29 Jul 2005**
PATENT GRANT DATE: **17 Feb 2009**
EXAMINER: **NOLAN, JASON MICHAEL**
USPTO CUSTOMER NO: **23914**

TRANSMITTED VIA EFS-WEB

Certificate of Corrections Branch
Commissioner for Patents
PO BOX 1450
Alexandria. VA 22313-1450

REQUEST FOR CERTIFICATE OF CORRECTION OF PATENT
FOR MISTAKES UNDER (37 C.F.R. §1.322) AND (37 C.F.R. § 1.323)

Sir:

The patentees through their attorney/agent hereby respectfully request that a certificate of correction be issued to correct printing errors in accordance with the attached Certificate of Correction Form 1050.

Pursuant to 37 C.F.R. §1.322, and 37 C.F.R. 1.323 patentees request that a certificate of correction enclosed herewith be issued for mistakes made by both the Patent and Trademark Office and the Applicant. The requested corrections are minor in character, are either clerical or typographical in nature and do not constitute new matter. The changes would not require reexamination. Support for the requested corrections can be found in the list of references cited by Applicant and considered by Examiner dated September 18, 2007 and Applicant's Amendment dated June 2, 2008.

Please send the certificate to the address registered with customer number 23914. The assignment on the above patent was recorded on September 21, 2005, and can be found on Reel 016564, Frame 0527 (10 pages) to Assignee, Bristol-Myers Squibb Company.

In that the errors listed above are ascribable to both the USPTO and Applicant, please charge the appropriate fee under 37 CFR §1.20(a) and any additional fees under 37 C.F.R. § 1.17 which may be required. to Account No. 19-3880 in the name of Bristol-Myers Squibb Company.

Respectfully submitted,

Bristol-Myers Squibb Company
Patent Department
P.O. Box 4000
Princeton, NJ 08543-4000

Date: 5|11|10

MARY VANATTEN
Attorney for Applicant
Reg. No. 39,408
Phone: 609-252-4379

Case: **10196ACIP**

UNITED STATES PATENT AND TRADEMARK OFFICE
CERTIFICATE OF CORRECTION

PATENT NO. : 7491725   Page 1 of 1
DATED: : FEBRUARY 17, 2009
INVENTOR(S) : JEAN LAJEUNESSE ET AL.

    It is certified that there is an error in the above-identified patent and that said Letters Patent is hereby corrected as shown below:

On the Title Page

    On the Title Page, Column 2, OTHER PUBLICATIONS, line 23, delete "AMinothioacryloyl" and insert --Aminothioacrylolyl --.

In the Claims:

    Column 48, line 66, Claim 2, delete "anaylsis" and insert --analysis --.

    Column 49, line 15, Claim 3, delete "γ" and insert -- λ --.

    Column 50, line 3, Claim 9, delete "13°" and insert -- 130° --.

    Column 50, lines 4 to 5, Claim 9, delete "thermo-gravitmetric" and insert -- thermogravimetric --.

    Column 50, line 28, Claim 12, delete "thermogravitmetric" and insert -- thermogravimetric --.

MAILING ADDRESS OF SENDER:
Bristol-Myers Squibb Company
Patent Department
P.O. Box 4000
Princeton, NJ 08543-4000